OPTIMIZATION AND MODELLING OF A PARTIALLY ACIDULATED PHOSPHATE ROCK (PAPR) FERTILIZER PILOT-PLANT USING CHILEMBWE PHOSPHATE ROCK

By

FREDRICK CHILESHE

A THESIS

Submitted to
University of Zambia
in fulfillment of the requirements for the degree of

DOCTOR OF PHILOSOPHY
(METALLURGY AND MINERAL PROCESSING)

School of Mines

(2004)

COPYRIGHT DECLARATION

This thesis represents my own work and has not been previously submitted for a degree at this or another university.

Signed

Fredrick Chileshe
(B.Min.Sc, PG Dip, MSc (Eng), AEIZ)

Supervisor's signature

Prof. S. Simukanga
(B.Min.Sc, M.Min.Sc, PhD, FEIZ, RENG, FSAIMM, MIMMM))

Dr. G. Nkonde
(M.Sc, D.Tech,MEIZ, RENG)

APPROVAL PAGE

This thesis of Fredrick Chileshe is approved in fulfillment of the requirement for the award of Doctor of Philosophy in Metallurgy and Mineral Processing by the University of Zambia.

Examiner's signatures

1. ______________________________

Chairman – Examining Board
Dr. F. Tembo
(B.Min.Sc, M.Min.Sc, PhD)

2. ______________________________

Prof. S. Simukanga
(B.Min.Sc, M.Min.Sc, PhD, FEIZ, RENG, FSAIMM, MIMMM))

3. E.H. Jere
____

Dr. E.H. Jere
(B.Sc, M.Sc, PhD)

4. ______________________________

Dr. J.B. Mwalula
(B.Sc, MSc, PhD)

TO FIDELIS CHIMFWEMBE CHILESHE

ABSTRACT

Improving food security by increasing crop production is currently Zambia's primary objective. Poor soil fertility and inadequate utilization of chemical fertilizers have often resulted in poor crop yields and that has exacerbated the problems of poverty and hunger in the country. Phosphorus is the most limiting nutrient after nitrogen in most of the Zambian soils. Currently, phosphate fertilizers are imported and are expensive for most of the low-resource farmers in the country. However, local phosphate deposits exist in Zambia but they have remained un-exploited and these include Chilembwe, Mumbwa, Nkombwa Hill, and Kaluwe. If exploited, indigenous phosphate resources could provide less expensive phosphate fertilizers that could help farmers increase crop production. In addition, indigenous phosphate resources could reduce the amount of foreign exchange currently spent on the importation of phosphate fertilizers. Previous research has revealed that Partially Acidulated Phosphate Rock (PAPR) produced using Chilembwe phosphate rock is just as agronomically effective as the imported superphosphate fertilizers on food crops in Zambia.

Partial acidulation of phosphate rock involves the reaction of finely ground phosphate rock with only a fraction (usually 50%) of the stoichiometric quantity of acid required to fully convert the apatite in the rock to a soluble form, mono-calcium phosphate. The process of producing PAPR is therefore less expensive in terms of acid consumption. The agronomic effectiveness of PAPR largely depends on the percentage of soluble phosphate (available P_2O_5) content in the

PAPR. During the processing of phosphate rock into PAPR the percentage of available P_2O_5 in the product depends largely upon the various process variables. These process variables include *reactiveness of phosphate rock, particle size of phosphate rock, degree of acidulation, acid concentration, process temperature profile, residence time of phosphate rock in the granulator and drying temperature of PAPR*. These variables differ from one phosphate rock to the other. Therefore, it was necessary to optimize the process variables in the pilot-plant during the production of PAPR using Chilembwe phosphate rock in order to improve the product quality and process efficiency.

The main units in the process (i.e. the ball mill in the comminution circuit and the granulator in the granulation circuit) were modelled in order to adopt the types of operation that gave optimum performance of the units. To model a system, a tracer was introduced in the feed stream as an instantaneous pulse while the product stream leaving the system was sampled and analyzed for the tracer concentration at discrete time intervals. The data for the tracer concentration with time was used to calculate the experimental residence time distribution curve which was simulated using the selective recycle model to obtain the number of cycles distribution curve. The number of cycles distribution curve showed the mass of tracer leaving the system after a given number of cycles and this was used in assessing the performance of the unit. It was assumed that flow in the main units (i.e. the ball mill and the granulator) was perfectly mixed whilst the classifying units (i.e. the hydrocyclone and the screens) were time delay units. In curve fitting, the generalized number of cycles distribution (NCD) and the inverse of the Laplace transform for a perfectly mixed reactor and a pure time delay unit were used.

Preliminary work involved characterization of a Chilembwe phosphate rock sample in order to determine the constituent mineral phases, the type of apatite, the grain size of apatite, and the chemical composition. Acidulation tests were carried out in the PAPR pilot-plant consisting of a rotary drum granulator, a rotary drum dryer, and a deck of screens. Prior to acidulation tests, phosphate rock sample containing an average of 26.4% CaO, 1.05% MgO, 0.75% K_2O, 0.08% Na_2O, 1.19% Al_2O_3, 1.60% Fe_2O_3, 22.5% P_2O_5, 1.79% F and 1.00% S was crushed and ground to a desirable particle size distribution.

Acidulation tests involved mixing the ground phosphate rock, with water and acid in the rotary drum granulator where the reactions occurred giving a granular PAPR product that was dried in the rotary drum drier. The product from the drier was sampled and analyzed for water-soluble P_2O_5 and neutral ammonium citrate (NAC)-soluble P_2O_5. The sum of water-soluble P_2O_5 and NAC-soluble P_2O_5 is the available P_2O_5 for uptake by plants when the fertilizer is applied in the field. Several process variables were studied during the acidulation tests aimed at optimizing the PAPR pilot-plant when using Chilembwe phosphate rock. These included *particle* size *of phosphate rock, degree of acidulation, acid concentration, initial temperature of phosphate rock, water and acid mixture,* *residence time of phosphate rock in the granulator, and drying temperature of PAPR.*

An economic evaluation for a 30 metric tons per hour PAPR project for an initial period of 15 years was finally carried out in order to assess the viability of commercial-scale production of PAPR. Methods employed in the analysis included the minimum rate of return, the Net Present Value, and Benefit-Cost ratio at various prices of the commodity.

Results of the powder X-ray diffraction studies revealed that the apatite in Chilembwe phosphate rock exists in the form of calcium manganese fluoride phosphate, $Ca_{9.3}Mn_{0.7}F_2\ (PO_4)$ suggesting the alteration of the ideal fluorapatite $Ca_{10}(PO_4)_6F_2$ by substitution of 0.7 Ca^{+2} with Mn^{+2} ions. The apatite grains are in the size range 400μm - 800μm as revealed by thin sections observation under the microscope. Results from size-sorting assays have shown that the bulk of the apatite could be liberated from the rock matrix by grinding to minus 106μm.

Acidulation test results showed that in the particle size range 42% - 79% minus 75μm the percentage of water-soluble P_2O_5 and Neutral Ammonium Citrate (NAC)-soluble P_2O_5 in PAPR remained constant. The percentage of available P_2O_5 in PAPR increased with the increase in the degree of acidulation (i.e. 40%, 50%, 60%, 70%, 80%, and 100%). Low acid concentrations, 50% to 70% H_2SO_4 gave high levels of water-soluble P_2O_5 and NAC-soluble P_2O_5 in PAPR. Acid concentration below 40% and above 70% lowered the percentage of water-soluble P_2O_5 and NAC-soluble P_2O_5 in PAPR. The initial temperature of the rock, water and acid before the reaction did not have a remarkable effect on the percentage of water-soluble P_2O_5 and NAC-soluble P_2O_5 in PAPR in the range 25°C to 110°C. The effect of residence time of phosphate rock in the granulator was that the percentage of water-soluble P_2O_5 and NAC-soluble P_2O_5 increased with the increase in residence time up to 3 minutes. After 3 minutes there was no significant change in the level of available P_2O_5 in the product. The drying temperature in the range of 90°C - 150°C did not affect the percentage of available P_2O_5 in PAPR. However, water-soluble P_2O_5 decreased with the increase in drying temperature whilst NAC-soluble P_2O_5 increased with the increase in drying temperature keeping the available P_2O_5 constant. The selective recycle model for a generalized NCD was effectively used to simulate the RTD's in the comminution of phosphate rock and in the acidulation and granulation processes. This resulted in the optimization of the operations of the main processing units (i.e. the ball mill in the comminution of phosphate rock and the granulator in the processing of phosphate rock into PAPR). The PAPR produced at optimum parameters contained an average of 9% available P_2O_5 and 18% total P_2O_5 at 50% degree of acidulation with H_2SO_4 at 50% concentration, 3 minutes residence time of phosphate rock in the granulator, and 120°C drying temperature, using phosphate rock containing about 23% P_2O_5 and particle size 42% minus 75μm.

Field tests were conducted by the School of Agricultural Sciences on maize, soya beans, sunflower, and groundnuts and results showed that PAPR was just as agronomically effective as the imported Mono-Ammonium Phosphate (MAP) in providing phosphorus to the plants. For soil re-captalization with phosphorus, PAPR was also found to be more suitable than MAP as it did not depress maize yields at higher application rates.

Economic evaluation of a 30 metric tons per hour PAPR project showed that the project could be profitable and the price of PAPR could be as low as K40,000 per 50kg bag. This price is about half that of compound fertilizers that are currently on the market.

This study has shown that Chilembwe phosphate deposit could indeed become an inexpensive source of phosphate that could partially substitute the imported phosphate and greatly benefit low-resource farmers in the enhancement of agricultural crop production in Zambia.

LIST OF PUBLICATIONS MADE DURING THE PhD WORK FROM APRIL 1999 TO OCTOBER 2002

(1) Zambian Phosphate Resources by F. Chileshe, G.K. Nkonde and S. Simukanga. Published in the PK Journal, March-April 2000, Issue No. 226, British Sulphur, pp 9-18.

(2) Application of least square method for calculating the RTD and NCD parameters in selective recycle systems by G.K. Nkonde and F. Chileshe. Presented by F. Chileshe at the MIC 2001 conference in Innsbruck Austria in February 2001, Published in the IASTED conference proceedings, MIC2001, Vol. II, pp781-786.

(3) Simulation of RTD in a closed comminution circuit using the selective recycle model by G. K. Nkonde, F. Chileshe and S. Simukanga. Published in the South African Journal of Chemical Engineering, Vol.13, Issue No. 2, pp 15-25.

(4) Optimization of process variables in the production of PAPR by F. Chileshe, S. Simukanga and G.K Nkonde. Published in the Zambian Engineer Magazine EIZ, Vol. 35, No. 1, pp 28 -31.

(5) Application of Number of Cycles Distribution (NCD) in a closed comminution circuit by G.K. Nkonde and F. Chileshe. Published in the Indian Chemical Engineer, vol. 44, No. 3, July – September 2002, pp 147-150.

(6) Factors affecting the level of available P_2O_5 in partially acidulated phosphate rock from Chilembwe phosphate deposit of Zambia by F. Chileshe, S. Simukanga and G.K Nkonde. Submitted to the IMPC 2003 SA (Abstract accepted for poster presentation).

TABLE OF CONTENTS

Page No.

LIST OF TABLES

LIST OF FIGURES

Page No.

CHAPTER 1

ACKNOWLEDGEMENT

Firstly I would like to thank the United Nations University, Institute for Natural Resources in Africa (INRA) for providing me with a scholarship for the first two years of my studies and the Copperbelt University for funding the last one and half years of my studies.

Secondly, I am sincerely grateful to my supervisors, Dr. G. K Nkonde and Prof. S. Simukanga for their contributions towards this work. I would also like to thank the technicians in the School of Mines, Mr. L. Njovu, F. Phiri and B. Mwango, who assisted me in carrying out some of the pilot-plant tests. I would like to also thank the Mr. P. F. R. Vivian-Neal, the Managing Director for the African Industrial Minerals Limited for providing the estimated costs for the commercial-scale PAPR project. Thanks to the Staff in the Mineral Resources Unit, Mr. V. Kawamya and Miss. M. Chisha for their cooperation in the use of computers and printers in the unit.

Finally, I would like to thank my wife, Helen, my son Fidelis, relatives and friends for their encouragement during my stay in Lusaka.

PREFACE

In recent years, there has been kin interest in research concerning the utilization of local phosphate resources aimed at improving crop production in order to increase food security in Zambia. Four phosphate deposits of igneous origin exist in Zambia namely, Chilembwe, Mumbwa, Nkombwa Hill and Kaluwe. None of these deposits has yet become commercialized for phosphate fertilizer production. This work was carried out in the pilot-plant at the University of Zambia, School of Mines and involved production of PAPR using Chilembwe phosphate rock. The process variables that affect the quality of PAPR in terms of available P_2O_5 were optimized. These included particle size of phosphate rock, degree of acidulation, acid concentration, initial temperature of acid at various concentrations, residence time of phosphate rock in the granulator and drying temperature. The main process units, i.e. the ball mill. in the comminution of phosphate rock and the granulator in the acidulation of phosphate rock were modelled using the Selective Recycle Model in order to improve their operations. The work also included an economic evaluation of a 30 metric tonnes per hour PAPR plant aimed at assessing the viability of a commercial-scale PAPR project in Petauke.

CHAPTER 1: LITERATURE REVIEW

INTRODUCTION

Zambia has experienced a rapid population growth that requires an increase in agricultural output to match the rising demand for food and reduce the escalating poverty levels. The country's economy has relied heavily on copper mining since independence in 1964. Unfortunately, in recent years copper production has severely declined resulting in the reduction of foreign exchange earnings from the mining sector.

Currently, the agricultural sector's enormous potential to contribute to the economic growth of the country remains largely untapped mainly due to poor crop yields caused mainly by low soil fertility and lack of affordable inputs such as fertilizers. Phosphorus is the most limiting nutrient after nitrogen in most Zambian soils [Bunyolo, 1991]. Hence, the use of phosphates in these soils is cardinal to the improvement of crop production. Currently, fertilizers are expensive for most of the low-resource farmers. Since local phosphate resources remain unexploited, the country imports all phosphates for its agricultural needs.

Known local phosphate resources in Zambia include Mumbwa, Chilembwe, Nkombwa Hill, and Kaluwe phosphate deposits. Chilembwe phosphate deposit is currently the most promising for possible exploitation. Local phosphate resources could partially substitute the imported fertilizers and provide the low-resource farmers in the country with inexpensive phosphate fertilizers. These local phosphate resources are of igneous origin, thus, are not reactive and therefore can not be applied directly for crop production [Phiri et al, 1991]. The International Fertilizer Development Center (IFDC) based in Alabama USA (IFDC, 1984, IFDC, 1986) has tested and recommended the use of Partially Acidulated Phosphate Rock (PAPR) as the best agronomically effective source of phosphorus from indigenous phosphate deposits in developing countries. The production of PAPR requires only a fraction (usually 50%) of the acid needed to produce Single Super-Phosphate (SSP) or Triple Super-Phosphate (TSP). This makes PAPR to cost less than SSP and TSP in terms of acid consumption. PAPR is suitable to acidic soils and it provides sulphur as an additional nutrient.

Early research on local phosphate resources in Zambia was for establishing beneficiation routes aimed at producing concentrates suitable for use in superphosphate production [JICA,1985, Lombe, 1985, Lukomona, 1989, Simukanga, 1986]. However, recent research has focused on the production and utilization of PAPR using Chilembwe phosphate rock. For example, in the 1990/91 planting season, the Mineral Exploration Department (MINEX) and the University of Zambia (UNZA) School of Mines produced PAPR using Chilembwe phosphate rock. Field tests on various food crops in the high rainfall zones of Zambia showed that PAPR was as agronomically effective as the imported superphosphates, SSP and TSP [Goma et al, 1991, Damaseke et al, 1993]. To enhance research in the development and use of local phosphate resources in Zambia, a PAPR pilot-plant was installed in the School of Mines in 1994.

The conventional method of producing partially acidulated phosphate rock (PAPR) is by the Run-of-Pile (ROP) Process [IFDC, 1986]. In the ROP Process, phosphate rock, acid and water are fed into a mixer (usually a pugmill type) where they are mixed rapidly for 30 to 60 seconds retention time. The slurry from the mixer is discharged into a den (batch or continuous type) and stored for a short time. The material from the den is stored and cured for 2 to 4 weeks to allow the reactions to approach completion. After the curing period the material is crushed, screened to pass a 4mm screen then bagged and shipped. A granular product can be produced by granulating the previously prepared ROP PAPR product using steam or water in a separate step. However, the ROP Process suffers from the following disadvantages [IFDC, 1986]:

(1) The product is not ready for use for several weeks after its production requiring more storage space and several additional handling steps to make a finished product and this adds to the production costs.

(2) The process is suitable for rocks that are relatively reactive and low in iron and aluminium oxide and other impurities.

The IFDC has recently developed a new process for producing granular PAPR which is known as Single-Step Acidulation / Granulation (SSAG) Process [IFDC, 1984, IFDC, 1986, IFDC, 1988]. The process has the following advantages over the conventional ROP Process:

(1) Suitability for relatively unreactive rocks high in iron and aluminium oxides. This is achieved through proper control of acidulation conditions resulting in selective attack on calcium phosphate to

minimize dissolution of undesirable iron and aluminium impurities in the rock. This results in a product with a desirable level of plant available phosphorus, low in free acid content, and with good physical properties (i.e. non –sticky and free flowing).

(2) Selectivity of acidulation to form available phosphate is improved, especially at high acidulation levels, by substituting part of the H_2SO_4 with HNO_3 or by addition of KCl or NaCl to the phosphate rock prior to or during acidulation. Since denning and curing stages are eliminated handling costs are reduced.

In the SSAG Process ground phosphate rock, acid, water, and recycle (undersize material from the screens) are fed continuously to a rotary drum type granulator. The granular product from the granulator enters the rotary kiln dryer for immediate drying. The dryer discharge is screened to yield a product 1 – 4 mm size range. The oversize fraction is crushed and sent back to the oversize screen whilst the undersize is sent to a product screen. The undersize together with part of the oversize from the product screen are recycled back to the granulator. The granular product is bagged and shipped.

The percentage of available P_2O_5 in PAPR is affected by process variables namely, reactivity of the rock, degree of acidulation, retention time, acid concentration, process temperature profile, and particle size of the phosphate rock. The extent to which the process variables affect the chemical and physical properties of PAPR products depends significantly on the type, origin and mineralogical composition of the phosphate rock being treated [IFDC, 1986].

This work involved the characterization of Chilembwe phosphate rock, optimization of process variables, modelling of comminution as well as granulation processes and economic evaluation of a commercial scale PAPR project.

Characterization of Chilembwe phosphate rock employed various techniques including, ore microscopy, X-ray diffraction, Atomic Absorption Spectrometer, UV spectrometer. Size-sorting assays supported by observations of thin sections under the microscope determined the liberation size for the apatite grains from the rock matrix.

Process variables studied in this work included particle size distribution of the rock, degree of acidulation, acid concentration, initial temperature of phosphate rock, water, and acid mixture, drying temperature and retention time in the granulator. The study has established the relationship between each of the variables and the amount of available P_2O_5 in PAPR when using Chilembwe phosphate rock under the specified conditions.

Conventional comminution techniques played an important role in the liberation of the apatite grains from the rock matrix before the material could be used as feed to the PAPR pilot-plant. This necessitated modelling of the closed comminution circuit in order to attain the economic utilization of the main unit in the circuit, the ball mill. Faults in the comminuting unit could adversely affect the economics of grinding. In this respect, a selective recycle model was used to diagnose faults in a ball mill in a closed comminution circuit during the grinding of the phosphate rock in order to improve its operating conditions. The same model was used to improve the operating conditions in the granulator. In both cases, tracers were used to obtain experimental RTD curves. The experimental RTD curves were thereafter simulated using the selective recycle model. This simulation gave parameters for the Number of Cycles Distribution (NCD) that indicated the mass of tracer leaving the system at a particular number of cycles providing a possibility to select the best operation conditions.

An economic evaluation to assess the viability of a 30 metric tonne per hour commercial PAPR Process for an initial period of 15 years of operation was also carried out in this work. The Net Present Value and Benefit – Cost ratio have been applied in the analysis that has given a competitive price of PAPR in Petauke (close to the Chilembwe Phosphate deposit) with extrapolations to other districts and towns in Zambia taking into account transportation costs.

Field tests aimed at assessing the agronomic effectiveness of the PAPR produced in the School of Mines have been conducted by the School of Agricultural Sciences for two consecutive planting seasons, 2000/2001 and

2001/2002. The results of these tests have been appended in order to show PAPR's performance compared to the imported Mono-Ammonium Phosphate (MAP).

CHAPTER 1

LITERATURE REVIEW

1.1 Population and food

Zambia has experienced a rapid population growth since 1950. The World Population Prospects [1996] has shown that the population of Zambia grew from 3.141 million in 1960 to an estimated 8.081 million in 1995 and the 2000 census has estimated Zambia's population at 10million. Population growth consequently demands a somewhat marched growth in agricultural output in order to meet the rising demand for food and other agricultural commodities. Like many countries in sub-Saharan Africa, Zambia currently experiences high levels of hunger and poverty primarily due to low production of food crops caused by poor yields.

1.2 Copper mining

Zambia's economy since independence in 1964 relies heavily on copper mining. However, there has been a progressive decline of copper production over the years from above 700000 metric tonnes in 1968 to below 400000 metric tonnes in 1998 [Bank of Zambia, 1978 and 1998, Economic Report, 1973 and 1997, Monthly Digest of Statistics, 1991]. The decline of copper production and the servicing of the huge external debt (US$7 billion) have reduced national income resulting in an increase in poverty.

1.3 Agriculture

The agricultural sector's potential to contribute to the economic growth of the country has remained largely untapped. Nevertheless, agriculture, forestry, and fishing are the largest contributors to Gross Domestic Product (GDP) in Zambia. According to the Economic Report [1997] agriculture, forestry and fishing made a total contribution of 17.2% to GDP in 1996 and 16.0% in 1997.

1.4 Soil fertility

Kang [1985] and Ssali et al [1985] have all reported that phosphorus is generally the most limiting nutrient element after nitrogen in Tropical Africa. In many cases were soils had adequate organic matter levels (and hence, soil nitrogen) phosphorus was found as the limiting nutrient. Although the total amount of phosphorus in tropical soils is variable, African soils generally are highly weathered with low total phosphorus. In addition, many soils sorb phosphorus from the soil solution and thus render it less available for plant uptake (phosphorus fixation). The magnitude of phosphorus fixation is related to pH, the iron and aluminium oxides in the soil, and the exchangeable aluminium. Thus, highly acidic and weathered clayey soils usually have high phosphorus fixation capacities due to their high amorphous oxide (including allophane) contents.

Kang [1985] further reported that large areas of humid and sub-humid tropical Africa are dominated by low-activity clay soils consisting of mainly alfisols and ultisols. These soils have major constraints for intensive and continuous arable crop production. Tropical farmers traditionally practice shifting cultivation and rely on the fallow period for restoring the soil fertility, which is exhausted during the short cropping cycle. However, shifting cultivation has never really solved the phosphorus problems in traditional agricultural systems but only helps farmers to maintain stable (but low) levels of productivity and avoid serious soil erosion. Population and urbanization pressures have been forcing traditional farmers away from traditional shifting cultivation of 6 to 15 fallow years to agricultural systems where the cropping cycles have become more frequent.

Phiri et al [1993] have reported that soils in the high rainfall zone of Zambia, namely Northern, Luapula, North Western and Copperbelt Provinces, known as region III, are inherently deficient in phosphorus, an essential element in plant growth.

Rainfall statistics show that Lusaka, Central, Eastern, Western, and Southern Provinces of Zambia generally receive annual rainfall of less than 1000mm and sometimes experience droughts. However, Northern, Luapula, North Western and Copperbelt Provinces always receive enough tropical rainfall of more than 1000mm annually (Table 1.1) [Economic Report, 1983]. The rain season starts in October and ends in April. Soils in the high rainfall region are acidic, highly weathered, clayey and have a high phosphorus fixing capacity. These soils produce high crop yields when phosphorus is used. Bunyolo [1991] reported that in all long-term trials with maize, in Central, Southern, Western, and Northern Provinces, significantly high yields were obtained only when phosphate fertilizer was applied together with other nutrients.

Table 1.1. Long term average rainfall (mm) between 1940 and 1970.

Province	Station	Oct	Nov	Dec	Jan	Feb	Mar	Apr	Total
Central	Kabwe	20	97	241	256	189	125	22	950
	Serenje	11	138	279	239	290	159	30	1146
Copper-belt	Ndola	18	130	279	306	243	178	38	1192
Eastern	Chipata	0	92	215	257	231	153	49	997
	Lundazi	8	65	191	218	196	156	27	861
Luapula	Mansa	37	167	282	256	217	187	48	1194
	Kawam-bwa	76	178	236	211	200	224	118	1243
Lusaka	Inter-Airport	0*	117*	33*	433*	251*	35*	18*	887*
Northern	Mpika	5	94	235	276	224	186	26	1046
	Kasama	21	148	265	278	231	244	69	1256
North-Western	Mwini-lunga	93	216	254	235	207	256	83	1344
	Zambezi	43	130	212	219	202	150	29	985
Southern	Living-stone	23	79	169	177	160	85	23	716
	Choma	22	91	208	199	183	79	22	804
Western	Mongu	27	121	211	221	217	146	45	988
	Kaoma	26	115	218	223	202	119	25	928

*Only 1992 figures. *Data source: Economic Report [1983].*

1.5 Fertilizer utilization in Zambia

1.5.1 Production

In Zambia, fertilizer is produced by the Nitrogen Chemicals of Zambia (NCZ). The NCZ plant produces ammonium nitrate from primary materials. The process involves the reaction of atmospheric nitrogen with hydrogen to produce ammonia. The hydrogen used in this process is produced by gassification of coal using steam. Part of the ammonia is oxidized with air to form nitric acid. Nitric acid and ammonia are reacted to form ammonium nitrate fertilizer.

To produce mixed fertilizers (i.e. compound fertilizers containing Nitrogen, Phosphorus and Potassium), imported superphosphates such as mono-ammonium phosphate or di-ammonium phosphate and potassium chloride are used to blend with the locally produced ammonium nitrate. At full capacity, the plant output of fertilizer exceeds 300,000 MT per annum, well above the country's requirements of about 200,000 MT per annum. The excess fertilizer is exported to Malawi and Congo D.R. In recent years, however, production has declined due to insufficient operating capital, aged infrastructure and machinery. This has forced government to import much of the fertilizer.

1.5.2 Marketing and distribution

Government is the major importer of fertilizer but the private sector also imports some fertilizer. Fertilizer importation has two main disadvantages in Zambia; firstly, a substantial amount of foreign exchange is required. Statistics (Table 1.2) show an increasing trend in the foreign exchange spent on fertilizer imports over the period 1992 to 1996. The other common problem is late delivery of fertilizers, which has an adverse effect on crop production. For example, maize production in the 1996 / 97 growing season was 31.9% less than that in the 1995 / 96 growing season. One of the main reasons given for the drastic drop was the late delivery of fertilizers [Economic report, 1997].

Table 1.2. Fertilizer imports for 1992-1996.

Year	US$'Million
1992	48.0
1993	69.7
1994	71.8
1995	79.7
1996	80.0

Data source: Economic Report [1997].

The fertilizer marketing policy changes with the wish of the government of the day. The 1992 policy removed subsidies and involved private traders without restrictions whereby traders determine their own prices according to the costs. This planting season (2002/2003), the bulk of the fertilizer is being distributed by the government. This is aimed at boosting crop production following the devastating impact of the 2001/2002 drought, which left many areas of the country in a hunger situation.

Of the ten provinces in Zambia, the Eastern, Southern, and Central Provinces account for about 65% of the total fertilizer use while Lusaka and Northern Provinces account for most of the balance. Fertilizer use in Zambia is seasonal and coincides with the rainfall pattern. With the rain season starting in October and ending in April, most fertilizer is applied in late November and early December. Maize is the major crop planted and accounts for 70% of the fertilizer used [Msiska, 1993].

Fertilizer distribution is according to the demand forecasted by national fertilizer committee, by region and by district. In recent years, in the nineties, there has been no capacity to distribute fertilizers to many areas of Zambia before the beginning of the planting season. This has often resulted in fertilizers either not being available in many areas or arriving late. Ideally, distribution must be done before the planting season or throughout the year, this has not been the case. The current government wishes to make fertilizers available to the farmers throughout the year as opposed to bringing the commodity when the planting season for maize begins.

1.5.3 Phosphate consumption

There has been a general decline in the consumption of phosphate in Zambia (Figure 1.1) from about 24,000 metric tonnes in 1987/88 to less than 15,000 metric tonnes in 1998/99.

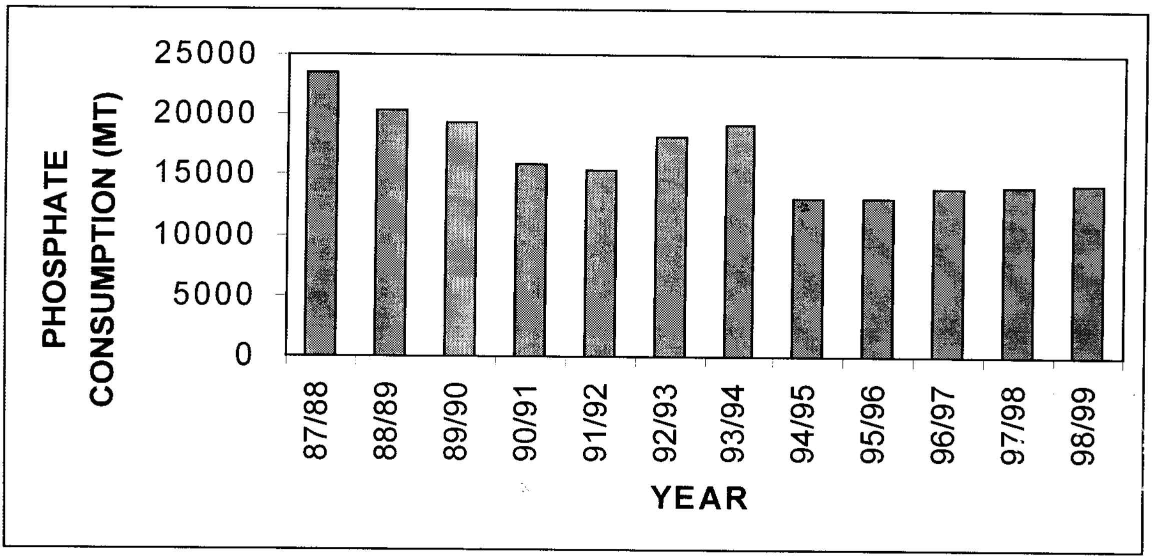

Figure 1.1. Phosphate (P_2O_5) consumption in Zambia for the period 1988/89 to 1998/99.

During the same period, South Africa's phosphate consumption was more than 10 times that of Zambia while Zimbabwe also consumed more than 2 times the amount consumed in Zambia [FAO, 1999].

1.6 Zambia's indigenous phosphate resources

Although Zambia relies entirely on imported phosphate fertilizers for its phosphorus needs indigenous phosphate deposits exist in the country at Chilembwe, Mumbwa, Nkombwa and Kaluwe. Although they may not completely substitute the imported phosphate fertilizers indigenous resources could be an important source of cheaper phosphate fertilizer for the resource poor farmers in the country and this could result in substantial savings in foreign exchange. Improving agricultural output is very vital to poverty reduction, creation of employment in agricultural related industries and stimulation of economic and industrial growth - which could be of great benefit to both rural and urban areas.

1.6.1 Distribution of phosphate deposits in Zambia

Tether and Money [1991], Sliwa [1991], and Mulela [1991] have reviewed the distribution and geology of phosphate deposits in Zambia. Figure 1.2 shows the location of phosphate deposits in Zambia. Three types of igneous deposits in Zambia are known; syenite-related, carbonatite-related, and supergene-enriched zone-related deposits. The supergene-enriched related deposits are associated with both syenite and carbonatite related deposits. Cabonatite – related phosphates are found at Kaluwe (Central Zambia) and Nkombwa Hill (Northern

Zambia). Syenite – related phosphates are located in Chilembwe area (Eastern Zambia) and north of Mumbwa in central Zambia. The syenite – related deposits in both cases are located with syenite bodies bordering large granite batholiths.

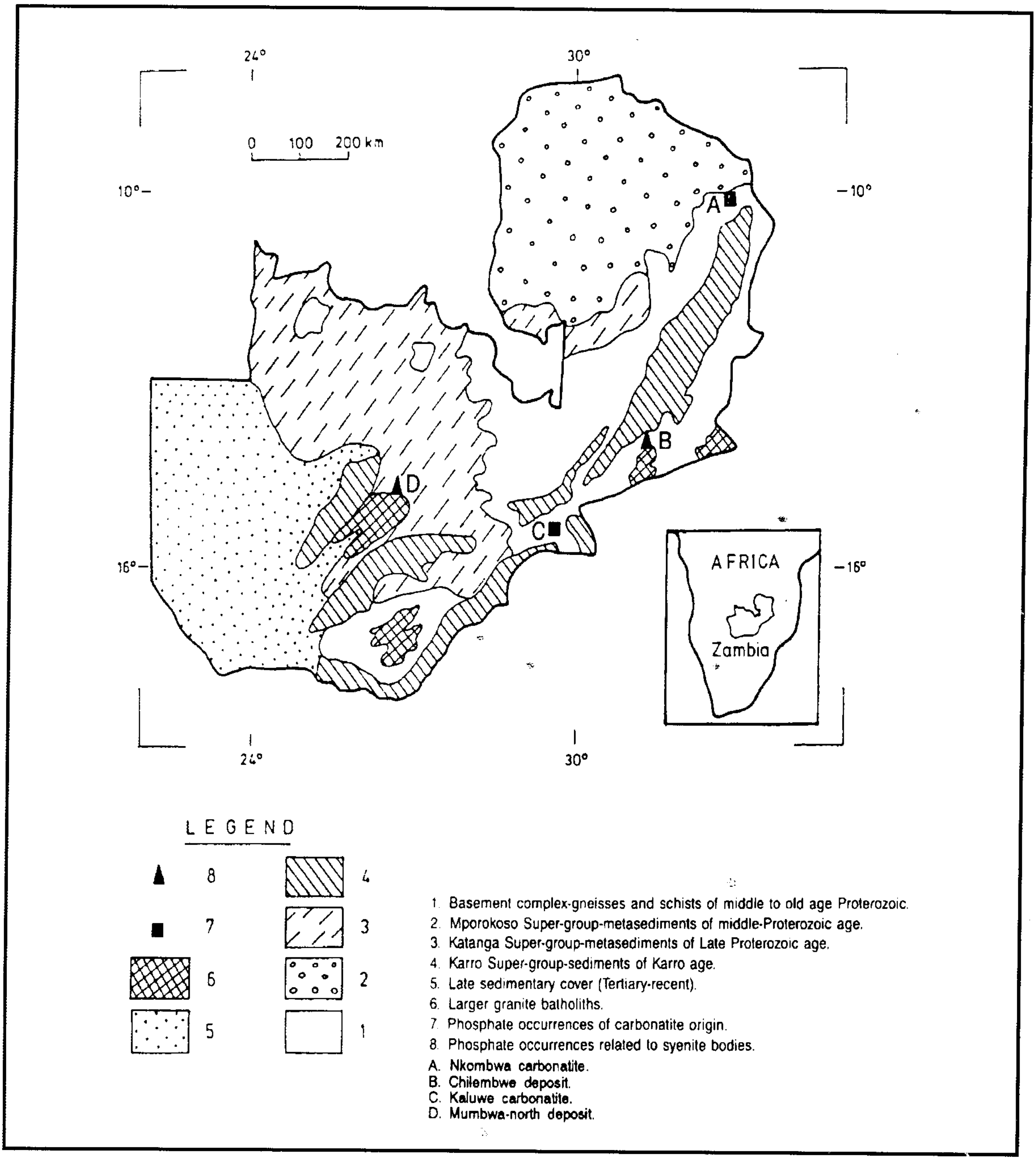

Figure 1.2. Location of phosphate deposits in Zambia. *Source: Sliwa [1991].*

1.6.2 Chilembwe phosphate deposit

Chilembwe phosphate deposit is located north of Sinda about 460 km east of Lusaka in the Eastern Province. Mineral Exploration Department (MINEX) discovered the deposit in 1978 and named it after a local village called Chilembwe at the time. The Japanese International Cooperation Agency (JICA) [1985] reported that most of the area is underlain by syenite and monzonite rocks which intruded into the Lusandwa Group of the Muva System. The syenites, in association with large granite, form a part of Sinda Batholith. The Lusandwa Group comprises concordant gneisses and associated metasediments in Chindeni Mobil Belt that trends north-northeast. All of these rocks are of the Precambrian age.

The area has been a subject of detailed geochemical, geophysical, and geological investigations. Mulela [1991] has reported that the area consists of five irregular ore bodies within a 4km radius in coarse-to-medium grained syenites on the northern margin of sinda batholith. Of the five ore bodies the two largest ones have been studied and evaluated. These are ore bodies No.2 and No.4. Orebody No.2 is the largest with reserves estimated at 1.4 million tonnes at 12% P_2O_5. The mineralized rock is composed of apatite and quartz with subordinate amounts of K-feldspar, biotite, amphibole (hornblende), and traces of pyroxenes.

Orebody No.4 is relatively small with reserves estimated at 220 000 tonnes at 9.9% P_2O_5. The ore comprises coarse – grained apatite with augite or hornblende as the second dominant mineral and subordinate biotite and feldspar. The apatite exists as hydroxy-fluorapatite, with some hydroxy chloroapatite occurring in the second (No.4) type bodies. Total reserves for the two orebodies have been estimated at 1.64 million tonnes at 11.8% P_2O_5 grade, mining, and dilution included. JICA [1985] used 6% P_2O_5 as the cut-of-grade in their pre-feasibility study to recover 35 000 tons per year concentrate at 30% P_2O_5 over a period of 14 years.

Chilembwe samples have been a subject of petrographic and mineralogical examination both locally and abroad. Van Kauwenbergh [1991]. studied Chilembwe phosphate rock samples by petrographic and mineralogical examination methods. He reported that the Chilembwe deposit could be of metasedimentary origin and could represent Xenolithic bodies with intrusive syenite mass as suggested by the texture, rather than intrusions in syenite country rock as was suggested by other researchers. Chlorine content in the sample from orebody No.2 averaged 735 ppm whilst that in samples from orebody No.4 averaged 4200ppm. Van Kauwenbergh observed that the chlorine content of the apatite in Chilembwe samples was above the limit for the wet-process phosphoric acid as corrosion problems could be severe at concentrations above 200 to 300 ppm.

1.6.3 Beneficiation tests for Chilembwe phosphate ore

Lombe [1985, 1991] undertook beneficiation studies for Chilembwe phosphate ore. Tables 1.3 and 1.4 show the chemical and mineralogical composition of Chilembwe phosphate ore samples used in the study.

Table 1.3. Chemical and mineralogical composition for No. 2 orebody of Chilembwe phosphate ore.

Chemical composition		Mineralogical composition		Approximate grain size	
P_2O_5	24.8%	Apatite	55.6%	Apatite	700 μm
CaO	27.4%	Quartz / feldspar	36.3%	Quartz	0.2 - 1.2 mm
MgO	2.0%	Hornblende	6.5%	Hornblende	0.4 - 1.5 mm
Al_2O_3	2.8%	Sphene	1.1%		
Fe_2O_3	1.1%	Pyroxene	0.15%	No inclusions or complex	
MnO	0.08%	Opaques	0.4%	intergrowths.	
SiO_2	53.2%				

Data source: Lombe [1991].

Table 1.4. Chemical and mineralogical composition for No.4 orebody of Chilembwe phosphate ore.

Chemical composition		Mineralogical composition		Approximate grain size	
P_2O_5	12.9%	Apatite	25.7%	Apatite	425 μm
CaO	21.8%	Hornblende/pyroxene	71%	Hornblende/pyroxene	0.4-2mm
MgO	3.0%	Biotite	1.1%		
Al_2O_3	6.8%	Fieldspar	1.4%		
Fe_2O_3	9.2%	Opaques	0.6%	Little or no intergrowths	
MnO	0.3%				
SiO_2	47.1%				

Data source: Lombe [1991].

By microscopic examination of the sample and size-sorting assays, Lombe reported that the bulk of the apatite was concentrated in the size range 850 – 212μm; and that substantial liberation of apatite was achievable below 850μm. A shaking table was successfully applied in the size range 212 - 600μm to produce a concentrate of 34% P_2O_5 grade at 70% recovery in a single pass. The concentrate was upgraded to at least 36% P_2O_5 in a cleaning stage whilst recovery was increased to 80% by recycling the initial tailings. Jigging did not yield comparable results due to its low concentration criterion.

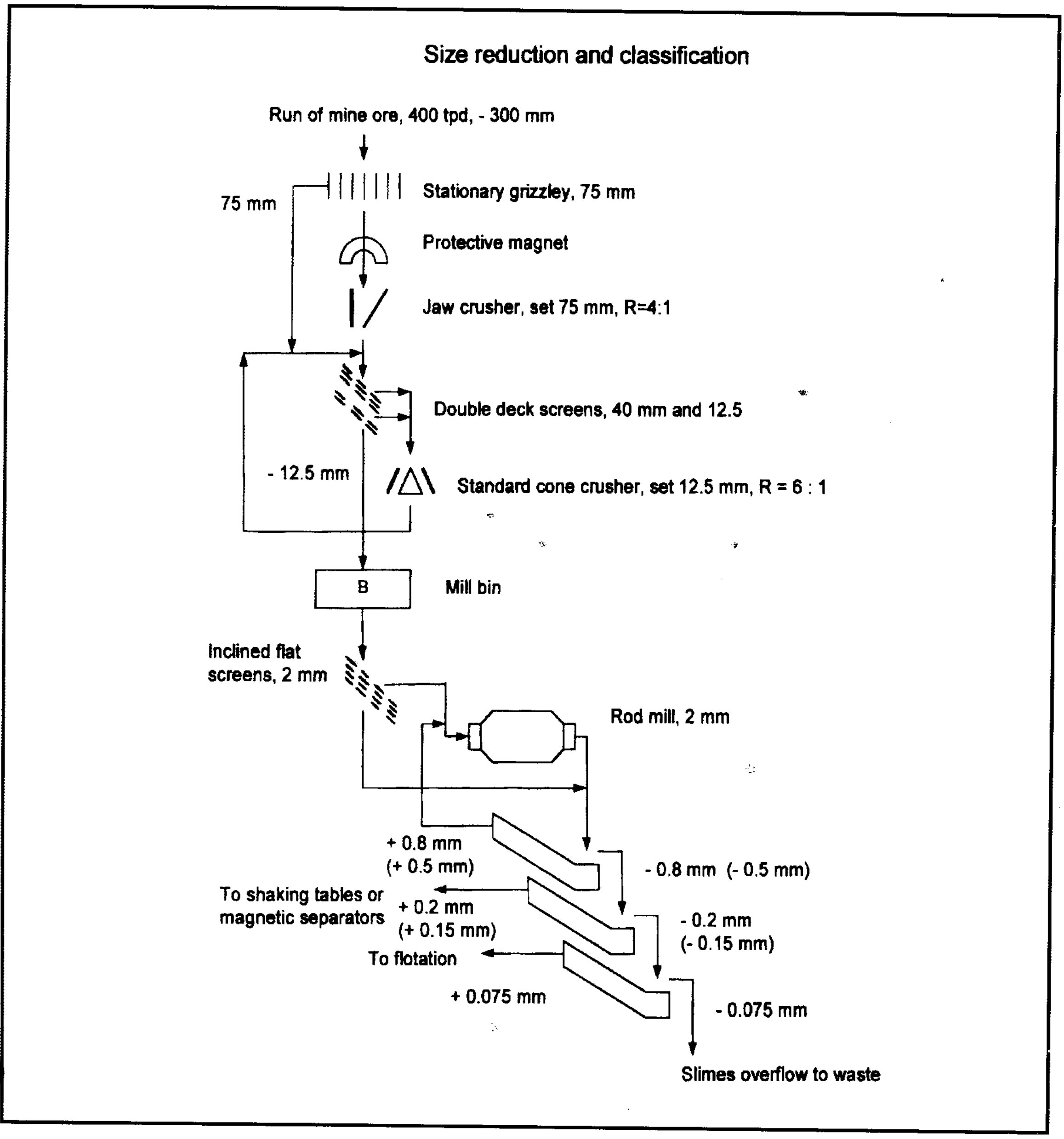

Figure 1.3. Proposed flowsheet for the beneficiation of Chilembwe phophate rock.
Source: Lombe [1985].

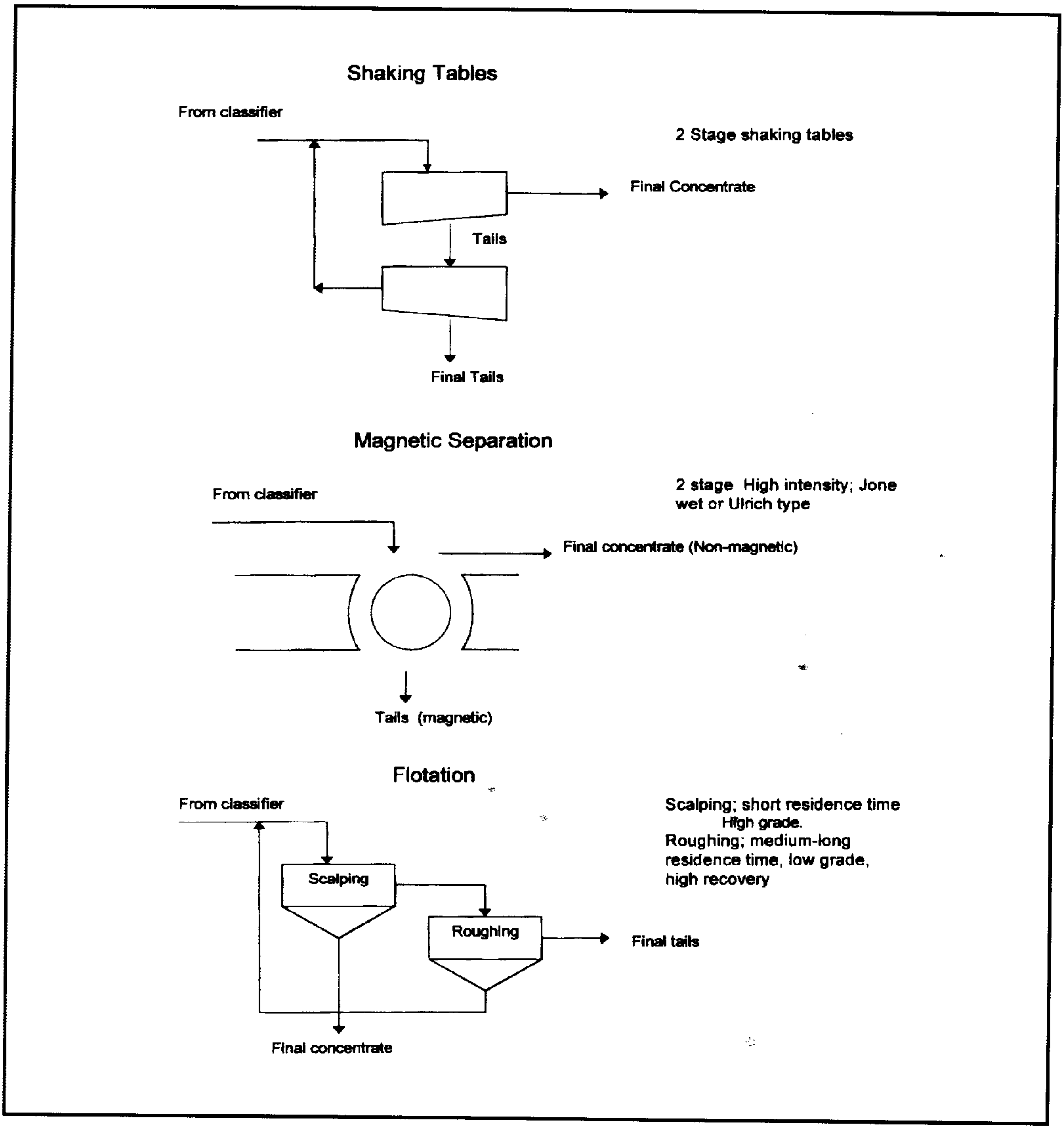

Figure 1.3. Continued.

The fraction finer than 212μm (about 30% of the ore) was successfully treated by apatite flotation with a fatty acid at alkaline pH and a petroleum sulphonate at acidic pH where the surface charge on the mineral was less negative. In both cases recoveries of at least 85% and grades with a minimum content of 33% P_2O_5 were obtained. For orebody No.4 the apatite was found to be substantially liberated below 425μm. Since the apatite and hornblende could not be separated by gravity due to similarities in densities, magnetic separation of the minerals was successfully employed in the size range 150 - 425μm which yielded a concentrate containing at least 36% P_2O_5 at about 80% recovery. The finer size fractions (i.e. 75 - 150μm) were treated by flotation in a similar manner as described for orebody No.2. In both cases grades of at least 36% P_2O_5 and recoveries of at least 85% were obtained for both orebodies No.2 and No.4. A beneficiation flowsheet (Figure 1.3) involving crushing, grinding, magnetic separation, gravity separation (shaking tables) and flotation was proposed. Only a small proportion of the ore needed concentration by costly flotation. Lombe [1991] suggested an alternative to flotation involving mixing of fines with concentrates from magnetic separation and shaking table and the material processed into a product such as PAPR fertilizer.

Simukanga et al [1991] reported that the bulk of the apatite mineral is concentrated in the size between 212 to 600μm and 106 to 425μm for orebodies No.2 and No.4 respectively. They also observed that the bulk of the gangue minerals (i.e. quartz and amphibole) are in the coarse size (above 425μm). Due to preferential grinding; apatite from orebodies No.2 and No.4 was found to be completely liberated below 600μm and 425μm respectively. These results confirmed Lombe's earlier observations already discussed in the above text.

JICA [1985] conducted beneficiation tests on Chilembwe phosphate ore in an attempt to upgrade the ore for use in the production of fused magnesium phosphate (FMP). These workers used combined samples from No.2 and No.4 orebodies (composite assay was 11.8% P_2O_5) in the tests. They initially screened the sample on a 48mesh sieve and then successfully treated the under size fraction (i.e. minus 48mesh size) by flotation using anionic phosphate collector, Keno-gard (Lila flot OS#100). The overall flotation test results gave a concentrate of grade 30% P_2O_5 at a recovery of 88.4% including slimes flotation. Heavy media separation did not yield comparable results.

1.7 Previous research on the utilization of Zambia's phosphate resources

In Zambia research aimed at utilizing local phosphate deposits as a source of fertilizer started in 1991 at The University of Zambia (UNZA) School of Mines and Mineral Exploration Department (MINEX). Before then research by Lombe [1985], Lukomona [1989] and Simukanga [1986] had been focused on beneficiating the ores to upgrade their P_2O_5 contents in order to produce a concentrate suitable for producing superphosphate fertilizers. A pre-feasibility study by the Japan International Cooperation Agency [JICA, 1985] involving the development the phosphate project at Chilembwe indicated that a marginal profit can be expected on a private mining enterprise. Moreover, the establishment of apatite mining required the existence of a phosphatic fertilizer plant in the country.

1.7.1 Direct application of ground phosphate rock

The cost of soluble (superphosphate) fertilizers is generally high making them expensive for low-resource farmers in developing tropical countries. Finely ground highly reactive phosphate rock (PR) has been used as a direct application fertilizer in some tropical countries [Roy and McClellan, 1985]. Technically the process of producing ground phosphate rock is simple, with the run-of-mine ore being crushed, ground, screened and applied directly into the field. The agronomic effectiveness of phosphate rock for direct application is largely influenced by its reactivity. Highly reactive rocks are more agronomically effective than less reactive ones. Sedimentary rocks tend to show a higher reactivity than igneous rocks. Rock reactivity depends on physical-chemical composition of the rock, crystalline structure, degree of carbonate substitution in the apatite structure, and association of other nutrients. The advantages of using ground phosphate rock as a direct application fertilizer are:

- low capital cost
- low energy requirements – about one third that for TSP
- use of rocks unsuitable for other types of processing
- production costs that are not too sensitive to economy of scale
- quick way of building a phosphate industry in a developing country.

The main disadvantages are that:

- unreactive rocks can not be used
- agronomic value can not be predicted
- limited to acidic soils

- a relatively low P_2O_5 compared to TSP
- handling problems due to dust. The dust problem can be overcome by granulation. The IFDC has developed a method of granulating ground phosphate rock into mini-granules using a binder [Phosphorus and Potassium, 1986].

In an effort to provide a cheaper source of P fertilizer to resource poor farmers in Zambia finely ground phosphate rocks from Mumbwa and Chilembwe with 28.0% and 15.2% total P_2O_5 and 1.0% and 1.3% citrate-soluble P_2O_5 respectively were tested for direct application. Agronomic tests on various crops, namely maize, groundnuts, beans, soya beans and sunflower were conducted between 1980 and 1991 in the high rainfall region III of Zambia. However, results showed that these phosphate rocks were not agronomically effective for direct application [Phiri et al, 1991 and 1993]. Mumbwa and Chilembwe phosphate rocks are of igneous origin and therefore are low in reactivity [Roy and McClellan, 1985].

1.7.2 Partially Acidulated Phosphate Rock (PAPR)

Partial acidulation of phosphate rock represents the best means of producing an agronomically effective source of phosphate. The technology of partial acidulation involves reacting finely ground phosphate rock with only *a fraction* of the amount of acid required to fully convert the apatite in the rock to soluble form, monocalcium phosphate. On the other hand, the production of superphosphate involves the reaction of phosphate rock with the *total* amount of acid required to fully convert the apatite to monocalcium phosphate. Thus, the production of partially acidulated phosphate rock (PAPR) requires less acid than the production of single super phosphate (SSP) or triple super phosphate (TSP) which makes it cheaper than SSP or TSP. Rocks which are unsuitable for producing SSP or TSP due to high levels of impurities such as iron and aluminium oxides can be used for producing PAPR. In addition sulphuric acid based PAPR also provides sulphur as one of the nutrients. In agronomy, PAPR provides a portion of P in a readily soluble form and the remainder in a residual form [IFDC, 1988]. This characteristic is desirable in the high rainfall zones where leaching is rapid. PAPR products have better physical properties than superphosphates for bulk blending with urea [Chein and Hammond, 1989]. In some countries several variations of partial acidulation have been tried or proposed [Slack and Rindt, 1964]. These are practically aimed at making a product for direct application rather than ammoniation. A partially acidulated superphosphate called "Kotka phosphate" is made in Finland by supplying about 10% of the P_2O_5 in the product as finely ground Morrocan rock, added to the conveyor belt as it leaves the den. The material is then cured in a normal manner. The acid soils of Finland provide the conditions necessary for effective use of this product. In South Africa a mixture called "super and raw" is produced that contains about half its phosphate as unreacted rock. The product can be made either by mixing the rock and superphosphate or by using only half of the usual amount of acid in acidulation [Chein and Menon, 1989], [Chein et al, 1987], [Govere, 1993], [Menon et al, 1991], [Slack and Rindt, 1964]. No denning is required in producing partially acidulated phosphate rock and the product is sold by the ton without reference to phosphate solubility and is recommended for acidic soils.

The IFDC carried out characterization and partial acidulation tests on a Chilembwe phosphate rock sample. Before acidulation tests, the sample was beneficiated to reduce the silica content of the ore. Direct anionic phosphate flotation provided the best results yielding a concentrate of 29.7% P_2O_5 at 89.4% recovery whilst the silica was reduced from 40% to 17.55%. The concentrate was used to produce 25% and 50% granular sulphuric acid-based PAPR. The 50% PAPR contained 23.3% P_2O_5 and had physical characteristics which were comparable to granular SSP. The cost of producing run-of-pile SAB-PAPR was reported to be 10% less than the run-of-pile SSP production when brought under the same conditions. Agronomic tests on maize and sorghum yielded comparable results to fully acidulated products [Frederick, 1991].

In 1991, following the IFDC's work on partial acidulation of Chilembwe phosphate rock, test work for the production and use of PAPR in Zambia were started at MINEX and University of Zambia (UNZA), School of Mines through collaboration with the IFDC [Nkonde and Simukanga, 1994]. In the 1990 / 91 growing season 50% sulphuric acid based PAPR containing 12.6% P_2O_5 was produced at MINEX in a concrete mixer. Boulders of Chilembwe phosphate rock were crushed and ground to minus 75μm. Fine rock was introduced into a concrete mixer and a calculated amount of sulphuric acid for 50% acidulation was added to the rock. A mixing (rotation) time of 15 minutes was allowed after acid addition. The PAPR product was cured for 4 weeks on a concrete floor in an iron sheet housing. The analysis showed 11.3% water-soluble P_2O_5, 12.6% NAC-soluble P_2O_5, 7%S and pH 5.0 [Zambezi and Chipola, 1991].

1.7.3 Agronomic performance of PAPR

Phiri et al [1991] conducted field experiments with PAPR in the high rainfall zones of Zambia on Mufulira and Konkola soil series.

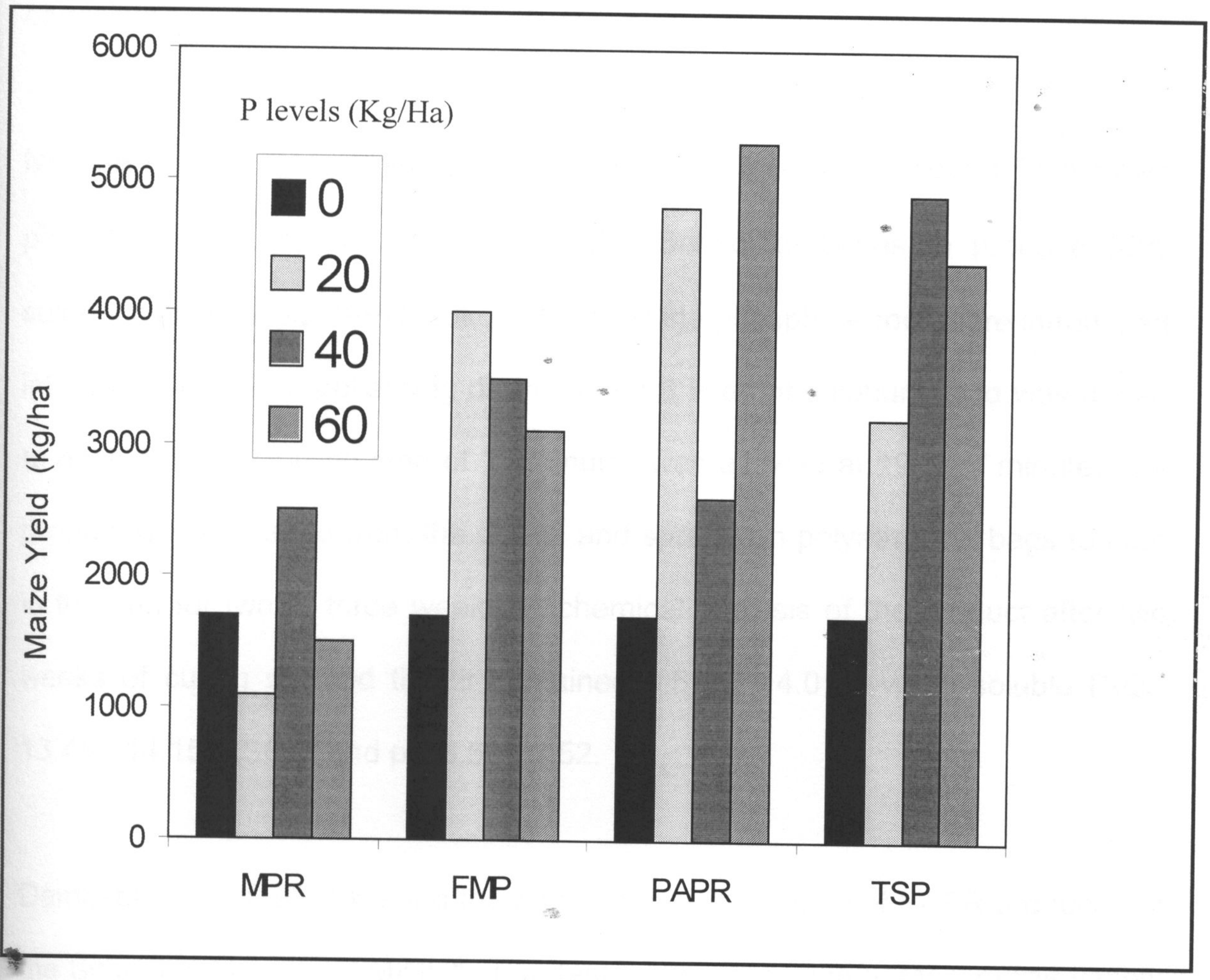

Figure 1.4. Maize yield under Mumbwa Phosphate Rock (MPR), Fused Magnesium Phosphate (FMP), Partially Acidulated Phosphate Rock (PAPR) and Triple Superphosphate (TSP) at different P levels on Konkola soil series. *Source: Phiri et al, [1993].*

They reported that in a highly P deficient and high P – fixing soil (e.g. Mufulira) PAPR was nearly as effective as TSP for maize and fingermillet crops but only half as effective for beans. Figure 1.4 shows some of the results of the tests on maize in which a comparison has been made using phosphate rock, fused magnesium phosphate, partially acidulated phosphate rock and triple superphosphate. These results support those of Hammond et al [1989] who earlier suggested that the maximum benefit from the use of PAPR for crop production, with respect to SSP, can be obtained on acid soils with high P-fixing capacity.

Nkonde et al [1991] carried out partial acidualtion of finely ground Chilembwe phosphate rock (minus 75μm) at UNZA, School of Mines to produce 50% sulphuric acid based PAPR. 10kg batches of the phosphate rock were introduced into each of the two pelletizing drums and 1.8 litres of sulphuric acid was added to each batch. A mixing time of 10 minutes was allowed at 19 rev / minute. The product was offloaded from the drums and spread on polyethylene bags to cure in the sun for two to three weeks. A chemical analysis of the product after two weeks of curing showed that it contained 3.51% - 4.01% water-soluble P_2O_5, 13.48 - 14.15% SO_4^{-2} and pH 3.58 - 3.52.

Damaseke et al [1993] studied the agronomic performance of PAPR produced at the School of Mines and MINEX. Two test crops were used namely maize variety (MM603) and soya beans variety (Santa Rosa). Three types of PAPR products were tested - University 50% sulphuric acid based PAPR (SAB PAPR-50) (processed by the School of Mines), MINEX SAB PAPR-50 (processed by MINEX), and nitric acid-based PAPR (HNO_3 – PAPR) processed by MINEX. From field test results it was concluded that all the sources; UNZA and MINEX processed PAPR were effective sources of phosphate which could supplement the conventional fertilizers on the market. Phiri et al [1993] also evaluated the agronomic performance of Chilembwe PAPR. Test crops included maize, finger millet, beans, soya beans, and groundnuts on acid (pH-$CaCl_2$ =4.2) Misamfu sandy loam, Mufulira mixed clay, Malashi clayey, and Maheba clayey soils with available P between 3 and 12 ppm (bray 1) and P-sorption ranging from low to very high across all soils. They reported that PAPR-50 was as agronomically effective as imported superphosphate fertilizer.

1.7.4 Preliminary financial evaluation for the production of PAPR at Chilembwe

Simukanga et al [1993] carried out a preliminary financial evaluation (Table 1.5) for producing PAPR from Chilembwe phosphate ore at 44,200 metric tonnes per annum. They compared the cost of producing PAPR at Chilembwe with the landed cost of TSP. TSP at Nitrogen Chemicals of Zambia (NCZ) in May 1993 cost US$284.55 / T and to this was added the cost of transporting TSP from NCZ to Chilembwe at US$45 / T which brought the total cost of TSP at Chilembwe to US$ 329.55 / T. The unit cost of P_2O_5 in TSP was US$ 7.01 / unit P_2O_5. The calculated unit cost of P_2O_5 in PAPR was US$ 6.48 / unit P_2O_5. It was found that the cost per unit P_2O_5 in PAPR was US$ 0.52 less than that of TSP despite an attempt to mechanize mining operations.

It was also noticed that the cost could be reduced if mining operations were made labour intensive. It was further found that a drastic reduction in the production cost per unit P_2O_5 in PAPR could be achieved by initially beneficiating the ore before partial acidulation.

Table 1.5. Summary of capital and operating costs for a 44,200 MT per annum PAPR project.

Life of plant = 5 years	**$ interest = 15%**	
	Cost/year (US$)	**Cost/T_{ore} (US$)**
Mining:		
Capital cost	43 055	0.97
Insurance, taxes and interest 15% of capital cost/year)	6 458	0.15
Operating cost	79 000	1.79
ROP-SAB PAPR PROCESS:		
Capital cost	15 790	0.30
Insurance, taxes and interest 15% of capital cost/year)	2 368	0.04
Operating cost	1 000 800	18.86
OTHER COSTS:		
Management	17 050	0.38
Bagging		9.80
Transport to Market		6.61
Total		38.9

Data source: Simukanga et al, [1993].

1.8 The Chemistry of partial acidulation

The chemistry of partial acidulation of phosphate rock is the same as that for complete acidulation to produce SSP or TSP [IFDC, 1986]. The water-soluble phosphate in PAPR, like in SSP and TSP, is monocalcium phosphate monohydrate. Other compounds present in the product include dicalcium phosphate dihydrate, calcium sulphate, calcium iron phosphate, calcium aluminium phosphate, and such inert materials as silica, fluosilicate salts, unreacted rock, organic matter, and phosphates of other metals present in the rock. Since apatite is the desired constituent of phosphate rock, the equation for using sulphuric acid may be written as:

$$\underset{\text{(fluorapatite)}}{Ca_{10}(PO_4)_6F_2} + \underset{\text{(sulphuric acid)}}{7yH_2SO_4} + \underset{\text{(water)}}{3yH_2O} = \underset{\text{(monocalcium phosphate)}}{3y\,Ca(H_2PO_4)_2.H_2O} +$$

$$\underset{\text{(calcium sulphate)}}{7yCaSO_4} + \underset{\text{(hydrofluoric acid)}}{2yHF} + \underset{\text{(fluorapatite)}}{(1\text{-}y)Ca_{10}(PO_4)_6F_2} \qquad (1.0)$$

where y represents the degree of acidulation. For example, y = 1.0 corresponds to 100% acidulation; y = 0.5 to 50% acidulation, and so on.

The above equation does not describe the complex chemistry involved in the reaction between phosphate rock and acid; it is a simplified model based on pure fluorapatite. In reality phosphate rock seldom contains pure fluorapatite and has other substitutions of CO_2, Na, Mg, Sr, Ba, Cl, OH, etc, in the apatite structure depending on the geological origin of the rock. It is difficult to judge with certainty how a particular phosphate rock will behave when treated with acid. The chemical transformation of the phosphate minerals in a rock during acidulation is usually affected by competing synergistic factors specific to each rock, including texture, surface area, and porosity, and the presence of associated compounds of calcium, iron, aluminium, magnesium, fluorine, and sulphur.

1.9 The partial acidulation of phosphate rock

1.9.1 The Run-Of-Pile (ROP) Process

The process of producing PAPR is similar to the conventional run-of-pile process (ROP) for SSP production [IFDC, 1986], [Slack and Rindt, 1964]. The run-of-pile (ROP) process is simple and involves three main steps, namely mixing, denning and curing (figure 1.7).

Mixing

The phosphate rock is mixed with acid (usually H_2SO_4) for a few minutes.

Denning

The slurry is discharged into a den where it is kept for few minutes to several hours.

Curing

The product is cured (stored) for 2 to 4 weeks to allow reactions to approach completion.

Granulation

The run-of-pile (ROP) PAPR product can be granulated if a granular product is needed.

1.9.2 The Run-Of-Pile (ROP) PAPR Process description

In the ROP Process (Figure 1.5), phosphate rock, acid and water are fed into a mixer (usually a pugmill type) where they are mixed rapidly for 30 to 60 seconds retention time. Rapid mixing and short retention time prevent agglomeration and caking of the material. The points of addition of rock, acid and water may be varied where necessary depending on process variables. The rotational speed of the mixer shafts and orientation of mixing paddles may be varied to achieve retention time for optimum mixing and reaction.

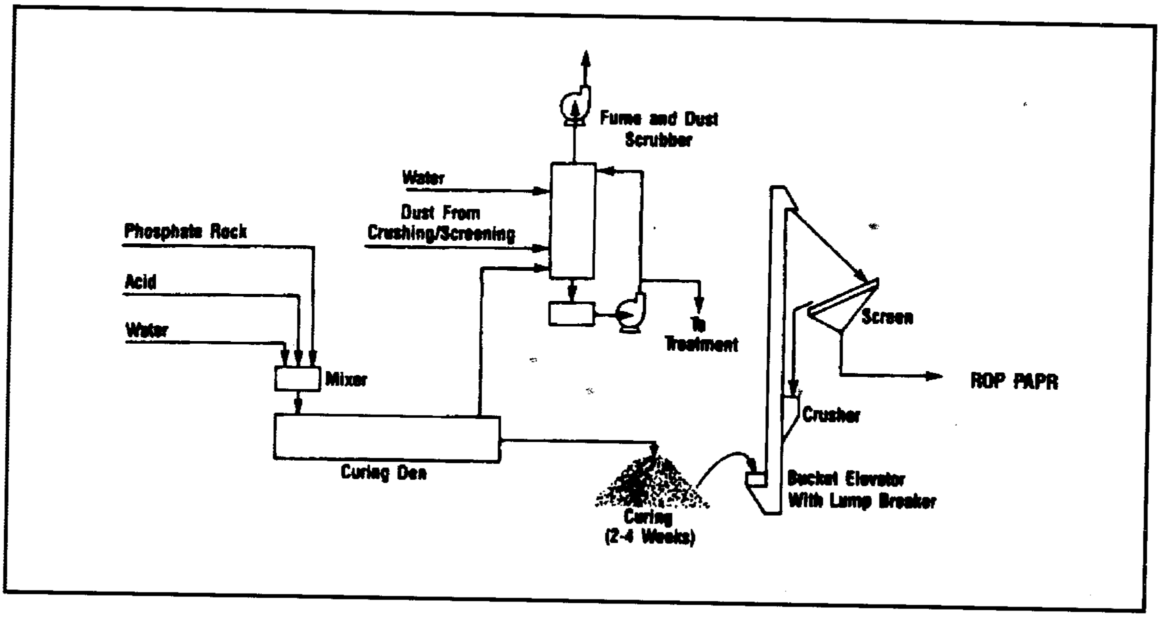

Figure 1.5. The Run-Of-Pile Process flowsheet for PAPR production. *Source: IFDC [1986].*

Other nutrients may be added to the mixer to improve acidulation or add nutrients to the product. The slurry from the mixer is discharged into a den (batch or continuous type) and stored for a short time. The material from the den is stored and cured for 2 to 4 weeks to allow the reactions to approach completion.

Depending on rock characteristics the material may be transferred straight to storage without denning. After the curing period the material is crushed, screened to pass a 4mm screen then bagged and shipped. A granular product can be produced by granulation of previously prepared ROP PAPR product using steam or water in a separate step.

1.9.3 Disadvantages of the ROP Process

The ROP PAPR Process has the following disadvantages:

(1) The product is not ready for use for several weeks after its production requiring more storage space and several additional handling steps to make a finished product and this adds to the production costs.

(3) The process is suitable for rocks that are relatively reactive and low in iron and aluminium oxide and other impurities.

1.9.4 The Single-Step Acidulation / Granulation (SSAG) Process

The IFDC has recently developed a new process for producing granular PAPR known as Single-Step Acidulation / Granulation (SSAG) Process (Figure 1.6) [IFDC, 1984] [IFDC, 1986] [IFDC, 1988]. In the SSAG process, ground phosphate rock, acid, water and recycle are fed continuously to a rotary drum type granulator. The recycle is the undersize material from the product screen. Typical recycle rate equivalent to a recycle-to-product ratio of about 2 is usually sufficient to maintain acceptable granulation. Different systems are used in addition of water and acid to the rolling bed of material in the drum. Retention time in the granulator depends on the degree of acidulation and rock composition. Typical retention time 5 – 8 minutes. The moist plastic material from the granulator is discharged into a co-current dryer. The drying temperature can be varied. Dust and gases are directed to a wet scrubber to remove fluorine and dust particles. The dryer discharge is screened to yield a product 1 – 4 mm size range. The oversize fraction is crushed and sent back to the oversize screen whilst the undersize is sent to a product screen. The undersize together with part of the oversize from the product screen are recycled back to the granulator. The granular product is bagged and shipped.

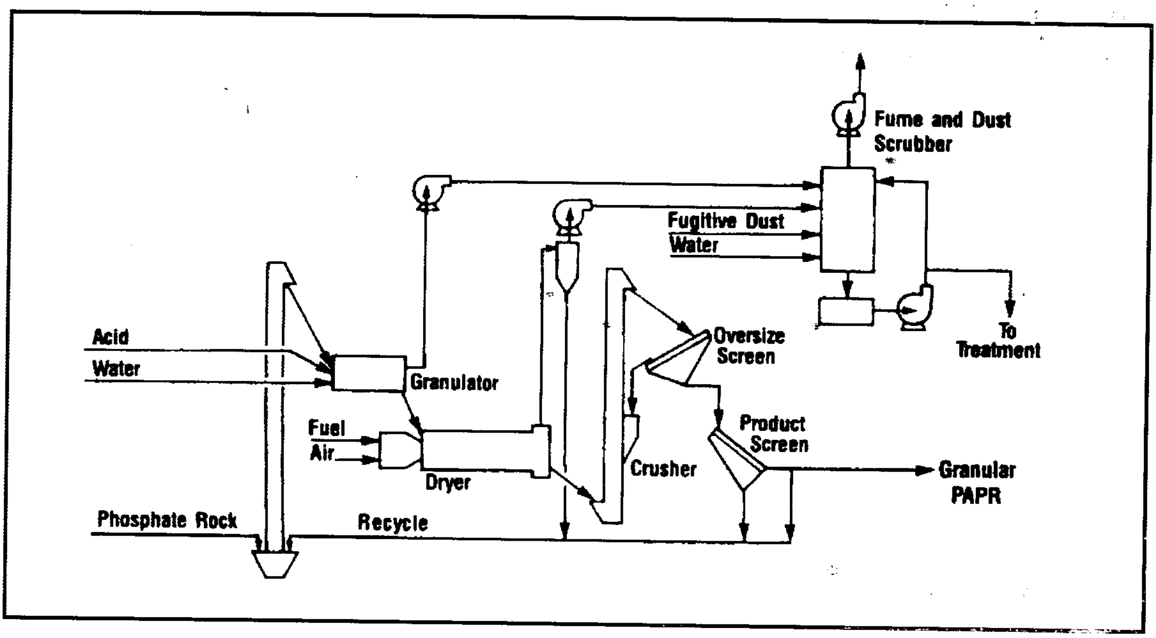

Figure 1.6. The Single-Step Acidulation / Granulator Process flowsheet for PAPR production. *Source: IFDC [1986].*

1.9.5 Advantages of the SSAG Process over the ROP Process

The process has many advantages over the conventional Run-Of-Pile Process including;

(1) Suitability for relatively unreactive rocks, high in iron and aluminium oxides. This can be achieved through proper control of acidulation conditions resulting in selective attack on calcium phosphate to minimize dissolution of undesirable iron and aluminium impurities in the rock. This results in a product with a desirable level of plant available phosphate, low in free acid content, and with good physical properties (i.e. non –sticky and free flowing)

(2) Selectivity of acidulation to form available phosphate is improved, especially at high acidulation levels, by substituting part of the H_2SO_4 with HNO_3 or by the addition of KCl or NaCl to the phosphate rock prior to or during acidulation. Denning and curing stages are eliminated resulting in reduced handling costs [IFDC, 1986].

1.10 Process variables

The process variables that affect the chemical and physical properties of PAPR fertilizer products are the following [IFDC, 1986]:

1) Rock reactivity
2) Particle size of the phosphate rock
3) Concentration of acid
4) Retention time
5) Degree of acidulation
6) Process temperature profile

1.10.1 Rock reactivity

The reactivity of a rock refers to the ease with which the phosphate can be converted to plant available form (by a chemical process or reaction in the soil) [Hatifield, 1964, IFDC, 1986]. It is an important factor influencing the agronomic effectiveness of the phosphate rock [Phosphorus and Potassium, 1987]. In the manufacture of superphosphate, an arbitrary scale of reactivity has been established using many properties of phosphate rock. Among them are specific surface, degrees of fluorination or carbonization, the rate of solution in dilute ammonium citrate or citric acid, the rate of solution in dilute phosphoric acid (38 percent H_3PO_4) and the agronomic response to the rock in a phosphorus deficient soil [Hatfield, 1964].

It has been established in tests with a number of phosphate rocks from South America, that reactivity depends on the origin of the rock [Phosphorus and Potassium, 1987]. Rocks of igneous and metamorphic origin tend to show the lowest solubility, while sedimentary phosphate rocks have a larger range of solubility in well established reagents such as neutral ammonium citrate and citric acid. Other factors influencing solubility include crystalline structure; degree of carbonate substitution in the apatite structure, association of other nutrients; and physical properties such as particle size, and porosity. It has been reported that with few exceptions, those rocks that display a high level of carbonate substitution within the apatite structure or have a high surface area are usually found to be the most reactive [Hatfield, 1964].

Particle size and surface area data for several phosphate rocks used in IFDC SAB-PAPR studies are shown in Table 1.6. It should be emphasized that a relatively large surface area does not always indicate a highly reactive rock. For example, the Kodjari (Burkina Faso) and Tilemsi Valley (Mali) phosphate rocks have a relatively high surface area (about $15m^2/g$ and $38m^2/g$, respectively). However, they are not highly reactive [IFDC, 1986]. In these examples most of the surface area is attributed to the clay particles (iron and aluminium compounds) in the rocks.

Table 1.6. Particle size and surface area data for selected phosphate rocks used in sulphuric acid based (SAB)-PAPR studies.

Phosphate rock source	Particle size		Average Particle Size	Median Particle size	Surface Area
	Passing 100 mesh %	Passing 200 mesh %			
Central Florida (USA)	99	95	14	25	13
Huila (Colombia)	93	80	12	24	6
Kodjari (Burkina Faso)	97	80	20	42	15
Medina Luna (Colombia)	92	77	12	28	6
Musoori (India)	92	77	14	32	2
Pesca (Colombia)	100	97	7	9	8
Tilemsi Valley (Mali)	100	96	13	6	38
Utah (USA)	91	77	28	63	3

Data source: IFDC [1986].

1.10.2 Particle size of phosphate rock

Results obtained by IFDC [1986] on laboratory scale performed on Hahotoe (Togo) and Pesca (Colombia) phosphate rocks considered to be low in reactivity showed that coarse material (65 - 80% passing 100 mesh and less than 50% passing 200 mesh) was difficult to process. The 35 –50% acidulated rock was extremely sticky and could not be properly granulated or dried because of an excessive amount of unreacted acid. When the rocks were finely ground (at least 80% passing 200 mesh), the problems of stickiness and high levels of unreacted acid were largely eliminated.

Table 1.7. Screen analysis of acidulation grades of Florida Land pebble.

Grade range BPL (percent)	Lots Analyzed (Number)	Fraction passing sieve 2		Fraction held on U.S. No. 35 sieve (Percent)
		U.S. No. 100 (Percent)	U.S. No. 200 (Percent)	
72 -75	3	74.5 – 75.2	51.9 – 52.8	0.4 – 5.4
68 – 77.5	5	78.6 – 84.7	57.0 – 66.3	0.4 – 2.5
72 – 75	4	89.7 – 91.3	68.6 – 69.5	0 – 0.2
68 – 76	4	92.6 – 98.2	73.6 – 86.8	0 –0.3

Data source: Hill [1964].

Hill [1964] has described rock fineness as another widely recognized index of quality in addition to P_2O_5 grade and percentage of oxides (Al_2O_3 + Fe_2O_3) in the manufacture of superphosphate fertilizers. Trade practices require the percentages that pass the 100- and 200-mesh sieves (US No.100 and 200 mesh), respectively (the latter by wet sieving). The finer the rock the more rapid is its reaction with the acidulant, so long as the effectiveness of a mixing device can keep pace with the fineness of the rock. However, under insufficient agitation, very fine rock tends to agglomerate into coarse aggregates, so that a particular plant may designate an optimal fineness in the use of rock for manufacture. Furthermore, since the cost mounts with fine grinding, a fineness that is economical to use is the one commonly sought. Table 1.7 shows results of screen analysis of Florida Land pebble.

It has been established that the effective surface area available to react with acid, for a particular size fraction (100 to 150 mesh), varies widely among rock types [Hatfield, 1964]. This is due to the variable porosity and large "inside' surfaces of the more reactive rocks. However, the effective surface area for a given rock increases with fineness of the particles. Figure 1.7 shows the effect of fine grinding of Morrocan rock on the rate of attack when two different concentrations of sulphuric acid are used [Hadfield, 1964]. Acid of 76% percent strength and at 59°F was used as the primary source (Figure 1.7, B), and this was diluted with water to give 70 percent H_2SO_4 for immediate use in the tests shown in figure 1.9, A. The amount of acid used was 60 parts of 100 percent H_2SO_4 per 100 parts of rock in each test. The abscissa of Figure 1.7 is a logarithmic scale, log (t+1), which elongates the shorter time periods. The ordinate is the percent of unreacted rock, as indicated by the citrate-insoluble P_2O_5 content of the solid residue after stopping the reaction at various lengths of period by diluting with acetone-dioxane solvent. The vertical line on each curve indicates the time for the complete disappearance of sulphuric acid in the reaction. The initial reaction is much more rapid for the more finely ground rock for both concentrations of sulphuric acid. For example the reaction is about 90% complete in 1 to 5 hours with rock ground to 93% minus 100 mesh, while 2 to 3 weeks are required to obtain this degree of conversion with rock that is 21 percent minus 100 mesh.

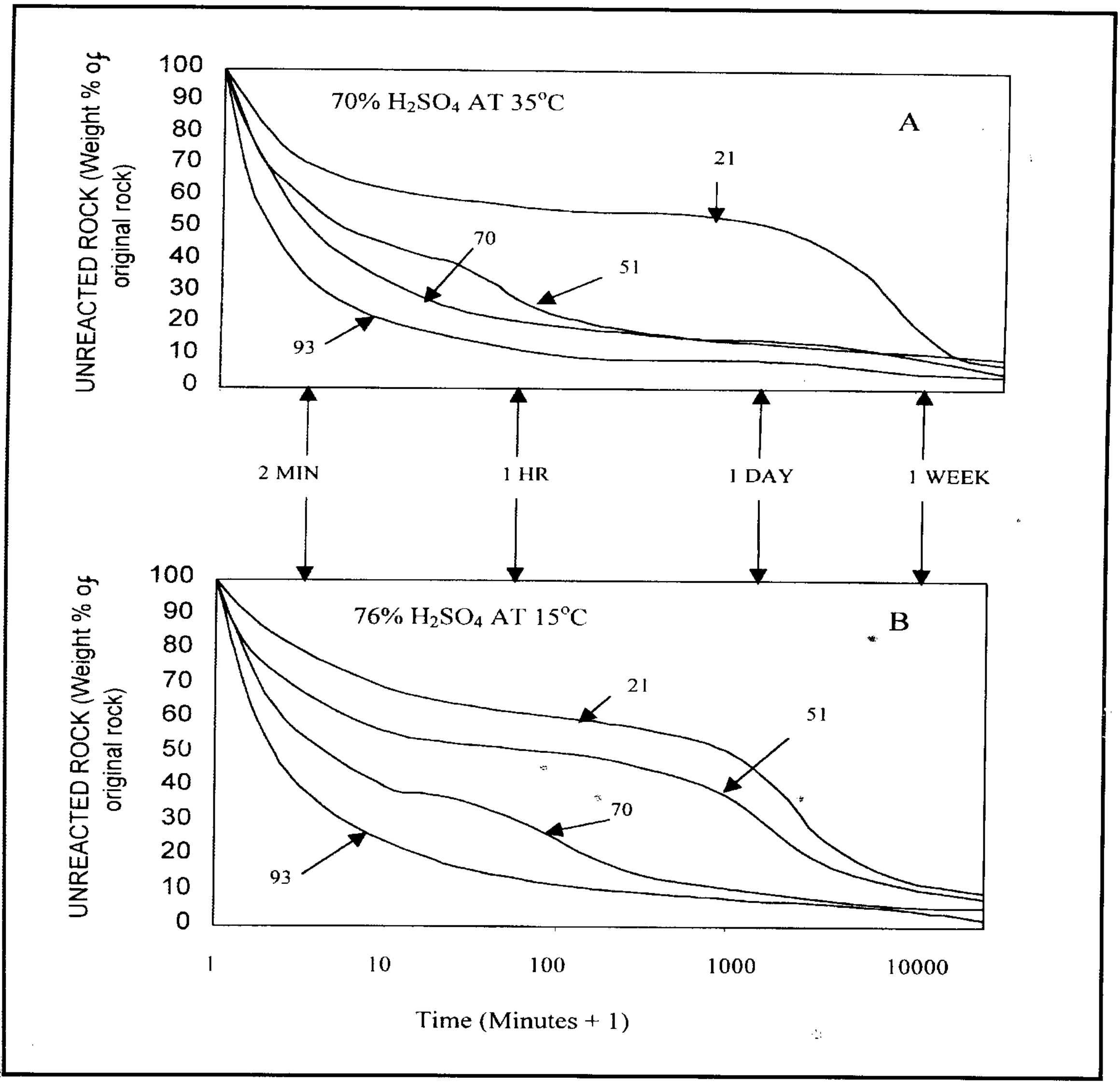

Figure 1.7. Effect of particle size and acid concentration on the rate of reaction of Moroccan rock. (Numbers on curves indicate percent passing 100 mesh British Standard Sieve. Vertical Marks show the time of disappearance of sulphuric acid.). *Source: Hatfield [1964].*

The curves for the coarser rocks show a relatively unreactive period from 10 minutes after mixing to about 3 days. This is exaggerated of coarse by the abscissa scale, but the illustrated leveling off of the reaction rate before the reaction is 70% complete demonstrates the importance of the effective rock surface for attack by sulphuric acid. The differences between the curves in Figure 1.7, A and B, for rocks of intermediate particle size are assumed to be largely due to the difference in temperature rather than the acid concentration.

1.10.3 Concentration of acid

The reaction between acid and phosphate rock is exothermic (about 90 Kcal / Kg of fuorapatite reacted with sulphuric acid) causing the temperature to rise significantly which results in the increase in the rate of reaction [IFDC, 1986]. This increase in the reaction rate is a disadvantage in unreactive rocks because surface precipitation reactions on rock particle surfaces tend to partially block the pores hence preventing further acid penetration into the inner rock matrix. The incomplete reaction leaves free acid which tends to react slowly with the iron and aluminium oxides to form insoluble phosphates.

The heat of reaction is greater for concentrated acids, and this tends to decrease the liquid phase by evaporation of water [Hatfield, 1964]. Calcium sulphate is also less soluble in the concentrated acid, and it precipitates from a strongly supersaturated liquid phase in a fine particle size on the surface of the unreacted rock. Thus, this results in an almost complete halt of the reaction, because of the coating and lack of liquid phase, when highly concentrated sulphuric acid is used.

Thus, determining the optimum range of acid concentration must involve the physical properties of the product as well as the rate of reaction.

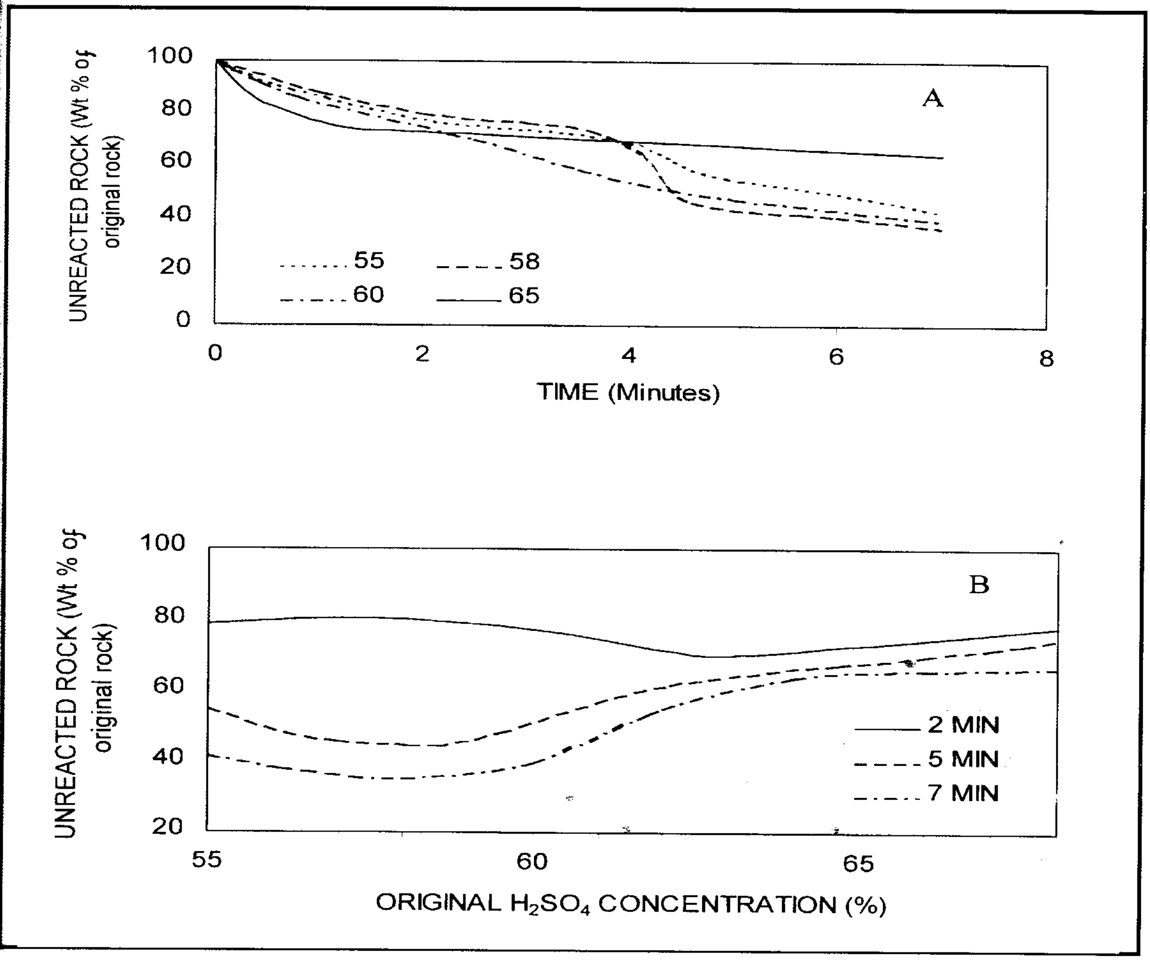

Figure 1.8. Kinetics in the early stages of normal superphosphate manufacture from Kola apatite: A, Rate curves; B, isochrones. (Temperature of acid, 60°C; acid: rock ratio, 110 percent of stoichiometric). *Source: Hatfield [1964].*

The kinetics during the early stages of the rock-sulphuric acid reaction are shown in Figure 1.8 as a function of acid concentration (slight excess of acid) and an acid temperature of 60°C. The rapid rate of reaction between 1 and 5 minutes, when the concentration is between 55 and 60 % H_2SO_4, shows the importance of sufficient liquid phase. The general nature of these curves indicates retardation of reaction by film around the rock particles through which the acid must diffuse to keep the reaction going. The same conclusion has been reached in a study of the action of a large excess of sulphuric acid on macrocrystalline apatite at constant temperature.

When a very dilute sulphuric acid is used, the amount of water is so large and the temperature rise so small that the rate of reaction is lessened; too dilute acid also requires artificial drying of the superphosphate to remove excessive moisture. In the partial acidulation of phosphate rock, it was reported that sulphuric acid with a concentration of 75 – 93% provided favourable results for more reactive rock, while 60 – 75% was more suited to less reactive ones. It was also found that unreactive rocks could be acidulated to 30 – 60% before free acid creates handling problems (i.e. a sticky product difficult to handle) [IFDC, 1986]. Pilot plant tests conducted by IFDC on a more reactive and a less reactive rock showed that when a more reactive rock (for example, Central Florida) was used the higher acid concentration 95% gave a slightly higher acidulation efficiency when measured in terms of water-soluble P_2O_5. However when a less reactive (Utah) rock was used, a slightly higher acidulation efficiency (water-soluble P_2O_5 basis after curing for 21 days), was obtained with a dilute acid (73%) acid.

1.10.4 Degree of acidulation

An increase in the degree of acidulation results in an increase in water-soluble P_2O_5 in the product. Degree of acidulation is not related to acidulation efficiency.

Acidulation efficiency is influenced by a combined effect of rock composition, reactivity and other process variables [IFDC, 1986]. It has been established that increasing the amount of acid per unit of rock increases the amount of liquid phase and thereby may increase the initial reaction rate [Hatfield, 1964]. The temperature of the reaction is controlled by two balancing forces – the increased rate of reaction tends to increase the temperature, but the additional heat capacity of the liquid requires more energy for a given temperature rise. When the excess of acid is sufficiently large, the latter effect predominates, that is, the increase in the rate of reaction is more than counterbalanced by the bulk of the liquid, and the temperature rise will not be as great as some small amount of acid. On the other hand, a stoichiometric deficiency of acid may actually give a slightly greater temperature rise because of the small amount of liquid phase.

Hatfield [1964] has reported that within practical limits of acid: rock ratio dictated by reasonable conversion and sufficiently low free acid in the product, the temperature rise is fairly constant for a given acid strength. The overall rate of reaction is affected mainly by the amount of liquid phase in this case. An increased amount of liquid phase increases the initial rate of reaction both by mass action effect and its ability to hold more calcium sulphate in solution. The latter fact is of less importance once precipitation is started than at the start of mixing. Increasing acid:rock ratio, say, from 90 percent to 100 percent of stoichiometric value, results in a greater percentage of increase in the rate of reaction than does an increase in the ratio from 100 percent to 110 percent of the stoichiometric value.

1.10.5 Retention time

In the full acidulation of phosphate rock to SSP a considerable period is given (i.e. the product is cured for 10 to 30 days to allow the reaction to approach completion). In the SSAG Process a much shorter retention time is allowed. Retention time in the equipment is based on mass flow through the granulator and dryer. Therefore the maximum production rate that can be achieved in a particular plant is determined by the retention time required for the particular phosphate rock after taking into account the required recycle-to-product ratio (total flow of material through the process equipment). In general, for a given acidulation level the retention time required to achieve optimum operation of the plant and conversion of the P_2O_5 to an available form increases as the reactivity of the rock decreases. A typical retention time of 4 minutes in the granulator and 12 minutes in the dryer is required for a rock with medium reactivity bringing the total to 16 minutes retention time [IFDC, 1986].

1.10.6 Process temperature profile

For unreactive rocks, a high temperature of the reaction causes a decrease in water-soluble P_2O_5 in the product due to surface precipitation reactions as discussed under concentration of acid. In the case of SSAG Process the drying temperature can also have an effect on the amount of water-soluble P_2O_5 in the finished product. Laboratory scale tests conducted at IFDC[1986] have indicated that the reversion of water-soluble P_2O_5 to NAC – soluble and insoluble compounds is minimized if the temperature of the material during drying does not exceed 120°C. However pilot plant tests were conducted in the temperature range 66 – 93°C and the results showed an increase of water–soluble P_2O_5 with increase in temperature in that range for both reactive and unreactive rocks.

1.11 Basis for kinetic models of normal superphosphate reactions

Hatifield [1964] has reported that a kinetic model of normal superphosphate reactions must take into consideration a number of factors, as follows:

1. The system is heterogeneous, one reactant being liquid and the other solid. Products are dissolved initially in the liquid phase. Some precipitate out ($CaSO_4$, $CaH_4P_2O_8.H_2O$); others enter into subsequent reactions (H_3PO_4, HF), while still others give rise to gases which are evolved partially or entirely (SiF_4, CO_2).
2. The system reactions are both consecutive and simultaneous.
3. The scale of intrinsic reactivity of the solid (phosphate rock) is important to the rate of reaction; at present this scale is qualitative only.
4. The effective surface area of the solid for attack by the liquid is related to the degree of fineness; a range of particle sizes, rather than uniform particles, must be considered. The effective surface diminishes as the reaction proceeds.

5. The amount of active reactant in the liquid phase (H^+ ion) is related to the initial acid concentration and temperature. As the reaction proceeds the liquid medium changes from one of sulphuric acid solution to a mixture of sulphuric acid and phosphoric acids and finally to phosphoric acid containing other cations and anions; supersaturated solutions of $CaSO_4$ and $CaH_4P_2O_8.H_2O$ exist during most of the reaction, the degree of supersaturation of each salt depending on the relative rates of attack on the rock and the rates of crystallization of salts from solution. It is in this changing medium that the hydrogen ion continues its attack on the rock. The hydrogen ion abundance diminishes with the degree of reaction primarily as the liquid phase diminishes; its concentration after the disappearance of aqueous sulphate, is largely determined by the temperature of the liquid phase.

6. The temperature of the reaction governs the rate constants and affects the amount of liquid phase as well as the hydrogen ion concentration therein. It affects the composition of the liquid phase with respect to dissolved salts and the rates of crystallization.

7. The reaction rate is retarded by the deposition of $CaSO_4$ and $CaH_4P_2O_8.H_2O$, by the decreasing surface of the rock, by the decreasing abundance of hydrogen ion, and by the decreasing temperature in the reaction mass.

Due to the complexity of the reactions, the perfect kinetic model, fitting all kinds of rock under all conditions, has not yet been advanced. The general approach to the kinetics of normal superphosphate has been to study one variable at a time and to define the variables in terms of practical controllable items such as original acid concentration, original acid temperature, etc. These measurable variables are indeed important as individual factors for any given set of conditions, but the prediction of their individual effects under all conditions of other variables is needed for an all-inclusive kinetic model. This task has been reported to be too great an undertaking experimentally, and hence the knowledge of fundamental properties of the phase systems has been insufficient to define and evaluate the proper "kinetic variables" for a generalized workable model [Hatfield, 1964]. The initial mechanism has been postulated to consist of several stages that occur simultaneously:

1. Diffusion of solvent ions toward the rock surface;
2. Chemical reaction between rock and acid;
3. Diffusion of reaction products into the bulk of the liquid phase;
4. Crystal formation of the new phase on the unreacted rock.

The slowest of these is the diffusion of the reaction products into the liquid phase, and the buildup of the product in the vicinity of its formation gives rise to a great degree of supersaturation and formation of a highly dispersed solid that makes further contact of reactants more difficult. Conditions that cause extremely high initial reaction rates, such as higher temperature and acid concentration, serve to intensify the degree of supersaturation and the deposition of product around the rock particles. This autoinhibition can be qualitatively visualized by comparing the early rate curves in figure 1.10, A; the stronger acid (65 percent H_2SO_4) is retarded rather quickly, even though its initial rate is the most rapid of those shown.

1.12 Determination of acid requirement

Determination of the quantity of acid required to fully acidulate phosphate rock is difficult because of the influence of variable amounts of the acid-producing and acid consuming components of the rock [IFDC, 1986]. In practice, a reasonable estimate of the stoichiometric amount of acid required can be made by multiplying the level of certain constituents in the rock by positive and negative factors (Table 1.8).

Table 1.8. Factors for estimating quantity of sulphuric acid required to fully acidulate phosphate rock [IFDC, 1986].

Phosphate rock component	Acidulation factor
MgO	2.433
CaO	1.749
Na_2O	1.582
K_2O	1.041
Al_2O_3	0.962
Fe_2O_3	0.614
F	(-) 1.650
SO_3	(-) 1.225
P_2O_5	(-) 0.691

Data source: IFDC [1986].

These factors describe the theoretical amount of acid required to convert each major constituent of phosphate rock into acidulation products normally found in

SSP. In most cases acid consumption data reported by commercial phosphate fertilizer producers agree closely with these estimates, although many producers may use slightly more acid than indicated (usually 5-10%) to compensate for normal process inefficiencies and to ensure optimum conversion of the phosphate to the available form.

To estimate kilograms of sulphuric acid (100% basis) required to fully acidulate 100kg of phosphate rock, the weight-percent of each component is multiplied by appropriate acidulation factor and totalled. The components with positive factors are the acid consumers while those with negative factors form acid during the reaction. For example, MgO forms $MgSO_4$ when it reacts with H_2SO_4 and consumes acid while P_2O_5 forms phosphoric acid H_3SO_4 when reacted with sulphuric acid.

1.13 Available phosphate

Available phosphate in this work refers to the amount of phosphate (expressed in terms of P_2O_5) that is soluble in a solution of Neutral Ammonium Citrate (NAC). This includes the water-soluble P_2O_5 and NAC-soluble P_2O_5 [IFDC, 1986].

1.14 Free acid

The free (H_3PO_4 expressed in $\%P_2O_5$) of the SAB-PAPR products is determined by washing the sample in acetone to remove residual phosphoric acid. In superphosphate chemistry, phosphoric acid is an intermediate product of the sulphuric acid and fluorapatite reaction. The phosphoric acid continues to react with more fluorapatite to form the final product-a mixture of mono- and dicalcium phosphate, calcium sulphate and unreacted fluorapatite (phosphate rock). A limitation of this determination is that free acidity contributed by unreated sulphuric acid is not detected. However, it is not likely that the PAPR products would contain free sulphuric acid [IFDC, 1986].

1.15 Granulation

Granulation is a method used to improve the handling properties of the fertilizer materials in the fertilizer industry. The term is commonly applied to describe a product which passes a 5mesh sieve and is retained on a 16 mesh sieve. This includes particles with mean diameters of 1 – 4 millimeters. Granular forms of individual commercial materials frequently have a narrower particle size range and occasionally an appreciable proportion of a semigranular or a so-called granular product passes a 16 mesh sieve. Fertilizers in this size range are classified as granular regardless of how they are produced – by cementing together of small particles, the mechanical disintegration of larger particles or mechanical removal of small ones from the body of the material [Hardesty, 1964].

Tumbling, rolling, or cascading the wetted material in the rotating cylinders is the most widely adopted technique for granulating superphosphate and mixed fertilizers containing superphosphate. The efficiency of this method of granulation necessitates adherence to the principles of agglomeration by effective use of the natural forces (i.e. surface tension and plasticity) which control size enlargement.

1.15.1 Surface tension

In the granulation of PAPR, surface tension between individual rock particles plays an important role. When a wettable solid particle is brought by mechanical force in proximity of another like system, the liquid films, by virtue of the force of surface tension, tend to coalesce and form a continuous film surrounding two solid particles [Hardesty, 1964]. The involvement of many like systems yields a loosely assembled plastic aggregate capable of being formed into various shapes and sizes, such as a molded building brick containing an assemblage of clay particles or a superphosphate granule containing an assemblage of superphosphate particles. There is a relationship between the force of surface tension and the formation of aggregates, which are illustrated in Figure 1.9. Weaker force of attraction and less coalescence are exhibited by nonwettable particles or subassemblies having irregular liquid distribution at their surfaces (Figure 1.9,A) than by particles that are easily and uniformly wetted (Figure 1.9, Aa). Weaker aggregates are formed when there is insufficient liquid present (Figure 1.9, B) than when there is sufficient liquid to fill the capillaries between the initial particles of the aggregate (Figure 1.9, Ba). Uniform size and shape of hard, dense, brittle particles and symmetrical packing result in a minimum number of contacts between particles per unit mass and the formation of a relatively weak aggregate (Figure 1.9, C).

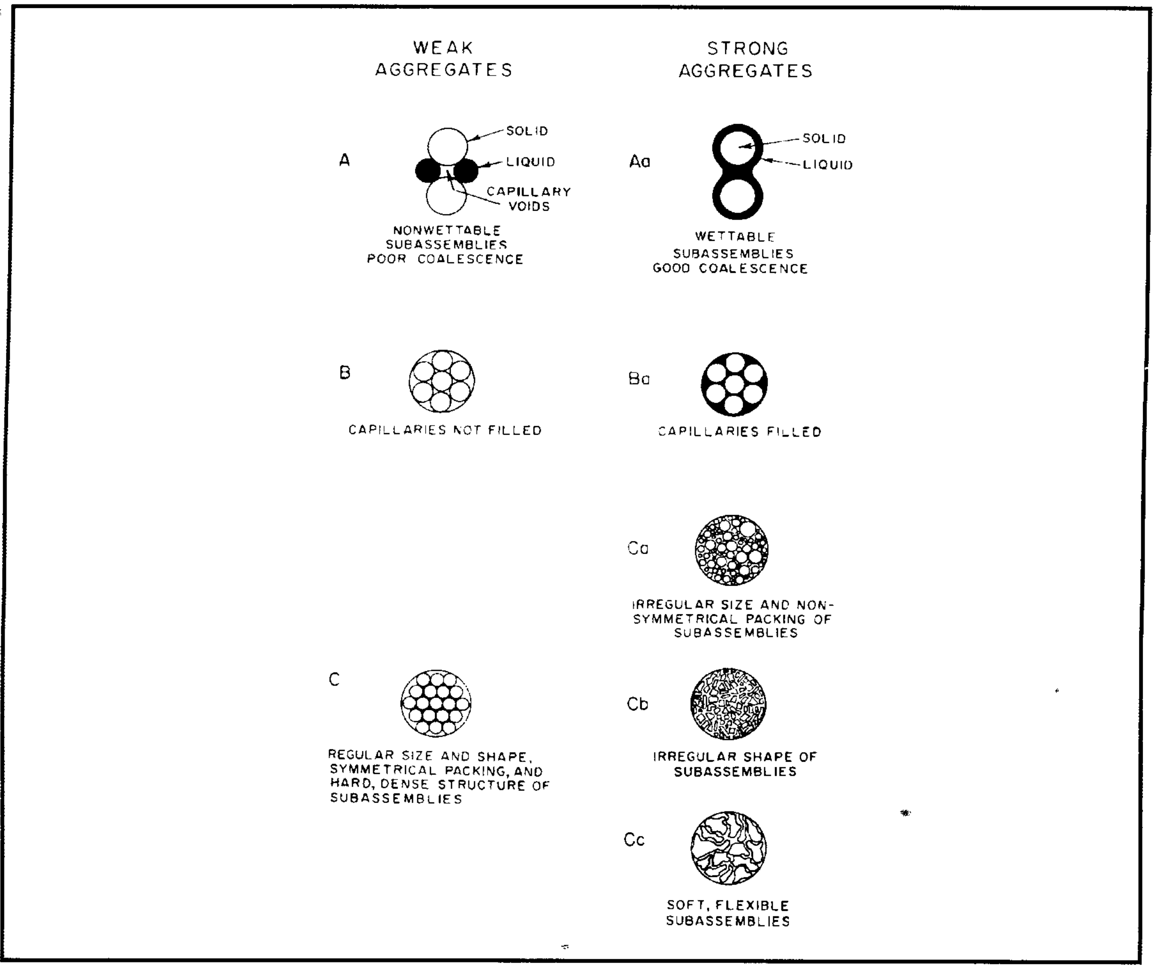

Figure 1.9. Characteristics of weak and strong aggregates. *Source: Hardesty [1964].*

An irregular size among particles and nonsymmetrical packing increases the number of contacts between particles (Figure 1.9, Ca), an irregular shape among particles forms an interlocking structure (Figure 1.9, Cb), and soft, pliable particles or subassemblages exhibit close packing in the aggregate (Figure 1.9, Cc) – all of which tend to produce a relatively strong aggregate. Surface tension is increased by the presence of highly ionized salts in solution and is generally decreased by increasing the temperature of agglomeration. However the net effect of increasing the temperature is generally favourable to agglomeration, as discussed later in connection with plasticity of the aggregate. Surface tension is also decreased by the presence of wetting agents, but sometimes this undesirable effect may be offset by the usefulness of the wetting agents in promoting uniform distribution of the liquid at the surface of the initial particles.

1.15.2 Plasticity

Another physical phenomenon that plays an important role in the granulation process is plasticity of the aggregates (granules) formed during the process. An aggregate is said to posses plasticity when it is capable of being deformed in any direction without rapture [Hardesty, 1964]. This property involves the freedom of slippage of individual particles within the aggregate under stress of natural forces (like capillary attraction and surface tension) and mechanical forces such as that applied to cause rolling or cascading of material in a rotating cylinder. The nechanical force serves to bring the finely divided, wetted particles of the mass nto contact so that capillary attraction can bring about their coalescence into the nost intimate packing habit. In the presence of an optimum proportion of well-istributed liquid phase, coalescence will continue until the fine particles have een used up, and, at this stage of the agglomeration process, the granules grow o longer because capillary attraction between them and the number of contacts er unit mass of the larger aggregates are insufficient to hold them together. lasticity can be enhanced artificially in three ways: (i). by adjusting the screen nalysis to get some particle mobility; (ii). by adding liquids (so called asticizers), which make it easier for fragments (particles) to slip into place; and (iii). by intimate mixing of plasticizers with fines to capitalize on liquid-to-solid surface tension.

LIQUID PHASE – The presence of water in fertilizers creates a liquid phase consisting of a solution of the soluble constituents present. The concentration of the liquid phase is dependent primarily on the quantity of water used and on the quantity and solubility of the salts present in the fertilizer: the concentration is also dependent on the temperature and the degree of saturation of the solution as influenced by the period of contact between solid and liquid. The volume of liquid phase is always greater than the volume of water present and is maximum at any given temperature when the liquid phase is saturated with salt. Thus, the liquid phase, rather than water alone, is the true plasticizer in the agglomeration step of the fertilizer granulation process. It supplies the medium for capillary attraction between particles and lubricates the particles so as to aid their migration to the optimum or equilibrium location within the aggregate.

Maximum efficiency of granulation is known to occur when the concentration of the liquid phase is constant during the agglomeration stage of the process [Hardesty, 1964]. Such a condition demands saturation of the liquid phase at constant temperature in a non-drying atmosphere. The equilibrium concentration of the liquid phase in superphosphates, especially in fresh goods, accounts largely for the ease with which they can be agglomerated. The volume of liquid phase, in mixtures containing high proportions of soluble salts such as ammonium nitrate and urea, can be several times the volume of water present and varies appreciably with 1° or 2° change in the temperature of processing; but in superphosphate alone, the magnitude of the difference between the volumes of liquid phase and of water present is not so great as to cause any appreciable change in volume of the liquid phase over a temperature range of several degrees.

INFLUENCE OF PARTICLE SIZE – The plasticity of the aggregates increases with the fineness of the particles owing to the increasing fineness of the capillaries and the resultant greater attractive force between particles.

A wetted crystalline material, such as ammonium nitrate exhibits much less plasticity in the coarse crystalline state than when a part of the salt is in a finely divided state resembling the condition represented by figure 1.11, Ca. A fresh damp superphosphate, consisting principally subassemblages of fine particles generally exhibits good plastic properties, owing to the flexibility in shape of the subassemblies of the aggregate, thus representing the condition represented by figure 1.11, Cc. This plastic property of superphosphate makes it more amenable to agglomeration under these conditions than any other fertilizer material. Its plasticity is largely responsible for the agglomerating characteristics of most mixed fertilizers. For example, in the agglomeration of minerals fines are important as a sufficient proportion of them in the aggregate occupy the voids between larger particles. The example is equally applicable to fertilizers. The resulting decrease in the size of the capillaries gives a corresponding increase in attractive force holding the particles of the aggregate together.

1.15.3 Granule strength

Particle size distribution and the packing characteristics of the particles have an influence on granule strength. It has been demonstrated experimentally that the magnitude of the suction potential holding the particles of a wet aggregate together increases with increase in closeness of particle parking and in surface tension of the plasticizer, and with decreases in the size of capillaries between particles and in the size of individual particles within the aggregate. Controlled drying of the aggregate after agglomeration usually serves to draw its constituent particles closer together by virtue of removal of liquid phase, thus increasing the physical stability of the dry product. Drying also improves aggregate stability by causing crystallization of soluble salts from liquid phase, thus cementing the particles of the aggregate together.

1.16 Process modelling and simulation

Mathematical modelling involves the formulation of mathematical relationships, which describe the behavior of the actual system such that dependent and independent variables and parameters of the model are directly related to the physical and chemical quantities in the system.

e general approach to process modelling consists of the following steps nfield and Lapidus, 1964]:

Definition of the problem. Type of system to be represented, uses of the model in such a system, complexity of process description, data against which the model is to be tested.

Collection of data from the process. Data can be collected from a normal operating system or from a perturbed system if needed.

Theoretical analysis of the nature of the system to generate a mathematical model.

(a) A model can be created which describes the physical and chemical processes occurring within the reactor. Such a model is described as a *mechanistic model* and would consist of the sets of equations developed for various reactors. Such a model is difficult to create because the physical and chemical steps involved must first be identified before modelling can be done and requires considerable research effort to identify the elementary steps occurring in the reactor. Such models are difficult to analyze because they can no longer be linearized and may contain too many parameters.

Semi empirical models are those that are not intended to be full despriptions of real processes. They lie between mechanistic and empirical models. Models of this type are relevant to chemical engineering.

(b) At the other extreme is the so-called "black box" model where essentially no priori information about the system is known. The model must be determined solely from the actual system.

(c) Most real situations lie somewhat intermediate between these two extremes.

4. Solution of the model. In general, linear models are amenable to analytical techniques, whereas non-linear models can be solved by numerical methods employing a computer.

5. Evaluation of the model. This refers to comparison of the model to the data. Depending on the type of model and data, the matching of the model and the data (also known as *simulation*) can follow a number of paths:

   (a) If the form of model is specified from basic principles, the matching of the model is usually accomplished by parameter estimation to produce an optimum fit.

   (b) If no priori information on the system exists other than output / input data, an *empirical model* of the system has to be constructed.

Once a model is available, it can be used as the centre of an experimental planning procedure which predicts which next experiments to carry out to obtain useful information. As long as the model has some mechanistic features, it can throw some light on the understanding of the reaction. If there are some experimental points that can not be predicted correctly by the model it is an indication that the mechanism contained by the model is in some way wrong or incomplete. A lack of fit indicates inadequate understanding of the physical and chemical processes occurring in the reactor.

The most preferred models in reactor design are semi empirical models. A semi empirical model that fits data correctly is of great comfort to a chemical engineer faced with scale up to full scale design. Although there is no guarantee that the scale up will be correct because the model is not garanteed to contain the correct mechanism, the chances are very high that the errors introduced by the inadequate mechanism will be tolerably small on the full scale plant. On the contrary, empirical models could give wild predictions outside the experimental region in large scale equipment.

Once a model is constructed it may be used to predict the future behavior of the system, reconstructing the past behavior of the system, outlining a form of control of the system, or indicating a better and improved set of operating conditions.

1.17 Types of flow in reactors

The two ideal limiting types of flow are perfectly mixed flow and plug flow. Flow patterns found in actual processes lie between these two limits. Channeling or by-pass represents a condition whereby some elements of the fluid pass through the vessel considerably faster than others. Dead space is when there is poor contacting or stagnant regions in the vessel. These conditions are detected experimentally by plotting a residence time distribution curve (RTD) using a tracer [Himmelblau, 1972, Levenspiel, 1972].

The residence time distribution E (t) is computed by injecting a tracer as an instantaneous pulse (delta function) into the system and measuring its response. Then

$$\mu C_o = \int_0^\infty C\, dt \cong \sum_{k=1}^{n} C_k \Delta t_k \qquad (1.1)$$

$$E(t) = \frac{C(t)}{t\, C_o} \qquad (1.2)$$

Where C_o is the quantity of tracer injected divided by the volume of the vessel, μC_o = the area under the response curve, C (t) is the response (concentration, or counts per minute etc) as a function of time, and n is the limit of summation. The symbol μ stands for the mean residence time which can be calculated from

$$\mu = \int_0^\infty t\, E(t)\, dt \cong \sum_{k=1}^{n} t_k E(t_k) \Delta t_k \qquad (1.3)$$

or from V/q, where V is the volume of the vessel and q the volumetric flowrate.

1.17.1 Models in the frequency domain

There are two primary reasons for employing frequency domain models in lieu of time domain models [Himmelblau, 1972]:

(a) The analytical solution of the model may be simpler in the frequency domain than the related solution of the model in the time domain.

(b) For some models, solutions can be obtained for frequency domain but not for the time domain. Or, the model response may be in the form of a complicated series which is hard to evaluate numerically.

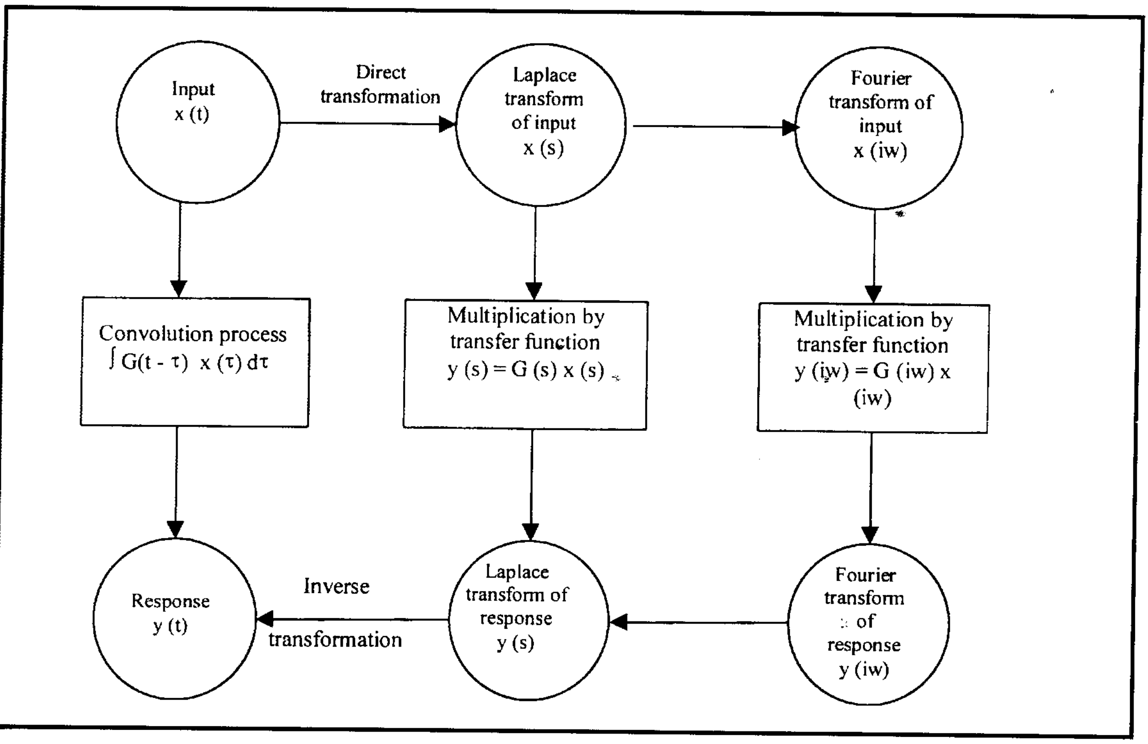

Figure 1.12. Representation of the relationship between the input and output of a linear subsystem. *Source: Himmelblau [1972].*

Direct transformation between the time and frequency domains, as shown in Figure 1.12 is possible in general only for models linear in the time domain.

However, satisfactory empirical models can be formulated directly in the frequency domain.

1.17.2 The transfer function

The transfer function is used as an alternative way to represent the relationship between the inputs and outputs of a constant-coefficient differential equation [Himmelblau, 1972]. For a general nth order differential equation, for example equation 1.4.

$$\frac{d^n y}{dt^n} + a_{n-1}\frac{d^{n-1} y}{dt^{n-1}} + \ldots + a_1 \frac{dy}{dt} + a_o y = x\,(t) \qquad (1.4)$$

The transfer function is defined as the ratio between the Laplace transform of the output divided by the Laplace transform of the input and it can be found by taking Laplace transforms of each side of equation 1.4 with $y\,(s) = y'(0) = \ldots = y^{(n-1)}(0) = 0$.

$$s^n\, y\,(s) + a_{n-1}\, s^{n-1}\, y\,(s) + \ldots + a_1\, sy\,(s) + a_0\, y\,(s) = x\,(s) \qquad (1.5)$$

Rearranging equation 1.4 gives

$$\frac{y\,(s)}{x\,(s)} = \frac{1}{s^n + a_{n-1}\, s^{n-1} + \ldots + a_1\, s + a_0} \qquad (1.6)$$

The transfer function corresponding to the subsystem differential equation is obtained from equation 1.6. If the input function x (t) is generalized to include derivatives of x (t), then a polynomial in s will appear in the numerator of the transfer function, equation 1.6. If the input to the subsystem is a delta function of the input

$$x(s) = L[x(t)] = L[\partial(t)] = \int_0^{\infty} e^{-st}\,\partial(t) = 1 \qquad (1.7)$$

and the right hand side of equation 1.6 is seen to be the Laplace transform of the impulse response

$$\frac{y(s)}{1} = g(s) = \frac{1}{s^n + a_{n-1}s^{n-1} + \ldots + a_1 s + a_0} \qquad (1.8)$$

Where

$$g(s) = L[g(t)]$$

Therefore, for an impulse input, the transfer function proves to be the Laplace transform of the impulse response function, and equation 1.6 can be written as

$$\frac{y(s)}{x(s)} = g(s) \qquad (1.9)$$

$$y(s) = g(s)\,x(s) \qquad (1.10)$$

1.17.3 Transfer functions for perfectly mixed flow and plug flow

The transfer function for perfectly mixed flow is given as $g(s) = 1/(1 + \tau s)$ and for plug flow $g(s) = e^{-\tau s}$ [Himmelblau, 1972]. Therefore, the transfer function for a perfectly mixed reactor in series with a plug flow reactor is given as,

$$g(s) = \frac{1}{\tau s + 1} e^{-\tau s}$$

or $\quad g(s) = g_1(s).g_2(s)$

1.17.4 The selective recycle model

In selective recycle systems particles are classified according to the number of cycles they have completed. A closed comminution circuit is an example of a system with selective recycling. Nkonde [1988, 1989] has used a selective recycle model shown in figure 1.13 to simulate the RTD of a ball mill in a closed comminution circuit consisting of a ball mill (unit 1) and a hydrocyclone (unit 2). Symbols used were Y_o for the net flowrate of the tracer through the system, Y_1 for the flowrate of the tracer leaving unit 1 and Y_2 for the flowrate of the recycle fraction of the tracer. In his study, he assumed perfectly mixed flow in unit 1 and plug flow in unit 2. The tracer response was used to plot an experimental RTD curve.

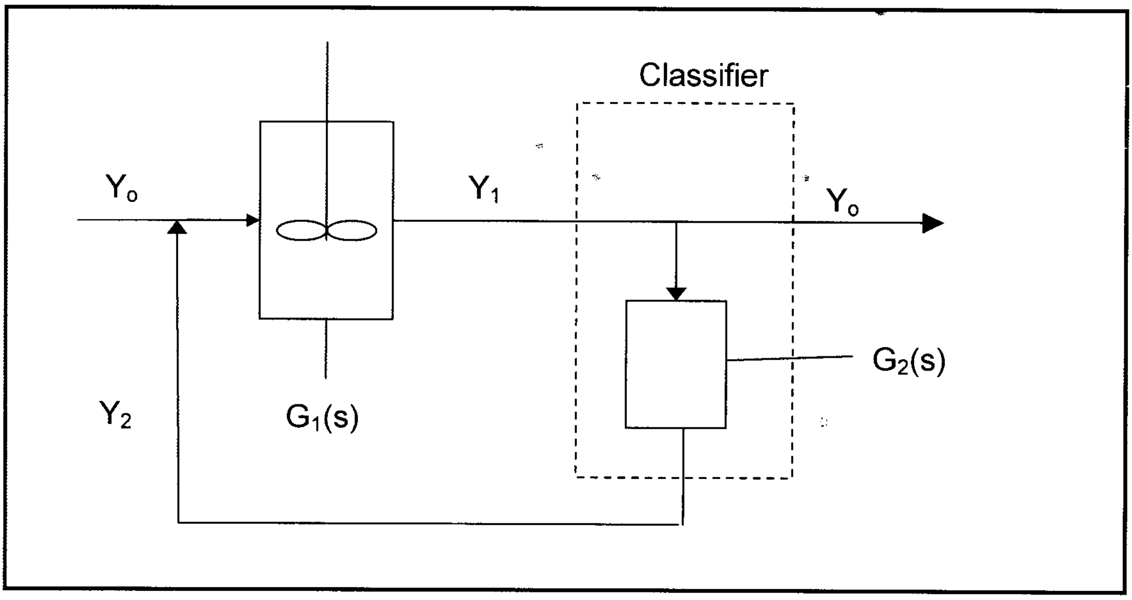

Figure 1.11. The selective recycle model. *Source: Nkonde [1988].*

To simulate the experimental RTD, he used transfer functions for perfect mixing $G_1(s) = 1/(1 + \tau_1 s)$ and for plug flow $G_2(s) = e^{-\tau_2 s}$ to compute the total transfer function of the system (equation 1.11).

$$G(s) = \sum_{n=1}^{\infty} b_n G_1^{\,n}(s)\, G_2^{\,n-1}(s) \tag{1.11}$$

where b_n is defined as the probability mass function specifying the number of cycles distribution (NCD) describing the probability of the original mass of a tracer to be removed from the recycle loop after the first, second, third and nth number of cycles. The sum of the probability mass functions is one as given in equation (1.12).

$$b_1 + b_2 + b_3 + \ldots + b_{n-1} + b_n = 1 \quad \text{or} \quad \sum_{n=1}^{\infty} b_n = 1 \tag{1.12}$$

The probability mass function b_n for the number of cycles distribution is expressed using different types of distributions such as gamma distribution. Nkonde used a generalized NCD for b_n to simulate the experimental RTD curve of a ball mill in a closed comminution circuit. His computations involved obtaining the inverse of the Laplace transform for a generalized NCD in equation (1.11) for $G_1(s) = 1/(1+\tau_1 s)$ and $G_2(s) = e^{-\tau_2 s}$. The mole fractions of the tracer for b_n were assumed to be $b_i + b_j = 1$ where b_i, and b_j are the mole fractions of original mass of the tracer leaving the selective recycle model after exactly the ith, and jth number of cycles through the main unit and τ_1 and τ_2 are the time constants in units 1 and 2 respectively. The RTD of the selective recycle model was obtained from the total transfer function of the selective recycle system in equation (1.11) by getting its inverse L^{-1} G(s) given in equation (1.13) below

$$L^{-1} G(s) = E(t)$$

$$= \frac{1}{\tau_1} \sum_{n=1}^{\infty} \frac{b_n}{(n-1)!} \left\{ \frac{t-(n-1)\tau_2}{\tau_1} \right\}^{n-1} e^{-(t-(n-1)\tau_2)/\tau_1} U(t-(n-1)\tau_2) \quad (1.13)$$

Where U is the step function.

$$E(t) = \frac{1}{\tau_1} \frac{b_i}{(i-1)!} \left\{ \frac{t-(i-1)\tau_2}{\tau_1} \right\}^{(i-1)} e^{-(t-(i-1)\tau_2)/\tau_1} U(t-(i-1)\tau_2) +$$

$$\frac{1}{\tau_1} \frac{b_j}{(j-1)!} \left\{ \frac{t-(j-1)\tau_2}{\tau_1} \right\}^{(j-1)} e^{-(t-(j-1)\tau_2)/\tau_1} U(t-(j-1)\tau_2) \quad (1.14)$$

The solution in equation (1.14) was obtained by minimizing the sum of the squared differences between the experimental RTD (RTD_{exp}) and the theoretical RTD (RTD_{theo}) as given in equation (1.15) below

$$F = \sum_{i=1}^{k} [RTD_{exp} - RTD_{theo}]^2 \quad (1.15)$$

where

$$RTD_{theo} = \frac{1}{\tau_1} \frac{b_i}{(i-1)!} \left\{ \frac{\theta-(i-1)\tau_2}{\tau_1} \right\}^{(i-1)} e^{-(\theta-(i-1)\tau_2)} U(\theta-(j-1)\tau_2 +$$

$$\frac{1}{\tau_1} \frac{b_j}{(j-1)!} \left\{ \frac{\theta-(j-1)\tau_2}{\tau_1} \right\}^{(j-1)} e^{-(\theta-(j-1)\tau_2)/\tau_1} U(\theta-(j-1)\tau_2)$$

F is the objective function to be minimized, $F \geq 0$. The summation outside the brackets is the total number of experimental points to be iterated. The six unknown parameters b_i, b_j, i, j, τ_1 and τ_2 were calculated by least square method shown in equation (1.15).

1.17.5 The Shrinking Core Model

The shrinking core model [Levenspiel, 1972] assumes particles of constant size. The reaction proceeds at a narrow front, which moves into solid particle. The reaction follows the following five steps:

Step 1. Diffusion of gaseous reactant A through film surrounding the particle to the surface of the solid.

Step 2. Penetration and diffusion of A through the blanket of ash to the surface of the unreacted core.

Step 3. Reaction of gaseous A with solid at this reaction surface.

Step 4. Diffusion of gaseous products through the ash back to the exterior surface of the solid.

Step 5. Diffusion of gaseous products through the gas film back into the main body of the fluid.

At times some of the steps do not exist. For example if no gaseous products are formed or if reaction is irreversible, steps 4 and 5 do not contribute directly to the resistance to reaction. Also, the resistances of the steps vary so that the step with the highest resistance is said to be rate controlling.

Film Diffusion Control

For film diffusion fractional time for complete conversion is given by:

$$t/T = (1 - (r_c/R)^3 \qquad 1.16a$$

where R is the total radius of particle and

r_c is the radius of the unreacted core

For a spherical particle, this can be written in terms of fractional conversion by noting that

$$1 - X_B = \left[\frac{\text{volume of unreacted core}}{\text{volume of particle}} \right] \qquad 1.16b$$

$$= 4\pi r_c^3 / 4\pi R^3 = (r_c / R)^3 \qquad 1.17$$

Therefore

$$t/T = (1 - (r_c / R)^3 = X_B \qquad 1.18$$

Where t = time for fractional conversion

T = time for complete conversion

Ash Diffusion Control

For ash diffusion control the progression of reaction in terms of time required for complete conversion is given by equation

$$t/T = 1 - 3(r_c / R)^2 + 2(r_c / R)^3 \qquad 1.19$$

Which in terms of fractional conversion is given as

$$t/T = 1 - 3(1 - X_B)^{2/3} + 2(1 - X_B) \qquad 1.20$$

Chemical Reaction Control

For chemical reaction control the increase in fractional conversion of the particle is given by equation

$$t/T = 1 - r_c / R = 1 - (1 - X_B)^{1/3} \qquad 1.21$$

The Theoretical Curve

Theoretical curve is plotted in figure 1.15.

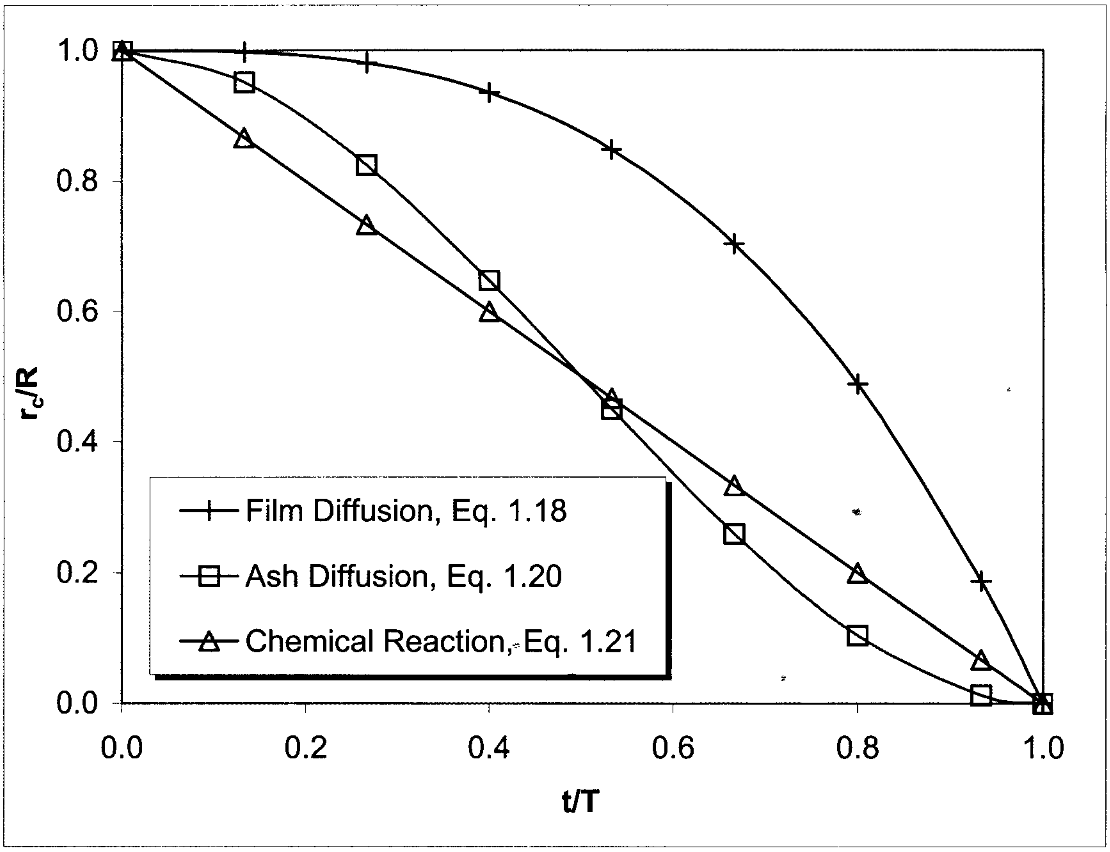

Figure 1.15. Progression of reaction of a single spherical particle with surrounding fluid measured in terms of time for complete reaction [Levenspiel, 1972].

The rate of a chemical process is controlled by the rate of the slowest step in the process. For the reaction between phosphate rock and sulphuric acid the data involving time for conversion of apatite into available P_2O_5 can be used to simulate the model in order to determine the rate-controlling step in the process.

CHAPTER 2: APPARATUS AND EXPERIMENTAL TECHNIQUES

CHAPTER 2

APPARATUS AND EXPERIMENTAL TECHNIQUES

2.1 Outline

The production of PAPR was carried out in a 25kg/hr pilot plant at the University of Zambia in the School of Mines. PAPR was produced by mixing phosphate rock with commercial sulphuric acid (98%H_2SO_4) and water (H_2O). Macrocrystalline apatites of igneous origin such as Chilembwe have their coarse apatite grains imbedded in a fine grained rock matrix and hence required to be liberated prior to processing into PAPR. The apatite grains were liberated by the process of comminution involving crushing and grinding of the rock to a suitable particle size distribution. In chemical reactions, the finer the particle the larger the surface area for the reaction between the acid and the apatite and the higher the process efficiency.

Techniques utilized in sample preparation involved primary crushing, secondary crushing, grinding, classification, thickening, filtration and drying at pilot plant scale (25kg/hr milling capacity). PAPR production involved acidulation and granulation followed by drying and sizing at pilot-plant scale (25kg/hr capacity).

Before carrying out acidulation experiments, the chemical composition of the feed was analyzed for CaO, P_2O_5, K_2O, Na_2O, MgO, Fe_2O_3, Al_2O_3, SO_3, and F. These chemical components were used to determine the amount of sulphuric acid required to achieve a desired degree of acidulation using the method given in chapter 1 section 1.12. The method of analysis included Atomic Absorption Spectrometry (AAS), UV-spectrometry and gravimetric techniques.

Comminution as well as acidulation processes required to be modelled in order to determine the flow behaviour of the material in the main units, the ball mill and the granulator, with an aim of optimizing their operations. In each modelling test the data for plotting the experimental Residence Time Distribution (RTD) curve was obtained by introducing a suitable tracer in the system in the form of an instantaneous pulse (or delta function). The tracer output was then closely monitored by sampling the exit stream at time intervals. A selective recycle model was then used to simulate the experimental RTD curve [Nkonde, 1988]. This particular model was chosen because the processes of closed grinding circuit as well as granulation and sizing systems include recycle streams.

2.2 Sampling

The sampling site at Chilembwe's number 2 orebody where the experimental sample was taken was an outcrop of phosphate ore. Boulders of phosphate rock were mined from the site. Picks and hammers were used by labour hired from the nearby Sambani village to dislodge and break large boulders to a size of about 20cm or less. Approximately 7 tonnes of phosphate rock was collected. Sampling was directed and monitored by a geologist from the Geology Department of the School of Mines who provided professional advice regarding this particular operation. The phosphate rock sample was transported to the School of Mines in Lusaka by a 10 tonne Mitsubishi truck and stockpiled prior to experimental work.

2.3 Comminution of phosphate rock

2.3.1 Primary and secondary crushing

Phosphate rock was collected from the pile and ferried by a trolley to a Pegson Osborn primary jaw crusher (Figure 2.1) with dimensions 320mm long 230mm wide at the mouth and the discharge set at 50mm crusher. The product from the primary crusher was minus 50mm in size and was transferred to a secondary crusher, a Denver type jaw crusher (Figure 2.2), with a mouth 100mm long and 60mm wide and the discharge set at 6mm.

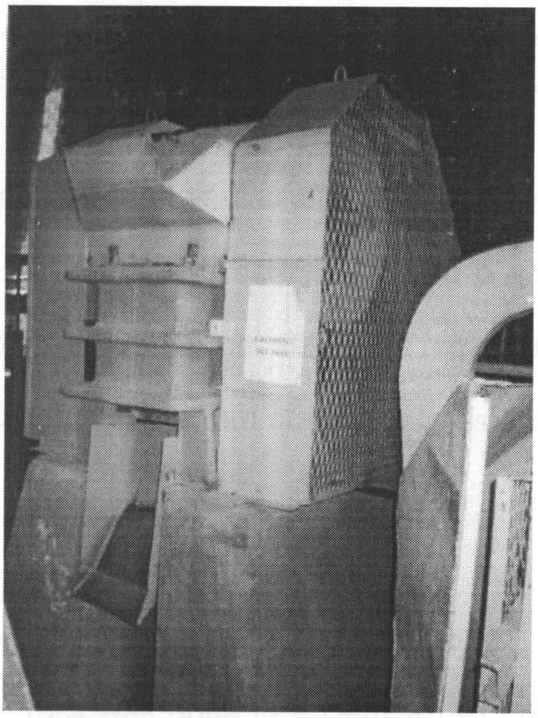

Figure 2.1. A Pegson Osborn primary jaw crusher at UNZA School of Mines.

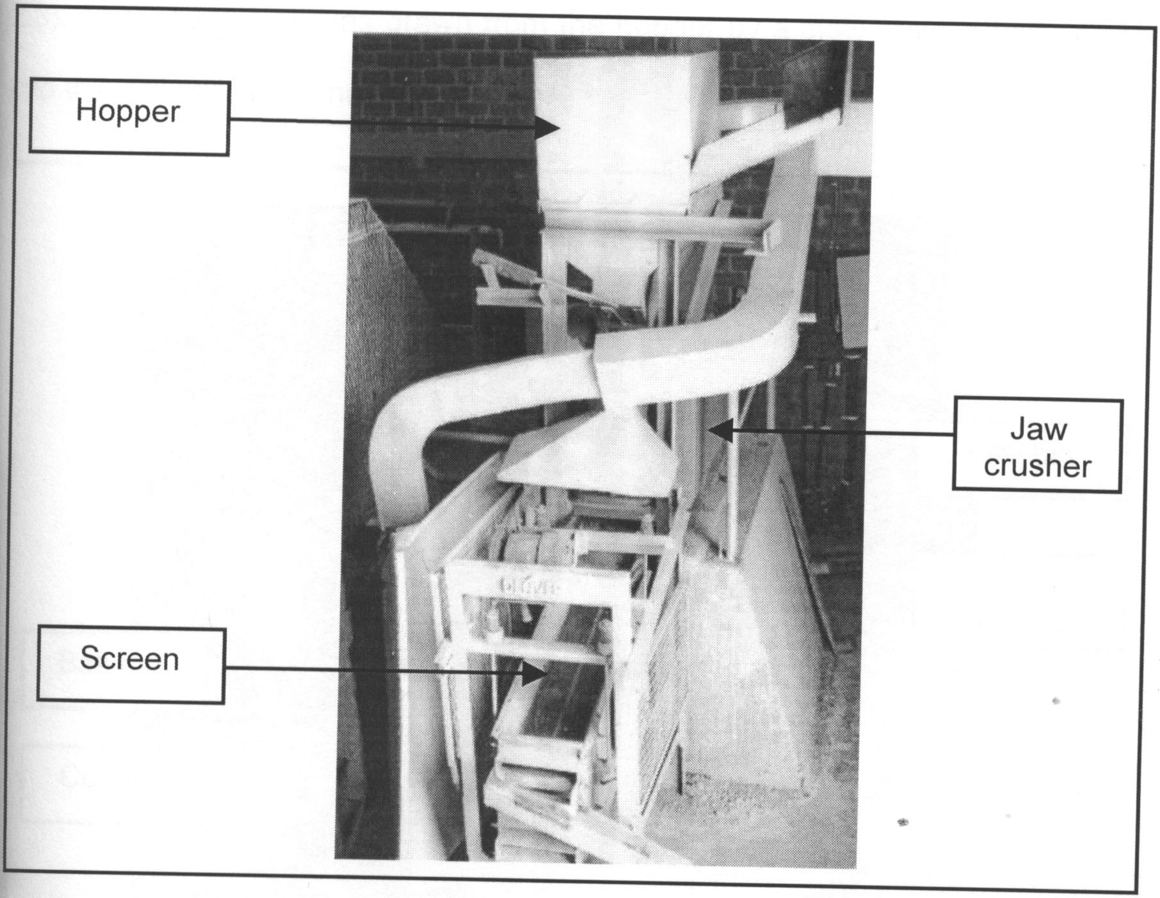

Figure 2.2. A Denver secondary jaw crusher at UNZA School of Mines. In front is the single deck vibrating screen.

The product from the secondary crusher discharged directly onto a 1000mm long and 300mm wide single deck vibrating screen carrying a wire mesh of 6mm aperture size. The oversize fraction (+6mm size) was recycled to the secondary crusher while the undersize fraction (-6mm size) was transferred to the grinding circuit.

2.3.2 Grinding and classification

Grinding of the phosphate rock was done in a Denver ball mill with dimensions 815mm long and 406mm diameter carrying a charge of 227kg steel balls (Figure

2.3). Phosphate rock was drawn from the hopper by a slow moving belt and fed into the ball mill via a chute.

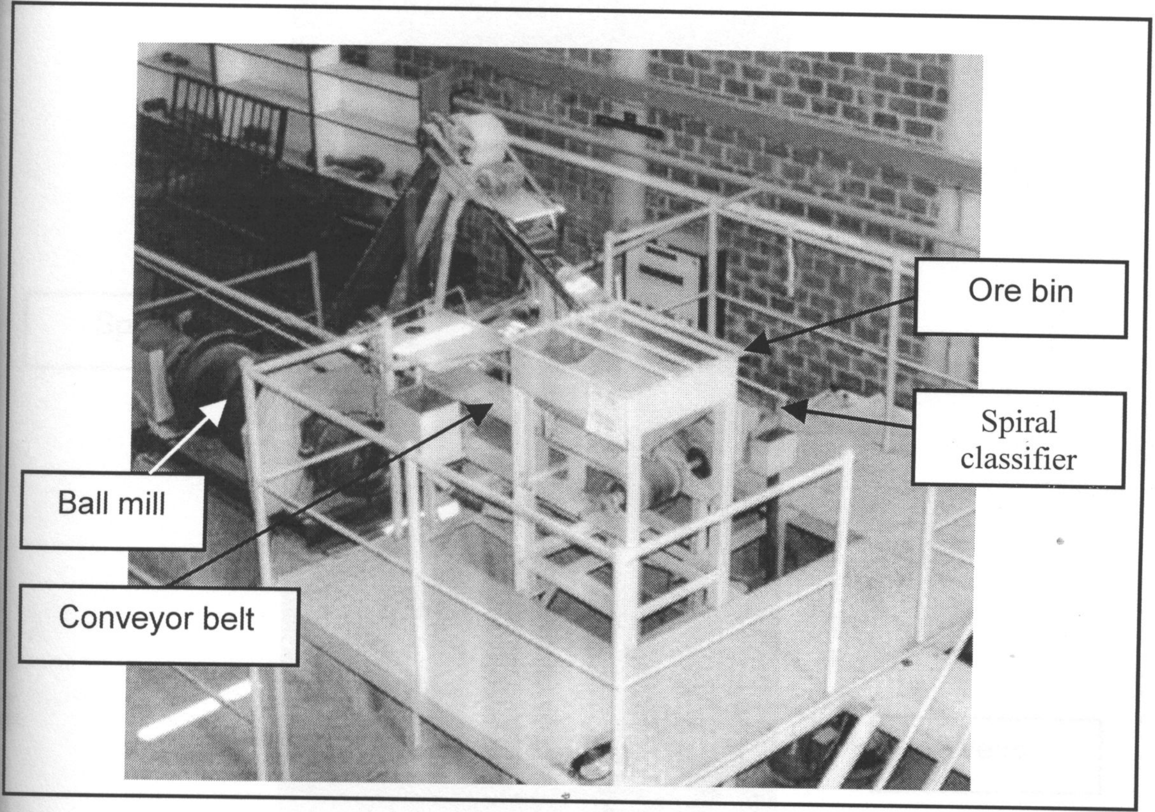

Figure 2.3. A closed grinding circuit pilot-plant at UNZA School of Mines.

The feed rate of the rock was adjusted by raising or lowering the screw gate on the ore bin. Rock feed rate was determined by measuring the weight of a sample collected over a period of 1 minute at the point where the belt discharged the rock into the chute leading to the ball mill. Tap water and classifier underflow streams joined the rock in the chute as it entered the ball mill. The mill product flowed through the trommel screen with dimensions 500mm long and 300mm diameter, with 0.8mm aperture to a Denver vertical pump that delivered the slurry to either a spiral classifier (Figure 2.4) or a hydrocyclone (Figure 2.5).

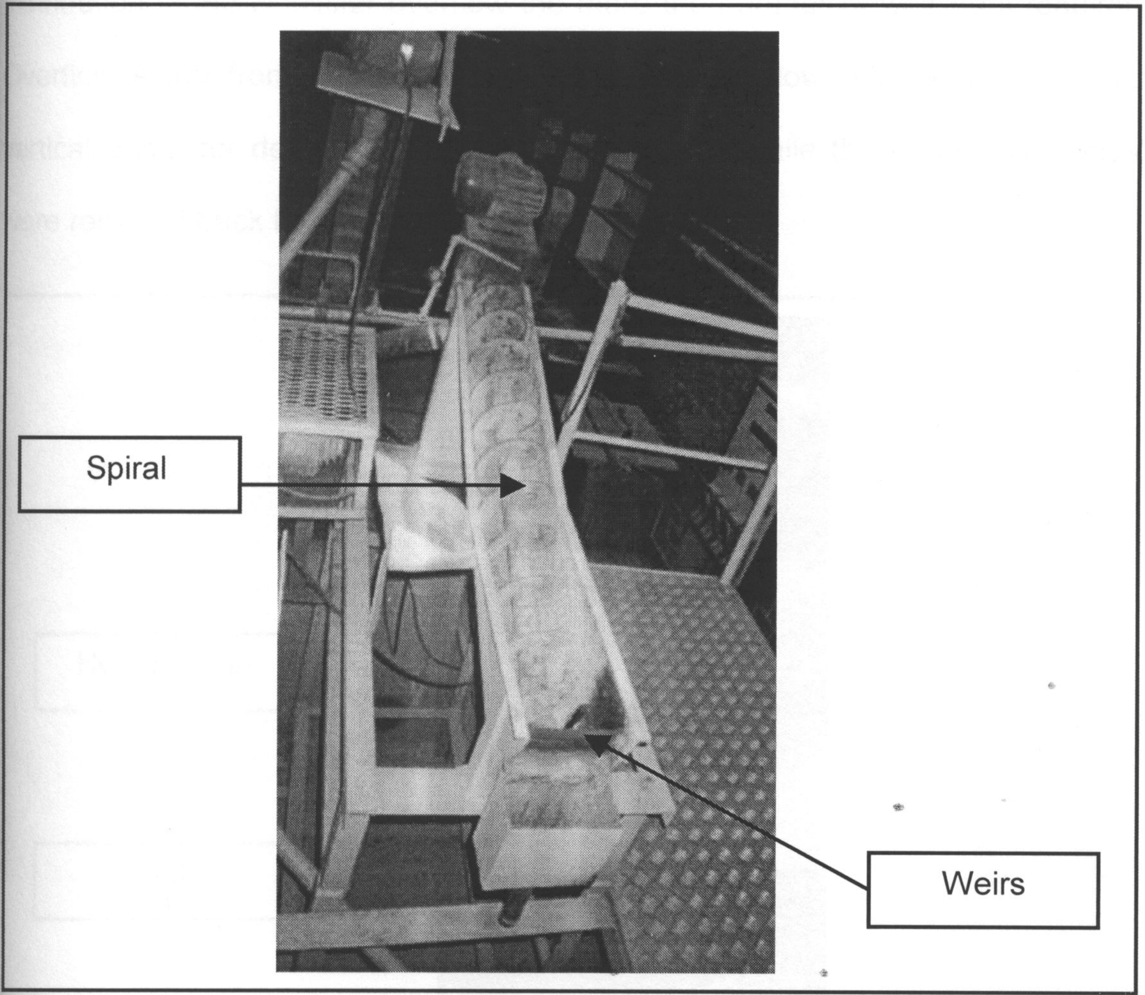

Figure 2.4. A Spiral classifier in closed-circuit with the ball mill at UNZA School of Mines pilot-plant.

The hydrocyclone was 500mm long with a spigot measuring 10mm internal diameter. The Denver type spiral classifier was 500mm long and 82mm diameter. At its overflow side, the classifier carried six weir bars that were used to alter the level or height of the overflow. Each weir bar measured 41mm high. Depending on the desired product size one or more of the weir bars could be used in order to vary the product particle size distribution. The product became finer as the total height of the weir bars increased. Hence, the finer the particle size distribution in the classifier overflow the more the number of weir bars required. Overflow slurry from the classifier or hydrocyclone flowed to another Denver vertical pump for delivery to the dewatering circuit while the underflow (sands) were recycled back to the ball mill for further grinding.

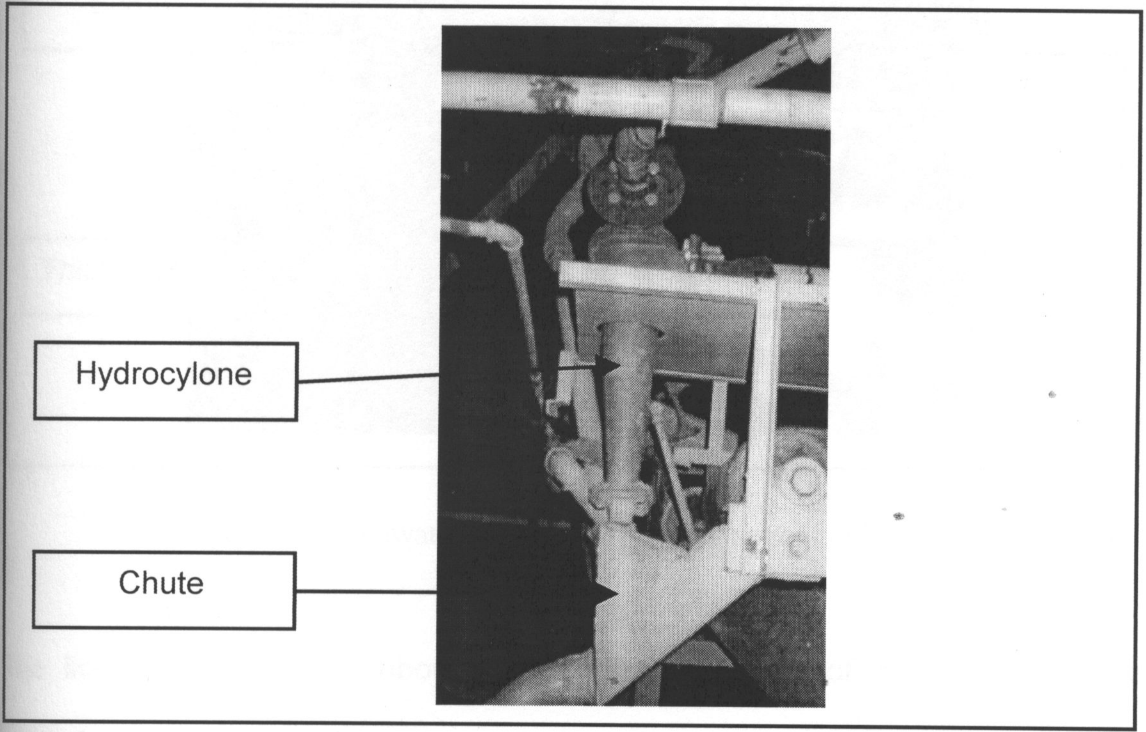

Figure 2.5. A hydrocyclone in closed-circuit with the ball mill at UNZA School of Mines.

2.4 Dewatering

The overflow from either the spiral classifier or hydrocyclone was pumped to a Denver thickener (Figure 2.6) with dimensions, 980mm diameter and 900 mm height where excess water was removed as clear overflow. The thickened slurry was drawn from the conical bottom of the thickener by a diaphram pump to a Denver rotary drum filter of dimensions 350mm length and 500mm diameter.

Control of the slurry level in the filter trough was done manually by switching the pump on and off at low and high levels respectively.

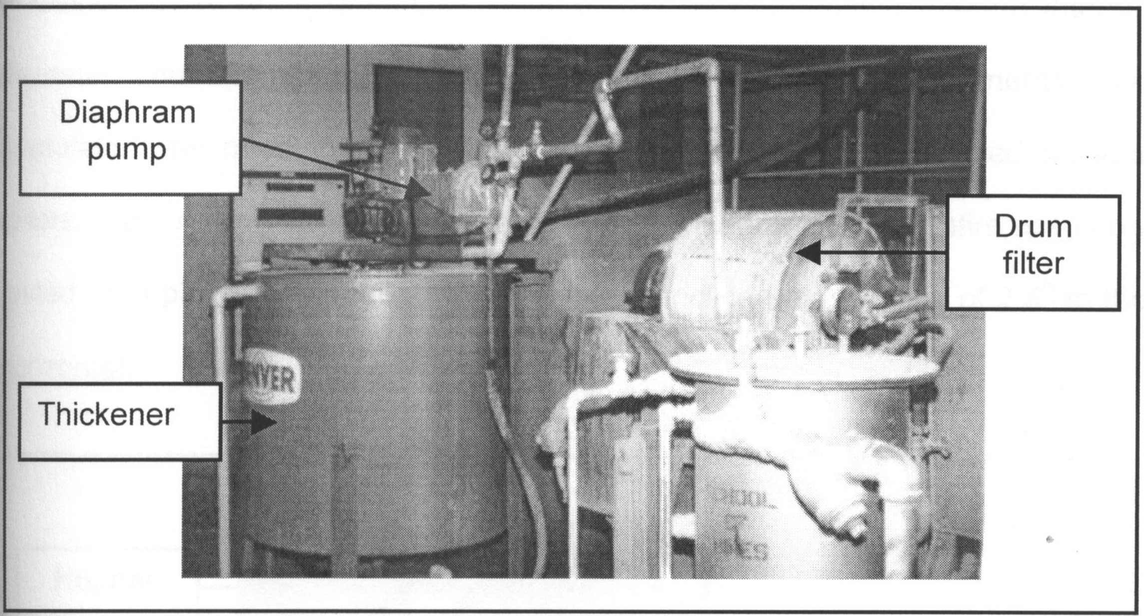

Figure 2.6. A dewatering circuit at UNZA School of Mines.

The filter cake contained about 8-9% moisture. Drying of the filter cake was carried out in an oven. The cake was put on plates and inserted in the oven set at a temperature of 125°C. Dry material consisted of weak aggromerates and these were broken up by simply rolling a metal pipe over them on a flat bench thereby producing fine rock powder suitable for conveyance by a screw feeder.

The fine rock powder was subjected to particle size analysis before it was used in the acidulation experiments. Laboratory sieves used in the particle size analysis were 1180 microns, 850 microns, 600 microns, 425 microns, 300 microns, 212 microns, 106 microns, 75 microns and 53 microns.

2.5 The PAPR pilot plant

2.5.1 The rotary drum granulator

A Leister rotary drum granulator (Figure 2.7) with dimension 380mm internal diameter and 820mm length was used in the acidulation experiments. The granulator was made of a stainless steel shell 10mm thick mounted on four rollers. Each roller was 35mm long and 140mm in diameter. The entire assembly rested on a platform supported by screws and inclined at an angle of 2.5° to the horizontal.

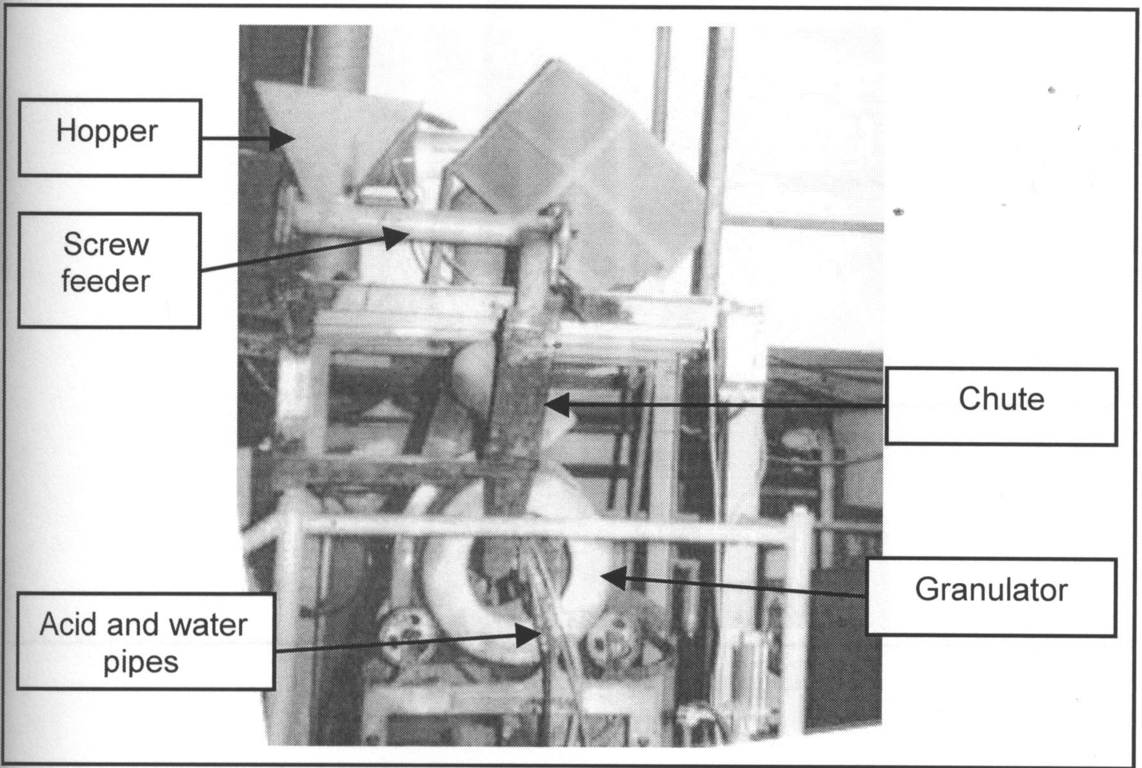

Figure 2.7. A granulator in the PAPR pilot-plant at UNZA School of Mines.

The angle of inclination could be altered by a mechanism of nuts and screws thus changing the residence time of the material in the granulator - as this depended on the angle of inclination at constant rock feed rate. In the interior of the granulator (Figures 2.8 and 2,9) were three 15mm diameter pipes, two for water and one for acid. Each pipe had a nozzle and was connected to a line of compressed air on one end and to water or acid on the other.

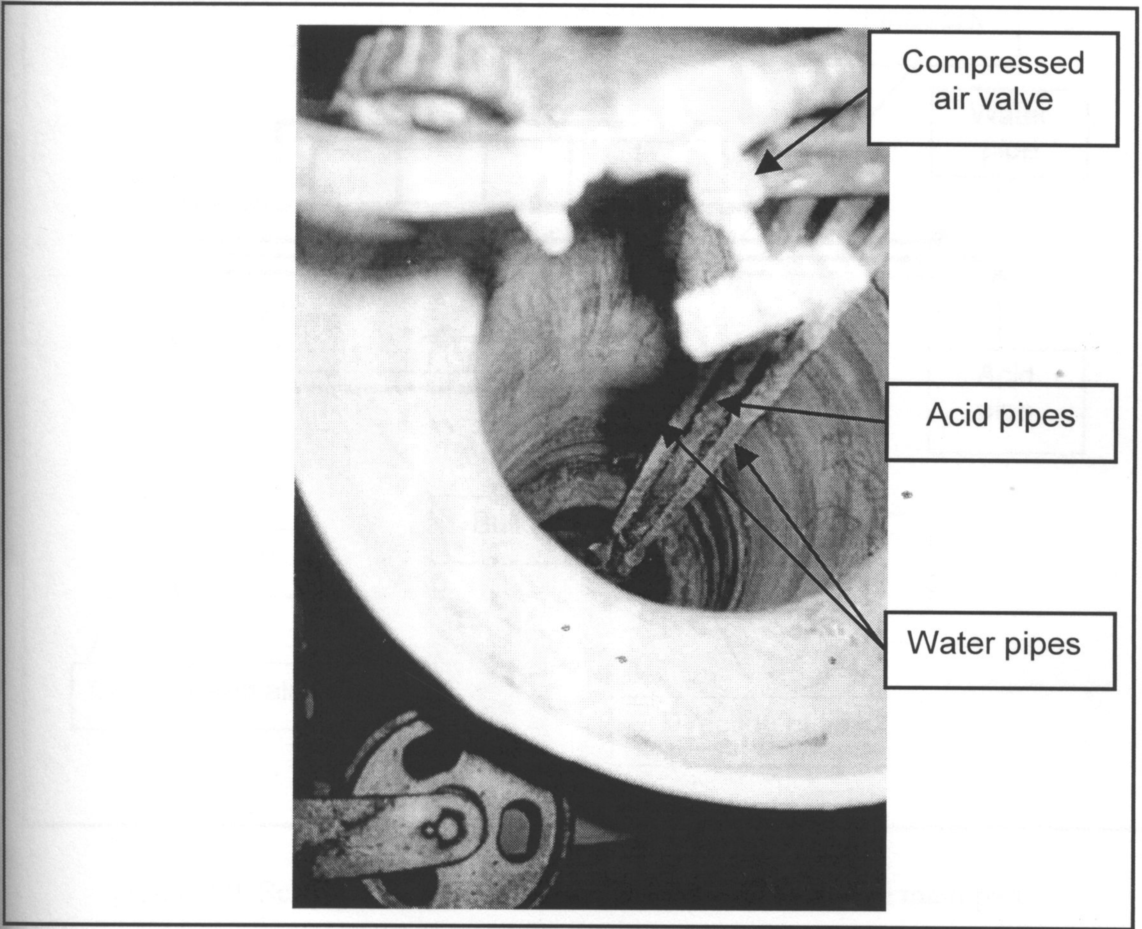

Figure 2.8. The interior of the granulator.

The compressed air forced liquid to go out of the nozzles in the form of a fine spray. Flow rates of water and acid were obtained from flow meters fitted on the respective tubes. The acid flow rate was determined by measuring the volume of acid collected in a measuring cylinder over a period of 1 minute at a given reading on the acid flow meter. A pneumatically operated scrapper moves to and fro inside the granulator. Its function is to remove any sticking PAPR granules from the wall (build up) in order to maintain a constant volume in the granulator.

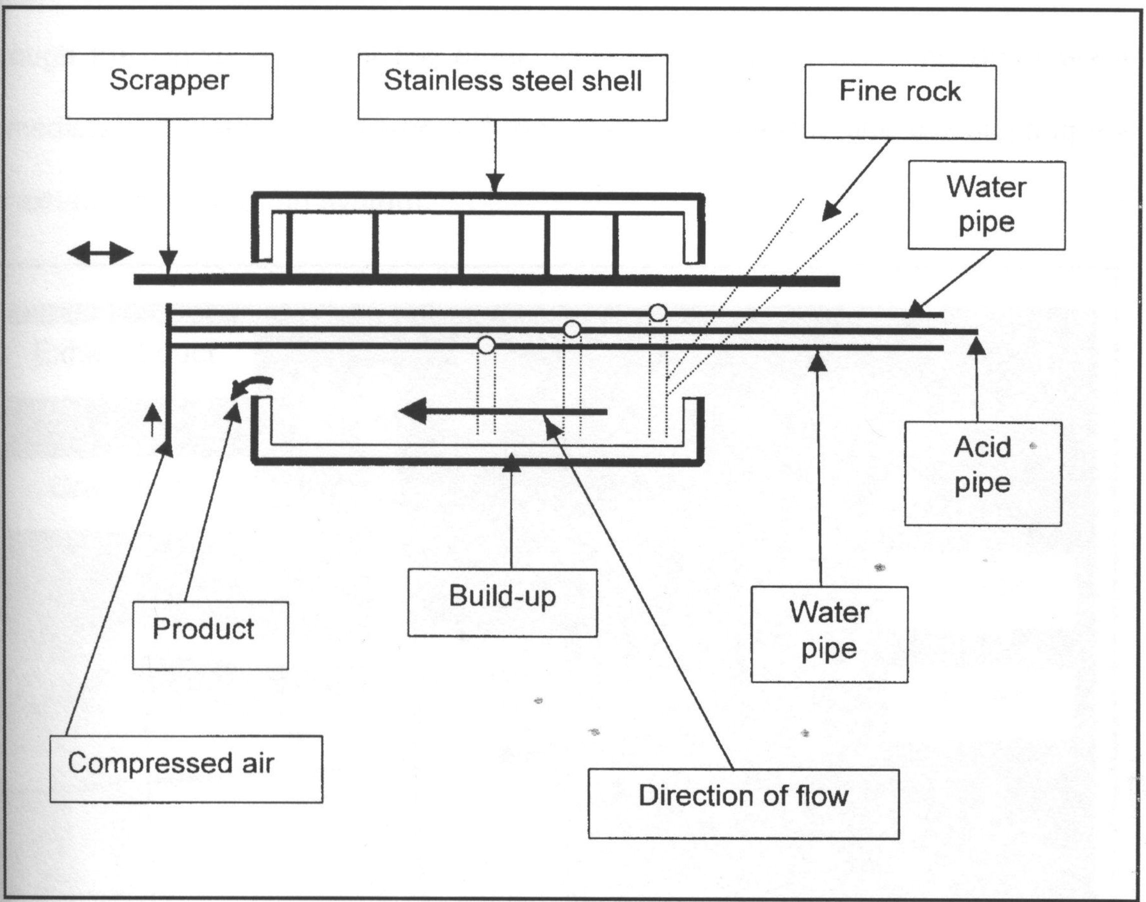

Figure 2.9. Schematic diagram of the granulator showing the main parts.

2.5.2 The rotary drum dryer

A Leister rotary drum dryer (Figure 2.10) was used in the drying of PAPR. The dryer was made of a 10mm thick stainless steel cylindrical drum 2080mm meters long and 350mm diameter. The drum was mounted on six rollers each with dimensions 35mm long and 140mm diameter and inclined towards the discharge end. The dryer was heated by an externally mounted Leister electric heater. The heater had two main parts, a blower and a heating chamber. Atmospheric air was sucked by the blower and forced through the heating chamber where its temperature was increased to a set point. Hot air from the heating chamber blew through the whole length of the dryer while waste gases from the dryer were immediately sucked and transported to the atmosphere out side the building via an exhaust duct and fan system.

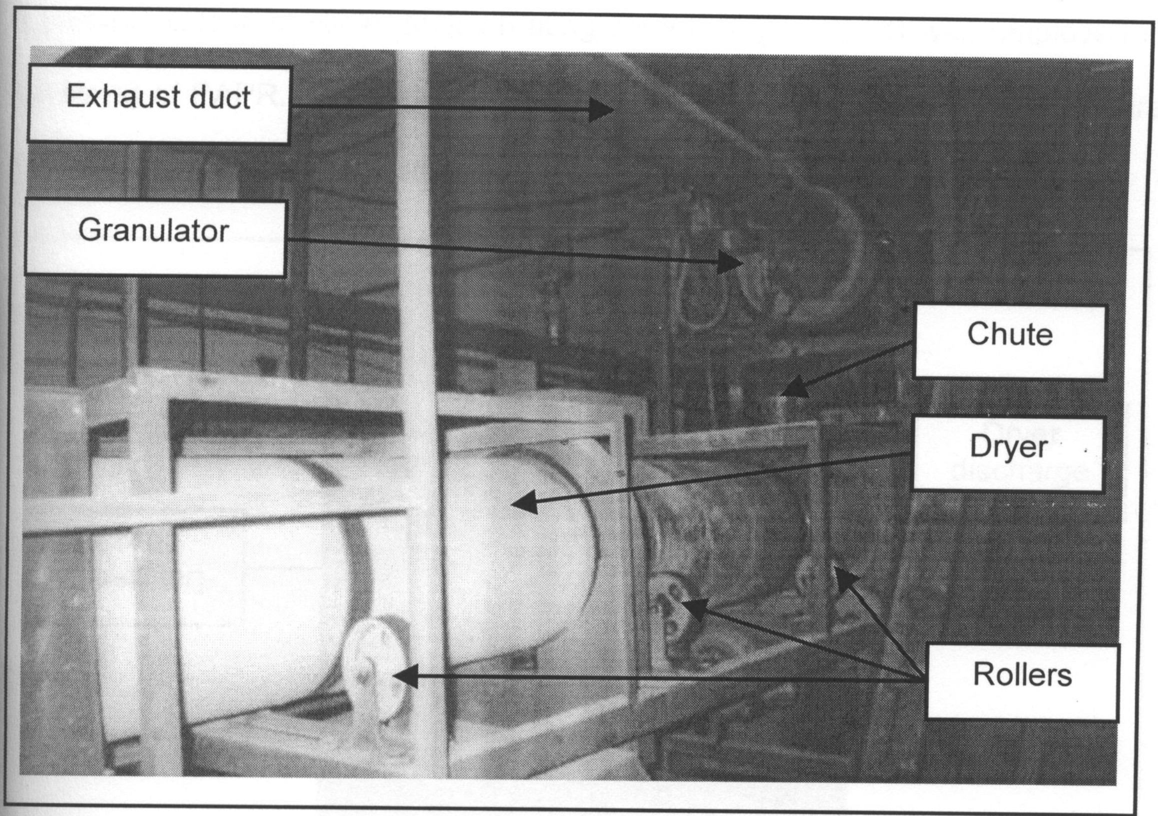

Figure 2.10. A rotary drum dryer in the PAPR pilot-plant at UNZA School of Mines.

The exhaust duct was essential in clearing the working environment of the toxic emissions such as fluorine gas and dust arising from the process. Inside the dryer were hammers that helped to remove any build-up of material from inside.

PAPR granules produced in the granulator entered the dryer via a chute and flowed co-currently with hot air. Heat flowed from the hot air to the granules resulting in the driving away of moisture from the granules. At constant throughput, the level of moisture in the dry PAPR granules depended on drying temperature.

2.5.3 The triple deck vibrating screen

A portable Gilson multiple deck vibrating screen (Figure 2.11) was employed in the sizing of PAPR. The multiple deck was fitted with two screens made of wire mesh 630mm long and 430 mm wide. Aperture sizes of the top and lower deck

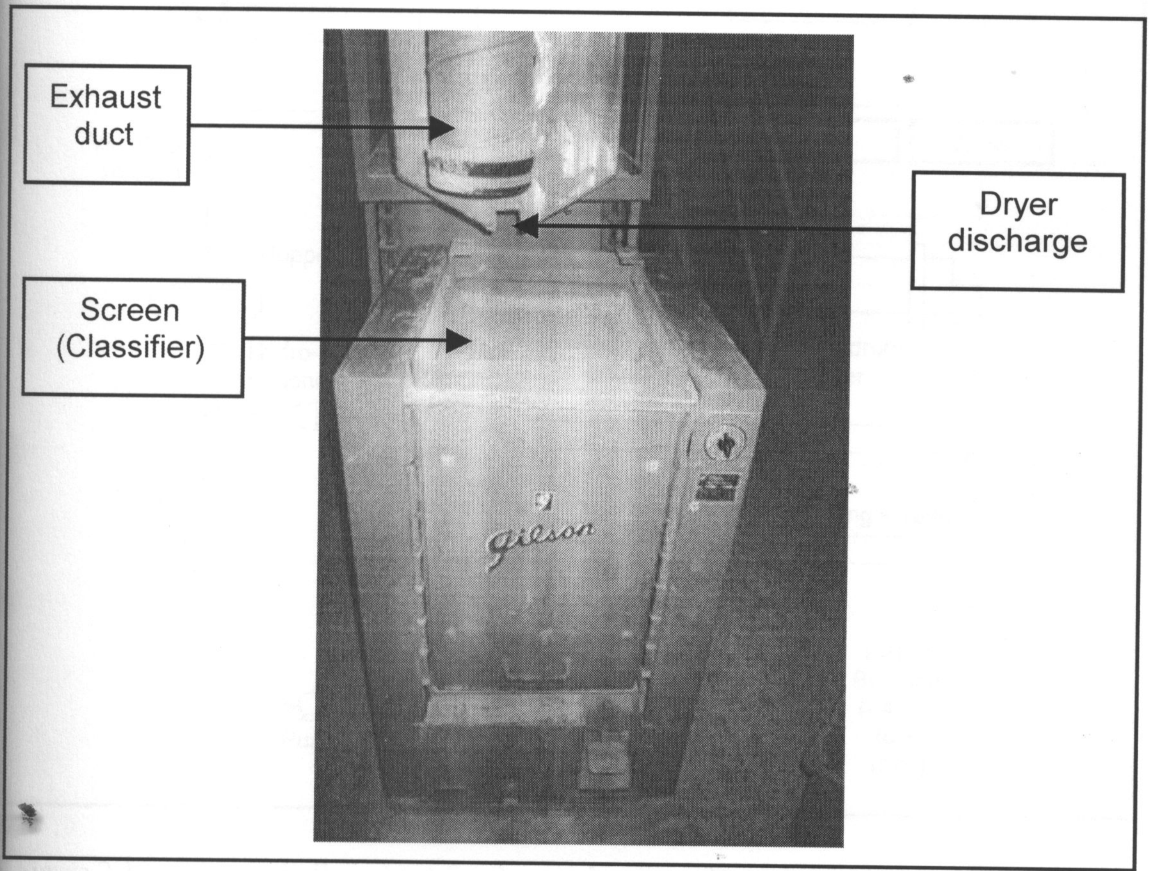

Figure 2.11. A Gilson multiple deck vibrating screen in the PAPR pilot-plant.

screens were 4mm and 1mm respectively. This resulted in the final product being in the size range –4mm to +1mm. The +4mm size fractions were sent to the crusher while the –1mm fraction was recycled to the granulation stage. Figure 2.12 shows the overall stages in the production of PAPR in the School of Mines.

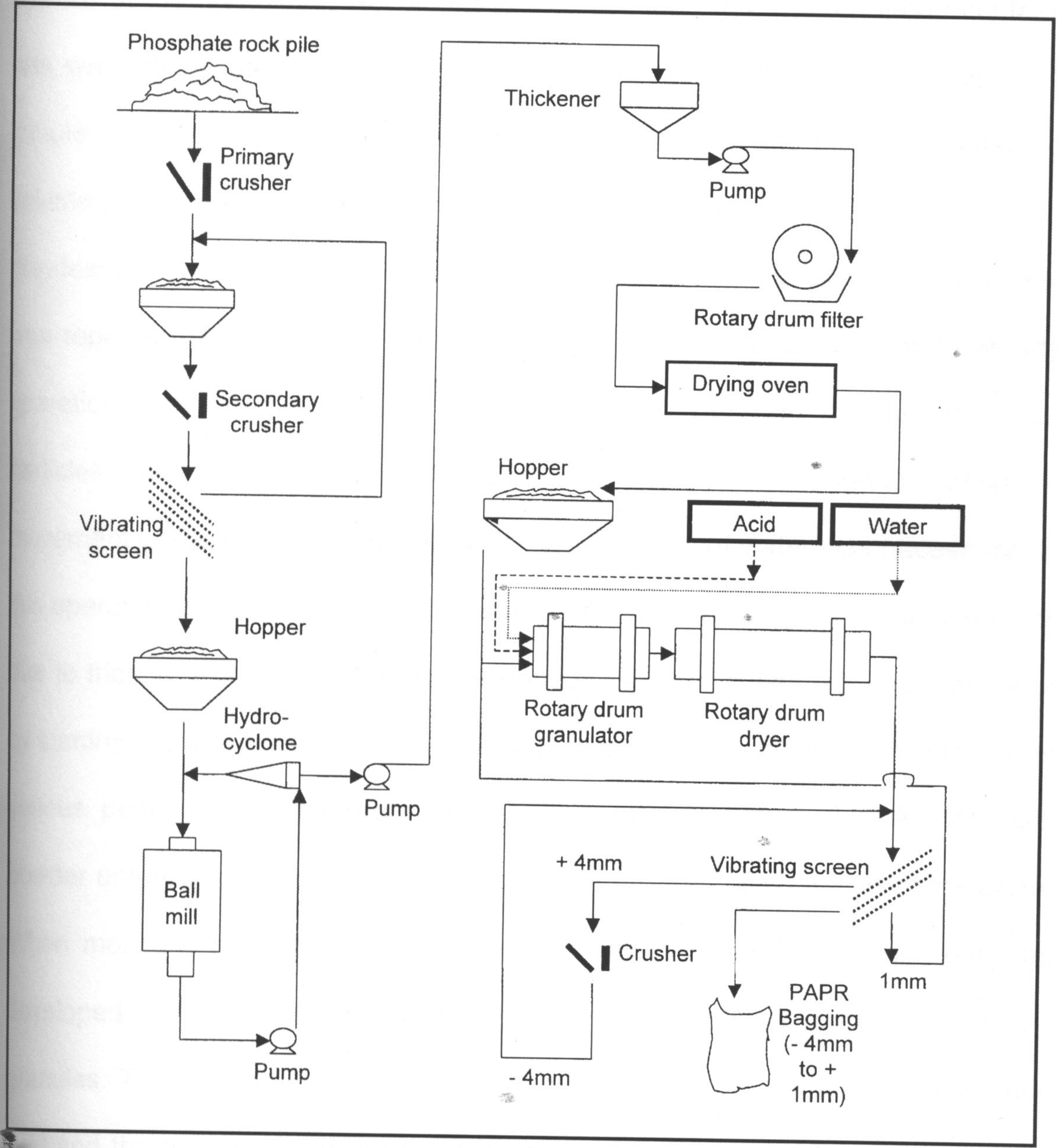

Figure 2.12. Schematic flowsheet for the production of PAPR in the School of Mines.

2.6 PAPR production process description

Operation of the PAPR pilot-plant always began with warming the dryer until the desired temperature was attained. After attaining the desired temperature, the dryer was switched on to start its rotary motion and compressed air lines were opened at the granulator. According to the rock feed rate the required acid feed rate was set by measuring the volume of acid collected from the nozzle in 1 minute. The valve was used for adjusting the acid flow rate until the measured volume was equal to the desired value. The flow meter reading corresponding to the desired flow rate was noted and maintained during the operation. The test was repeated several times to ensure the correct acid feed rate before steady operation could begin. Water was introduced in order to moisten the rock particles. The calculated amount of water was normally not enough to sustain the movement of the scrapper. Hence, an excess amount of water was necessary for this operation to work. Inadequate water resulted in the scrapper becoming stuck due to friction. Rock powder from the hopper was introduced into the granulator by starting the screw feeder. Sulphuric acid and water sprays were maintained at various points inside the granulator as illustrated in Figure 2.9. As the rock powder entered the granulator, it was subjected to the rolling action of the drum. When moisture was introduced by the first spray the individual rock particles developed some degree of plasticity causing them to start agglomerating into granules. The rolling bed of granules soon passed below the spray of sulphuric acid and the reaction between the rock and the acid started. The second water spray served to increase the amount of liquid phase in the bed resulting in the increase in granule sizes. At the discharge end of the granulator the granules overflowed the circular opening into the dryer chute and entered the rotary drum dryer. The dry granules were discharged onto the multiple deck vibrating screen. Sampling of PAPR for analysis was done by collecting the product from the dryer before sieving. The freshly produced PAPR was then allowed to remain overnight before assaying could start. During assaying the PAPR sample was crushed and split to approximately 200g each. The split samples were pulverized and analyzed for total P_2O_5, water-soluble P_2O_5 and Neutral Ammonium Citrate (NAC)-soluble P_2O_5. The sampling point is shown in Figure 2.13.

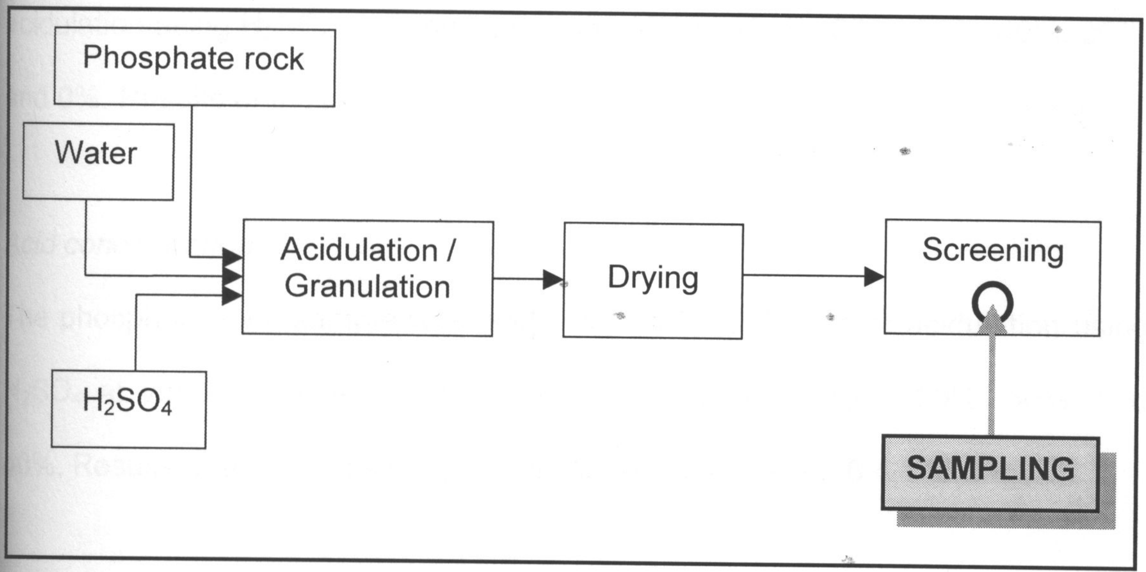

Figure 2.13. Experimental flowsheet for PAPR production and sampling.

2.6.1 Experiments for the optimization of process variables

Particle size of phosphate rock

Phosphate rock was ground to the following particle size distributions:

(1) 79% minus 75 μm

(2) 62% minus 75 μm

(3) 51% minus 75 μm

(4) 42% minus 75 μm

Each of the above samples were acidulated to 50% degree of acidulation using H_2SO_4 at a concentration of 70%. Results of these tests are given in Appendix B Tables 6.2.1 to 6.2.12.

Degree of acidulation

The phosphate rock sample was acidulated to the following degrees of acidulation using H_2SO_4 at a concentration of 70%, 100%, 80%, 60%, 40%, 20%, and 0%. Results of these tests are given in Appendix C Tables 6.3.1 to 6.3.8.

Acid concentration

The phosphate rock sample was acidulated to 50% degree of acidulation using H_2SO_4 at various concentrations including, 98%, 80%, 70%, 60%, 50%, and 40%. Results of these tests are given in Appendix D Tables 6.4.1 to 6.4.8.

Acid concentration and temperature

H_2SO_4 concentrations of 50%, 70%, and 98% and initial temperatures of 25°C, 50°C, 80°C, and 110°C were used to acidulate phosphate rock to 50% degree of acidulation. Results of these tests are given in Appendix E Tables 6.5.1 to 6.5.14.

Residence time of phosphate rock in the granulator

The residence time of phosphate rock in the granulator was varied by changing the angle of inclination as follows:

(1) 2^{o} (7 minutes)

(2) 5^{o} (5 minutes)

(3) 10^{o} (3 minutes)

(4) 15^{o} (1 minute)

Results of these tests are given in Appendix F Tables 6.6.1 to 6.6.6.

Drying temperature

PAPR from the granulator was dried at the following temperatures:

(1) $90^{o}C$

(2) $120^{o}C$

(3) $150^{o}C$

Results of these tests are given in Appendix G Tables 6.7.1 to 6.7.4.

2.7 Determination of the experimental RTD curves

2.7.1 RTD for the closed comminution circuit

The Residence Time Distribution (RTD) curves for the closed comminution circuit were obtained by using a tracer of sodium chloride (NaCl). Figure 2.14 shows the flowsheet for the experimental determination of the RTD in the closed comminution circuit. In each excursion, 200 ml of 50g/l NaCl solution was injected instantaneously into the ball mill inlet and the stop watch was simultaneously started.

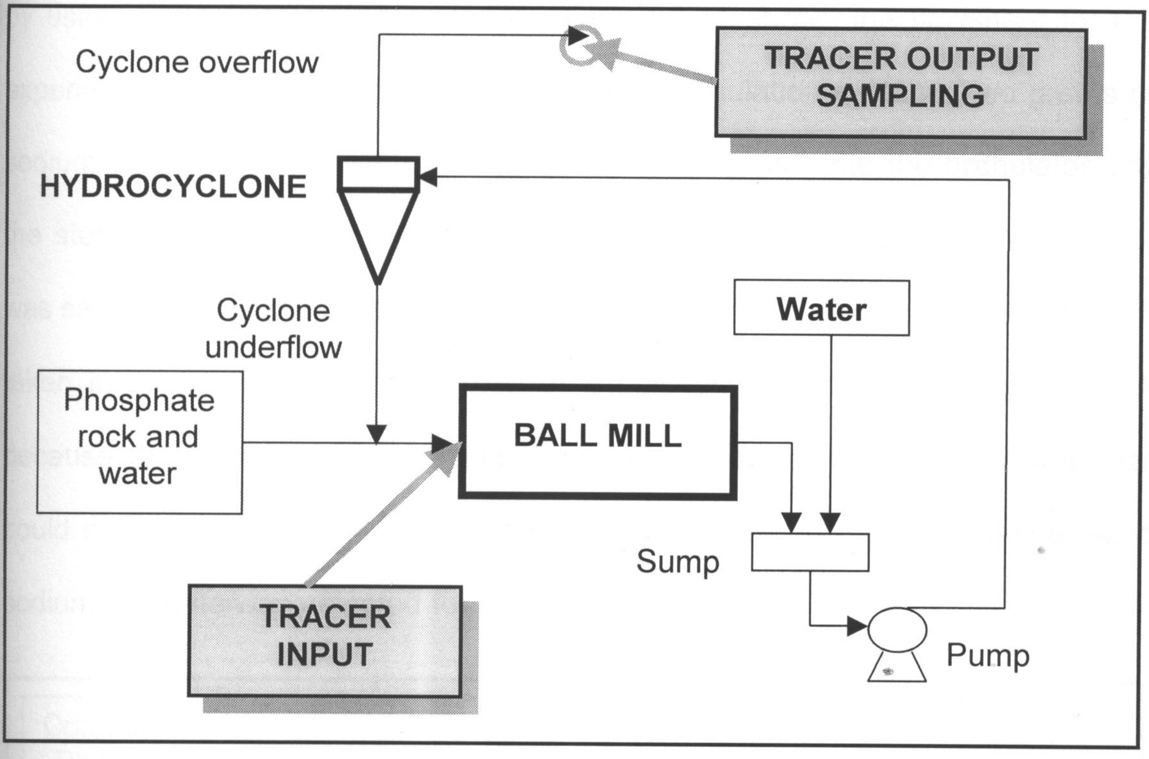

Figure 2.14. Flowsheet for the experimental determination of RTD in the closed comminution circuit at UNZA School of Mines.

The hydrocyclone overflow slurry was sampled after every 15 seconds using 100ml plastic bottles. About 60 samples were taken in each run to ensure that there was no tracer remaining in the system. Every sample was filtered into a 50ml plastic bottle and the filtrate was analyzed for chloride content using the method given in section 2.9 of this chapter. The percent chloride content was then converted to percent sodium chloride and the data was used to determine the RTD curve according to the method given in section 2.7.3. Results of these tests are given in Appendix H Tables 6.8.1 to 6.8. 7.

2.7.2 RTD for the granulation system

The Residence Time Distribution (RTD) curves for the granulator were obtained by using a tracer of sodium sulphate. Figure 2.15 shows the flowsheet for the experimental determination of the RTD in the granulation system. Two grams of sodium sulphate grains were introduced instantaneously into the granulator and the stop watch was started simultaneously. The product leaving the granulator was sampled at intervals of 30 seconds into plastic bags. About 50 samples were taken in each experiment. The use of a solution as a tracer did not go well because the area where the solution landed simply formed one big lump that could not trace the actual path of the granules in the rolling bed. Hence, solid sodium sulphate was selected for the operation.

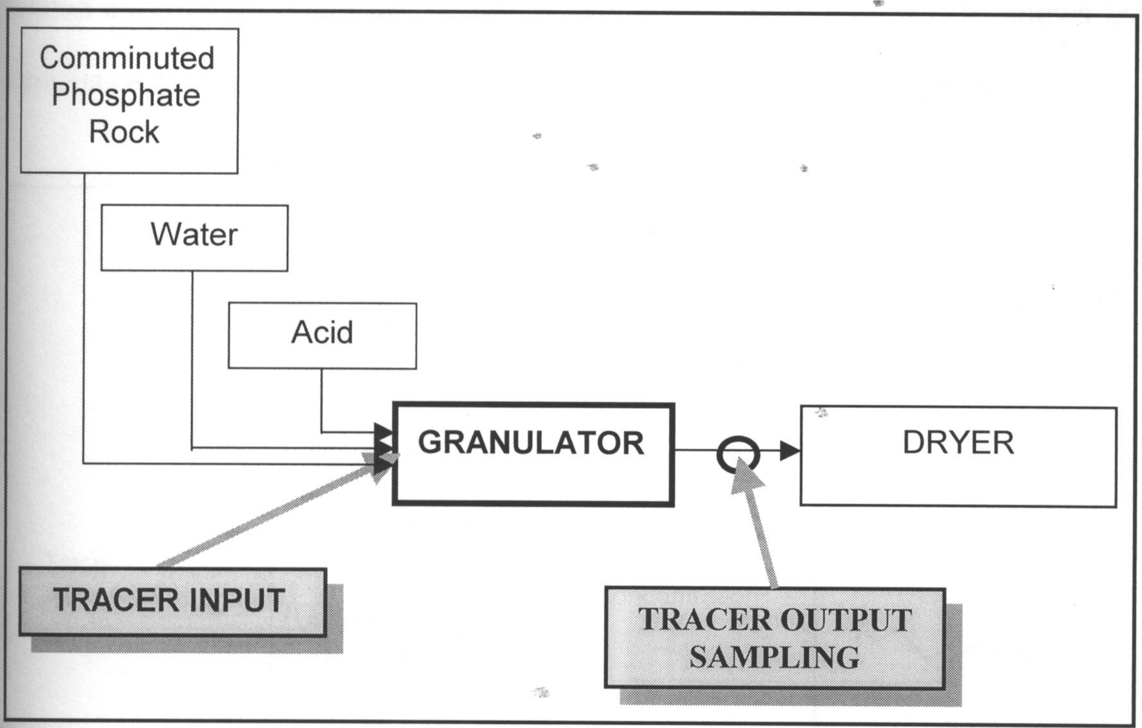

Figure 2.15. Flowsheet for the experimental determination of RTD in the granulation system at UNZA School of Mines.

Each individual sample was crushed, weighed, mixed with 100ml of water followed by shaking for 30 minutes and filtration into a 100ml plastic bottle. Analysis of sodium in the individual filtrates was done by atomic absorption spectrometer. Results of time against percent sodium sulphate were used to calculate the RTD of the system according to the procedure given in section 2.7.3. Results of these tests are given in Appendix I Tables 6.9.1 to 6.9.2.

2.7.3 Procedure for the calculation of RTD curve

A number of experimental techniques are used to characterize the extent of non-ideality of flow in a reactor. In all such experiments, flow is disturbed and its response to the stimulus is recorded. An analysis of the response gives the desired information about the system [Levenspiel, 1972]. Figure 2.16 shows the stimulus-response techniques commonly used to study flow in vessels.

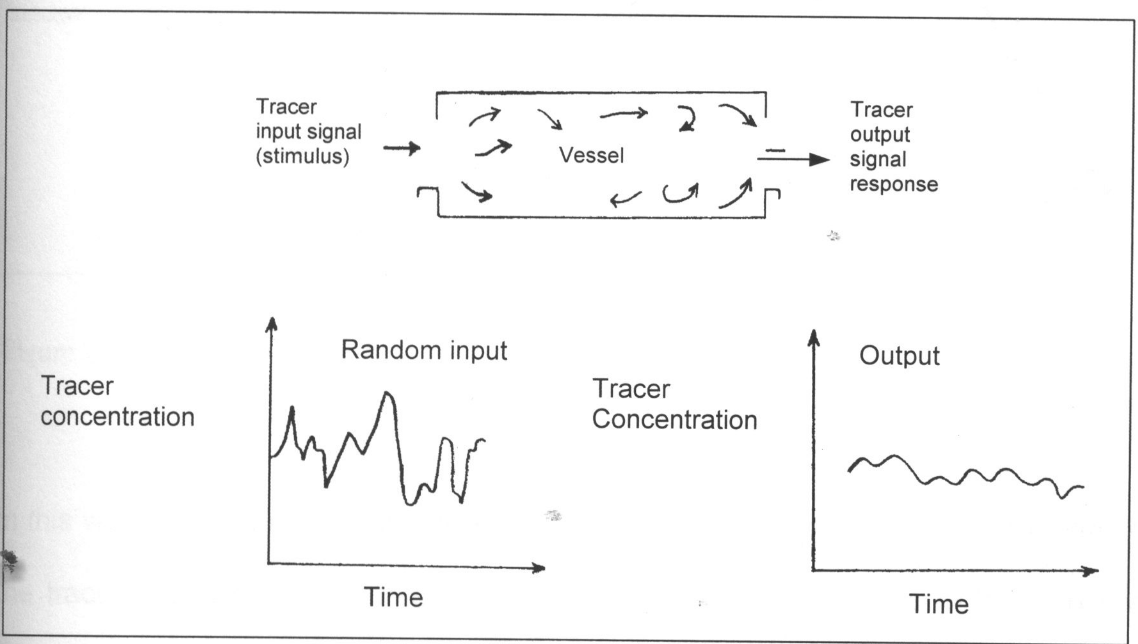

Figure 2.16 Stimulus –response techniques commonly used to study flow in vessels.

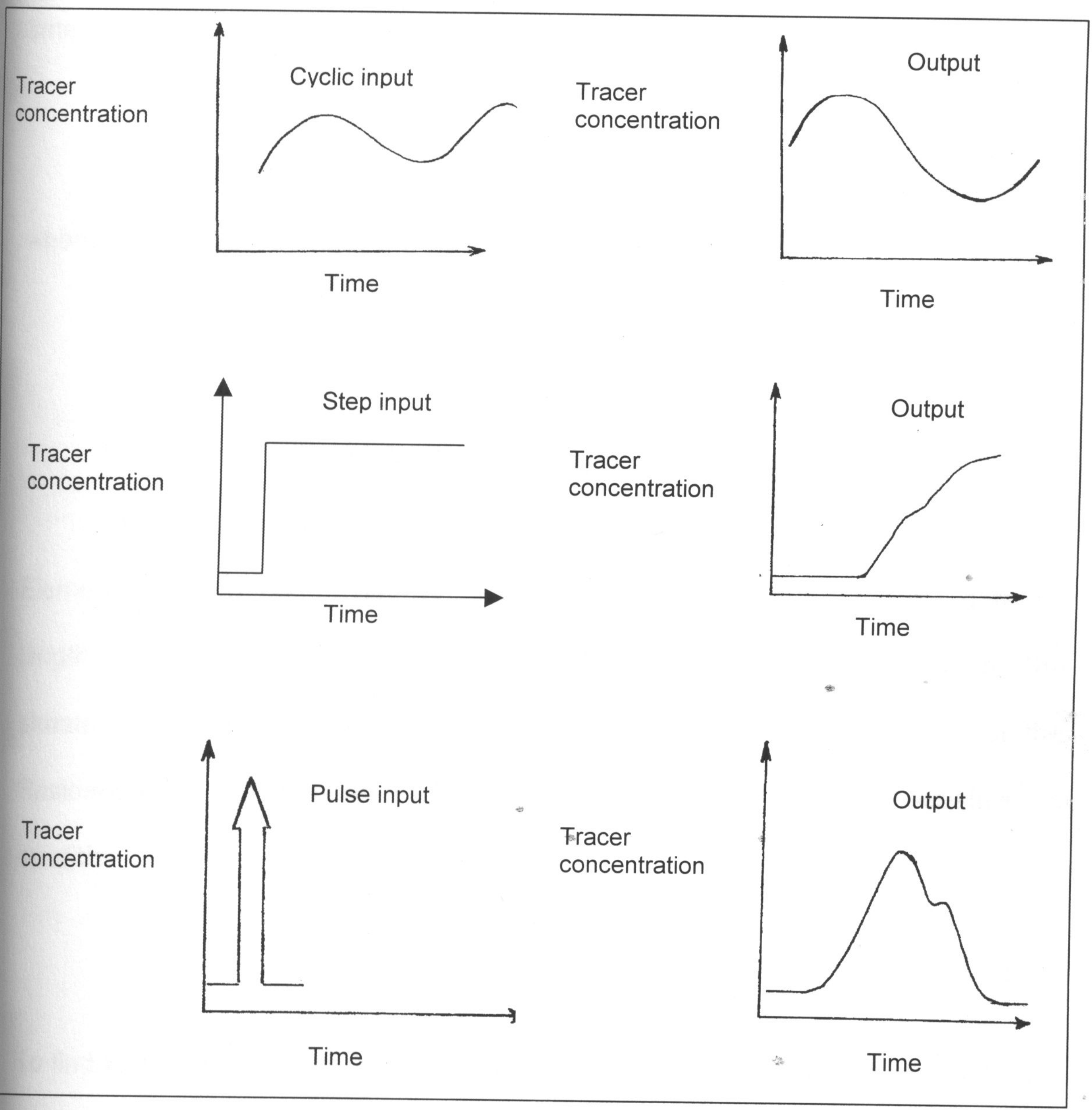

Figure 2.16 continued

In this work, the type of stimulus technique applied was the pulse input in which the tracer was introduced into the system as an instantaneous pulse and the response was recorded in the form of a concentration time curve. The method of determining a Residence Time Distribution (RTD) curve from the concentration time curve has been given by [Levenspiel, 1972].

$$Q = \sum_{i=1}^{k} C_i \, \Delta t \qquad 2.1$$

where Q = total area under the concentration time curve

$$MT = \frac{\Sigma ti \Sigma i}{\Sigma i}$$

C_i = concentration at discrete times (g/l)

Δt = time intervals

Elements of fluid taking different routes through the reactor require different lengths of time to pass through the vessel. The distribution of these times for the stream of fluid leaving the vessel is called the exit age distribution E, or the Residence Time Distribution (RTD) of the fluid. The normalized RTD satisfies the condition:

$$\int_0^{\infty} E dt = 1 \qquad 2.2$$

To find E, the area under the concentration time curve must be unity; hence the concentration readings must be divided by Q, giving

$$E = C_i / Q \qquad 2.3$$

The mean (μ_T)

For discrete measurements

$$\mu_T = \sum t_i E_I \Big/ \sum E_I \qquad 2.4$$

Dimensionless time units (θ)

In treating residence time distribution models it is convenient to measure the time in units of mean residence time. This gives:

$$\theta = t/\mu_T \text{ and } d\theta = dt/\mu_T \qquad 2.5$$

where μ_T is the mean residence time.

The dimensionless curve based on θ is denoted by $E(\theta)$ in this work.

2.8 Sample preparation for size sorting assays

Several boulders of approximately 200kg of Chilembwe phosphate rock sample were crushed to –6mm and split with a Johns Riffle to 10kg packs. Using a 2mm laboratory sieve, one of the 10kg samples was sieved to –2mm. The + 2mm size fraction was crushed with a laboratory jaw crusher and sieved again on the same sieve. This was repeated until the entire sample passed the 2mm sieve. The –2mm sample was again split with a riffle to obtain three sets of about 300g each. Each of the –2mm rock sample was sieved on a pack of 11 laboratory sieves including; 1400μm, 1180μm, 850μm, 600μm, 425μm, 300μm, 212μm, 150μm, 106μm, 75μm, and 53μm. The size fractions obtained were individually analyzed for their percent P_2O_5. Results of these tests are given in appendix A.

2.9 Determination of sodium chloride in the samples

The Mohr method was used to analyze for sodium chloride in the filtrates obtained from tracer tests [Snell, 1970, Young, 1971]. In this method silver combines with chlorine in the presence of a chromate ion preferentially; so long as soluble chloride is present the silver chromate formed initially is decomposed. When all the chlorine has combined with silver, an excess of potassium chromate at once forms a red silver chromate, which indicates the end point of the reaction.

The solutions used in the analysis were as follows:

(a) 0.1 N $AgNO_3$ = 17.0 g/l

(b) 0.1 N NaCl = 5.846 g/l

To a sample solution of known volume in a flask four drops of indicator solution, potassium chromate ($KCrO_4$) were added to obtain a light green tint. This was titrated against 0.1N silver nitrate solution in a burette with vigorous stirring of the sample until a permanent red tint was obtained. The burette reading for silver nitrate was recorded. 0.1N Sodium chloride solution was now added from a burette until the red tint just disappeared and the burette reading was recorded. The weight in grams of chloride in the sample is given by subtracting the volume of 0.1N NaCl from the volume of 0.1N $AgNO_3$ added to the sample.

Calculation

$$\text{Weight of Cl (g) in the sample} = \text{volume of } AgNO_3 - \text{volume of NaCl} \qquad 2.6$$

Therefore, the weight of NaCl (g) can be calculated by equation 2.7.

$$\text{NaCl (g)} = \left[\frac{\text{Molecular mass of NaCl}}{\text{Molecular mass of Cl}}\right] \text{Cl (g)} \qquad 2.7$$

Hence, the NaCl concentration in g/l can be determined by equation 2.8.

$$\text{NaCl concentration (g/l)} = \left[\frac{\text{NaCl (g)}}{\text{Volume of sample analyzed (l)}}\right] \text{dilution factor} \qquad 2.8$$

2.10 Determination of phosphorus in phosphate rock

Principle

The method used in this work involves the formation of the yellow mixed heteropoly phosphovanadomolybdic acid complex in a 0.8M nitric acid, 0.002M ammonium vanadate, 0.008M ammonium molybdate medium. Phosphorus is determined spectrophotometrically by measuring the absorbance of the complex at 460nm [Elsie, 1982].

Outline

The sample is decomposed with hydrofluoric and nitric acids and the solution is evaporated to dryness. The salts are dissolved in dilute nitric acid and residual fluoride is subsequently complexed with boric acid. Acid-insoluble material is removed by filtration, ignited and fused with sodium carbonate to convert refractory titanium and zirconium phosphates to soluble sodium phosphate. The melt is digested in water and the hydrous oxides of the above elements are removed by filtration. The filtrate is ultimately combined with initial filtrate. The resulting solution is analyzed for phosphorus.

Interferences

Large amounts of Zirconium, thorium and titanium interfere with the analysis because they form insoluble phosphates. However, up to approximately 0.25mg of zirconium, 1mg of thorium or 5mg of titanium can be present during complex formation without producing appreciable error in the phosphorus result.

Interferences from coloured ions – chromium (III), chromium (VI), iron (III), copper (II), nickel and cobalt – is avoided by using an identical aliquot of the sample solution, not treated with ammonium vanadate and ammonium molybdate, as the reference solution.

Up to at least 50mg of aluminium, barium, calcium, magnesium, manganese (II), silicate, alkali metals, beryllium, cadmium, mercury (II), uranium (VI), zinc, lead, silver, molybdate and selenate do not interfere. Germanium and more than 1 mg of arsenic intefere because they form similar heteropoly vanadomolybdic acid or heteropoly molybdate compounds. Tungsten interferes by forming a heteropoly compound with phosphorus, and cerium and tin precipitate as phosphates during complex formation.

Range

This method is suitable for samples containing approximately 0.01% or more of phosphorus.

Reagents

Standard phosphorus solution, 0.2mg/l, was prepared by dissolving 0.4584g of anhydrous di-sodium hydrogen phosphate (Na_2HPO_4)- dried at 105°C for 1-2 hours– in water and diluted to 500ml in a volumetric flask.

Ammonium vanadate solution, 0.25% m/v, was prepared by dissolving 2.5g of ammonium meta vanadate (NH_4VO_3) in about 500ml of water, 20ml of concentrated nitric acid was added and the solution was diluted to 1000ml in a volumetric flask.

Ammonium molybdate solution, 5% m/v, was prepared by dissolving 50g of ammonium molybdate [$(NH_4)_6Mo_7O_{24}.H_2O$] in about 500ml of warm water. The solution was diluted to 1000ml in volumetric flask.

Boric acid solution, 5% m/v, was prepared by dissolving 50g of the reagent in about 800ml of hot water. The solution was cooled and diluted to 1000ml.

Nitric acid, 50% v/v, was boiled to remove oxides of nitrogen.

Procedure

Approximately 0.5g of powdered sample was transferred to a 250ml teflon beaker. 5ml of water was added in order to moisten the sample. 10ml of concentrated HNO_3 was added slowly to decompose any carbonates present. 10ml of HF was added and the mixture evaporated to dryness at low heat on a hot plate. The dried mixture was cooled and water was used to wash down the sides of the teflon beaker. 5ml each of HNO_3 and HF were added and the sample was evaporated to dryness. The sample was cooled once more and 20ml of 50% HNO_3 was added and evaporated to dryness again. Heating the sample was continued for a further 30 minutes in order to expel volatile fuorides. The sample was then cooled and leached with 20ml of 50% oxygen free HNO_3 and 10ml of 5% boric acid solution at low heat on a hot plate. A clear solution was obtained without any precipitate. This was filtered through No.40 Whatman filter paper into a 100ml volumetric flask and made up to the mark with water. The subsequent ignition and fusion procedure by addition of sodium carbonate to the residue was not done due to the absence of residue after dissolution of the sample in the nitric and boric acids solution. A reagent sample blank was carried along the preparation steps.

Measurement

5ml of the blank and sample solutions were transferred to two separate 100ml volumetric flasks. 5ml of concentrated HNO_3 acid were added to each flask. Water was added to bring the volume to approximately 50ml. 10ml of 0.25% ammonium vanadate solution was added. 20ml of 5% ammonium molybdate solution was added followed by the addition of water up to the mark and thorough mixing. A reference sample was prepared by transferring 10 ml of sample solution to a 100ml volumetric flask and adding water only up to the mark. The solution was left to stand for 30 minutes. The concentration was measured at 460nm using the Perkin Elmar VIS / UV spectrophotometer.

2.11 Determination of P_2O_5 in phosphate fertilizers

2.11.1 Determination of total phosphoric anhydride (P_2O_5) in PAPR

This method is applicable to all fertilizers and ground phosphate rock. The appropriate dissolution method has to be followed depending on the characteristics of the fertilizers. About 1.0g sample was transferred to a 250ml conical beaker. 40ml of HNO_3 and 5ml HCl were added. The mixture was boiled gently until the brown films had ceased. The resultant clear solution had a volume of around 15-20ml. The sides of the beaker were washed with water until the volume was about 70ml. Dissolved gases were boiled off and the mixture was cooled to room temperature and then filtered into a 500ml volumetric flask and brought to the mark with water. A 10ml aliquot of this sample transferred to a 100ml volumetric flask and analyzed for phosphorus using the spectrophotometric molybdophosphate method described in section 2.10 under '*measurement*'.

2.11.2 Determination of water-soluble P_2O_5 in PAPR

About 1g sample was weighed into a 250ml conical flask. 100ml of distilled water was added at room temperature. The mixture was put on a shaker and agitated for one hour. The mixture was filtered using No.4 Whatman filter paper into a 250ml volumetric flask and made up to the mark with water [Horwitz, 1965]. A 10ml aliquot of this sample was transferred to a 100ml volumetric flask and analyzed for phosphorus using the spectrophotometric molybdophosphate method described in section 2.10 under '*measurement*'.

2.11.3 Determination of P_2O_5 soluble in neutral ammonium citrate (NAC) solution

Outline

The P_2O_5 soluble in neutral ammonium citrate (NAC) is determined indirectly by first analyzing for the citrate-insoluble P_2O_5. The NAC-soluble phosphate is then calculated by subtracting the water-soluble P_2O_5 and citrate-insoluble P_2O_5 from the total P_2O_5. The method of analyzing for the citrate-insoluble P_2O_5 is described below.

Citrate-Insoluble P_2O_5

Ammonium Citrate solution, Sp. Gravity = 1.09 at 20°C and pH 7 as determined by pH meter. 370g of crystalline citric acid was prepared by dissolving 370g crystalline citric acid in 1.5 litres of water and nearly neutralized by adding 340ml of NH_4OH (28-29%). The solution was cooled and the pH was adjusted to 7 by adding NH_4OH or citric acid. This was stored in a 2.5 litre plastic container. Before use the pH was checked and adjusted to 7 if it had changed.

Method of operation

1g sample of PAPR was weighed into a 250ml conical flask and water-soluble P_2O_5 was removed as described in section 2.11.2. The residue from filtration of water-soluble P_2O_5 was transferred to 250ml conical flask. 100ml ammonium citrate solution at pH 7 was added to the sample and the flask was closed tightly with a stopper. The mixture was shaken vigorously using a mechanical shaker until the filter paper was reduced to pulp. Pressure due to gaseous films was relieved by removing the stopper momentarily. The flask was continuously agitated in a water bath maintained at 65°C. After exactly 1 hour the flask was removed from the water bath and contents filtered with No.5 filter paper. The residue was washed with hot water at 65°C allowing thorough drainage before adding more water until the volume of the filtrate was about 350ml. Filter paper and residue were placed into a 250ml beaker and 30ml HNO_3 and 10ml HCl were added and boiled to the complete discharge of red brown fumes. The solution was cooled and filtered into 250ml volumetric flask and made up to the mark with water [Horwitz, 1965]. A 10ml aliquot of this sample was transferred to a 100ml volumetric flask and analyzed for phosphorus using the spectrophometric molybdophosphate method described in section 2.10 under '*measurement*'.

2.12 Determination of sodium, magnesium, calcium, potassium, and aluminium in phosphate rock

Principle

Aluminium, calcium and magnesium are determined by atomic absorption spectrophotometry in a nitrous oxide-acetylene flame after the addition of a solution of high potassium content to both sample and the calibration solutions [Elsie, 1982].

Outline

The sample is decomposed with hydrofluoric, hydrochloric and perchloric acids. The solution is evaporated to near dryness and the salts are dissolved in dilute hydrochloric acid. The resulting solution is analyzed for sodium, magnesium, calcium, potassium, and aluminium.

Operation method

0.2g sample was weighed into a teflon beaker and moistened with water. 15ml HF was added and the mixture was evaporated to dryness on a hot plate. 2ml of

$HClO_4$ was added and the mixture was evaporated to dryness. Again 3ml $HClO_4$ and 15ml HF were added and the mixture was evaporated to dryness. 2ml of $HClO_4$ were again added and the mixture evaporated to dryness. 10ml of 33% HCl were added and the mixture boiled to dissolve the salts. The resulting solution was filtered through No.40 Whatman filter paper to a 100ml volumetric flask and made up to the mark with water.

For the analysis of Na and Al, a solution of KCl was added to give a final concentration of 2000ppm and for the analysis of Mg and Ca Lanthanum chloride and strontium chloride were added to give a final concentration of 2000ppm each.

Reagents

KCl, 5%, was prepared by transferring 48g of KCl into a 500ml volumetric flask and adding water up to the mark.

SrCl, 5%, was prepared by transferring 42g of $SrCO_3$ into a 500ml volumetric flask, adding 80ml of HCl and diluting to 500ml with water.

LaCl, 5%, was prepared by transferring 29g of La_2O_3 into a 500ml volumetric flask, adding 80ml of HCl and diluting to 500ml with water.

4ml of each of the above reagents contained 2000ppm in 100ml solutions.

2.13 Analysis of sulphur

About 0.5g of sample was weighed into a 500ml beaker. 20ml of potassium chromate-bromine mixture was added and allowed to stand for 15minutes. 15ml of HNO_3 was added and the mixture was allowed to stand for 15 minutes at room temperature. After 15 minutes the mixture was evaporated slowly to dryness on a hot plate. The dry residue was moistened with HCl and again evaporated to dryness in order to dehydrate silica completely. 5 ml of HCl and 50ml of hot water were added and the mixture was boiled and filtered through No.40 Whatman filter paper. The filtrate was diluted to 300ml and boiled. To the hot mixture was added 50ml of 10% BaCl solution. The solution was allowed to stand overnight and then filtration was done using No. 40 Whatman filter paper followed by washing the precipitate with hot 1% HCl and thoroughly with hot water. The filter paper and precipitate were transferred to a porcelain crucible, dried, charred and ignited for 30 minutes at 900°C followed by cooling and weighing of the precipitate [Elsie, 1982].

Reagents

Potassium chromate-bromine mixture was prepared by initially dissolving 16g of $KCrO_4$ in 50ml H_2O. 10ml Br_2 was added and made up to 100ml with water.

10% BaCl solution was prepared by dissolving 10g of salt in water in a 100ml volumetric flask and making up to the mark with water.

2.14 Analysis of iron

Principle

The sample is decomposed with hydrofluoric, hydrochloric and perchloric acids. The solution is evaporated to dryness and the salts are dissolved in dilute hydrochloric acid. The resulting solution is analyzed for iron by atomic absorption spectrometer [Elsie, 1982].

Procedure

0.5g sample was transferred to a 250ml teflon beaker and 20ml of concentrated hydrofluoric acid was added. The mixture was allowed to digest for 30 minutes at room temperature. 10ml each of perchloric and hydrochloric acids were added to the mixture and the resulting solution was evaporated to fumes of perchloric acid. The solution was cooled and 10ml each of water, concentrated hydrofluoric and hydrochloric acids were added and again evaporated to fumes of perchloric acid. Where necessary the addition of hydroflouric and hydrochloric acids was repeated until the decomposition of the sample was complete. The solution was cooled and the sides of the beaker were washed with water. The solution was evaporated again to fumes of perchloric acid. The washing and evaporation was repeated to ensure the complete removal of hydrofluoric acid. The solution was then evaporated until about 1.5ml of perchloric acid was remaining. To this was added 10ml of water and 4ml of 50% hydrochloric acid and the solution was heated gently until the solution became clear. The solution was cooled and transferred to a 100ml volumetric flask and diluted to the mark. The solution was then analyzed for iron by atomic absorption spectrometer.

CHAPTER 3: RESULTS AND DISCUSSIONS

CHAPTER 3

RESULTS AND DISCUSSIONS

3.1 Outline

In this study, process variables optimized for acidulation of Chilembwe phosphate rock included particle size of phosphate rock, degree of acidulation, acid concentration, initial temperature of the rock, water and acid, residence time in the granulator and drying temperature of PAPR. Before optimizing any of the above parameters, tests were conducted in order to determine the particle size at which the apatite could be liberated from the rock matrix. This was done first by measuring the size of the apatite grains in thin sections under an ore microscope followed by carrying out size sorting assays of a rock sample crushed to minus 2000μm.

In order to understand the operations of the main units – that is (i) the ball mill in the comminution circuit, and (ii) the granulator in the granulation circuit, tracer tests were performed to give residence time distribution (RTD) curves. Simulation of RTD was done using the selective recycle model. The number of cycles distribution (NCD) graphs revealed the type of operation that could maintain satisfactory performance of the important units in the process.

The agronomic effectiveness of PAPR was compared with that of commercial mono-ammonium phosphate (MAP). Field trials were conducted the School of Agricultural Sciences.

3.2 Characterization

3.2.1 Microscopic observation

Figure 3.1 shows micrographs of thin sections of Chilembwe phosphate rock samples B and C from No.2 ore body. Sample C indicated that the rock is composed of mainly (~80%) apatite (grey) phenocrysts, with minor (<1%) quartz and hornblende set in a fine-grained crystalline matrix.

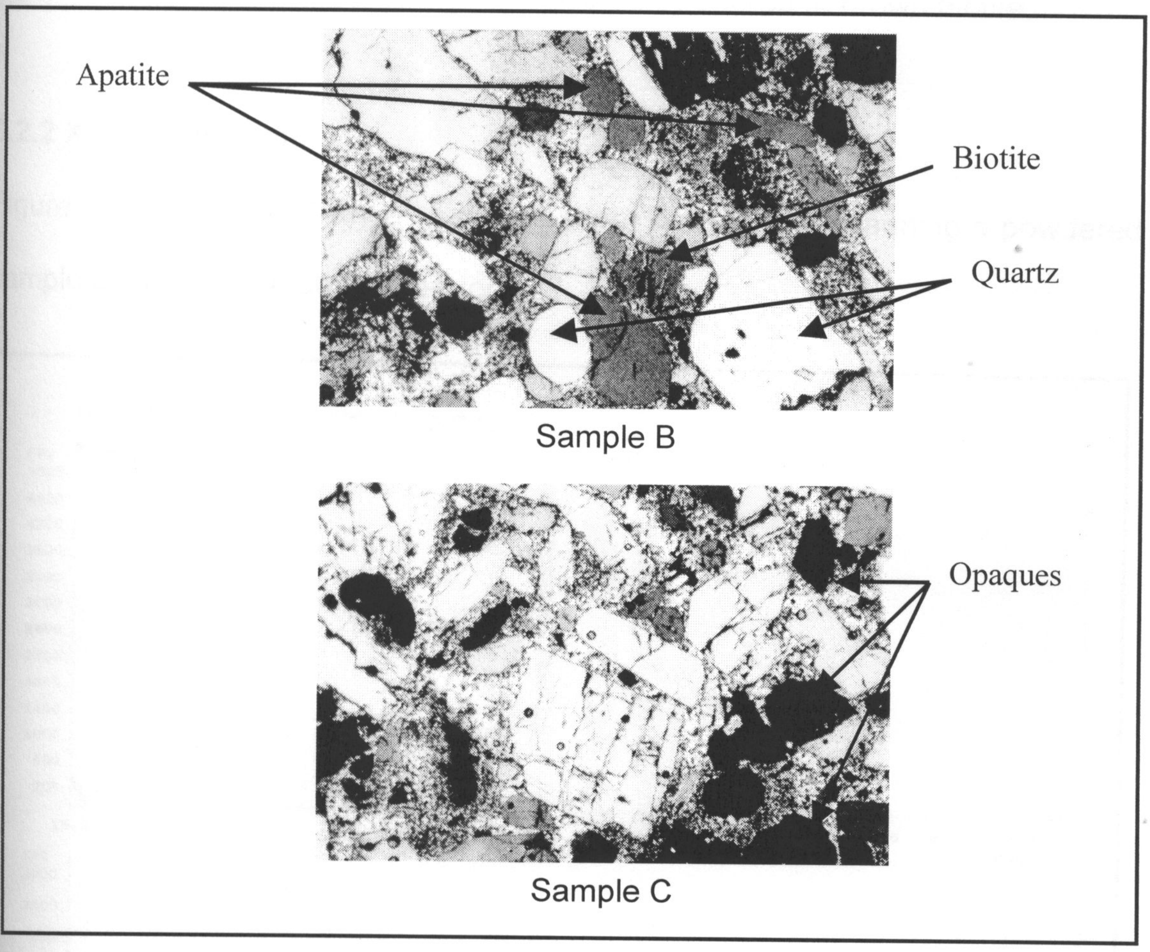

Figure 3.1. Microstructure of Chilembwe phosphate rock samples from ore body No. 2 at x2.5 objective x25 magnification. Field of view = 4400 microns.

Accessory minerals include sphene, opaques and zircon. The apatite phenocrysts range in shapes from subhedral to euhedral, and are up to 4mm in size. Most of the phenocrysts are fractured and fresh. Hornblende occurs as isolated interstitial phenocrysts. Most of the hornblende crystals are partially altered along the margins and cleavage to brown biotite. The matrix is composed of an equiangular intergrowth of mainly feldspar and minor quartz. The feldspars are partly altered on the surface to a brown turbid material. In thin section, sample B is compositionally similar to sample C, except that there is a relatively higher content of hornblende, which is also partly altered to brown biotite.

3.2.2 X-ray diffraction

Figure 3.2 shows the X-ray diffraction pattern obtained by scanning a powdered sample of Chilembwe phosphate rock.

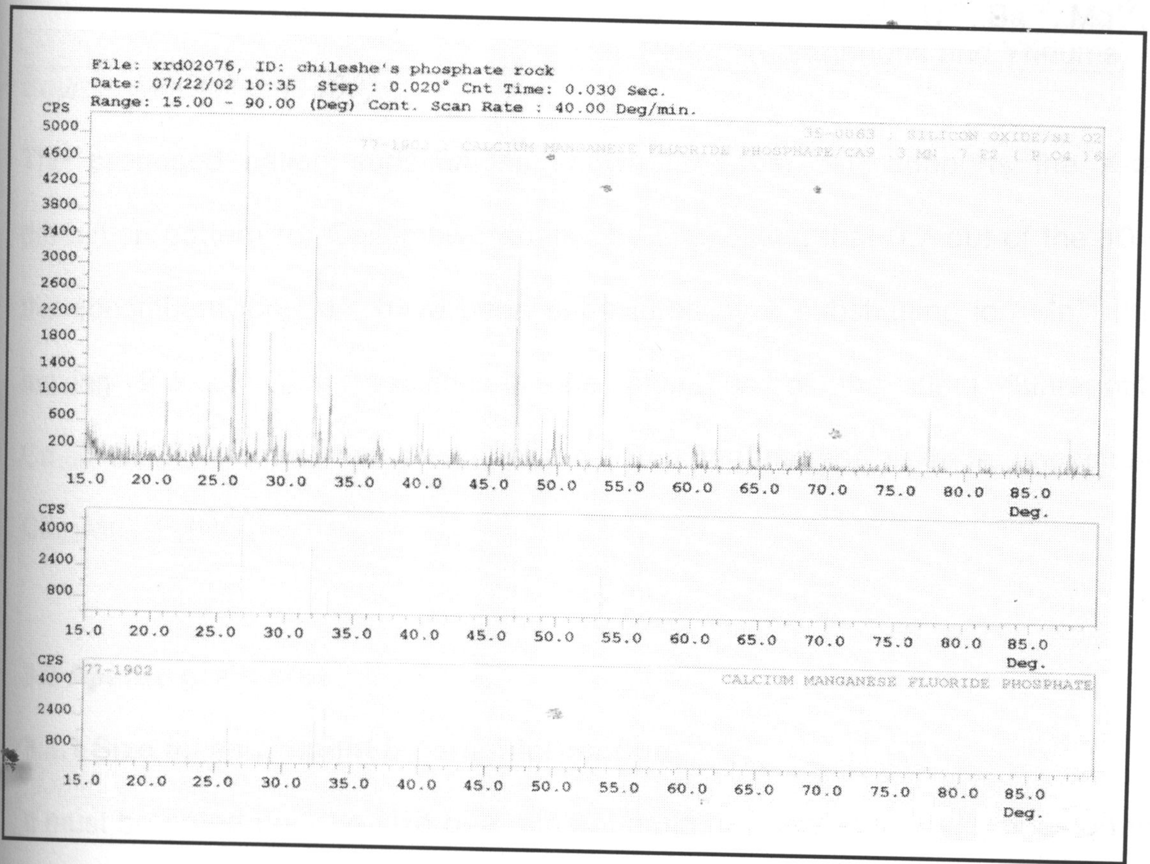

Figure 3.2. XRD pattern for Chilembwe phosphate rock from No.2 orebody.

The X-ray diffraction pattern revealed that phosphorus in the Chilembwe phosphate rock sample exists in the form of calcium manganese fluoride phosphate with the chemical formula $Ca_{9.3}Mn_{0.7}F_2(PO_4)_6$. The other crystalline phase present in the same sample was identified as silicon oxide, SiO_2. Patterns of other apatite structures such as fluorapatite, hydroxyapatite, chloroapatite, and carbonate fuorapatite failed to match the pattern produced by Chilembwe apatite. In the study of the mineralogy of carbonate fluorapatites, McClellan [1980] has referred to some proposed substitutions in the apatite structure as given in table 3.1.

Table 3.1. Some proposed cation substitutions in the apatite structure.

Fluorapatite $Ca_{10}(PO_4)_6F_2$	
Constituent ion	Substituting ion
Ca^{+2}	Na^{+}, Sr^{+2}, Mn^{+2}, K^{+1}, U^{+4}, Ba^{+2}, Mg^{+2}, $RE^{+2,+3}$ (Lanthanons and Yttriums)

Source: McClellan [1980].

The proposed cation substitutions shown in Table 3.1, supports the X-ray diffraction pattern for Chilembwe apatite by suggesting that 0.7 out of the 10 of the constituent ion Ca^{+2} have been substituted by a substituting ion Mn^{+2} thus leaving 9.3 of Ca^{+2} resulting in the alteration of the ideal fluorapatite, $Ca_{10}(PO_4)_6F_2$, to another structure - calcium manganese fluoride phosphate, $Ca_{9.3}Mn_{0.7}F_2(PO_4)_6$.

3.3 Apatite grain size

3.3.1 Size measurement by ore microscope

It must be noted that the size of a mineral grain in a thin section depends on the orientation of that particular grain because the thin section does not present a three dimensional view of the grains. As a result of this problem measurement errors become inevitable when determining the grain size of the mineral. Such errors are minimized by using several thin sections and also by measuring the sizes of many grains in every thin section. In this work three thin sections were used and more than 300 apatite grains were measured. Figure 3.3 shows the frequency of occurrence of the various sizes of apatite in the samples. Measurements showed that the apatite grains are coarse and that they occur mostly in the size range 200 to 1100μm. 600μm is the most frequent size. Lombe [1985] reported an average grain size of apatite of 700μm for samples from the same ore body. In this work, the calculated average grain size was 641μm - close to that reported by Lombe.

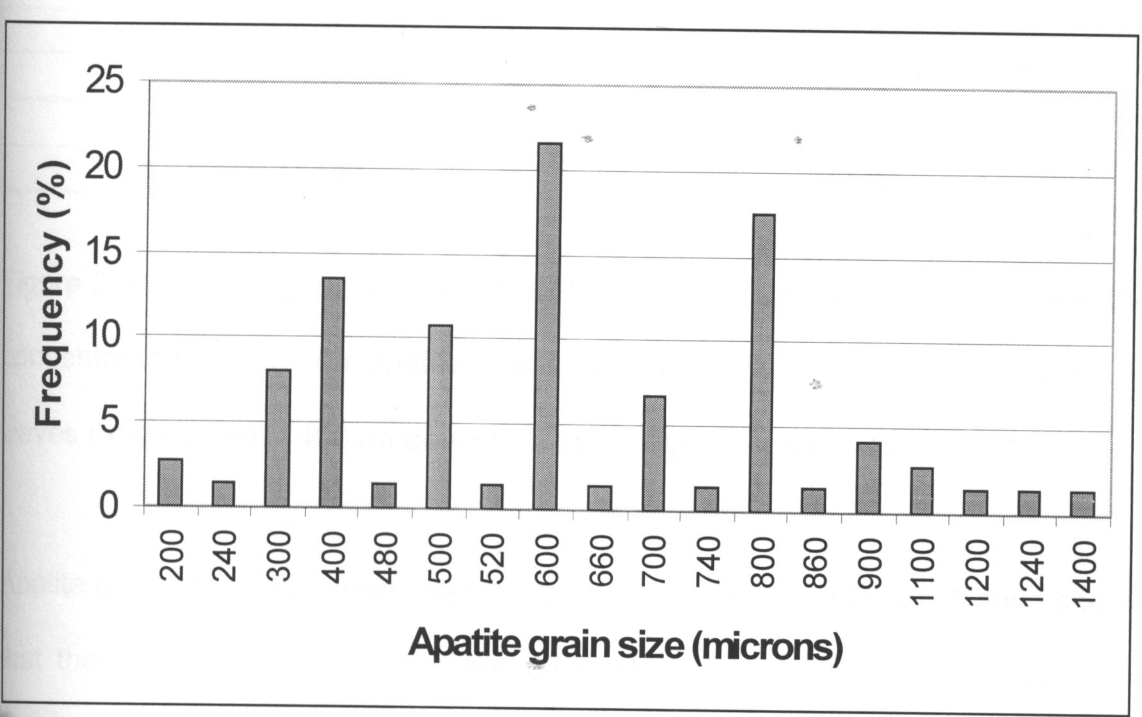

Figure 3.3. Frequency of occurrence of apatite grains of various sizes in three samples of apatite rock from ore body No.2.

3.3.2 Size-sorting assays

Table 3.2 shows the percentage of P_2O_5 in various size fractions of phosphate rock retained by sieving a –2000μm sample assaying 23.2% P_2O_5 on a pack of laboratory sieves: 1400μm, 1180μm, 850μm, 600μm, 425μm, 300μm, 212μm, 150μm, 106μm, 75μm, and 53μm.

Table 3.2. P_2O_5 content in various size fractions of phosphate rock retained on the sieves.

Sieve size (microns)	Assay (% P_2O_5)
1400	16.81
1180	17.65
850	18.54
600	23.81
425	27.38
300	27.26
212	26.99
150	26.06
106	25.39
75	21.57
53	22.00
-53	20.52
Head assay	**23.20**

Figure 3.3 shows the graph of percent P_2O_5 against particle size tracing how the concentration of P_2O_5 (or apatite grains) varied with size in material retained on sieves ranging from 1400μm down to 53μm as given in table 3.2.

Apatite grain size measurements by ore microscope in section 3.3.1 have shown that the grains are coarse and are concentrated in the size range 800μm to 400μm with 600μm being the most frequently occurring size. Therefore, by comparing with size-sorting assays results in figure 3.4 it can be confirmed that the bulk of the apatite grains can be liberated from the rock matrix by grinding to minus 106μm. Sieve analysis of products from classifier and hydrocyclone overflow streams in the School of Mines grinding plant showed that more than 90% by weight of particles were below 106μm thereby ascertaining liberation of the bulk of the apatite grains. However, the optimum grind size is also a subject of the efficiency of the subsequent acidulation process.

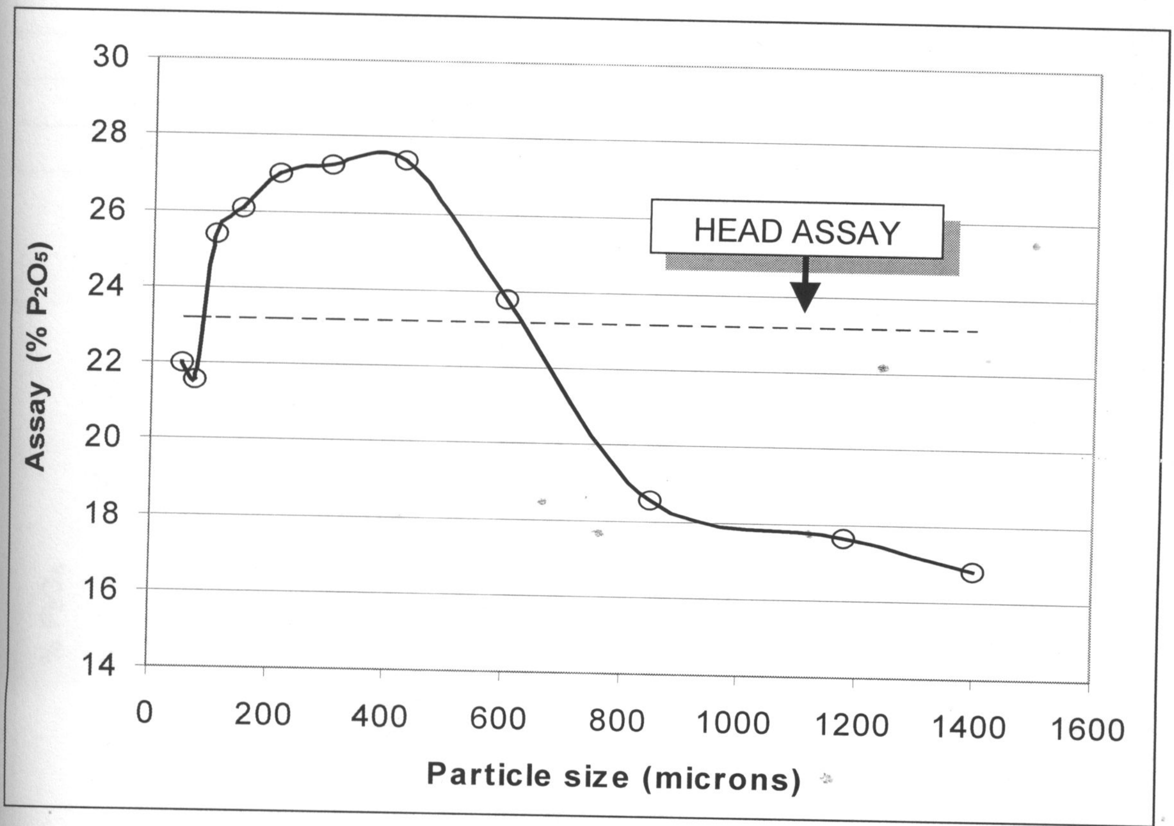

Figure 3.4. P_2O_5 content in different size fractions.

It is anticipated that the finer the particles the larger the surface area of the reaction between the acid and the rock and the more efficient the acidulation process.

3.4 Acidulation of phosphate rock

3.4.1 Particle size of phosphate rock

Table 3.3 shows the results of the effect of particle size of Chilembwe phosphate rock on percent soluble P_2O_5 in PAPR products at 50% degree of acidulation.

Table 3.3. Effect of particle size of phosphate rock on soluble P_2O_5 in PAPR.

Particle size (% minus 75μm)	Water-soluble P_2O_5 (%)	NAC-soluble P_2O_5 (%)	Available P_2O_5 (%)
79	4.92	4.18	9.10
62	5.59	3.07	8.66
51	2.59	2.59	5.18
42	4.62	4.91	9.53

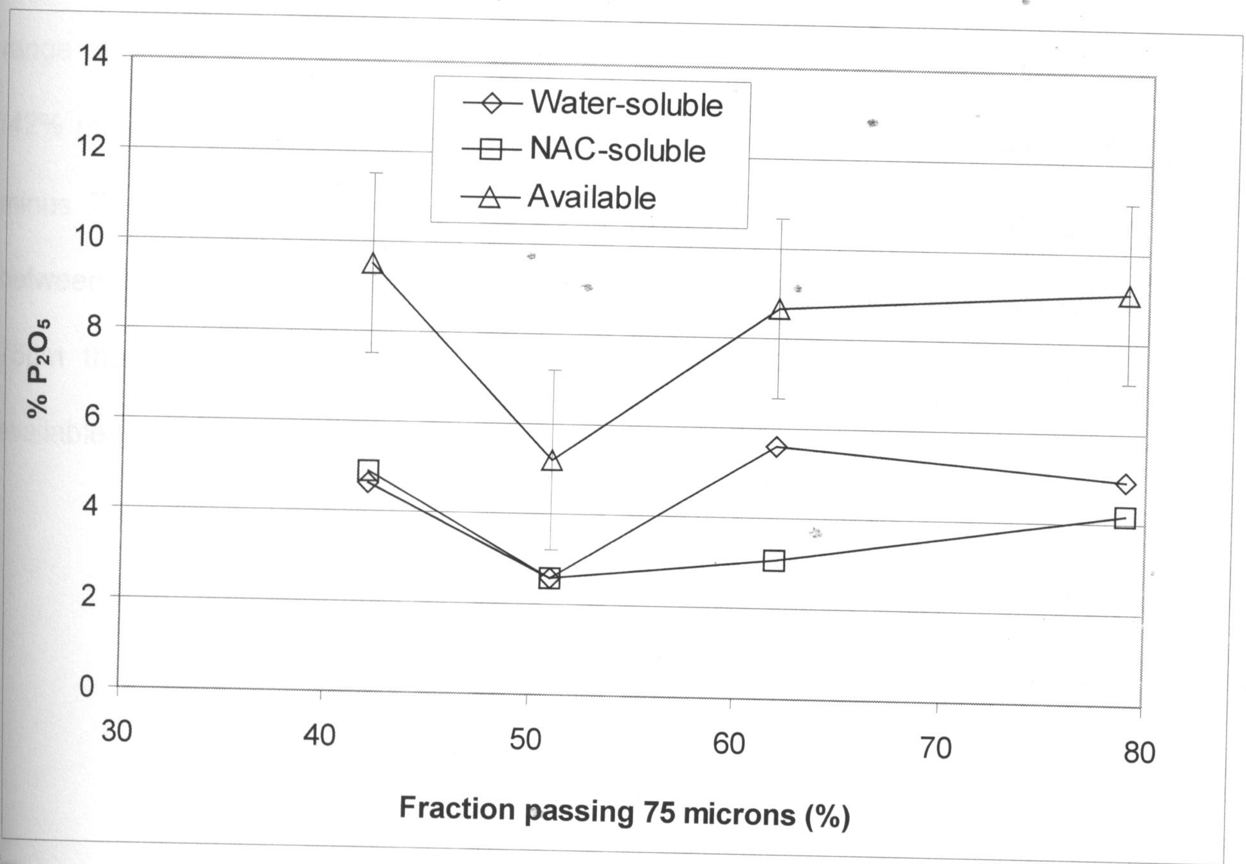

Figure 3.5. Effect of particle size of phosphate rock on soluble P_2O_5 in PAPR.

Trends in figure 3.5 showed that within the particle size range of the feeds (i.e. 42% - 79% minus 75μm) there were no significant differences in the percentage of water-soluble P_2O_5, Neutral Ammonium Citrate (NAC)-soluble P_2O_5 and hence available P_2O_5 in the PAPR products. For the 51% - 75μm size the error amount calculated by error bars was as follows:

Fixed value = 2

Percentage = 5%

Standard deviation = 1

Considering the above fixed value (2), percentage (5%) and standard deviation (1) it could be concluded that the available P_2O_5 for the 51% -75m was within the range obtained at the other three particle sizes. Moreover the coarse size feed (42% minus 75μm) gave 9.59% available P_2O_5 whilst the finest size feed (79% minus 75μm) gave 9.66% available P_2O_5 showing no remarkable differences between the two extreme sizes. Hence, in the particle size range 42 - 79% minus 75μm the percentage of water-soluble P_2O_5, NAC-soluble P_2O_5 as well as available P_2O_5 remained constant.

3.4.2 Residence time of phosphate rock in the granulator

Phosphate rock of 79% minus 75μm was acidulated at 50% degree of acidulation at varying residence times in the granulator. The residence time of phosphate rock in the granulator was varied by changing the angle of inclination of the granulator against the horizontal. Angles of inclination considered in the experiments were 2° (7minutes), 5° (5 minutes), 10° (3 minutes), 15° (1 minute). Table 3.4 below shows the results of the effect of residence time on soluble P_2O_5.

Table 3.4. Effect of residence time in the granulator on soluble P_2O_5 in PAPR.

Time (min)	Water-soluble P_2O_5 (%)	NAC-soluble P_2O_5 (%)	Available P_2O_5 (%)
1	3.65	2.66	6.31
3	4.61	4.29	8.90
5	4.59	3.97	8.55
7	4.60	3.83	8.42

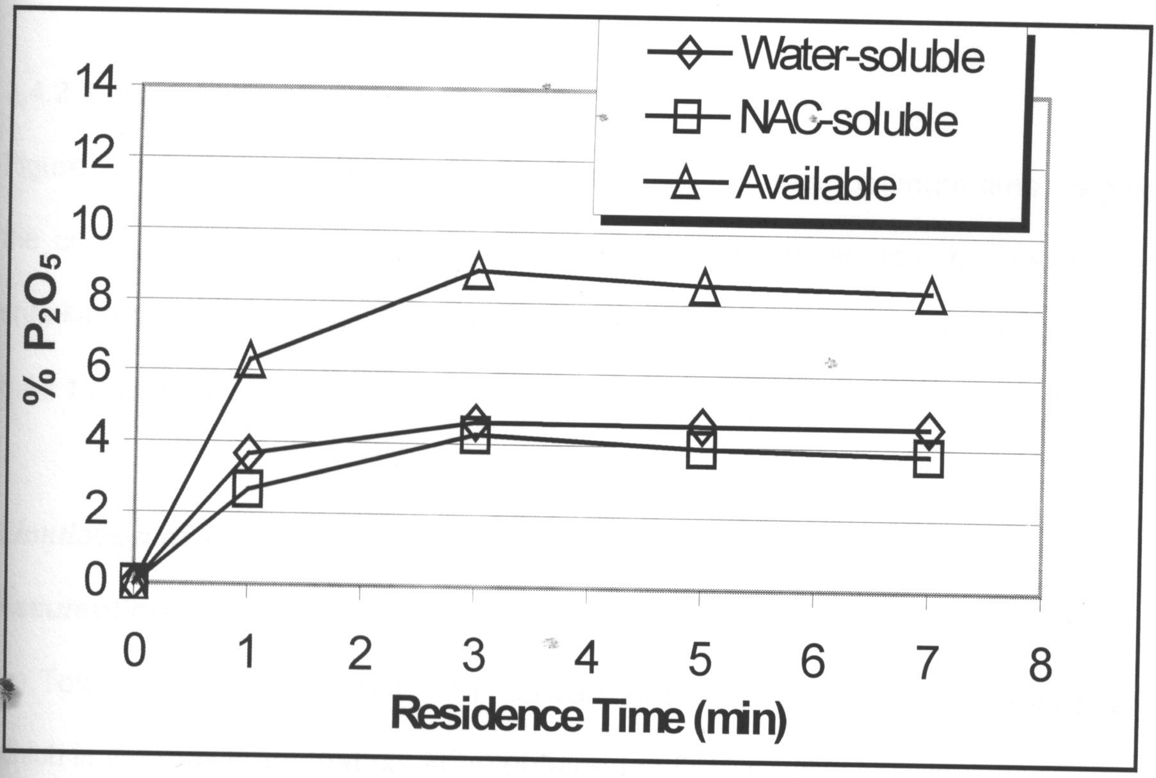

Figure 3.6. Effect of residence time in the granulator on soluble P_2O_5 in PAPR.

Trends in Figure 3.6 showed an increase in percent water-soluble P_2O_5, NAC-soluble P_2O_5 and available P_2O_5 in PAPR from 0 to 3 minutes residence time in the granulator. Beyond 3 minutes there was no noticeable increase in percent water-soluble P_2O_5, NAC-soluble P_2O_5 and available P_2O_5 in PAPR. This was so because initially the rate of reaction was fast but eventually became slow as the concentrations of the reactants decreased with time. Beyond the residence time of 3 minutes, the reaction was already too slow to effect any remarkable increase in the percentage of water-soluble P_2O_5, NAC-soluble P_2O_5 and available P_2O_5 within the limited residence time in the granulator. From the granulator the PAPR entered the dryer where it lost the liquid phase causing the reaction to stop. This results can be explained by the shrinking core model (Section 1.17.5 in Chapter 1).

3.4.2.1 Shrinking Core Model

Figure 3.6 was redrawn for the time range 0 to 3 minutes (optimum time) to give the curve shown in Figure 3.7, which was used to obtain data for testing the shrinking core model. The data for the model can be found in Appendix J Tables 6.10.1 and 6.10.2.

Simulation of experimental results using the Shrinking Core Model

Assumptions:

(a) Total conversion of apatite will convert all the apatite to 9% available P_2O_5 which is the maximum that could be obtained at 50% degree of acidulation.

(b) The unreacted core will shrink with time from 0 to 3 minutes.

(c) The particle volume remains constant although in practice this is not true due to the formation of calcium sulphate and monocalcium phosphate.

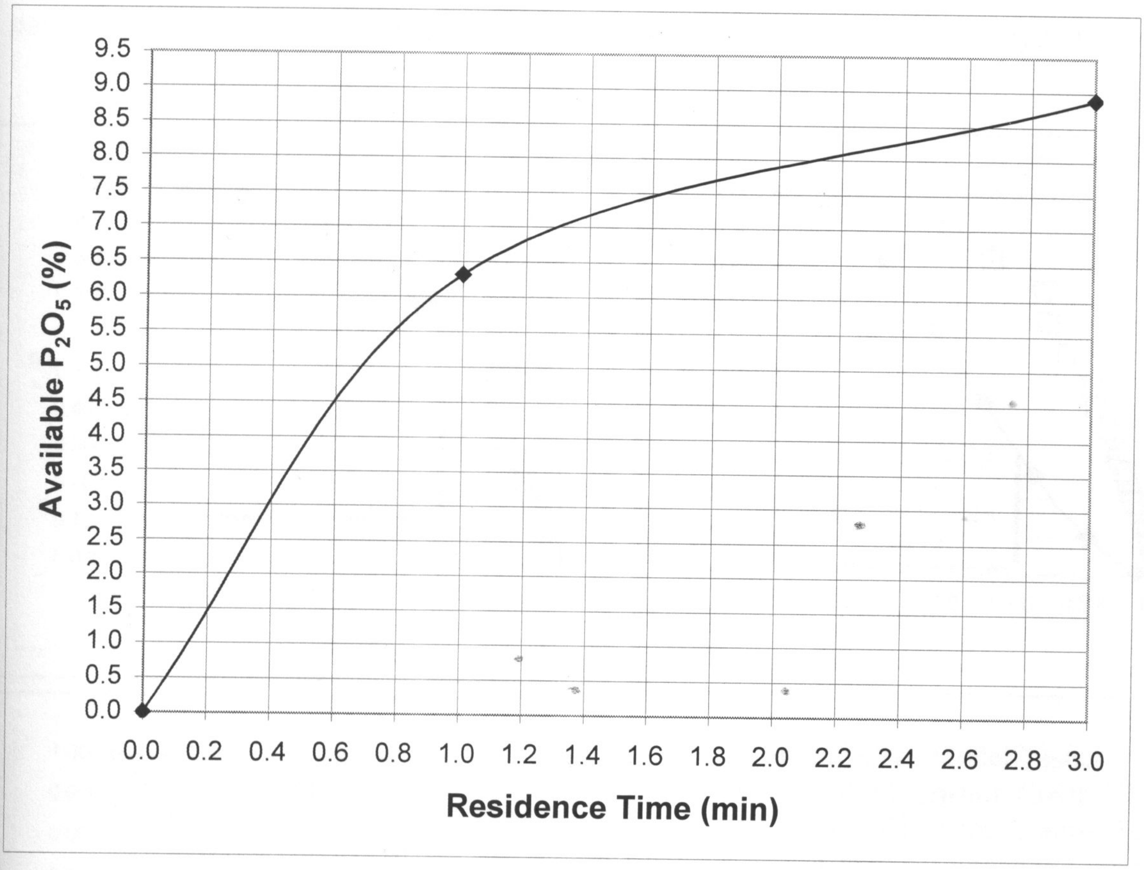

Figure 3.7. Effect of residence time in the granulator on available P_2O_5 from 0 to 3 minutes.

Film diffusion control

The experimental data fitted the *film diffusion control mechanism of the* Shrinking Core Model (Figure 3.8). This means that the limiting step in the conversion of apatite to available P_2O_5 is the diffusion of the liquid reactant species H_2SO_4 through a thin liquid film surrounding the particle to the reaction zone and diffusion of the product HF through the diffusion layer back to the rest of the liquid. The solid products of the reaction (i.e. $CaSO_4$ and Monocalcium phosphate monohydrate) join the product and insoluble layer surrounding the particle thus increasing the thickness of the solid product layer (or "ash layer").

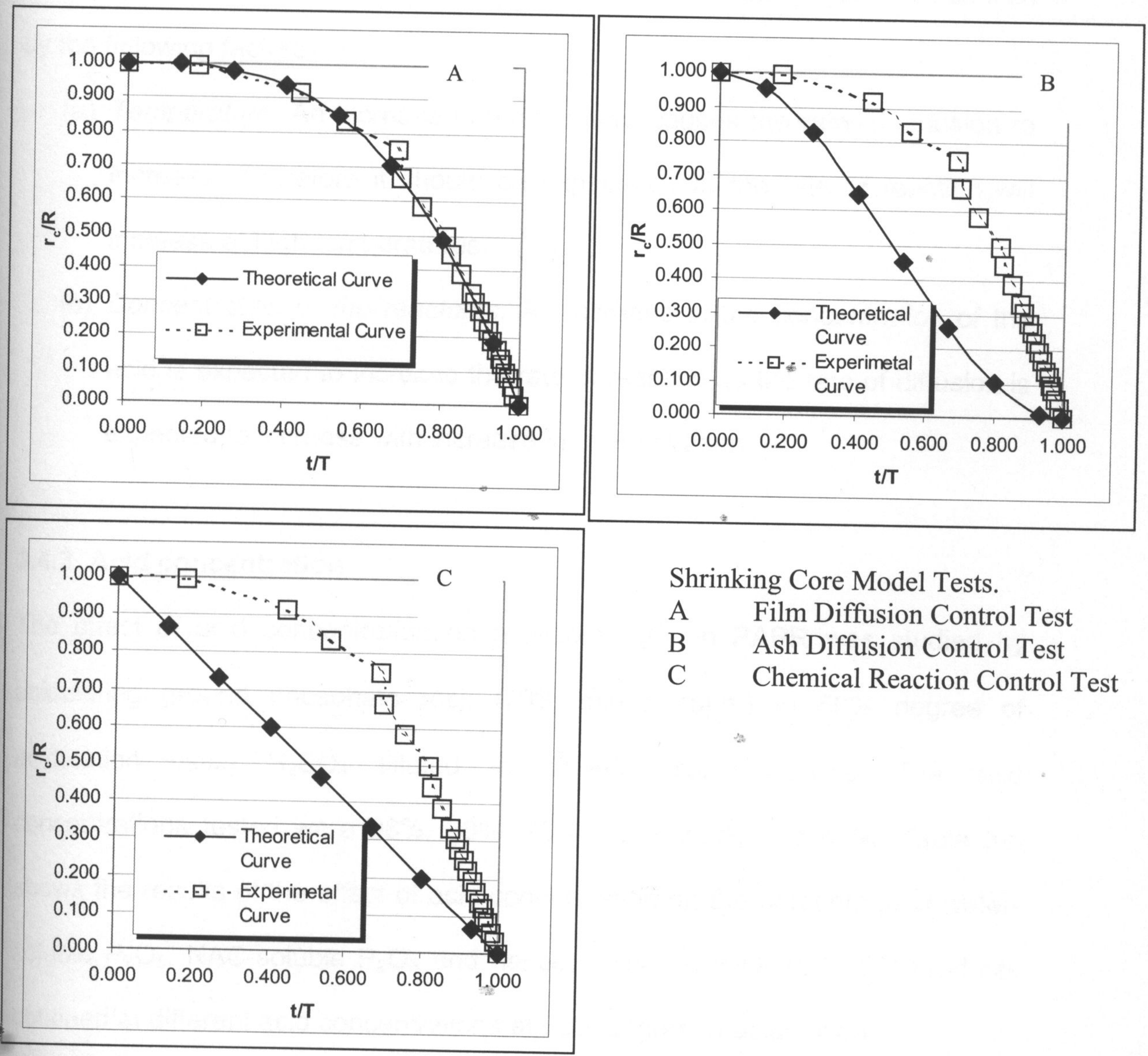

Figure 3.8. Comparison between the experimental curve and the theoretical curve for shrinking core model.

Ash diffusion (solid product layer diffusion) control and ***chemical reaction control*** did not fit the experimental curves suggesting that they do not control the rate of conversion of apatite to available P_2O_5.

In general the rate of diffusion through the liquid film (diffusion layer) is influenced by the following factors:

(a) *Temperature*. An increase in temperature causes the rate of diffusion to increase. Therefore it should be expected that the rate of reaction will increase at high temperatures.

(b) *Concentration of the reactants*. An increase in the concentration of the acid is expected to increase the rate of reaction as the rate of diffusion is expected to increase with increase in concentration.

3.4.3 Acid concentration

The effect of acid concentration on available P_2O_5 in PAPR was studied by acidulating ground phosphate rock (79% minus 75μm) to 50% degree of acidulation using H_2SO_4 diluted to different concentrations. The acid concentrations tested were 98%, 80%, 70%, 60%, 50%, and 40%. Table 3.6 shows the results of the effect of acid concentration on the percentage of water-soluble P_2O_5, NAC-soluble P_2O_5 and hence, available P_2O_5 in PAPR products obtained at different acid concentrations at 50% degree of acidulation.

Trends in Figure 3.9 showed that the percentage of water-soluble P_2O_5, NAC-soluble P_2O_5 and hence available P_2O_5 generally increased with decreasing acid concentration to an optimum at 50% H_2SO_4. However, 40% sulphuric acid gave the lowest conversion of P_2O_5 to soluble form although it was the most dilute.

Theory in f chapter 1 section 1.10.3 explains that the reaction between sulphuric acid and rock is exothermic causing temperature to rise according to the concentration of the acid used in the operation. The significant rise in temperature also increases the rate of diffusion according to the liquid film diffusion control mechanism confirmed by the shrinking core model in section 3.4.2 above.

The high rate of reaction causes the calcium sulphate to precipitate from a strongly supersaturated liquid phase in a fine particle size on the surface of unreacted rock particles thereby partially blocking contact between the liquid phase and the unreacted rock particles resulting in the poor conversion of apatite to soluble forms. This is the reason why experimental results at high acid concentrations showed low percentages of water-soluble and NAC-soluble P_2O_5 in PAPR.

At low acid concentrations, the rate of reaction is slow and so is the precipitation of calcium sulphate. The slow rate of calcium sulphate precipitation allows more contact between the liquid phase and the rock particles resulting in the increased conversion of apatite to soluble forms.

Table 3.5. Effect of acid concentration on soluble P_2O_5 in PAPR.

Acid concentration (%)	Water-soluble P_2O_5 (%)	NAC-soluble P_2O_5 (%)	Available P_2O_5 (%)
98	4.26	1.34	5.60
80	4.50	1.32	5.82
70	4.55	1.50	6.05
60	4.61	1.49	6.10
50	4.81	1.48	6.28
40	3.46	1.06	4.51

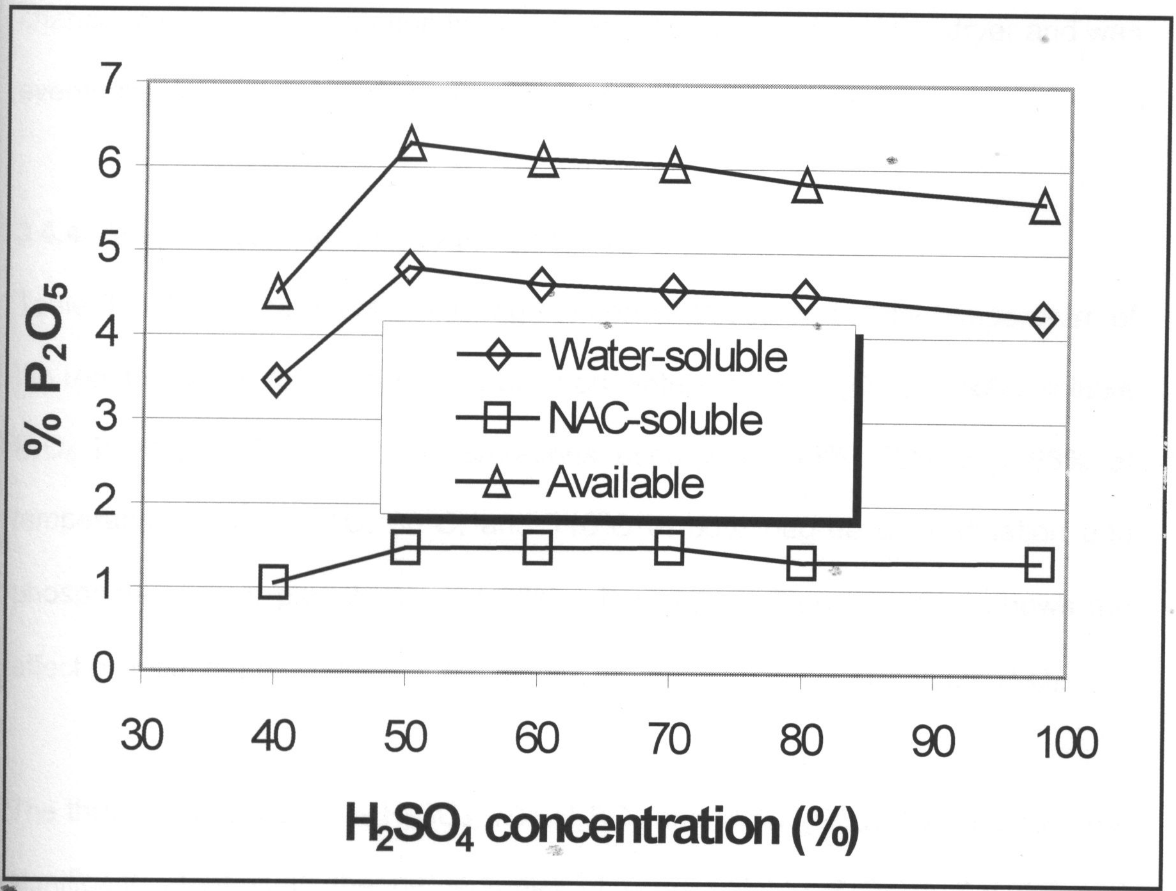

Figure 3.9. Effect of acid concentration on soluble P_2O_5 in PAPR.

Experimentally obtained data is in close agreement with the theoretical explanation and the film diffusion control mechanism of the Shrinking Core Model. As can be observed in Figure 3.9 the percentage of water-soluble P_2O_5, NAC-soluble P_2O_5 and available P_2O_5 in PAPR increased with the decreasing acid concentration giving an optimum at 50% acid concentration. However, when acid concentration was too low such as 40% H_2SO_4, the reaction rate became exceedingly slow. As residence time in the granulator was limited, there was no chance to prolong the reaction in the material before it entered the dryer and was eventually deprived of liquid phase causing the reaction to stop.

3.4.4 Acid concentration and temperature

Table 3.6 shows the effect of varying the concentration and initial temperature of the reactants (i.e. rock, acid and water) on water-soluble P_2O_5 and NAC-soluble P_2O_5 in PAPR. The acid concentrations used were 50%, 70% and 98% at temperatures 25°C, 50°C, 80°C, and 110°C at 50% degree of acidulation and phosphate rock of particle size of 78% minus 75μm. Figure 3.10(a) shows the effect of initial temperature of the rock, water and acid on water-soluble P_2O_5.

The three curves (i.e. 50% H_2SO_4, 70%H_2SO_4 and 98%H_2SO_4) did not show any significant variation in the percentages of water-soluble P_2O_5 at the different initial temperatures of the reactants in the range 25 to 110°C. Only the acid concentration played a significant role on influencing the percentage of water-soluble P_2O_5 in the PAPR products. Indeed the more dilute acid, 50% H_2SO_4 gave a product with a higher content of water-soluble P_2O_5 followed by the 70% H_2SO_4 and 98% H_2SO_4.

Table 3.6. Effect of H_2SO_4 concentration and temperature on soluble P_2O_5 in PAPR.

H_2SO_4 conc.	**Initial T °C**	**Water-soluble P_2O_5** (%)	**NAC-soluble P_2O_5** (%)
50	25	6.08	2.02
	50	6.09	2.26
	80	6.39	2.23
	110	6.65	1.37
70	25	5.87	4.14
	50	5.19	2.49
	80	5.16	3.74
	110	5.03	3.73
98	25	4.65	4.26
	50	4.81	3.34
	80	4.72	3.57
	110	4.74	3.25

In Figure 3.10(b) the initial temperature of the reactants did not have any significant influence on the NAC-soluble P_2O_5 in PAPR products in the temperature range 20 to 110°C. Each acid concentration showed approximately a constant percentage of NAC-soluble P_2O_5 in PAPR at all temperatures from 25 to 110°C. However, the percentage of NAC-soluble P_2O_5 in PAPR was affected by the acid concentration. Hence, NAC-soluble P_2O_5 was more in the 50% H_2SO_4 and 70% H_2SO_4 but low in the 98% H_2SO_4 in the initial temperature range 25 to 110°C. Therefore theoretical explanation given in section 3.4.3 under acid concentration also applies here.

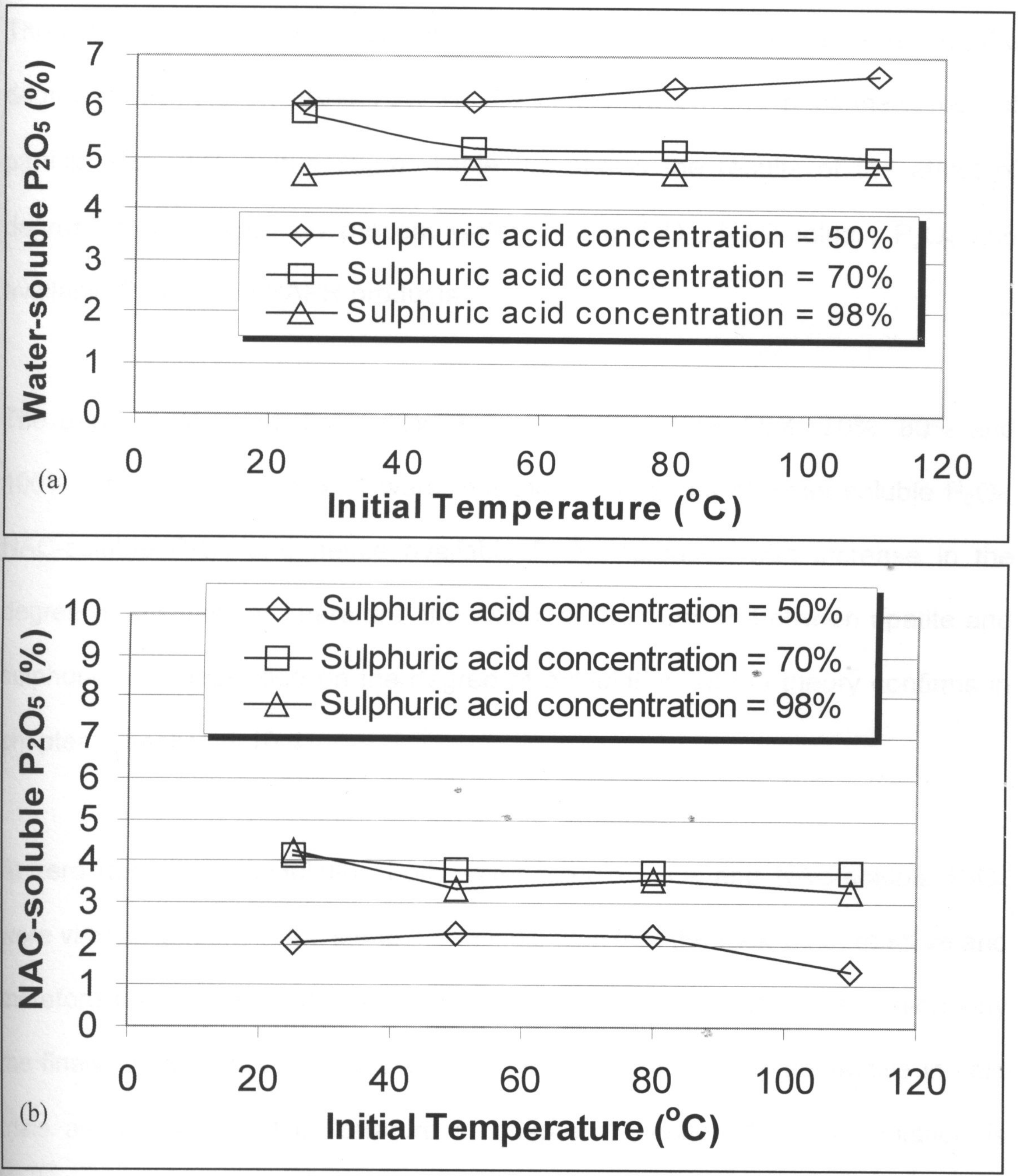

Figure 3.10. Effect of initial temperature of rock, acid and water on water- and NAC-soluble P_2O_5 in PAPR.

3.4.5 Degree of acidulation

The effect of degree of acidulation on soluble P_2O_5 was studied by varying the degree of acidulation using 70% H_2SO_4 concentration and phosphate rock of particle size 79% minus 75μm. Table 3.7 shows the results of the effect of degree of acidulation on percent water-soluble P_2O_5, NAC-soluble P_2O_5 and available P_2O_5 in the PAPR products.

The degrees of acidulation tested were 0%, 20%, 40%, 60%, 70%, 80% and 100%. Trends in Figure 3.11 were that the percentages of water-soluble P_2O_5, NAC-soluble P_2O_5 and hence available P_2O_5 increased with increase in the degree of acidulation. Therefore, the extent of the reaction between apatite and sulphuric acid depended on the degree of acidulation as the theory confirms in chapter 1, section 1.10.4.

At zero degree of acidulation both water-soluble P_2O_5 and NAC-soluble P_2O_5 were virtually absent in the sample - an indication that the rock is not reactive and therefore unsuitable for direct application as a fertilizer. This is the reason why the finely ground rock sample was found to be agronomically ineffective in field trials as reported in the literature in chapter 1 section 1.7.1. Acidulation is therefore a very necessary step in the utilization of Chilembwe phosphate rock for agricultural purposes.

Table 3.7. Effect of degree of acidulation on soluble P_2O_5 in PAPR.

Degree of acidulation	Water-soluble P_2O_5 (%)	NAC-soluble P_2O_5 (%)	Available P_2O_5 (%)
100	6.92	2.53	9.44
80	6.08	3.09	9.17
60	4.50	2.03	6.53
40	3.18	2.07	5.26
20	1.25	0.00	1.25
0	0.00	0.00	0.00

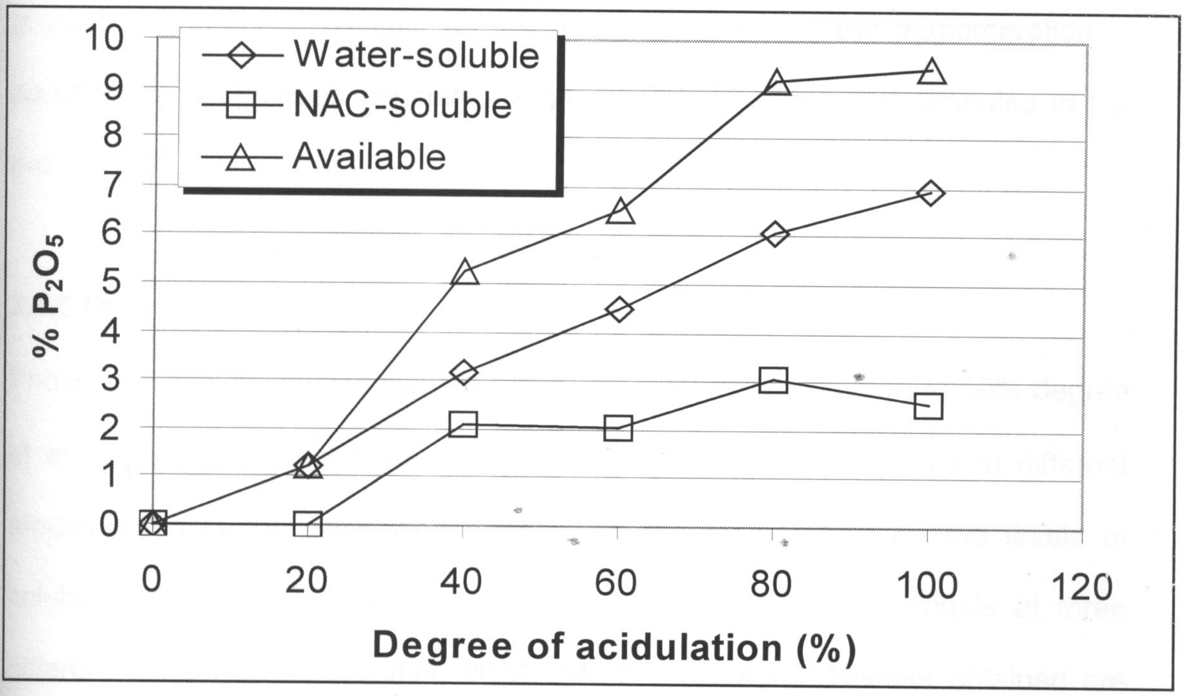

Figure 3.11. Effect of degree of acidulation on soluble P_2O_5 in PAPR.

The optimum degree of acidulation is normally determined by the cost of acid rather than the available P_2O_5 in the PAPR product. As a matter of choice 50% acidulation cuts down the expense on acid by 50% therefore making the process less expensive in terms of acid consumption. The remaining unreacted rock in the PAPR converts slowly to soluble form in acidic soils, thus giving long term benefits in providing residual phosphorus to the plants (See chapter 1 section 1.7.2).

At higher degrees of acidulation, 80% and above, the product became sticky. This was caused by the high levels of free acid in it. The sticky product made the granulation operation difficult, as it tended to accelerate the agglomeration of particles in the process causing a high proportion of oversize granules in the product.

3.4.6 Drying temperature

Phosphate rock of particle size 79% minus 75μm was acidulated to 50% degree of acidulation using sulphuric acid of 70% concentration and dried at different temperatures in the drier. The effect of drying temperature on the levels of soluble P_2O_5 in PAPR products was studied by drying the products at three different temperatures including 90°C, 120°C and 150°C. Results obtained are given in Table 3.8. Trends in Figure 3.12 showed that water-soluble P_2O_5 in PAPR decreased gradually with increase in the drying temperature from 5.49% P_2O_5 to 3.3% P_2O_5 in the range 90 to 150°C. NAC-soluble P_2O_5 increased with increase in drying temperature from 3.7% P_2O_5 to 5.67% P_2O_5 in the range 90 to 150°C. However, the available P_2O_5 remained constant at approximately 9% P_2O_5 throughout the temperature range 90 to 150°C.

Low temperature drying allowed the water-soluble P_2O_5 to remain stable. At higher temperatures part of the water-soluble P_2O_5 was converted to NAC-soluble P_2O_5 due to the driving away of the bound water above 100°C. The best temperature should be 100 to 120°C due to increased drying rate but water-soluble P_2O_5 was still more than the NAC-soluble P_2O_5.

Table 3.8. Effect of drying temperature on soluble P_2O_5 in PAPR.

Drying temp. (°C)	Water-soluble P_2O_5	NAC-soluble P_2O_5	Available P_2O_5
90	5.49	3.70	9.19
120	4.94	4.31	9.24
150	3.30	5.88	9.18

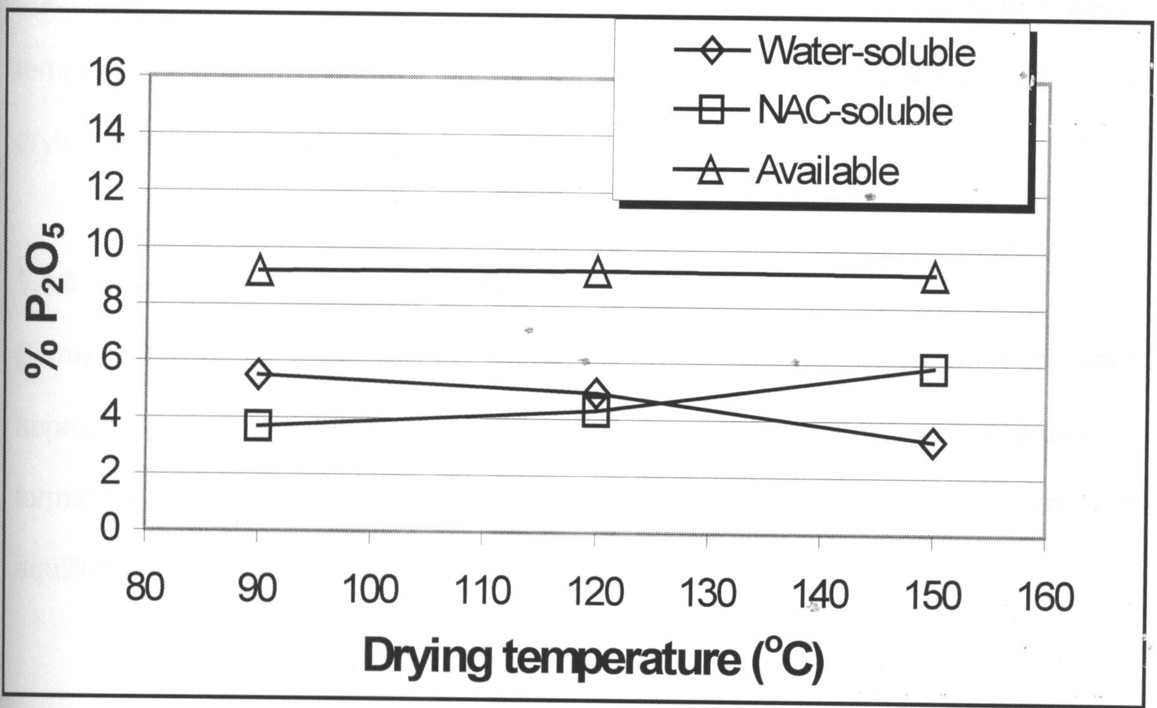

Figure 3.12. Effect of drying temperature on soluble P_2O_5 in PAPR.

3.4.7 Optimum parameters

The optimized parameters were as follows:

- Particle size of phosphate rock: any size from 42 – 79% minus 75μm.

- Degree of acidulation: 50%.
- Acid concentration: 50 – 70%.
- Initial temperature of rock, water and acid: ambient (25°C)
- Residence time of phosphate rock in the granulator: 3 minutes.
- Drying temperature: 100 -120°C.

The results for optimized parameters are given in Figure 3.12, which was obtained by using optimum particle size (79% minus 75μm), optimum degree of acidulation (50%), optimum acid concentration (70%), and optimum initial temperature (25°C). The available P_2O_5 remained at about 9% P_2O_5 at every drying temperature.

3.4.8 Equilibrium Constant Approach

Some of the results could have been explained by using the equilibrium constant approach. However, due to the non-availability of the standard free energies of formation of fluorapatite and monocalcium phosphate monohydrate the equilibrium constant approach was not used.

3.5 MODELLING OF COMMINUTION AND GRANULATION PROCESSES

3.5.1 Simulation of RTD curves in comminution and granulation

Figure 3.13 shows a schematic flowsheet of the selective recycle model representing a closed comminution circuit shown in chapter 2 Figure 2.14. The same model also applies to the granulation system shown in chapter 2 Figure 2.15. Slurry flow in the ball mill (main unit) was assumed as perfectly mixed while in the hydrocyclone plug flow (time delay) was assumed.

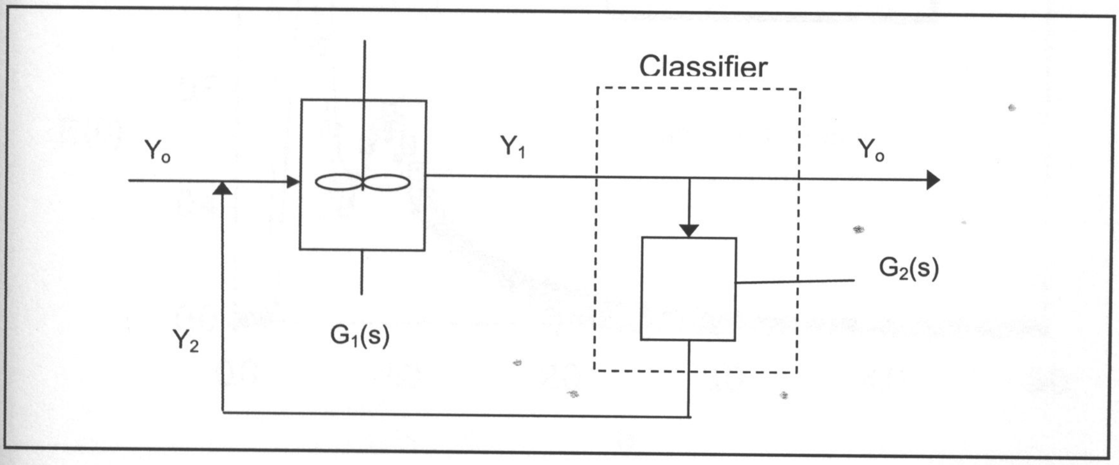

Figure 3.13. The selective recycle model.

Like wise, in the granulation system perfect mixing in the granulator (main unit) and plug flow at the classification stage after drying were assumed.

3.5.1.1 Simulation of RTD in the comminution of phosphate rock

A tracer of sodium chloride solution was used to obtain the experimental residence time distribution (RTD) curve shown in Figure 3.14. Detailed procedure for plotting RTD curves is given in chapter 2 section 2.7.3. The RTD curve of the tracer showed that there was internal circulation in the ball mill. This was revealed by the presence of two peaks in the RTD curve as can be seen in Figure 3.14.

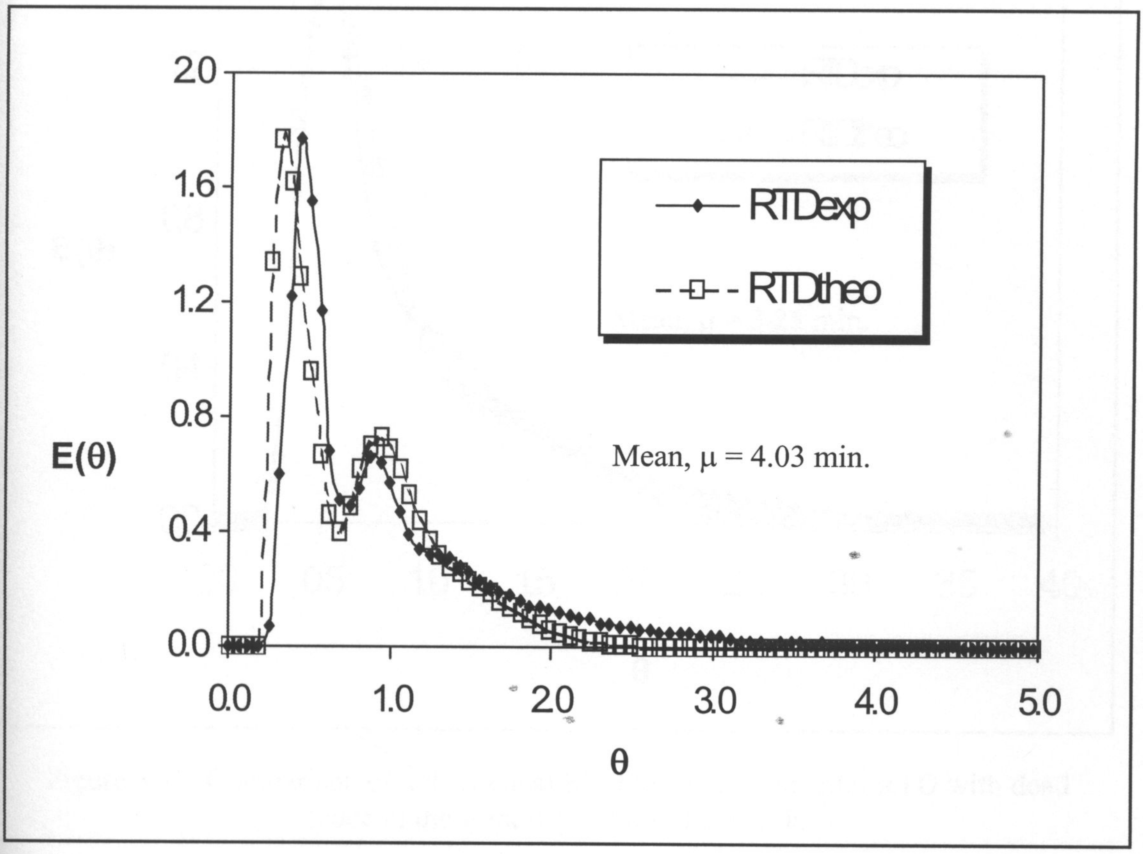

Figure 3.14. Comparison of a theoretical RTD to an experimental RTD with internal circulation in the grinding of phosphate rock.

The mill was opened and the composition of the grinding media was found to be 25% 1.8cm diameter, 25% 2.4cm diameter and 50% 3.8cm diameter steel balls. The composition of the grinding media was changed to 20% 2.4cm diameter and 80% 3.8cm diameter steel balls and a fresh tracer test showed that the ball mill had some of dead space in it but was sufficiently close to a normal RTD. This was revealed by the long tail in the RTD curve as can be seen in figure 3.15.

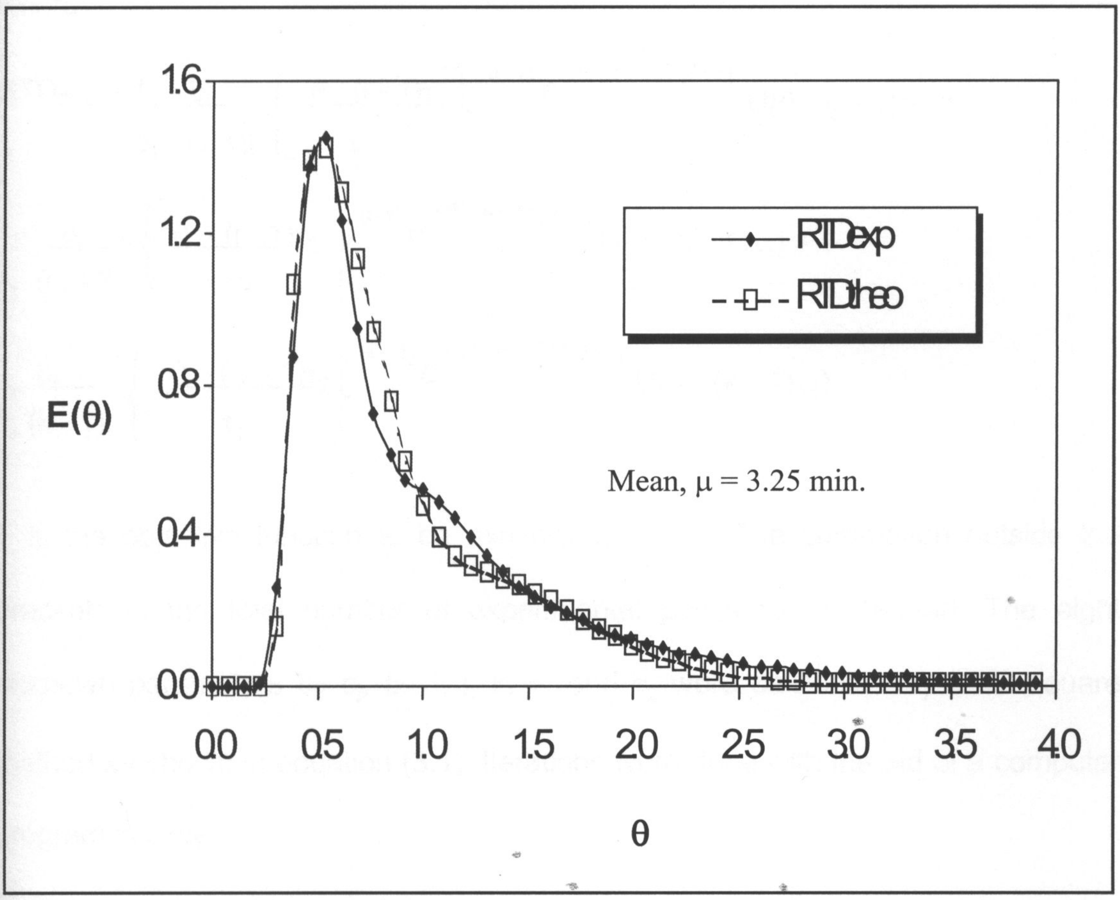

Figure 3.15. Comparison of a theoretical RTD to an experimental RTD with dead space in the grinding of phosphate rock.

Simulation of the experimental RTD curves was done using the method of least squares according to the procedure and equations explained in the theory in chapter 1 section 1.17.4. Hence, the solution was obtained by minimizing the sum of the squared differences between the experimental RTD (RTD_{exp}) and the theoretical RTD (RTD_{theo}) as given in equation (3.1)

$$F = \sum_{i=1}^{k} [RTD_{exp} - RTD_{theo}]^2 \qquad (3.1)$$

where

$$RTD_{theo} = \frac{1}{\tau_1}\frac{b_i}{(I-1)!}\left\{\frac{\theta-(i-1)\tau_2}{\tau_1}\right\}^{(i-1)} e^{-(\theta-(i-1)\tau_2)/\tau_1} U(\theta-(j-1)\tau_2 +$$

$$\frac{1}{\tau_1}\frac{b_j}{(j-1)!}\left\{\frac{\theta-(j-1)\tau_2}{\tau_1}\right\}^{(j-1)} e^{-(\theta-(j-1)\tau_2)/\tau_1} U(\theta-(j-1)\tau_2) +$$

$$\frac{1}{\tau_1}\frac{b_k}{(k-1)!}\left\{\frac{\theta-(k-1)\tau_2}{\tau_1}\right\}^{(k-1)} e^{-(\theta-(k-1)\tau_2)/\tau_1} U(\theta-(k-1)\tau_2)$$

F is the objective function to be minimized, $F \geq 0$. The summation outside the brackets is the total number of experimental points to be iterated. The eight unknown parameters b_i, b_j, b_k, i, j, k, τ_1 and τ_2 were calculated by least square method as shown in equation (3.1). Iterations were done with the aid of a computer program in excel.

THE NUMBER OF CYCLES DISTRIBUTION

The parameters obtained from equation (3.1) for the RTD with internal circulation (Figure 3.12) and RTD with dead space (Figure 3.13) are given in Table 3.9.

Table 3.9. Parameters obtained from the simulation of RTDs using least square method.

Optimized Parameters	Values for RTD with internal circulation	Values for RTD with dead space
i	2	2
j	4	4
k	6	8
b_i	0.56	0.82
b_j	0.35	0.17
b_k	0.09	0.01
τ_1	0.116 minutes	0.210 minutes
τ_2	0.200 minutes	0.297 minutes

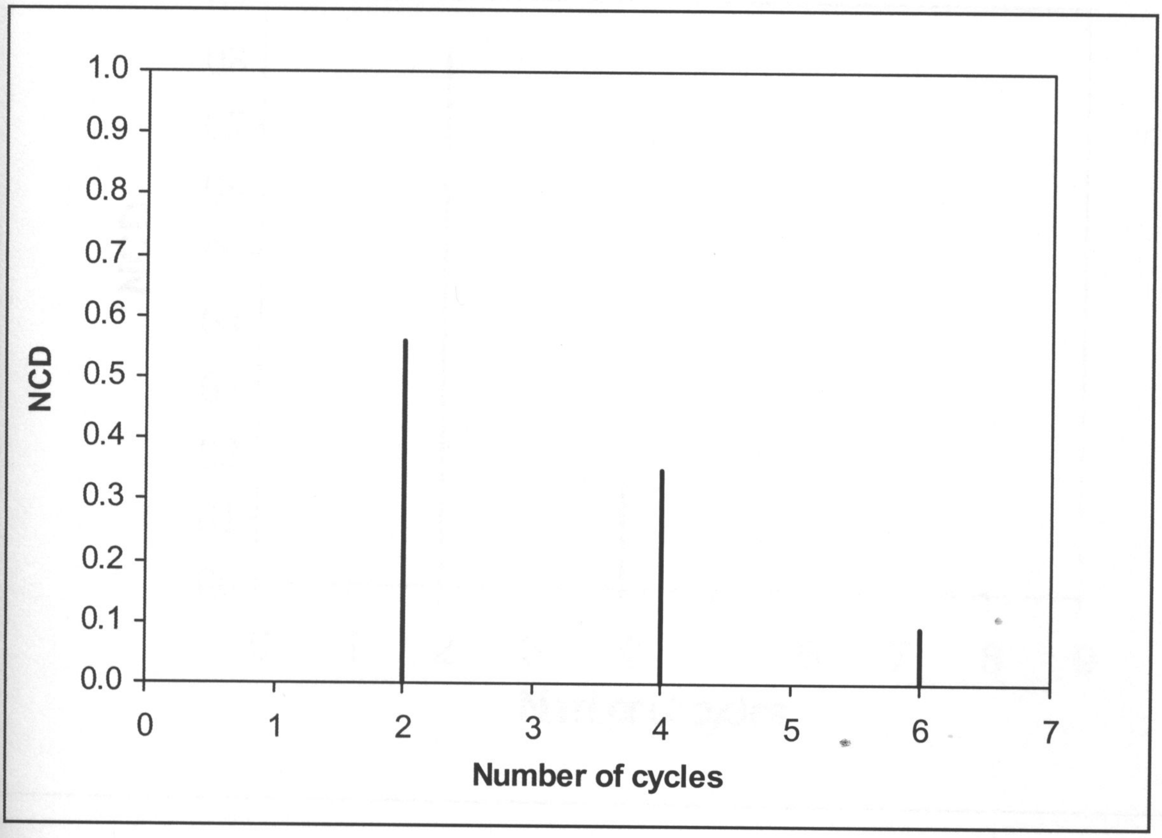

Figure 3.16. NCD for RTD with Internal circulation

The Number of Cycles Distribution (NCD) graphs, Figures 3.16 and 3.17, were plotted from the optimized parameters - values of b_i, b_j, and b_k were plotted against values of i, j, and k. For the RTD with internal circulation, the values of b_i, b_j, and b_k can be interpreted to mean that 56% of the tracer left the closed comminution circuit after exactly 2 number of cycles through the ball mill, 35% of the tracer left after 4 number of cycles and 9% of the tracer left after exactly 6 number of cycles through the ball mill.

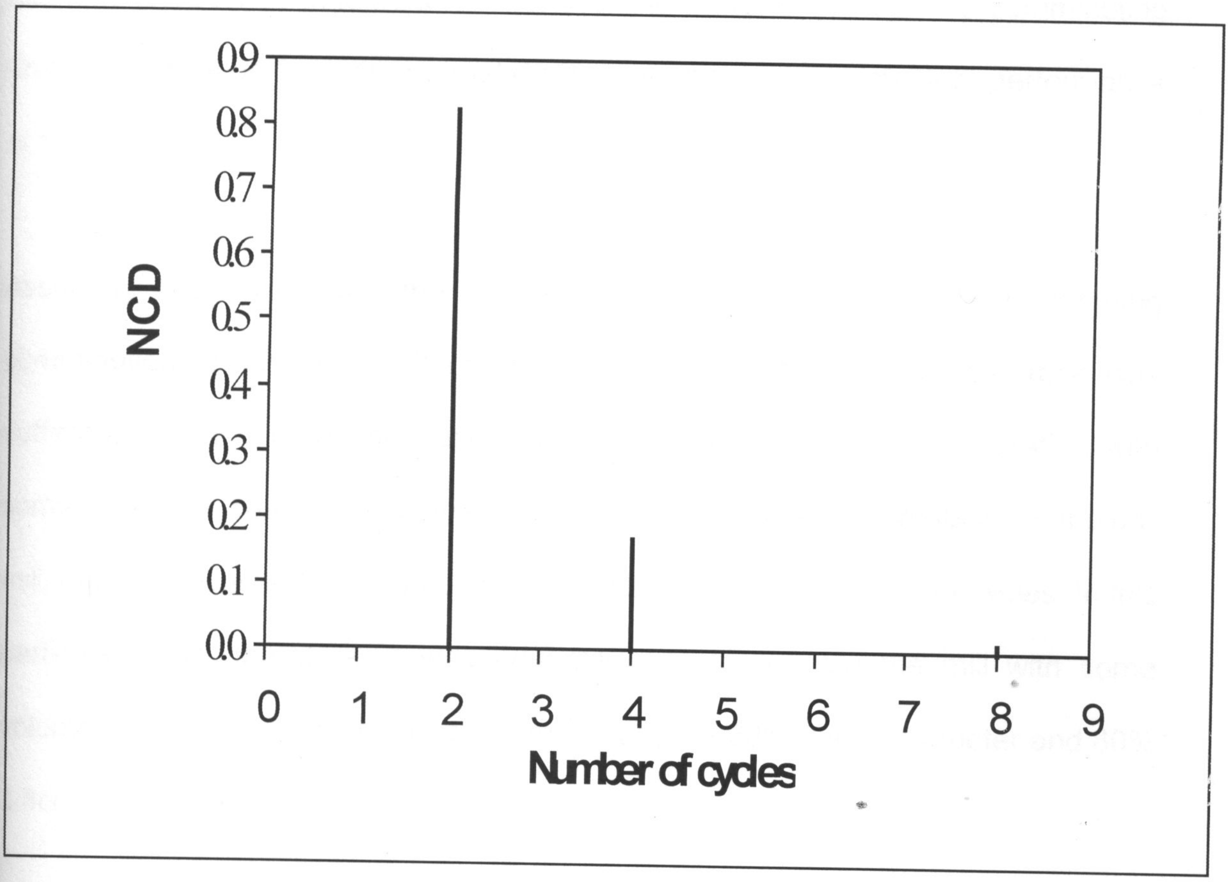

Figure 3.17. NCD for RTD with dead space

For the RTD with dead space, the values of b_i, b_j, and b_k can be interpreted to mean that 82% of the tracer left the closed comminution circuit after exactly 2 number of cycles, 17% of the tracer left after 4 number of cycles and 1% of the tracer left after exactly 8 number of cycles.

Any malfunctioning of the comminuting unit, ball mill or rod mill such as dead space in the mill, can result in uneconomical utilization of the equipment, loss of optimum output of material per given time and a high recycle ratio. It is therefore essential from time to time to check for any malfunctioning of the equipment using for example a tracer to determine the RTD of the material through the comminuting unit. Any deviation from the normal RTD curve means unsatisfactory performance of the unit.

Assuming the tracer was the actual particles of phosphate rock undergoing comminution. Then the NCD graphs would mean that 82% of the rock was sufficiently comminuted after just 2 number of cycles during the operation with some volume of dead space in the ball mill. With some internal circulation in the ball mill, only 56% was sufficiently comminuted after the same number of cycles. In this particular case, therefore, it was advantageous to operate the mill with some volume of dead space by using a ball mill charge of 20% 2.4cm diameter and 80% 3.8cm diameter steel balls.

3.5.1.2 Simulation of RTD in the granulation of phosphate rock

A tracer of sodium sulphate powder was used for testing the granulation system in order to obtain the experimental RTD curves. Details of the experimental procedure is given in chapter 2 section 2.7.3. The RTD curve obtained at a mean residence time of 3.2 minutes had two peaks indicating internal circulation as given in Figure 3.16. The angle of inclination of the granulator was altered to increase the mean residence time of the material to 6.7 minutes and a fresh tracer test conducted. The resulting RTD curve showed an almost normal RTD (Figure 3.17).

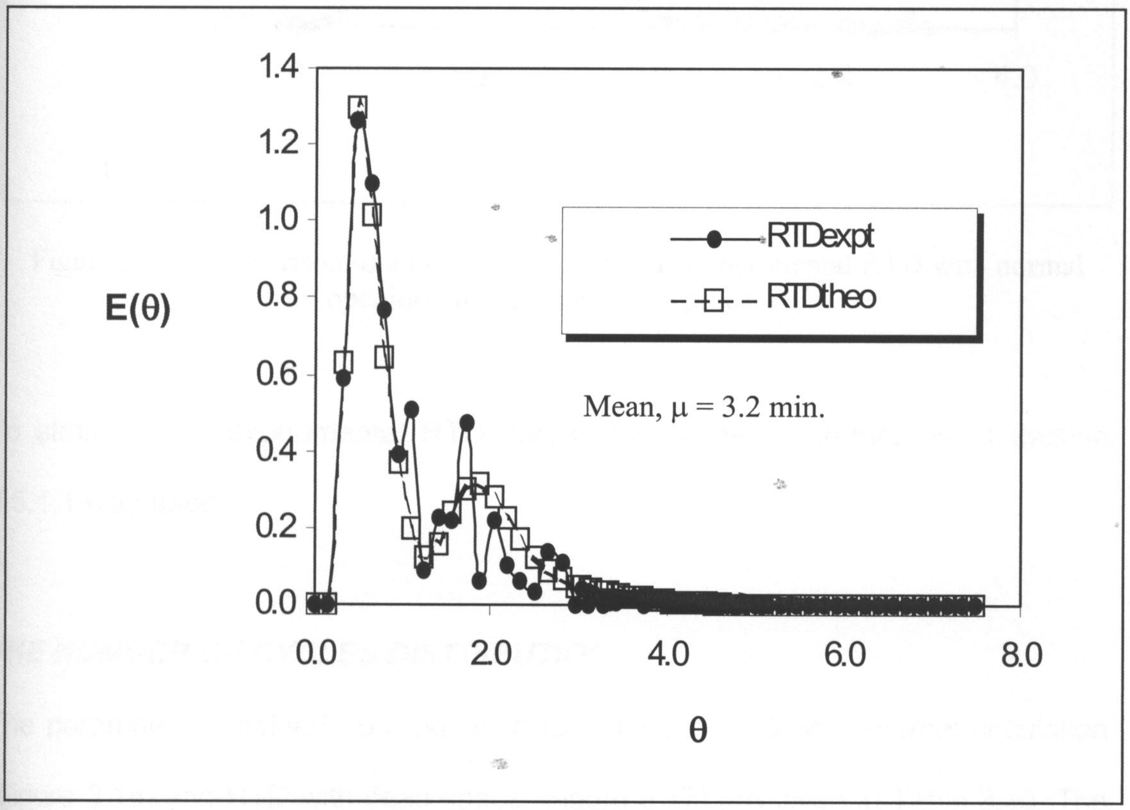

Figure 3.18. Comparison of a theoretical RTD to an experimental RTD with internal circulation in the granulation process.

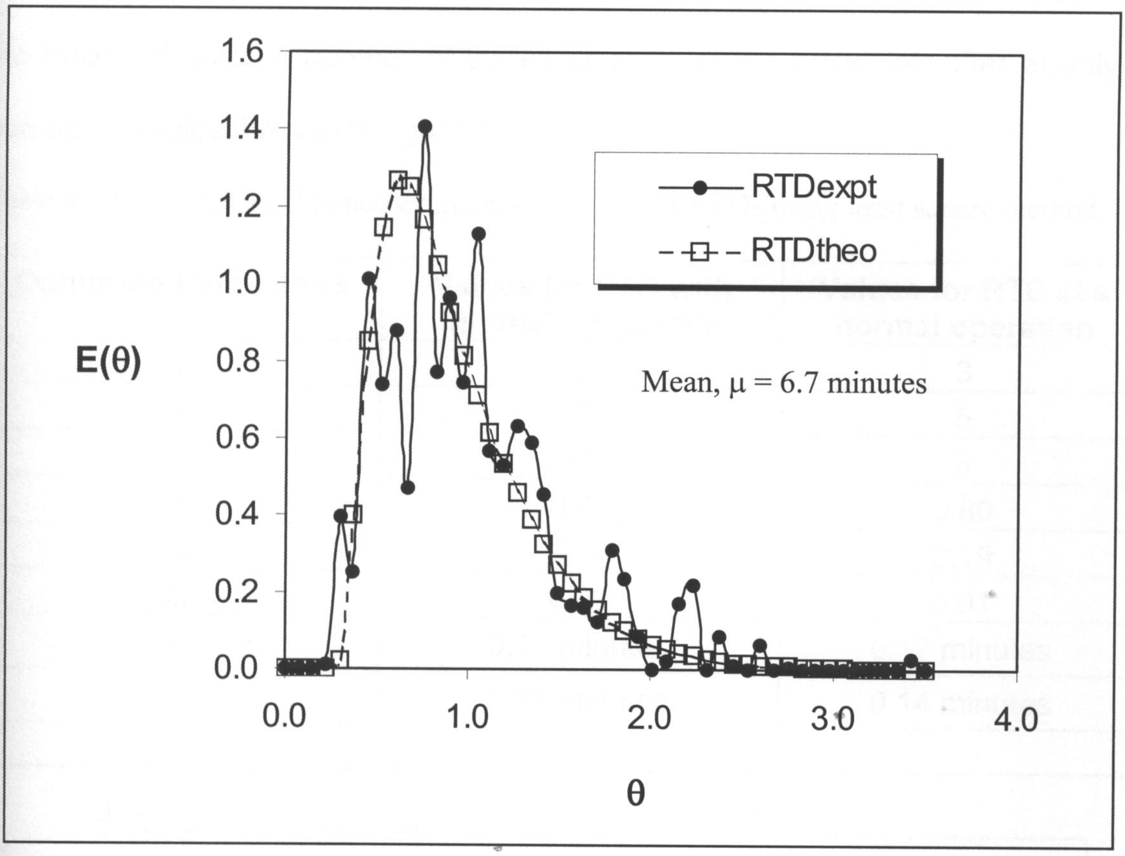

Figure 3.19. Comparison of a theoretical RTD to an experimental RTD with normal operation in the granulation process.

To simulate the experimental RTD curves the same procedure as in section 3.5.1.1 was used.

THE NUMBER OF CYCLES DISTRIBUTION

The parameters obtained from equation (3.1) for the RTD with internal circulation (Figure 3.16) and RTD with dead space (Figure 3.17) are given in Table 3.10. The values of b_i, b_j, and b_k were plotted against the values of i, j, and k to obtain the NCD graphs shown in Figures 3.18 and 3.19. For the RTD with internal circulation, the values of b_i, b_j, and b_k can be interpreted to mean that 67% of the tracer left the granulation circuit after exactly 2 number of cycles through the granulator, 30% of the tracer left after 5 number of cycles and 3% of the tracer left after exactly 8 number of cycles through the granulator.

Table 3.10. Parameters obtained from the simulation of RTDs using least square method.

Optimized Parameters	Values for RTD with internal circulation	Values for RTD at a normal operation
i	2	3
j	5	5
k	8	8
b_i	0.67	0.80
b_j	0.30	0.19
b_k	0.03	0.01
τ_1	0.19 minutes	0.17 minutes
τ_2	0.27 minutes	0.14 minutes

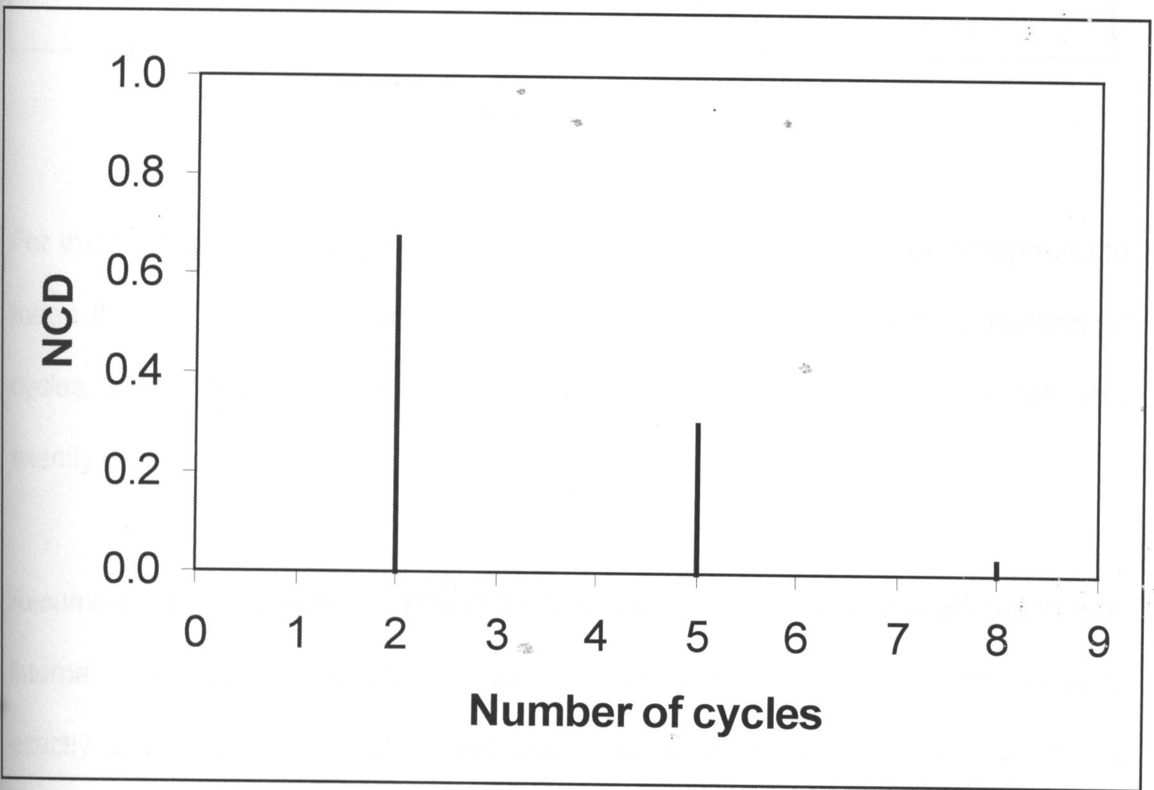

Figure 3.20. NCD for the RTD with internal circulation.

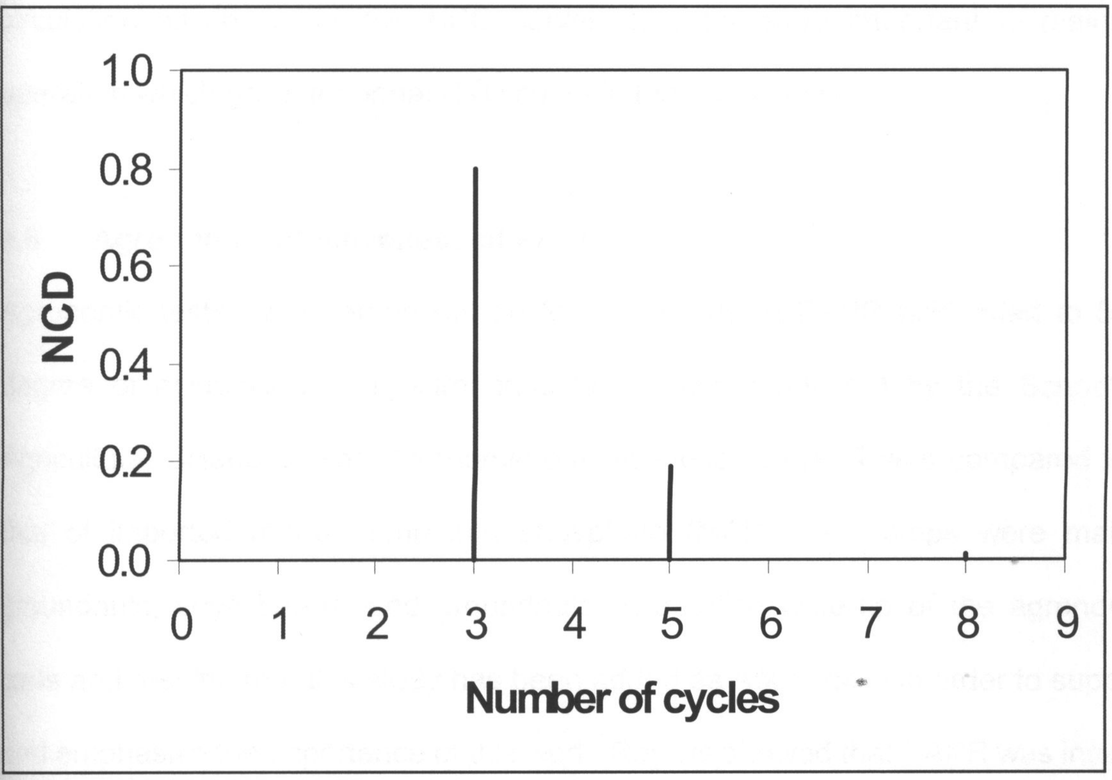

Figure 3.21. NCD for the RTD with dead space.

For the RTD with normal operation, the values of b_i, b_j, and b_k can be interpreted to mean that 80% of the tracer left the granulation circuit after exactly 3 number of cycles, 19% of the tracer left after 5 number of cycles and 1% of the tracer left after exactly 8 number of cycles.

Assuming the tracer was the PAPR itself, it would mean that in the operation with internal circulation (Figure 3.18) the total amount of PAPR leaving the system after exactly 2 and 5 number of cycles sums up to 97%. Similarly, in the normal operation (Figure 3.19) the total amount of PAPR leaving the system after exactly 3 and 5 number of cycles would add up to 99%. Therefore, the normal operation gave more PAPR before exactly 8 number of cycles than the operation with internal circulation as shown by the NCD curves. It is therefore important to maintain operation which gives a normal RTD curve in the tracer tests.

3.6 Agronomic effectiveness of PAPR

Agronomic tests were carried out on food crops using PAPR acidulated to 50% degree of acidulation. The agronomic tests were conducted by the School of Agricultural Sciences. The agronomic effectiveness of PAPR was compared with that of imported mono-ammonium phosphate (MAP). Test crops were maize, groundnuts, soya beans, and groundnuts. A detailed write-up of the agronomic tests and results from this study has been added as Appendix J in order to support and emphasize the importance of this work. Results showed that PAPR was indeed just as agronomically effective as Mono-Ammonium Phosphate (MAP) in providing phosphorus to crops.

CHAPTER 4: ECONOMIC EVALUATION OF A 30 TPH COMMERCIAL-SCALE PAPR PROJECT

CHAPTER 4

ECONOMIC EVALUATION OF A 30TPH COMMERCIAL-SCALE PAPR PROJECT

4.1 Outline

The main production stages for PAPR include mining and processing. Mining involves drilling, blasting and hauling of the waste rock and the run-of-mine ore. The run-of-mine ore requires transportation by road from Chilembwe phosphate deposit to the processing plant to be located at the proposed site in Petauke. The processing of PAPR would involve primary and secondary crushing, dry milling, partial acidulation of the fine rock followed by drying, screening, and finally bagging. Capital costs, annual costs and processing costs have been used to carryout an economic analysis in order to assess the viability of a 30TPH commercial project for an initial period of 15 years of operation. The Net Present Value and Benefit-Cost ratio have been applied in the analysis and a competitive price of PAPR has been determined and extrapolated to various towns/districts in Zambia.

4.2 Process scale-up from pilot-plant

The throughput rate of the pilot-plant was 25kg/hr, the large scale plant will have a throughput rate of 30 tonnes per hour. Equipment manufacturers require specification in terms of volumetric flow rate and the type of material being handled in order to supply the correct size of equipment. Therefore, the processing equipment has been scale-up according to the following:

(a) ***Materials Flow***

From pilot-plant data (Appendix D, table 6.4.1) at 50% degree of acidulation 129.3 g/min rock requires 11.47 ml/min sulphuric acid.

Volume of acid X density = weight of acid

= 11.47 X 1.83 = 20.9901 g/min, but only 98% is H_2SO_4 while the rest is water.

Therefore weight of acid = 98% X 20.9901 = 20.5703 g/min

Assuming no losses weight of PAPR will be weight of acid + weight of phosphate rock = 129.3 + 20.5703 = 149.8703 g/ min

Rock / PAPR ratio = 129.3 / 149.8703 = 0.8627

On large scale PAPR = 30 tonnes per hour.

Hence, phosphate rock required = 30 X 0.8627 = 21 tonnes per hour.

Acid / rock ratio = 11.47 / 129.3 = 0.0887 ml/g = 88.7 liters / tonne of phosphate rock.

(b) ***Primary crusher***

Density of uncrushed phosphate rock (15-30cm size) = 3.1g/cm^3 = 3.1 tonnes/m^3

Throughput rate = 21 tonnes per hour

Feed rate = 21 / 3.1 = 6.8 m^3/hour

(c) ***Secondary crusher***

Bulk density of the material crushed to -50mm is = 2g/cm^3 = 2 tonnes/m^3

Throughput rate = 21 tonnes / hour

Feed rate = 21 / 2 = 10.5 m^3/hour

(d) Grinding Mill

Bulk density of the material crushed to -6mm = 1.5g/m^3 = 1.5 tonnes/m^3

Feed rate = 21 tonnes / hour

Feed rate = 21 / 1.5 = 14 m^3 / hour

Process will employ dry milling using a Euromag mill.

(e) Granulator

Bujlk density of ground material = 1g/cm^3

Rock feed rate = 21 tonnes / hour

Rock feed rate = 21 / 1 = 21 m^3/hour

Acid feed rate = 88.7 X 21 = 1862.7 liters / hour

(f) PAPR drier & vibrating screen

Bulk density of PAPR = 1.1g/cm^3 = 1.1 tonnes/m^3

PAPR throughput rate = 30 tonnes/hour

PAPR volumetric throughput rate = 30 / 1.1 = 27.3 m^3/hour

Maximum drying temperature = 150°C

Maximum moisture content of feed = 12%

Moisture content of dry PAPR = 0.8% - 1%

The vibrating screen will have the same throughput rate as the drier in order for it to handle material from the drier.

4.3 Location

Petauke district has been proposed for siting the processing plant for PAPR. The main advantages of locating the plant in Petauke include:

(1) Proximity to the 33kV electricity power line. The Chilembwe phosphate deposit is 65km away from the closest power line (Figures 4.1 and 4.2). Siting the process plant near the deposit in Chilembwe would require

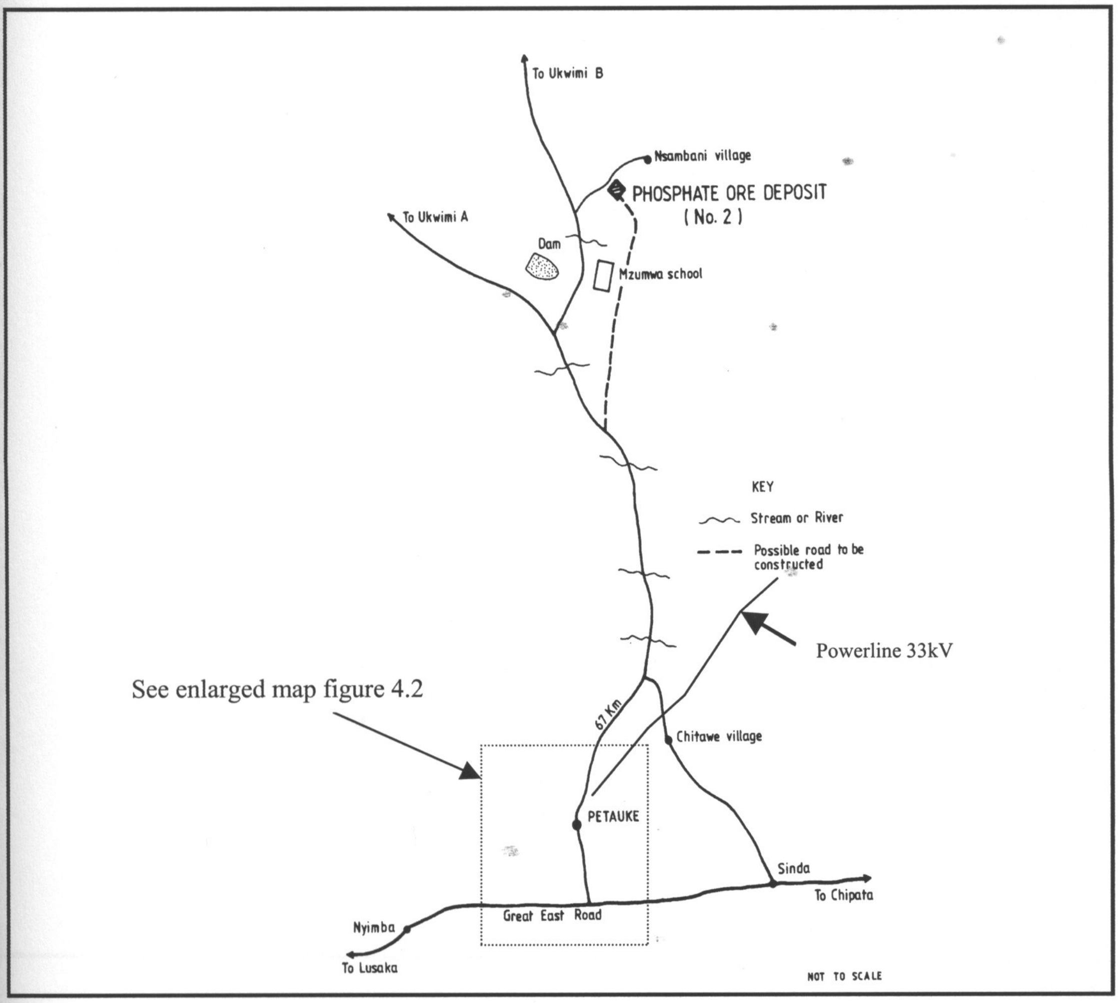

Figure 4.1. Relative position of Chilembwe phosphate deposit.

extension of the power line over a distance of 65km from Petauke to Chilembwe. Such a move would be difficult in terms of the extra capital needed to undertake it in the short term unless the cost of constructing it is wholly met by the power company, the Zambia Electricity Supply Corporation (ZESCO) itself. The selected site for processing of the ore is close to the power line, therefore, the run-of-mine ore requires transportation from Chilembwe to the proposed site for a distance of 65km.

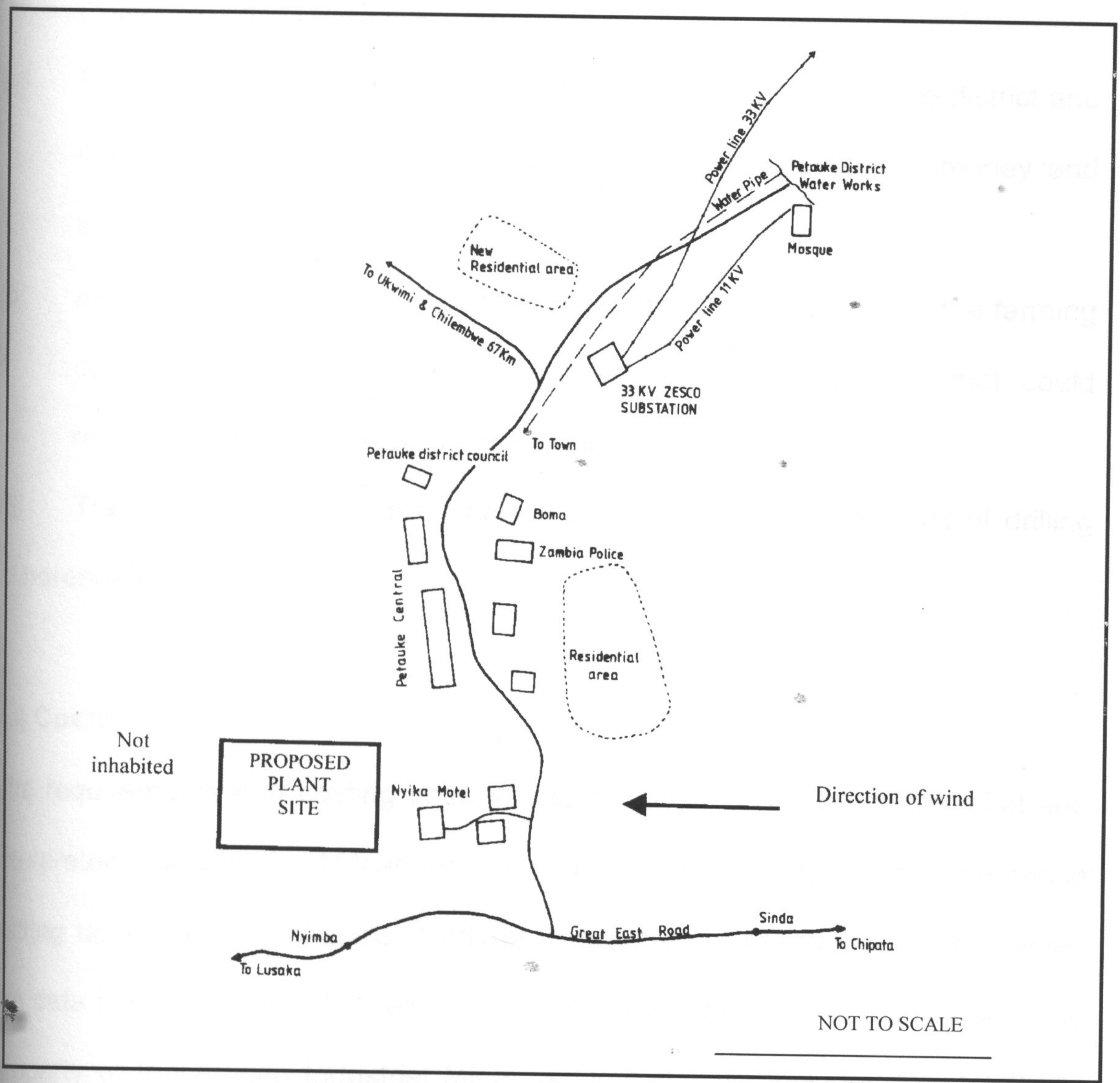

Figure 4.2. Proposed site for PAPR processing plant.

(2) *Petauke is close to the Great East Road* which is the main tarred road leading to Lusaka and Chipata giving an extra advantage in terms of transportation of finished PAPR to the market areas.

(3) *Shops, accommodation* and most of the *social amenities* required by the labour force in the processing plant already exist in Petauke. The labour force at the mine site in Chilembwe will be recruited from the nearby Sambani village. Only one mining engineer will be commuting to Chilembwe from Petauke.

(4) The investment would further enhance the *development* of the district and surrounding areas due to the anticipated increased flow of money and traffic to the area.

(5) *Inexpensive PAPR basal fertilizer* could be readily available to the farming community in the district and the surrounding areas and that could remarkably increase crop production in the region.

(6) There is readily available *water* and this would avoid the cost of drilling boreholes.

4.4 Costs

The requirements and costing used in this evaluation have been compiled and interpreted solely by the African Industrial Minerals Limited, which is interested in setting up a commercial-scale PAPR processing plant in Petauke. In this work, the data has been utilized purely for academic purposes and remains strictly the property of the African Industrial Minerals Limited. This includes Capital Costs

(Table 4.1), Operating Costs (Table 4.2), Processing Costs (Table 4.3), Production and Sales (Table 4.4) and Cost of Production (Table 4.5). The proposed production scale is 30 Mt per hour of PAPR attainable in the third year of operation. Some of the equipment has been bought second hand locally and these will require rehabilitation as shown in Table 4.1.

Table 4.1. Capital costs.

As at 5 Aug 2002

Capital costs	**US $ Projection**	**Remarks**
Chilembwe		
Environmental report + license	5,000	
Mining plan and Tech transfer	5,000	
Mechanical equipment:		
CAT D4 Dozer	45,000	subject to survey
F E Loader		lease
Tractor/trailer unit	150,000	tbd
Tools (Compressor, Mech, Hand)	13,100	quote
Fence	21,875	quote
Road	60,000	based upon quote
Utility X 2	38,000	quote
Radio	1,600	quote
Solar panels batteries and pumps	11,250	quote
Office and first aid equip	4,000	quote
Lab equip	5,000	quote
Civil works	35,750	based upon quote
Sub Total	395,575	
Petauke		
Site acquisition	2,000	estimate
Loader and forklift		lease
Utility vehicles	76,000	quote
Civil Works + Warehousing	115,000	indication
Bore holes X2	14,450	
Weighbridge	57,500	
Electrical substation	15,000	indication
Generators – 2 x 500Kva		See milling quote
Primary crushers	8,500	Quote

Rehabilitation	2,000	Estimate
Motor and spares	6,000	Indication
Lifting	4,300	Quote
Secondary crusher		See milling quote
Mill	650,000	Indication
Granulator	7,500	Quote
Rehabilitation	3,000	Estimate
Motor and spares	12,000	Indication
Compressor and acid feeds	6,000	Quote
Rubber lining	12,000	Indication
Dryer	7,500	Quote
Rehabilitation	2,500	Estimate
Motor and spares	8,000	Indication
Lifting	3,936	Quote
Heater	10,000	Estimate
Conveyors (fabrication at Kabwe)	7,500	Estimate
Hoppers	35,000	Quote + estimate
Extractor & Scrubbing system	6,000	Estimate
Bagging plant	68,200	Quote
Compressor and wiring	6,000	
Delivery & Commissioning:		
Euromag mill		See milling quote
Ex Kabwe	5,760	Quote
Chemical plant	15,000	Estimate
Bagging plant	16,313	Quote
Scania trucks X 3	300,000	
Laboratory equipment	5,000	Quote
Office equipment	28,000	Quote
Workshop equipment	26,000	
Mining software	4,000	Indication
Acid tank & Rehabilitation (60, 000 lt)	6,672	tbc
Sub Total	1,552,631	
TOTAL	1,948,206	
Contingence @20%	389,641	
TOTAL CAPITAL COSTS	**2,337,847**	

Table 4.2. Operating costs.

Operating Costs	**US $**	
Labour (p.a)		
Managing Director	60,000	Estimate
Workforce – Processing	104,370	Estimate
Workforce – Mine	55,000	Estimate

Geologist	5,000	Estimate
Tech consultancy	4,000	Estimate
Financial Controller	12,000	Estimate
Sub Total	240,370	
Annual Operating Costs		
Water	5,000	Estimate
Workmans'compensation		Covered in salary calculations
Insurances	25,000	Estimate
Maintenance/Spares	52,000	Estimate
Directors expenses	160,000	
MD fee Professional Services	36,000	Corpus Globe
Marketing	35,000	
R & D (Sch Mines etc)	5,000	
Fuel and Office consumables	28,000	Suggestion
Accomodation (X 8 p.a.)	14,400	Quote
Sub Total	360,400	
Annual costs	600,770	
Contingiency @ 20%	120,154	
Total Annual Costs	720,924	
Annual Cost inflation:	0.12	

Table 4.3. Processing costs.

Processing Costs (US$/Mt)			
Extraction Cost	1.00	Explosives etc	
Generator fuel	3.00	Indication	
Hammermill wear	0.33	Indication	
Sulfuric Acid (@ $110 per Mt)	10.00	Calculation Zincorp S. A.	
Bags (@ $0.31 incl printing)	6.20	Quote	
Plant hire:			
Front end loader (@$55 Hr)	2.75	Quote	
Tipper truck (@$27 per load)	2.70	Quote	
Fork lift	0.60		
Tractor (@ 12 Hr)	0.60	Quote	
Front end loader (@$55 Hr)	2.75	Quote	
Transport from Chilembwe (fleet)	2.50		
Transport from Chilembwe (Sub-contract)		Indication	10.00
Pallets	3.00		
Sub Total	35.43		
Contingency @ 20%	7.09		
Processing cost US$/ Mt	**42.52**		

Table 4.4. Production and sales.

Production and Sales

Production	Year 1	Year 2	Year 3
Mt per hour	15.00	20	30
Hours per day	8.00	12	12
Days per Month	16.00	20	20
Mt per Month	1,920.00	4,800	7,200
Months of Production	9.50	12	12
Mt produced in Year	18,240.00	57,600	86,400
Mt per annum (annualized)	*23,040.00*		

Table 4.5. Cost of production.

Cost of production	Year 1	Year 2	Year 3
Total Annual Costs (US$)	720,924.00	847,086	995,326
Processing Cost (US$/Mt)	42.52	50	59
Total Annual production (Mt)	18,240.00	57,600	86,400
Total Cost US$/Mt	**82.04**	**65**	**70**
Annualized Cost US$/Mt	***73.81***		

Utilizing the above data, the following calculations were performed.

Mineable ore (Mt) 1,640, 000 Mt

Extraction (Mt per annum) yr 1 (18240Mt), yr 2 (57600Mt), yr 3 (86400Mt). It has been assumed that after 3 years the production rate will remain constant at 86,400Mt per annum for the remaining years of the mine life unless more investment is made. Hence, mineable ore after 2 years will be 1,564,160 Mt at 86,400Mt per year and this could be mined for 18 years. Hence, the mine life is 20 years. However, in this work, economic evaluation has considered 15 years of operation by assuming that beyond 15 years more capital would be required to sustain the operation. The Net Present Value (NPV) and the Benefit to Cost ratio (B/C) have been used as the main methods of analyzing the project economics.

Net Present Value

Net Present Value (NPV) = Net Present Worth Positive and Negative Cash Flows at the minimum Rate of Return (ROR). A positive NPV means satisfactory project economics and a negative NPV means unsatisfactory project economics. At break-even the NPV becomes zero.

Benefit-Cost ratio

The ratio of the present Worth Net Positive Cash Flows to the present Worth Net Negative Cash Flows, commonly called Benefit-Cost ratio (B/C Ratio) is defined as follows:

$$\text{Benefit Cost Ratio} = \frac{\text{Present Worth Net Positive Cash flow @ i*}}{\left|\text{Present Worth Net Negative Cash flow @ i*}\right|}$$

A B/C Ratio greater than 1.0 indicates satisfactory project economics, a B/C ratio equal to 1 indicates break-even economics with investing elsewhere at a Rate of Return (ROR) equal to the minimum ROR, "i*", and a B/C ratio less than 1.0 indicates unsatisfactory project economics compared to investing elsewhere at "i*". B/C ratio is also sometimes referred to as Profitability Index, or, "PI".

The numerator, "present Worth Net Positive Cash Flow @ i*, is the present Worth of Net Positive Cash Flow not required to pay off future negative cash flows. The denominator, "present Worth Net Negative Cash flow @ i*", represents the absolute or positive value of present worth negative cash flow not offset by positive cash flow generated in earlier project years. The denominator is reflective of those cash flows that cause project Cumulative NPV to reach its lowest point or "maximum capital at risk" in the project. This is the money an investor would have set aside today, (time zero) at the minimum Rate of Return in order to cover all of the negative cash flow realized in the project that is not projected to be covered by project positive cash flows in earlier years. Down stream costs that are covered or paid off by positive cash flow in earlier years do not impact the ratio denominator because no additional investment needs to be made by the investor. For example, down stream expansion, abandonment or reclamation costs that are offset, or can be paid off either by revenues in the year they are incurred or by preceding positive cash flow do not impact ratio denominators [Stermole and Stermole, 1996].

Loan

Capital = $2337847

Working capital = processing costs + total annual costs in year 3 = $5097600 + $995326 = $6092926 per annum.

Or $507743.83 per month.

Assuming the working capital could cover only the first 3 months during which PAPR stocks will be built for sale. Hence,

Working capital = $1523232.

The loan has to cater for the capital as well as the working capital. Hence,

Loan = $2337847 + $1523232 = $3861079.

The loan repayment period is assumed to be 10 years in equal instalments.

Cash flow

Pre-Tax Net = Revenue – Processing Costs – Annual Costs – Loan Repayment – Interest on loan – Depreciation.

Mineral Loyalty @ 2% = Pre-Tax Net x 2/100

Depreciation is calculated by dividing the capital by 15 years and subtracted in equal amounts for 15 years.

Amortization and Depletion (not considered in the Zambian government's taxation policy on mining).

Net-Taxable = Pre-Tax Net – Mineral Loyalty

Company Tax @ 35% = Net-Taxable x 35/100

Net After Tax = Net-Taxable – Company Tax

Net Cash Flow = Net after Tax + Depreciation + Capital Expenditure + Working Capital + Salvage.

Discounted Cash Flow = Net Cash Flow X $(1/(1 + i)^n)$

Where i = discount rate

n = operating year

Net Present Value (NPV) and Benefit to Cost Ratio (Refer to Section 4.2).

4.5 Source of capital

In this work, an assumption is made that money has to be sourced by the following means:

(i) *Loan* from a banking institution within Zambia. Interest rates on loans as at 25th August, 2002 were as follows:

(7) Zambia National Commercial Bank Ltd (ZANACO) 53% interest.

(8) Development Bank of Zambia (DBZ) 8 – 12% interest depending on the source of funding. DBZ is currently undergoing restructuring and has no money to lend until government sources some funds from partners abroad.

(ii) *Sale of shares.* Money could be sourced through the sale of shares by floating them to the public on the Lusaka Stock Exchange Market.

(iii) *Private investors from outside Zambia* could source funds from banks in their country(ies) at competitive interest rates, such as 12% interest.

The loan is estimated at US$ 3.91 million at a competitive interest rate to make the investment feasible. Ten years has been assumed as the loan repayment period. Taxes include *mineral loyalty* at 2% of the gross value and *company tax* at 35% of the net as stipulated in the government's taxation policy on mining and processing. *Depreciation* on capital equipment costs is currently at 100% according to information obtained from the Zambia Revenue Authority. *Amortization and depletion* have not been provided for in the current taxation policy and are therefore non-existent.

At the high interest rate, 53%, the actual amount of money required to be paid back to the ZANACO bank as interest in the first year of operation would be a staggering $1,842,000 (table 4.6). Adding this to the initial installment of $386,000 towards the loan, the total equals $2,228,000. In addition, processing costs and annual costs would require a further $1,497,000.

Table 4.6. Interest rate at 53% and price at $177.78 per Mt or K40,000 per 50kg bag.

All figures in US$' 000'

Operating year	0	1	2	3	4	5	6	7	8	9	10	11	12	13	14	15
Revenue	0	3243	10240	15360	15360	15360	15360	15360	15360	15360	15360	15360	15360	15360	15360	15360
Processing costs	0	776	2880	5098	5098	5098	5098	5098	5098	5098	5098	5098	5098	5098	5098	5098
Annual costs	0	721	847	995	995	995	995	995	995	995	995	995	995	995	995	995
Loan repayment (10 years)	0	386	386	386	386	386	386	386	386	386	386	0	0	0	0	0
Interest on loan @ 53%	0	1842	1637	1432	1228	1023	819	614	409	205	0	0	0	0	0	0
Depreciation @ 100%	0	156	156	156	156	156	156	156	156	156	156	156	156	156	156	156
Pre-tax net	0	-637	4334	7293	7497	7702	7907	8111	8316	8521	8725	9111	9111	9111	9111	9111
Mineral loyalty @ 2%	0	0	87	146	150	154	158	162	166	170	175	182	182	182	182	182
Net taxable	0	0	4247	7147	7348	7548	7749	7949	8150	8350	8551	8929	8929	8929	8929	8929
Company tax @ 35%	0	0	1487	2501	2572	2642	2712	2782	2852	2923	2993	3125	3125	3125	3125	3125
Net after tax	0	-637	2761	4646	4776	4906	5037	5167	5297	5428	5558	5804	5804	5804	5804	5804
Depreciation	0	156	156	156	156	156	156	156	156	156	156	156	156	156	156	156
Capital expenditure	-2338	0	0	0	0	0	0	0	0	0	0	0	0	0	0	0
Working capital	-1523	0	0	0	0	0	0	0	0	0	0	0	0	0	0	1523
Salvage	0	0	0	0	0	0	0	0	0	0	0	0	0	0	0	30
Net Cash Flow	-3861	-482	2917	4801	4932	5062	5192	5323	5453	5584	5714	5960	5960	5960	5960	7513
Discount Cash Flow @ 30%	-3861	-370	1726	2185	1727	1363	1076	848	669	527	414	333	256	197	151	147

NPV 7387 Satisfactory Economics

Benefit-Cost ratio 2.75 Satisfactory Economics

Although the project economics would be satisfactory, unfortunately, the revenue in the first year of operation would only be $3,243,000 and this would be grossly insufficient to meet the anticipated financial requirements. Hence, 53% interest rate renders the investment a non-starter. Therefore, the loan must be obtained from DBZ at 12% interest rate.

4.6 Price of PAPR and Project Economics

The minimum rate of return is the discount rate where the Net Present Value (NPV) equals zero and the Benefit-Cost ratio (B/C) equals 1, indicating the break-even point of the project. If other factors in the cash flow would remain constant, the price would vary with the minimum rate of return assuming the project is at break-even. This is because the price of the commodity directly determines the revenue generated from the sales. Therefore, the variation of the price of PAPR with the minimum rate of return has been carried out in order to determine the most competitive price when compared with the basal fertilizer that is currently on the Zambian market. Table 4.7 shows the minimum rates of return with their corresponding prices of PAPR. The exchange rate as at 30th August, 2002 was taken as K4500 per US$1. In each scenario the price was determined by trial and error using a computer program in excel.

The price that gave a NPV of approximately $0 and a Benefit-Cost ratio of approximately 1 was taken as being the price at the minimum rate of return (at break-even).

Table 4.7. Price of PAPR obtained at the various minimum rates of return.

Minimum rate of return	Price US $ per Mt	Price Kwacha per 50kg bag
0%	78.12	17577
30%	108.18	24341
50%	134.33	30224
100%	220.14	49532

At 0% minimum rate of return, the price of PAPR would be $78.12 per Mt or K17,577 per 50kg bag. This kind of scenario assumed that the Dollar must remain at its present value for 15 years. This certainly can not be possible because the Dollar will lose some of its value in the period under consideration and besides no investor puts money in a 0% rate of return project with prior knowledge. The second scenario assumes 30% minimum rate of return and the price in this case changes to $108.18 per Mt or K24,341 per 50kg bag. If the actual discount rate would be lower than 30% then the project could give favourable economics. As a matter of safety, in this work, a 30% discount rate has been assumed. Hence, this scenario puts the project at break-even. The third scenario assumes 50% minimum rate of return and the corresponding price would be $134.33 per Mt or K30,224 per 50kg bag. With the discount rate at 30% per annum, the NPV and B/C would be $3.68 million and 1.95 respectively, indicating satisfactory project economics. The fourth scenario assumed 100% minimum rate of return and the corresponding price would be $220.14 per Mt or K49532 per 50kg bag.

Table 4.8. Minimum rate of return at $177.78 per Mt or K40,000 per 50kg bag.
All figures in US$' 000'

Operating year	0	1	2	3	4	5	6	7	8	9	10	11	12	13	14	15
Revenue	0	3243	10240	15360	15360	15360	15360	15360	15360	15360	15360	15360	15360	15360	15360	15360
Processing costs	0	776	2880	5098	5098	5098	5098	5098	5098	5098	5098	5098	5098	5098	5098	5098
Annual costs	0	721	847	995	995	995	995	995	995	995	995	995	995	995	995	995
Loan repayment (10 years)	0	386	386	386	386	386	386	386	386	386	386	0	0	0	0	0
Interest on loan @ 12%	0	417	371	324	278	232	185	139	93	46	0	0	0	0	0	0
Depreciation @ 100%	0	156	156	156	156	156	156	156	156	156	156	156	156	156	156	156
Pre-tax net	0	787	5600	8401	8447	8494	8540	8586	8633	8679	8725	9111	9111	9111	9111	9111
Mineral loyalty @ 2%	0	16	112	168	169	170	171	172	173	174	175	182	182	182	182	182
Net taxable	0	772	5488	8233	8278	8324	8369	8415	8460	8505	8551	8929	8929	8929	8929	8929
Company tax 35%	0	270	1921	2882	2897	2913	2929	2945	2961	2977	2993	3125	3125	3125	3125	3125
Net after tax	0	501	3567	5351	5381	5410	5440	5469	5499	5529	5558	5804	5804	5804	5804	5804
Depreciation	0	156	156	156	156	156	156	156	156	156	156	156	156	156	156	156
Capital expenditure	-2338	0	0	0	0	0	0	0	0	0	0	0	0	0	0	0
Working capital	-1523	0	0	0	0	0	0	0	0	0	0	0	0	0	0	1523
Salvage	0	0	0	0	0	0	0	0	0	0	0	0	0	0	0	30
Net Cash Flow	-3861	657	3723	5507	5537	5566	5596	5625	5655	5684	5714	5960	5960	5960	5960	7513
Discounted Cash Flow @76.96%	-3861	371	1189	994	565	321	182	104	59	33	19	11	6	4	2	1

NPV 0 Break-even

Benefit-Cost ratio 1.00 Break-even

If the discount rate remains at 30%, the economics of the project would be very favourable. However, this price seems to be on the high side because of the low percentage of available P_2O_5 in PAPR when compared with the basal fertilizer currently on the market. It is necessary to note that PAPR produced from unbeneficiated Chilembwe phosphate rock contains less than 10% available P_2O_5 with about 7% S whilst its competitor, basal compound fertilizer, contains 18% available P_2O_5, and in addition it also contains 6%N, 8% K_2O and 8.5% S. It must also be noted that N and K are virtually absent in PAPR. These two components if needed would have to be applied separately by the farmers themselves.

Therefore in view of the above concerns, a competitive price of K40,000 per 50kg bag of PAPR would be reasonable bearing in mind that the cost of basal fertilizer in Petauke is about K80000 per 50kg bag. At K40,000 per 50kg bag of PAPR the NPV and B/C would be $9.58 million and 3.48 respectively at 30% discount rate, indicating favourable project economics (table 4.8).

The price of K40,000 per 50kg bag of PAPR in Petauke would give sufficient profit and make the commodity highly competitive. The minimum rate of return at K40,000 per bag would be 76.96% and that is very high indicating good profits if discounting is done at 30%. Figure 4.3 shows how the cumulative NPV varies with the project life when the price of PAPR is maintained at $177.78 per Mt or K40,000 per 50kg bag. The payback period for the project would be 2.5 years.

Maximum capital at risk appears at year 0 just when money has been borrowed as a lump figure. The negative part of the curve shows the region of zero profits. The payback period appears at the point where the cumulative NPV becomes equal to zero. Net profits begin to accumulate after the payback period at 2.5 years.

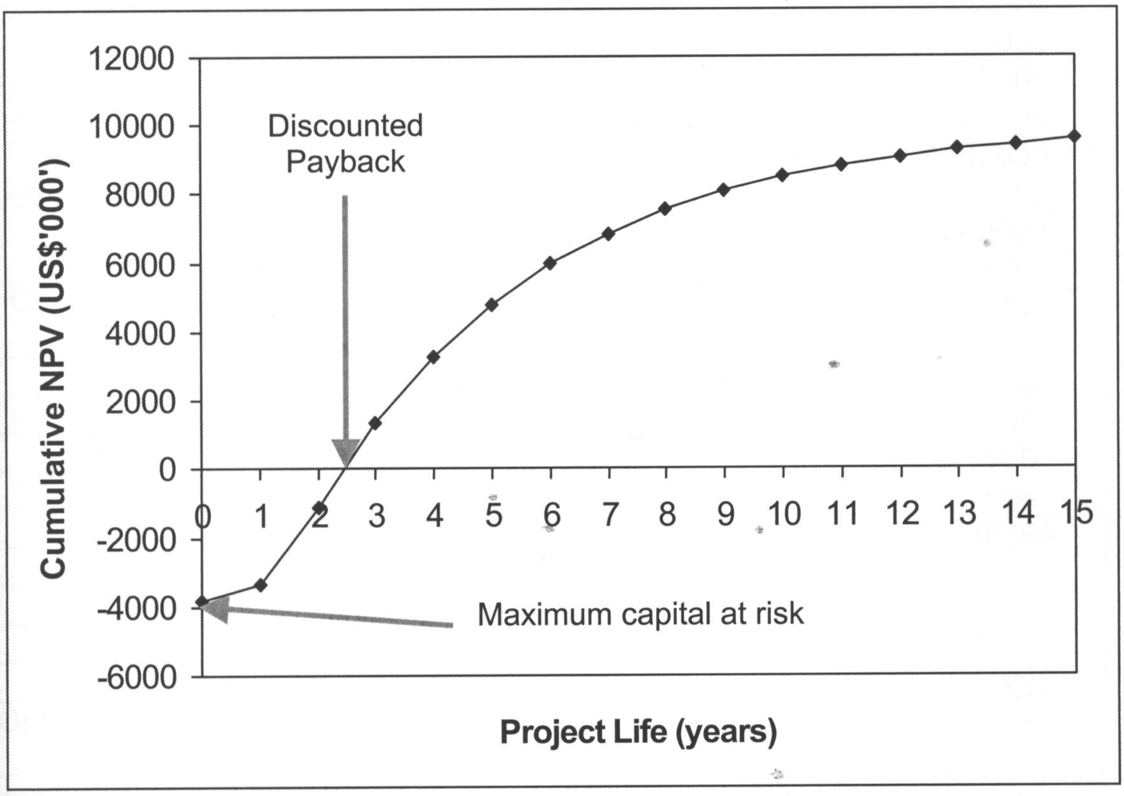

Figure 4.3. Graphical illustration of payback using cumulative NPV @ 30% discount rate and the price of PAPR at K40000 per 50kg bag.

4.6.1 Labour

Table 4.9 shows the projected labour requirements and their monthly emoluments. These values were estimated by referring to the already estimated labour costs in Table 4.2.

Table 4.9. Labour

Labour Costs	No.	US$ per annum	Total	K per month per person
Managing Director	1	60000	60000	22500000
Financial Controller	1	12000	12000	4500000
Sub-Total	**2**	**72000**	**72000**	**27000000**
WORKFORCE				
Processing:				
Process Engineer	1	12000	12000	4500000
Foreman	2	5000	10000	1875000
Operator (Materials Handling)	2	3000	6000	1125000
Operator (Processing)	2	3000	6000	1125000
Operator (Packaging)	2	3000	6000	1125000
Laboratory Technician	1	4970	4970	1863750
Mechanic	1	3200	3200	1200000
General workers	26	1200	31200	450000
Clerks (stores, sales, purchasing)	3	2500	7500	937500
Drivers	5	2100	10500	787500
Secretary	2	2000	4000	750000
Mail	1	900	900	337500
Cleaner	3	700	2100	262500
Sub-Total	**51**	**43570**	**104370**	**16338750**
Mining:				
Mining Engineer	1	12000	12000	4500000
Mine Captain	1	5000	5000	1875000
Operators (Drilling and Blasting)	5	3100	15500	1162500
Drivers (loading and hauling)	5	2100	10500	787500
General workers	10	1200	12000	450000
Sub-Total	**22**	**23400**	**55000**	**8775000**
Geologist	1	5000	5000	1875000
Tech consultancy	1	4000	4000	1500000
Sub-Total	**2**	**9000**	**9000**	**3375000**
GRAND TOTAL	**77**	**147970**	**240370**	**55488750**

With the exclusion of the managing director, at least 76 people could be employed in this industry and more than K30 million per month as salaries would end up in Petauke district. This could have a positive impact on the economy of the district.

4.6.2 Government Revenue

The mineral loyalty and company tax would earn government more than $3 million per annum attainable in the third operating year and the rest of the project life. An indirect benefit would result from the partial reduction in the total foreign exchange currently spent on the importation of phosphate fertilizers since part of the phosphate requirements would be met by the local phosphate resource.

4.7.3 PAPR price variation with distance from Petauke

Transportation costs generally increases the price of fertilizers. Figure 4.4 show the projected prices of PAPR extrapolated by considering the distance from Petauke where the commodity would cost K40000 per 50kg bag. The transportation cost based on Dar Farms and Transport International, Lumumba and Mwembeshi Road, Lusaka is currently quoted as K300 per Mt per km.

The most distant place would be Mbala where the price would reach a maximum of K60,745 per 50kg bag of PAPR. Indeed PAPR would be inexpensive for the resource poor farmers in Zambia and setting up an industry to produce the commodity is highly recommended by this research project.

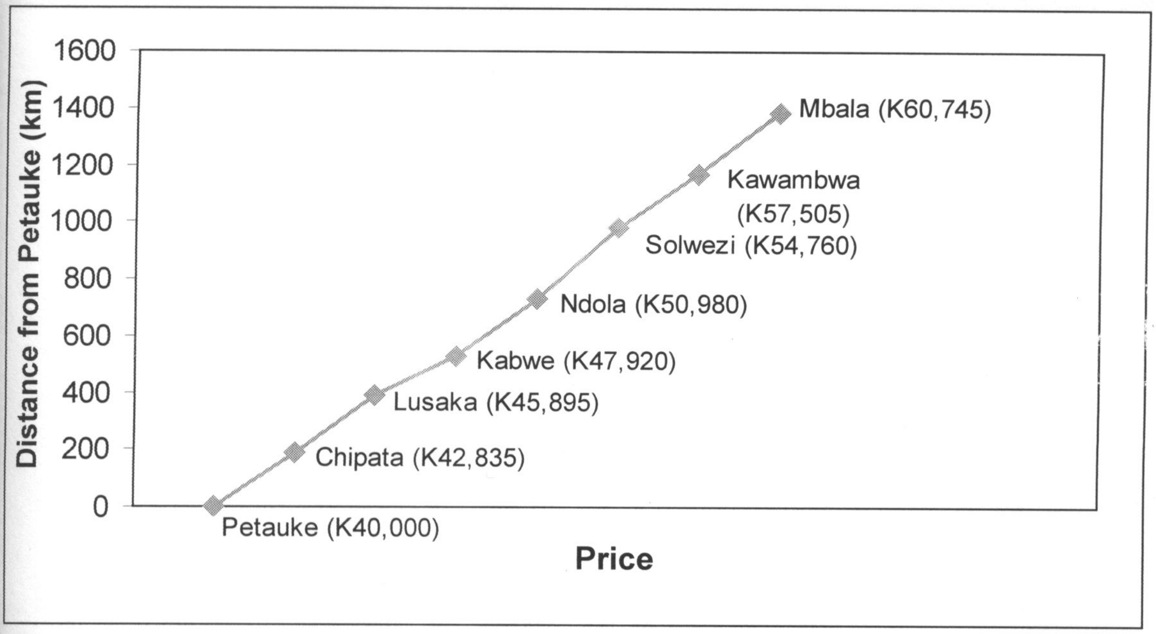

Figure 4.4. Estimated price per 50kg Bag of PAPR in the selected towns/districts in Zambia

The estimated rate of return is high at a very competitive price on the Zambian market.

CONCLUSIONS

CONCLUSIONS

Considering all the areas covered in this research, the following conclusions have been drawn:

(1) The apatite in Chilembwe phosphate rock exists in the form of calcium manganese fluoride phosphate with the chemical formula $Ca_{9.3}Mn_{0.7}F_2(PO_4)_6$ suggesting that 0.7 out of 10 of the constituent ion Ca^{+2} have been substituted by a substituting ion Mn^{+2} thus leaving 9.3 of the Ca^{+2} that has resulted in the alteration of the ideal fluorapatite, $Ca_{10}(PO_4)_6F_2$ to the present mineral $Ca_{9.3}Mn_{0.7}F_2(PO_4)_6$.

(2) The apatite in Chilembwe phosphate rock is coarse grained, most of it being in the size range 400μm to 800μm. Whilst 600μm is the most frequent size, the average grain size is approximately 641μm. In the comminution process the bulk of the apatite mineral is liberated from the rock matrix by grinding to minus 106μm.

(3) In the particle size range 42 to 79% minus 75μm the percentage of water soluble P_2O_5 and NAC-soluble P_2O_5 in PAPR remains constant.

(4) The percentage of available P_2O_5 in PAPR increases with the increase in the degree of acidulation (i.e. 40%, 50%, 60%, 70%, 80%, and 100%).

(5) The rate of reaction between phosphate rock and sulphuric acid is controlled by film diffusion control mechanism. Therefore the rate of diffusion and indeed the rate of reaction is high at high acid concentrations and at high temperatures.

(6) Low acid concentrations, 50 to 70% H_2SO_4 gives high levels of water-soluble P_2O_5 and NAC-soluble P_2O_5 in PAPR. Acid concentration below 40% and above 70% lowers the percentage of water-soluble P_2O_5 and NAC-soluble P_2O_5 in PAPR. This is because a high acid concentration results in a high temperature and a high rate of reaction which causes the calcium sulphate to precipitate from a strongly supersaturated liquid phase in a fine particle size on the surface of the unreacted rock particles thereby partially blocking contact between the liquid phase and the unreacted rock particles resulting in the poor conversion of apatite to soluble forms. On the other hand at 40% acid concentration the reaction is too slow to give a good conversion of apatite to soluble P_2O_5.

(7) The initial temperature of the rock, water and acid before the reaction did not have a remarkable effect on the percentage of water-soluble P_2O_5 and NAC-soluble P_2O_5 in PAPR in the range 25 to 110°C. Hence the initial temperature should remain at ambient temperature.

(8) The optimum residence time in the granulator was found to be 3 minutes. Beyond 3 minutes, there was no significant change in the percentage of water-soluble P_2O_5 and NAC-soluble P_2O_5.

(9) The drying temperature in the range of 90°C to 150°C did not affect the percentage of total available P_2O_5 in PAPR. However, water-soluble P_2O_5 decreased with the increase in drying temperature whilst NAC-soluble P_2O_5 increased with the increase drying temperature keeping the total available P_2O_5 constant.

(10) The selective recycle model for a generalized NCD has been effectively used to simulate the RTD's in the comminution of phosphate rock and in the acidulation and granulation processes. This resulted in the optimization of the operations of the main processing units (i.e. the ball mill in the comminution of phosphate rock and the granulator in the production of PAPR).

(11) The PAPR produced at optimized parameters contained 9% available P_2O_5 and 18% total P_2O_5 at 50% degree of acidulation using phosphate rock with original assay of about 23% P_2O_5.

(12) Field test results on maize, soya beans, sunflower, and groundnuts have shown that PAPR is as agronomically effective as imported mono-ammonium phosphate (MAP). In addition, PAPR is more suitable than MAP in recapitalizing the soil with phosphorus, as it does not depress maize yields at high application rates.

(13) Economic evaluation of a 30TPH commercial production of PAPR has shown that, indeed the production of PAPR could become a commercially viable project with a pay back period of two and half years. The price of PAPR could be about half that of the compound basal fertilizer that is currently on the market and this would vary with distance from K40,000 in Petauke to K60,745 in Mbala which is at the furthest distance from Petauke.

(14) Chilembwe phosphate deposit could indeed become an inexpensive source of phosphate that could partially substitute the imported phosphate

APPENDICES

and greatly benefit the low-resource farmers in the enhancement of agricultural crop production in Zambia.

APPENDIX A

6.1 Size sorting assays

6.1.1 Results

Table 6.1.1. Particle size analysis of phosphate using a pack of laboratory sieves.

Sieve size (microns)	Weight retained (%) Test 1	Test 2	Test 3	Average wt. retained (%)
1400	9.49	9.96	9.44	9.63
1180	5.58	5.73	5.59	5.63
850	9.01	10.27	9.17	9.48
600	11.65	12.40	12.04	12.03
425	11.62	11.98	12.00	11.87
300	10.98	11.01	11.18	11.06
212	9.26	9.00	9.26	9.18
150	6.46	6.14	6.39	6.33
106	6.26	5.70	5.98	5.98
75	5.37	4.84	5.06	5.09
53	3.52	3.08	3.33	3.31
-53	10.79	9.89	10.54	10.41
TOTAL	100.00	100.00	100.00	100.00

Table 6.1.2. P_2O_5 content in various size fractions.

Sieve size (microns)	% P_2O_5 Test 1	% P_2O_5 Test 2	% P_2O_5 Test 3	Average % P_2O_5
1400	17.14	17.13	16.14	16.81
1180	18.15	17.75	17.06	17.65
850	19.07	18.43	18.13	18.54
600	24.65	23.13	23.66	23.81
425	27.83	26.96	27.35	27.38
300	28.15	26.67	26.96	27.26
212	27.62	26.73	26.63	26.99
150	26.99	25.95	25.24	26.06
106	26.02	25.05	25.11	25.39
75	20.57	21.53	22.62	21.57
53	23.43	21.76	20.81	22.00
-53	21.21	20.08	20.26	20.52

APPENDIX B

6.2 RESULTS FOR THE EFFECT OF PARTICLE SIZE OF PHOSPHATE ROCK ON SOLUBLE P_2O_5 IN PAPR PRODUCTS.

6.2.1. Particle size analysis results

Table 6.2.1. Particle size analysis of phosphate rock ground to four different particle size distributions.

Particle size (microns)	Particle size distribution (Cum. wt % passing)			
	A	B	C	D
600	99.96	100.00	99.99	99.93
425	99.89	99.98	99.83	99.62
300	99.61	99.51	98.95	97.51
212	98.94	98.11	96.09	90.20
150	97.63	95.78	87.61	77.91
106	92.65	83.53	68.90	58.94
75	**79.00**	**62.00**	**51.25**	**41.72**
53	63.43	45.86	38.93	30.38

6.2.2. Chemical analysis of samples A, B, C and D summary

Table 6.2.2. Chemical composition of granulator feeds of various particle size distributions.

Components	Particle size distribution (Fraction passing 75 microns)			
	A (79% -75μm)	B (62% -75μm)	C (51% -75μm)	D (42% - 75μm)
CaO	26.37	26.57	28.42	28.47
MgO	1.05	0.94	0.89	1.14
K_2O	0.75	0.71	0.67	0.60
Na_2O	0.08	0.11	0.36	0.17
Al_2O_3	1.19	0.93	1.05	1.03
Fe_2O_3	1.60	1.69	1.53	1.43
P_2O_5	22.50	23.10	24.42	24.37
F	1.79	1.80	1.93	1.93
S	1.0	1.0	1.0	1.0

6.2.3 Experimental conditions

Degree of acidulation: 50%.

Acid concentration: 70% H_2SO_4 v/v.

Residence time in the granulator: 3 minutes.

PAPR drying temperature: 100°C.

Table 6.2.3. Rock feed rates to the granulator.

Feed rates	Particle size distribution (Fraction passing 75 microns)			
	A (79% -75μm)	B (62% -75μm)	C (51% -75μm)	D (42% -75μm)
Rock (g/min)	132.19	144.64	166.60	169.36
70% H_2SO_4 (ml/min)	16.41	17.66	21.89	22.37
Water (ml/min)	10.73	11.43	12.28	12.40

6.2.4 Summary of results

Table 6.2.4. Effect of particle size of phosphate rock on soluble P_2O_5 in 50% PAPR.

Particle size dist. (mμ)	Water-soluble P_2O_5				NAC-soluble P_2O_5			
	Test 1	Test 2	Test 3	Average	Test 1	Test 2	Test 3	Average
A	4.91	4.97	4.88	4.92	6.05	-	4.30	5.18
B	5.78	5.40	5.61	5.59	2.83	3.19	3.20	3.07
C	2.66	2.68	2.41	2.59	1.73	2.55	3.50	2.59
D	4.87	4.27	4.73	4.62	4.56	5.66	4.51	4.91

Particle size dist. (mμ)	Available P_2O_5
	Average
A	9.10
B	8.66
C	5.18
D	9.53

6.2.5 Particle size analysis of samples A, B, C and D detailed results

Granulator feed A was obtained in the closed grinding circuit pilot-plant using the hydrocylcone at an overflow pulp density of 1010gpl and 102.1ml/sec flowrate. The feed rate of the rock to the ball mill was maintained at 25kg/hr.

Table 6.2.5. Particle size analysis of granulator feed A.

Particle size (microns)	Cum. wt% passing			
	Test 1	Test 2	Test 3	Average
600	99.98	99.93	99.97	99.96
425	99.92	99.84	99.90	99.89
300	99.63	99.56	99.64	99.61
212	98.96	98.88	98.97	98.94
150	97.64	97.59	97.65	97.63
106	92.50	92.69	92.74	92.65
75	78.59	79.19	79.23	**79.00**
53	62.81	63.68	63.80	63.43

Granulator feed B was obtained in the closed grinding circuit pilot-plant using the classifier with weir bars set at 24.2cm from the bottom at an overflow pulp density of 1015gpl and 9.5ml/sec flowrate. The feed rate of the rock to the ball mill was maintained at 25kg/hr.

Table 6.2.6. Particle size analysis of granulator feed B.

Particle size (microns)	Cum. wt% passing			
	Test 1	Test 2	Test 3	Average
600	100.00	100.00	100.00	100.00
425	99.95	100.00	100.00	99.98
300	99.27	99.60	99.65	99.51
212	97.85	98.22	98.28	98.11
150	95.54	95.87	95.93	95.78
106	83.35	83.50	83.74	83.53
75	61.89	61.78	62.34	**62.00**
53	45.56	45.99	46.03	45.86

Granulator feed C was obtained in the closed grinding circuit pilot-plant using the classifier with weir bars set at 20.1cm from the bottom at an overflow pulp density of 1015gpl and 9.5ml/sec flowrate. The feed rate of the rock to the ball mill was maintained at 25kg/hr.

Table 6.2.7. Particle size analysis of granulator feed C.

Particle size (microns)	Cum. wt% passing			
	Test 1	Test 2	Test 3	Average
600	99.98	100.00	100.00	99.99
425	99.84	99.83	99.81	99.83
300	98.99	98.96	98.89	98.95
212	96.19	96.14	95.95	96.09
150	87.77	87.74	87.33	87.61
106	69.08	68.99	68.64	68.90
75	51.68	51.12	50.95	**51.25**
53	39.47	38.92	38.38	38.93

Granulator feed D was obtained in the closed grinding circuit pilot-plant using the classifier with weir bars set at 16cm from the bottom at an overflow pulp density of 1015gpl and 9.5ml/sec flowrate. The feed rate of the rock to the ball mill was maintained at 25kg/hr.

Table 6.2.8. Particle size analysis of granulator feed D.

Particle size (microns)	Cum. wt% passing			
	Test 1	Test 2	Test 3	Average
600	99.94	99.95	99.91	99.93
425	99.65	99.64	99.58	99.62
300	97.59	97.51	97.42	97.51
212	90.28	90.24	90.08	90.20
150	77.96	78.01	77.76	77.91
106	58.89	59.14	58.80	58.94
75	41.58	41.95	41.65	**41.72**
53	29.85	30.79	30.50	30.38

Table 6.2.9. Percent soluble P_2O_5 in PAPR produced using rock of particle size distribution A (79% minus 75μm).

Test No	Assay % P_2O_5				
	Total	Water-soluble	NAC-insoluble	NAC-soluble	Available
1	21.83	4.91	10.87	6.05	10.96
2	13.93	4.97	10.98	-	2.95
3	20.27	4.88	11.09	4.30	9.18
Average	21.05	4.92	11.04	5.18	10.07

Table 6.2.10. Percent soluble P_2O_5 in PAPR produced using rock of particle size distribution B (62% minus 75μm).

Test No	Assay % P_2O_5				
	Total	Water-soluble	NAC-insoluble	NAC-soluble	Available
1	22.89	5.78	14.28	2.83	8.61
2	22.76	5.40	14.17	3.19	8.59
3	22.85	5.61	14.04	3.20	8.81
Average	22.83	5.59	14.16	3.07	8.67

Table 6.2.11. Percent soluble P_2O_5 in PAPR produced using rock of particle size distribution C (51% minus 75μm).

Test No	Assay % P_2O_5				
	Total	Water-soluble	NAC-insoluble	NAC-soluble	Available
1	17.09	2.66	12.70	1.73	4.39
2	18.30	2.68	13.07	2.55	5.23
3	18.03	2.41	12.12	3.50	5.91
Average	17.81	2.59	12.63	2.59	5.18

Table 6.2.12. Percent soluble P_2O_5 in PAPR produced using rock of particle size distribution D (42% minus 75μm).

Test No	Assay % P_2O_5				
	Total	Water-soluble	NAC-insoluble	NAC-soluble	Available
1	23.25	4.87	13.82	4.56	9.43
2	23.23	4.27	13.30	5.66	9.93
3	22.99	4.73	13.75	4.51	9.24
Average	23.16	4.62	13.62	4.91	9.53

APPENDIX C

6.3 RESULTS FOR THE EFFECT OF DEGREE OF ACIDULATION ON SOLUBLE P_2O_5 IN PAPR

6.3.1. Feed composition summary

Table 6.3.1 Chemical composition of the feed.

Com	CaO	MgO	K_2O	Na_2O	Al_2O_3	Fe_2O_3	P_2O_5	F	SO_3
(%)	26.37	1.05	0.75	0.08	1.19	1.60	22.50	1.79	1.0

6.3.2 Experimental conditions

Acid concentration: 70% H_2SO_4. Residence time in the granulator: 3 minutes.
Drying temperature for PAPR: 100°C.

Table 6.3.2. Feed rates of components at the various degrees of acidulation.

Degree of acidulation	100	80	60	40	20	0
Rock feed rate (g/min)	129.3	129.3	129.3	129.3	129.3	-
Acid flowrate (ml/min)	32.1	25.68	19.27	12.84	6.42	-

Additional water varied from 25 to 42ml/min according to the degree of acidulation.

6.3.3 Summary of results

Table 6.3.3. Effect of the degree of acidulation on soluble P_2O_5 in PAPR products.

Degree of acidulation	Water-soluble P_2O_5 (%)				NAC-soluble P_2O_5 (%)			
	Test 1	Test 2	Test 3	Average	Test 1	Test 2	Test 3	Average
100	6.87	6.94	6.94	6.92	2.98	2.12	2.48	2.53
80	5.95	6.22	6.07	6.08	2.76	4.01	2.50	3.09
60	4.48	4.55	4.47	4.50	1.67	2.21	2.22	2.03
40	3.11	3.15	3.28	3.18	1.95	1.94	2.33	2.07
20	1.36	1.30	1.09	1.25	0.00	0.00	0.00	0.00
0	0.00	0.00	0.00	0.00	0.00	0.00	0.00	0.00

Degree of Acidulation	Available P_2O_5 (%)
	Average
100	9.44
80	9.17
60	6.53
40	5.26
20	1.25
0	0.00

6.3.4 Effect of degree of acidulation on soluble P_2O_5 in PAPR: detailed results

Table 6.3.4. Percent soluble P_2O_5 in PAPR at 100% degree of acidulation.

Test No	Assay % P_2O_5				
	Total	Water-soluble	NAC-insoluble	NAC-soluble	Available
1	17.83	6.87	7.98	2.98	9.85
2	17.67	6.94	8.61	2.12	9.06
3	17.92	6.94	8.50	2.48	9.42
Average	17.81	6.92	8.36	2.53	9.44

Table 6.3.5. Percent soluble P_2O_5 in PAPR at 80% degree of acidulation.

Test No	Assay % P_2O_5				
	Total	Water-soluble	NAC-insoluble	NAC-soluble	Available
1	17.81	5.95	9.10	2.76	8.71
2	19.34	6.22	9.11	4.01	10.23
3	17.72	6.07	9.15	2.50	8.57
Average	18.29	6.08	9.12	3.09	9.17

Table 6.3.6. Percent soluble P_2O_5 in PAPR at 60% degree of acidulation.

Test No	Assay % P_2O_5				
	Total	Water-soluble	NAC-insoluble	NAC-soluble	Available
1	18.71	4.48	12.56	1.67	6.15
2	19.15	4.55	12.39	2.21	6.76
3	19.02	4.47	12.33	2.22	6.69
Average	18.96	4.50	12.43	2.03	6.53

Table 6.3.7. Percent soluble P_2O_5 in PAPR at 40% degree of acidulation.

Test No	Assay % P_2O_5				
	Total	Water-soluble	NAC-insoluble	NAC-soluble	Available
1	19.89	3.11	14.83	1.95	5.06
2	19.78	3.15	14.69	1.94	5.09
3	20.43	3.28	14.82	2.33	5.61
Average	20.03	3.18	14.78	2.07	5.25

Table 6.3.8. Percent soluble P_2O_5 in PAPR at 20% degree of acidulation.

Test No	Assay % P_2O_5				
	Total	Water-soluble	NAC-insoluble	NAC-soluble	Available
1	18.27	1.36	17.70	0.00	1.36
2	19.95	1.30	19.21	0.00	1.30
3	17.45	1.09	17.88	0.00	1.09
Average	18.56	1.25	18.26	0.00	1.25

Table 6.3.9. Percent soluble P_2O_5 in PAPR at 0% degree of acidulation.

Test No	Assay % P_2O_5				
	Total	Water-soluble	NAC-insoluble	NAC-soluble	Available
1	19.74	0.00	19.43	0.00	0.00
2	18.59	0.00	19.53	0.00	0.00
3	18.95	0.00	18.95	0.00	0.00
Average	19.09	0.00	19.30	0.00	0.00

APPENDIX D

6.4 RESULTS FOR THE EFFECT OF ACID CONCENTRATION ON SOLUBLE P_2O_5 IN PAPR

6.4.1 Experimental conditions

Degree of acidulation: 50%.
Drying temperature: 100°C.
Residence time in the granulator: 3 minutes.
Rock composition and particle size distribution A.

Table 6.4.1. Feed rates of rock, acid and water at various acid concentrations.

Feed rates	H_2SO_4 concentration					
	98%	80%	70%	60%	50%	40%
Rock (g/min)	129.3	129.3	129.3	129.3	129.3	129.3
H_2SO_4 (ml/min)	11.47	14.05	16.05	18.73	22.48	28.10

Additional water 25 – 30 ml/min.

6.4.2 Summary of results

Table 6.4.2. Effect of acid concentration on soluble P_2O_5 in PAPR.

Acid conc. (% v/v)	Water-soluble P_2O_5				NAC-soluble P_2O_5			
	Test 1	Test 2	Test 3	Average	Test 1	Test 2	Test 3	Average
98	4.55	3.79	4.43	4.26	-	1.48	1.20	1.34
80	4.42	4.60	4.48	4.50	1.42	0.93	1.62	1.32
70	4.57	4.47	4.61	4.55	2.13	1.92	0.46	1.50
60	4.40	5.07	4.37	4.61	2.53	0.44	1.49	1.49
50	5.12	4.48	4.82	4.81	1.59	1.38	1.46	1.48
40	3.38	3.47	3.52	3.46	0.84	1.71	0.62	1.06

Acid conc. (v/v)	Available P_2O_5
	Average
98	5.60
80	5.82
70	6.05
60	6.10
50	6.28
40	4.51

6.4.3 P_2O_5 assays in PAPR produced at various acid concentrations

Table 6.4.3. Percent P_2O_5 in PAPR produced using 98% H_2SO_4 concentration.

Test No	Assay % P_2O_5				
	Total	Water-soluble	NAC-insoluble	NAC-soluble	Available
1	20.68	4.55	16.83	-	4.55
2	20.4	3.79	15.13	1.48	5.27
3	20.41	4.43	14.78	1.20	5.63
Average	20.50	4.26	15.58	1.34	5.15

Table 6.4.4. Percent P_2O_5 in PAPR produced using 80% H_2SO_4 concentration.

Test No	Assay % P_2O_5				
	Total	Water-soluble	NAC-insoluble	NAC-soluble	Available
1	19.52	4.42	13.68	1.42	5.84
2	19.5	4.6	13.97	0.93	5.53
3	19.62	4.48	13.52	1.62	6.10
Average	19.55	4.50	13.72	1.32	5.82

Table 6.4.5. Percent P_2O_5 in PAPR produced using 70% H_2SO_4 concentration.

Test No	Assay % P_2O_5				
	Total	Water-soluble	NAC-insoluble	NAC-soluble	Available
1	19.75	4.57	13.05	2.13	6.70
2	19.93	4.47	13.54	1.92	6.39
3	19.45	4.61	14.38	0.46	5.07
Average	19.71	4.55	13.66	1.50	6.05

Table 6.4.6. Percent P_2O_5 in PAPR produced using 60% H_2SO_4 concentration.

Test No	Assay % P_2O_5				
	Total	Water-soluble	NAC-insoluble	NAC-soluble	Available
1	20.41	4.4	13.48	2.53	6.93
2	19.67	5.07	14.16	0.44	5.51
3	20.09	4.37	14.23	1.49	5.86
Average	20.06	4.61	13.96	1.49	6.10

Table 6.4.7. Percent P_2O_5 in PAPR produced using 50% H_2SO_4 concentration.

Test No	Assay % P_2O_5				
	Total	Water-soluble	NAC-insoluble	NAC-soluble	Available
1	20.03	5.12	13.32	1.59	6.71
2	19.47	4.48	13.61	1.38	5.86
3	19.39	4.82	13.11	1.46	6.28
Average	19.63	4.81	13.35	1.48	6.28

Table 6.4.8. Percent P_2O_5 in PAPR produced using 40% H_2SO_4 concentration.

Test No	Assay % P_2O_5				
	Total	Water-soluble	NAC-insoluble	NAC-soluble	Available
1	19.99	3.38	15.77	0.84	4.22
2	20.55	3.47	15.37	1.71	5.18
3	19.45	3.52	15.31	0.62	4.14
Average	20.00	3.46	15.48	1.06	4.51

APPENDIX E

6.5 RESULTS FOR THE EFFECT OF INITIAL TEMPERATURE OF ROCK, ACID AND WATER ON SOLUBLE P_2O_5 IN PAPR

6.5.1 Experimental conditions

The experiment was carried out as a semi batch operation. 153.2g of the rock was mixed 30ml of water in a beaker and heated to the desired initial temperature on a hot plate. A measured volume of acid required for 50% degree of acidulation was heated separately in a beaker to the desired initial temperature. When the temperature had been attained the acid was poured into the beaker containing the rock and water at the same temperature and thoroughly mixed for 1 minute and the contents emptied into the granulator for the process to continue. Temperatures are given in table 6.5.1 below.

Table 6.5.1. Initial temperatures and concentrations tested.

Acid conc.	Initial Temperatures	
	Rock and water	Acid
50% H_2SO_4	25°C, 50°C, 80°C, 110°C	25°C, 50°C, 80°C, 110°C
70% H_2SO_4	25°C, 50°C, 80°C, 110°C	25°C, 50°C, 80°C, 110°C
98% H_2SO_4	25°C, 50°C, 80°C, 110°C	25°C, 50°C, 80°C, 110°C

6.5.2 Summary of results

Table 6.5.2. Effects of initial temperature of rock, acid and water on soluble P_2O_5 in PAPR.

H_2SO_4 Conc. (% v/v)	Initial T °C	Water-soluble P_2O_5				NAC-soluble P_2O_5			
		Test 1	Test 2	Test 3	Avg	Test 1	Test 2	Test 3	Avg
50	25	5.85	5.76	6.64	6.08	1.77	2.21	2.08	2.02
	50	6.07	5.69	6.50	6.09	2.65	2.46	1.66	2.26
	80	6.31	6.26	6.61	6.39	2.54	2.03	2.12	2.23
	110	6.69	5.68	7.57	6.65	1.28	2.30	0.53	1.37
70	25	5.06	7.52	5.04	5.87	3.48	4.43	4.50	4.14
	50	5.34	5.14	5.09	5.19	2.64	2.50	2.32	2.49
	80	5.11	5.19	5.18	5.16	4.34	3.21	3.66	3.74
	110	4.97	5.09	5.04	5.03	3.70	3.59	3.89	3.73
98	25	4.48	5.08	4.40	4.65	4.01	3.54	5.22	4.26
	50	4.82	5.11	4.49	4.81	4.01	2.65	3.37	3.34
	80	4.62	5.12	4.42	4.72	3.85	2.90	3.97	3.57
	110	4.65	5.22	4.35	4.74	3.62	2.37	3.77	3.25

6.5.3 P_2O_5 assays in PAPR produced at various initial temperatures detailed results

Table 6.5.3. P_2O_5 assays in PAPR produced using 50% H_2SO_4 concentration at 25°C initial temperature of rock, water and acid.

Test No	Assay % P_2O_5				
	Total	Water-soluble	NAC-insoluble	NAC-soluble	Available
1	16.80	5.85	9.18	1.77	7.62
2	16.37	5.76	8.40	2.21	7.97
3	17.12	6.64	8.40	2.08	8.72
Average	16.76	6.08	8.66	2.02	8.10

Table 6.5.4. P_2O_5 assays in PAPR produced using 50% H_2SO_4 concentration at 50°C initial temperature of rock, water and acid.

Test No	Assay % P_2O_5				
	Total	Water-soluble	NAC-insoluble	NAC-soluble	Available
1	17.35	6.07	8.63	2.65	8.72
2	16.81	5.69	8.66	2.46	8.15
3	16.93	6.5	8.77	1.66	8.16
Average	17.03	6.09	8.69	2.26	8.34

Table 6.5.5. P_2O_5 assays in PAPR produced using 50% H_2SO_4 concentration at 80°C initial temperature of rock, water and acid.

Test No	Assay % P_2O_5				
	Total	Water-soluble	NAC-insoluble	NAC-soluble	Available
1	17.05	6.31	8.2	2.54	8.85
2	16.43	6.26	8.14	2.03	8.29
3	16.82	6.61	8.09	2.12	8.73
Average	16.77	6.39	8.14	2.23	8.62

Table 6.5.6. P_2O_5 assays in PAPR produced using 50% H_2SO_4 concentration at 110°C initial temperature of rock, water and acid.

Test No	Assay % P_2O_5				
	Total	Water-soluble	NAC-insoluble	NAC-soluble	Available
1	16.76	6.69	8.79	1.28	7.97
2	16.7	5.68	8.72	2.30	7.98
3	16.68	7.57	8.58	0.53	8.10
Average	16.71	6.65	8.70	1.37	8.02

70% Acid concentration

Table 6.5.7. P_2O_5 assays in PAPR produced using 70% H_2SO_4 concentration at 25°C initial temperature of rock, water and acid.

Test No	Assay % P_2O_5				
	Total	Water-soluble	NAC-insoluble	NAC-soluble	Available
1	17.33	5.06	8.79	3.48	8.54
2	16.96	7.52	5.01	4.43	11.95
3	17.05	5.04	7.51	4.50	9.54
Average	17.11	5.87	7.10	4.14	10.01

Table 6.5.8. P_2O_5 assays in PAPR produced using 70% H_2SO_4 concentration at 50°C initial temperature of rock, water and acid.

Test No	Assay % P_2O_5				
	Total	Water-soluble	NAC-insoluble	NAC-soluble	Available
1	16.89	5.34	8.91	2.64	7.98
2	16.38	5.14	8.74	2.50	7.64
3	16.38	5.09	8.97	2.32	7.41
Average	16.55	5.19	8.87	2.49	7.68

Table 6.5.9. P_2O_5 assays in PAPR produced using 70% H_2SO_4 concentration at 80°C initial temperature of rock, water and acid.

Test No	Assay % P_2O_5				
	Total	Water-soluble	NAC-insoluble	NAC-soluble	Available
1	17.59	5.11	8.14	4.34	9.45
2	16.72	5.19	8.32	3.21	8.40
3	16.89	5.18	8.05	3.66	8.84
Average	17.07	5.16	8.17	3.74	8.90

Table 6.5.10. P_2O_5 assays in PAPR produced using 70% H_2SO_4 concentration at 110°C initial temperature of rock, water and acid.

Test No	Assay % P_2O_5				
	Total	Water-soluble	NAC-insoluble	NAC-soluble	Available
1	16.55	4.97	7.88	3.70	8.67
2	16.55	5.09	7.87	3.59	8.68
3	16.89	5.04	7.96	3.89	8.93
Average	16.66	5.03	7.90	3.73	8.76

98% acid concentration

Table 6.5.11. P_2O_5 assays in PAPR produced using 98% H_2SO_4 concentration at 25°C initial temperature of rock, water and acid.

Test No	Assay % P_2O_5				
	Total	Water-soluble	NAC-insoluble	NAC-soluble	Available
1	16.94	4.48	8.45	4.01	8.49
2	17.29	5.08	8.67	3.54	8.62
3	18.03	4.4	8.41	5.22	9.62
Average	17.42	4.65	8.51	4.26	8.91

Table 6.5.12. P_2O_5 assays in PAPR produced using 98% H_2SO_4 concentration at 50°C initial temperature of rock, water and acid.

Test No	Assay % P_2O_5				
	Total	Water-soluble	NAC-insoluble	NAC-soluble	Available
1	17.86	4.82	9.03	4.01	8.83
2	17.34	5.11	9.58	2.65	7.76
3	17.51	4.49	9.65	3.37	7.86
Average	17.57	4.81	9.42	3.34	8.15

Table 6.5.13. P_2O_5 assays in PAPR produced using 98% H_2SO_4 concentration at 80°C initial temperature of rock, water and acid.

Test No	Assay % P_2O_5				
	Total	Water-soluble	NAC-insoluble	NAC-soluble	Available
1	17.09	4.62	8.62	3.85	8.47
2	17.27	5.12	9.25	2.90	8.02
3	17.29	4.42	8.90	3.97	8.39
Average	17.22	4.72	8.92	3.57	8.29

Table 6.5.14. P_2O_5 assays in PAPR produced using 98% H_2SO_4 concentration at 110°C initial temperature of rock, water and acid.

Test No	Assay % P_2O_5				
	Total	Water-soluble	NAC-insoluble	NAC-soluble	Available
1	16.98	4.65	8.71	3.62	8.27
2	16.69	5.22	9.1	2.37	7.59
3	17.32	4.35	9.2	3.77	8.12
Average	17.00	4.74	9.00	3.25	7.99

APPENDIX F

6.6 RESULTS FOR THE EFFECT OF RESIDENCE TIME OF PHOSPHATE ROCK IN THE GRANULATOR ON SOLUBLE P_2O_5 IN PAPR

6.6.1 Experimental conditions

Degree of acidulation: 50%.
Acid concentration: 70%
Rock composition, As given in Appendix III Table 6.3.1.

Table 6.6.1. Variation of residence time of phosphate rock in the granulator by changing the angle of inclination.

Granulator angle of inclination	Residence time
2°	7
5°	5
10°	3
15°	1

6.6.2 Summary of results

Table 6.6.2. Summary of results of the effect of residence time of phosphate rock in the granulator on soluble P_2O_5 in PAPR.

Time (min)	Water-soluble P_2O_5				NAC-soluble P_2O_5			
	1	2	3	Average	1	2	3	Average
1	3.63	3.74	3.59	3.65	2.69	2.07	3.22	2.66
3	4.53	4.64	4.65	4.61	4.37	4.26	4.23	4.29
5	4.56	4.62	4.58	4.59	4.26	3.89	3.76	3.97
7	4.54	4.69	4.56	4.60	4.18	3.61	3.70	3.83

Time (min)	Available P_2O_5 Average
1	6.31
3	8.90
5	8.55
7	8.42

6.6.3 P_2O_5 assays in PAPR produced at various residence times of phosphate rock in the granulator

Table 6.6.3. P_2O_5 assays in PAPR after 1 minute residence time of phosphate rock in the granulator.

Test No	Assay % P_2O_5				
	Total	Water-soluble	NAC-insoluble	NAC-soluble	Available
1	17.06	3.63	10.74	2.69	6.32
2	16.79	3.74	10.98	2.07	5.81
3	17.20	3.59	10.39	3.22	6.81
Average	17.02	3.65	10.70	2.66	6.31

Table 6.6.4. P_2O_5 assays in PAPR after 3 minutes residence time of phosphate rock in the granulator.

Test No	Assay % P_2O_5				
	Total	Water-soluble	NAC-insoluble	NAC-soluble	Available
1	17.4	4.53	8.5	4.37	8.90
2	17.16	4.64	8.26	4.26	8.90
3	17.23	4.65	8.35	4.23	8.88
Average	17.26	4.61	8.37	4.29	8.89

Table 6.6.5. P_2O_5 assays in PAPR after 5 minutes residence time of phosphate rock in the granulator.

Test No	Assay % P_2O_5				
	Total	Water-soluble	NAC-insoluble	NAC-soluble	Available
1	17.8	4.56	8.98	4.26	8.82
2	17.17	4.62	8.66	3.89	8.51
3	17.21	4.58	8.87	3.76	8.34
Average	17.39	4.59	8.84	3.97	8.56

Table 6.6.6. P_2O_5 assays in PAPR after 7 minutes residence time of phosphate rock in the granulator.

Test No	Assay % P_2O_5				
	Total	Water-soluble	NAC-insoluble	NAC-soluble	Available
1	17.75	4.54	9.04	4.17	8.71
2	17.19	4.69	8.89	3.61	8.30
3	17.22	4.56	8.96	3.70	8.26
Average	17.39	4.60	8.96	3.83	8.42

APPENDIX G

6.7 RESULTS FOR THE EFFECT OF DRYING TEMPERATURE ON SOLUBLE P_2O_5 IN PAPR

6.7.1 Experimental conditions:

Residence time in the granulator: 3 minutes.
Acid concentration: 70%.
Degree of acidulation 50%.
Rock composition; As given in appendix B table 6.4.1.

6.7.2 Summary of results

Table 6.7.1. Percent P_2O_5 in PAPR dried at various temperatures.

Drying temp. (°C)	Water-soluble P_2O_5				NAC-soluble P_2O_5			
	Test 1	Test 2	Test 3	Avg	Test 1	Test 2	Test 3	Avg
90	5.38	5.58	5.51	5.49	3.80	3.61	3.70	3.70
120	4.91	4.89	5.01	4.94	4.27	4.38	4.27	4.31
150	3.29	3.38	3.23	3.30	5.91	5.76	5.97	5.88

Drying temp. (°C)	Available P_2O_5
	Average
90	9.19
120	9.24
150	9.18

6.7.3. P_2O_5 assays in PAPR dried at various temperatures

Table 6.7.2. P_2O_5 assays in PAPR at 90°C drying temperature.

Test No	Assay % P_2O_5				
	Total	Water-soluble	NAC-insoluble	NAC-soluble	Available
1	17.97	5.38	8.79	3.80	9.18
2	18.03	5.58	8.84	3.61	9.19
3	18.1	5.51	8.89	3.70	9.21
Average	18.03	5.49	8.84	3.70	9.19

Table 6.7.3. P_2O_5 assays in PAPR at 120°C drying temperature.

Test No	Assay % P_2O_5				
	Total	Water-soluble	NAC-insoluble	NAC-soluble	Available
1	17.82	4.91	8.64	4.27	9.18
2	17.66	4.89	8.39	4.38	9.27
3	18.14	5.01	8.86	4.27	9.28
Average	17.87	4.94	8.63	4.31	9.24

Table 6.7.4. P_2O_5 assays in PAPR at 150°C drying temperature.

Test No	Assay % P_2O_5				
	Total	Water-soluble	NAC-insoluble	NAC-soluble	Available
1	17.97	3.29	8.77	5.91	9.20
2	17.87	3.38	8.73	5.76	9.14
3	17.94	3.23	8.74	5.97	9.20
Average	17.93	3.30	8.75	5.88	9.18

APPENDIX H

6.8 RESULTS FOR THE DETERMINATION OF RTD CURVE FOR THE CLOSED COMMINUTION CIRCUIT

(For the experimental conditions refer to chapter 2 section 2.7.3).

6.8.1 Experimental conditions during tracer test 1

Mill ball Charge: 25% 1.8cm diameter, 25% 2.4cm diameter and 50% 3.8cm diameter steel balls. Tracer volume 500ml sodium chloride solution.

Table 6.8.1. Residence time distribution data from test 1.

Time (min)	NaCl (g/l)	E (t)	θ	E (θ)
0.00	0.00	0.000	0.000	0.000
0.25	0.00	0.000	0.088	0.000
0.50	0.82	0.044	0.175	0.125
0.75	1.88	0.100	0.263	0.286
1.00	2.14	0.114	0.351	0.325
1.25	3.31	0.177	0.439	0.504
1.50	6.81	0.364	0.526	1.037
1.75	14.33	0.765	0.614	2.182
2.00	7.58	0.405	0.702	1.153
2.25	5.11	0.273	0.789	0.778
2.50	4.17	0.223	0.877	0.635
2.75	4.11	0.220	0.965	0.626
3.00	3.47	0.185	1.052	0.528
3.25	2.82	0.151	1.140	0.429
3.50	2.35	0.125	1.228	0.358
3.75	2.11	0.113	1.316	0.322
4.00	2.00	0.107	1.403	0.304
4.25	1.23	0.066	1.491	0.188
4.50	1.29	0.069	1.579	0.197
4.75	1.12	0.060	1.666	0.170
5.00	0.94	0.050	1.754	0.143
5.25	0.82	0.044	1.842	0.125
5.50	0.70	0.038	1.930	0.107
5.75	0.59	0.031	2.017	0.089

6.00	0.47	0.025	2.105	0.072
6.25	0.47	0.025	2.193	0.072
6.50	0.41	0.022	2.280	0.063
6.75	0.29	0.016	2.368	0.045
7.00	0.35	0.019	2.456	0.054
7.25	0.23	0.013	2.543	0.036
7.50	0.18	0.009	2.631	0.027
7.75	0.18	0.009	2.719	0.027
8.00	0.23	0.013	2.807	0.036
8.25	0.18	0.009	2.894	0.027
8.50	0.23	0.013	2.982	0.036
8.75	0.12	0.006	3.070	0.018
9.00	0.06	0.003	3.157	0.009
9.25	0.12	0.006	3.245	0.018
9.50	0.07	0.004	3.333	0.011
9.75	0.05	0.003	3.421	0.007
10.00	0.04	0.002	3.508	0.005
10.25	0.06	0.003	3.596	0.009
10.50	0.04	0.002	3.684	0.007
10.75	0.04	0.002	3.771	0.005
11.00	0.02	0.001	3.859	0.004
11.25	0.03	0.001	3.947	0.004
11.50	0.72	0.038	4.035	0.109
11.75	0.03	0.001	4.122	0.004
12.00	0.01	0.001	4.210	0.002
12.25	0.03	0.002	4.298	0.004
12.50	0.01	0.001	4.385	0.002
12.75	0.01	0.001	4.473	0.002
13.00	0.02	0.001	4.561	0.003
13.25	0.03	0.002	4.648	0.005
13.50	0.01	0.001	4.736	0.002
13.75	0.02	0.001	4.824	0.003
14.00	0.08	0.004	4.912	0.013
14.25	0.15	0.008	4.999	0.023
14.50	0.08	0.004	5.087	0.012
14.75	0.05	0.003	5.175	0.007
15.00	0.06	0.003	5.262	0.008

6.8.2 Experimental conditions during tracer test 2

Mill ball Charge: 25% 1.8cm diameter, 25% 2.4cm diameter and 50% 3.8cm diameter steel balls. Tracer volume 500ml sodium chloride.

Table 6.8.2. Residence time distribution data from test 2.

Time (min)	NaCl (g/l)	E (t)	θ	E (θ)
0.00	0.00	0.000	0.000	0.000
0.25	0.01	0.000	0.062	0.0008
0.50	0.01	0.000	0.124	0.0008
0.75	0.03	0.001	0.187	0.0021
1.00	1.03	0.018	0.249	0.0735
1.25	8.34	0.148	0.311	0.596
1.50	17.04	0.303	0.373	1.2172
1.75	24.79	0.440	0.435	1.7712
2.00	21.74	0.386	0.497	1.553
2.25	16.33	0.290	0.560	1.1668
2.50	9.58	0.170	0.622	0.6842
2.75	7.11	0.126	0.684	0.5079
3.00	6.81	0.121	0.746	0.4869
3.25	7.75	0.138	0.808	0.554
3.50	9.22	0.164	0.870	0.659
3.75	8.99	0.160	0.933	0.6422
4.00	8.05	0.143	0.995	0.575
4.25	6.64	0.118	1.057	0.4743
4.50	5.40	0.096	1.119	0.3861
4.75	4.76	0.085	1.181	0.3400
5.00	4.52	0.080	1.243	0.3232
5.25	4.46	0.079	1.306	0.319
5.50	4.35	0.077	1.368	0.3106
5.75	3.99	0.071	1.430	0.2854
6.00	3.70	0.066	1.492	0.2644
6.25	3.23	0.057	1.554	0.2308
6.50	2.91	0.052	1.616	0.2078
6.75	2.64	0.047	1.679	0.1889
7.00	2.53	0.045	1.741	0.1805

7.25	2.26	0.040	1.803	0.1616
7.50	2.03	0.036	1.865	0.1448
7.75	1.94	0.034	1.927	0.1385
8.00	1.88	0.033	1.989	0.1343
8.25	1.70	0.030	2.052	0.1217
8.50	1.53	0.027	2.114	0.1091
8.75	1.41	0.025	2.176	0.1007
9.00	1.35	0.024	2.238	0.0965
9.25	1.17	0.021	2.300	0.0839
9.50	1.12	0.020	2.363	0.0797
9.75	0.97	0.017	2.425	0.0693
10.00	0.94	0.017	2.487	0.0672
10.25	0.91	0.016	2.549	0.0651
10.50	0.82	0.015	2.611	0.0588
10.75	0.73	0.013	2.673	0.0525
11.00	0.70	0.013	2.736	0.0504
11.25	0.68	0.012	2.798	0.0483
11.50	0.65	0.011	2.860	0.0462
11.75	0.59	0.010	2.922	0.0420
12.00	0.53	0.009	2.984	0.0378
12.25	0.53	0.009	3.046	0.0378
12.50	0.47	0.008	3.109	0.0336
12.75	0.35	0.006	3.171	0.0252
13.00	0.30	0.005	3.233	0.0216
13.25	0.30	0.005	3.295	0.0216
13.50	0.12	0.002	3.357	0.0084
13.75	0.25	0.004	3.419	0.018
14.00	0.22	0.004	3.482	0.0156
14.25	0.22	0.004	3.544	0.0156
14.50	0.18	0.003	3.606	0.0132
14.75	0.23	0.004	3.668	0.0168
15.00	0.18	0.003	3.730	0.0132
15.25	0.15	0.003	3.792	0.0108
15.50	0.16	0.003	3.855	0.0114
15.75	0.15	0.003	3.917	0.0108
16.00	0.15	0.003	3.979	0.0108
16.25	0.12	0.002	4.041	0.0084

16.50	0.13	0.002	4.103	0.0096
16.75	0.10	0.002	4.165	0.0072
17.00	0.10	0.002	4.228	0.0072
17.25	0.10	0.002	4.290	0.0072
17.50	0.09	0.002	4.352	0.0066
17.75	0.08	0.001	4.414	0.006
18.00	0.08	0.001	4.476	0.006
18.25	0.05	0.001	4.538	0.0036
18.50	0.07	0.001	4.601	0.0048
18.75	0.07	0.001	4.663	0.0048
19.00	0.07	0.001	4.725	0.0048
19.25	0.05	0.001	4.787	0.0036
19.50	0.05	0.001	4.849	0.0036
19.75	0.05	0.001	4.912	0.0036
20.00	0.05	0.001	4.974	0.0036

6.8.3 Experimental conditions during tracer test 3

Mill ball Charge: 10% 2.4cm diameter and 90% 3.8cm diameter steel balls.

Tracer volume 500ml sodium chloride solution.

Table 6.8.3. Residence time distribution data from test 3

Time (min)	NaCl (g/l)	E (t)	θ	E (θ)
0.00	0.00	0.000	0.000	0
0.25	0.01	0.000	0.077	0.0011
0.50	0.02	0.001	0.153	0.0021
0.75	0.09	0.003	0.230	0.0085
1.00	2.84	0.079	0.306	0.2581
1.25	9.56	0.266	0.383	0.868
1.50	15.16	0.422	0.460	1.3756
1.75	15.96	0.444	0.536	1.4481
2.00	13.58	0.378	0.613	1.2327
2.25	10.39	0.289	0.689	0.9427
2.50	7.92	0.220	0.766	0.7187
2.75	6.70	0.186	0.843	0.6078

3.00	6.02	0.167	0.919	0.546
3.25	5.69	0.158	0.996	0.5161
3.50	5.33	0.148	1.073	0.4841
3.75	4.86	0.135	1.149	0.4415
4.00	4.37	0.122	1.226	0.3967
4.25	3.76	0.105	1.302	0.3412
4.50	3.36	0.093	1.379	0.305
4.75	2.89	0.080	1.456	0.2623
5.00	2.61	0.073	1.532	0.2367
5.25	2.35	0.065	1.609	0.2133
5.50	2.10	0.058	1.685	0.1909
5.75	1.89	0.053	1.762	0.1717
6.00	1.68	0.047	1.839	0.1525
6.25	1.50	0.042	1.915	0.1365
6.50	1.36	0.038	1.992	0.1237
6.75	1.21	0.034	2.068	0.1098
7.00	1.08	0.030	2.145	0.0981
7.25	0.96	0.027	2.222	0.0874
7.50	0.88	0.025	2.298	0.08
7.75	0.80	0.022	2.375	0.0725
8.00	0.72	0.020	2.451	0.065
8.25	0.65	0.018	2.528	0.0586
8.50	0.59	0.016	2.605	0.0533
8.75	0.53	0.015	2.681	0.048
9.00	0.48	0.013	2.758	0.0437
9.25	0.42	0.012	2.835	0.0384
9.50	0.38	0.010	2.911	0.0341
9.75	0.35	0.010	2.988	0.032
10.00	0.31	0.008	3.064	0.0277
10.25	0.28	0.008	3.141	0.0256
10.50	0.26	0.007	3.218	0.0235
10.75	0.23	0.007	3.294	0.0213
11.00	0.21	0.006	3.371	0.0192
11.25	0.19	0.005	3.447	0.0171
11.50	0.18	0.005	3.524	0.016
11.75	0.15	0.004	3.601	0.0139

12.00	0.15	0.004	3.677	0.0139
12.25	0.13	0.004	3.754	0.0117
12.50	0.12	0.003	3.830	0.0107
12.75	0.12	0.003	3.907	0.0107
13.00	0.11	0.003	3.984	0.0096
13.25	0.09	0.003	4.060	0.0085
13.50	0.09	0.003	4.137	0.0085
13.75	0.07	0.002	4.214	0.0064
14.00	0.07	0.002	4.290	0.0064

6.8.4 Experimental conditions during tracer test 4

Mill ball Charge:10% .2.4 cm diameter and 90% 3.8cm diameter steel balls.

Tracer volume 250mls sodium chloride solution.

Table 6.8.4. Residence time distribution data from test 4.

Time (min)	NaCl (g/l)	E (t)	θ	E (θ)
0.000	0.00	0.000	0.000	0
0.250	0.00	0.000	0.082	0
0.500	0.02	0.002	0.163	0.0067
0.750	0.09	0.009	0.245	0.0268
1.000	1.16	0.108	0.327	0.3316
1.250	3.57	0.333	0.408	1.0181
1.500	5.02	0.467	0.490	1.4301
1.750	4.89	0.455	0.572	1.3932
2.000	4.01	0.373	0.653	1.142
2.250	2.95	0.275	0.735	0.8406
2.500	2.31	0.216	0.817	0.6598
2.750	1.95	0.182	0.898	0.5559
3.000	1.77	0.165	0.980	0.5057
3.250	1.68	0.156	1.062	0.4789
3.500	1.53	0.142	1.143	0.4354
3.750	1.36	0.127	1.225	0.3885
4.000	1.20	0.112	1.307	0.3416
4.250	1.05	0.097	1.388	0.2981

4.500	0.93	0.086	1.470	0.2646
4.750	0.81	0.075	1.552	0.2311
5.000	0.74	0.069	1.633	0.211
5.250	0.65	0.060	1.715	0.1842
5.500	0.59	0.055	1.797	0.1675
5.750	0.52	0.048	1.878	0.1474
6.000	0.45	0.042	1.960	0.1273
6.250	0.42	0.039	2.042	0.1206
6.500	0.36	0.034	2.123	0.1038
6.750	0.33	0.031	2.205	0.0938
7.000	0.29	0.027	2.287	0.0837
7.250	0.27	0.025	2.368	0.077
7.500	0.23	0.022	2.450	0.067
7.750	0.21	0.020	2.532	0.0603
8.000	0.19	0.018	2.613	0.0536
8.250	0.18	0.016	2.695	0.0502
8.500	0.15	0.014	2.777	0.0435
8.750	0.14	0.013	2.858	0.0402
9.000	0.13	0.012	2.940	0.0368
9.250	0.13	0.012	3.022	0.0368
9.500	0.11	0.010	3.103	0.0301
9.750	0.09	0.009	3.185	0.0268
10.000	0.09	0.009	3.267	0.0268
10.250	0.08	0.008	3.349	0.0234
10.500	0.07	0.007	3.430	0.0201
10.750	0.06	0.005	3.512	0.0167
11.000	0.06	0.005	3.594	0.0167
11.250	0.06	0.005	3.675	0.0167
11.500	0.05	0.004	3.757	0.0134

6.8.5 Experimental conditions during tracer test 5

Mill ball Charge: 30% 2.4cm diameter and 70% 3.8cm diameter steel balls.

Tracer volume 250ml sodium chloride solution.

Table 6.8.5. Residence time distribution data from test 5.

Time (min)	NaCl (g/l)	E (t)	θ	E (θ)
0.00	0.00	0.0000	0.0000	0.0000
0.25	0.00	0.0000	0.0855	0.0000
0.50	0.00	0.0000	0.1710	0.0000
0.75	0.00	0.0000	0.2565	0.0000
1.00	0.89	0.0884	0.3420	0.2584
1.25	3.27	0.3233	0.4276	0.9453
1.50	4.96	0.4908	0.5131	1.4350
1.75	5.03	0.4978	0.5986	1.4554
2.00	4.04	0.4001	0.6841	1.1698
2.25	2.94	0.2908	0.7696	0.8501
2.50	2.21	0.2187	0.8551	0.6393
2.75	1.86	0.1838	0.9406	0.5373
3.00	1.73	0.1710	1.0261	0.4999
3.25	1.64	0.1628	1.1116	0.4761
3.50	1.56	0.1547	1.1972	0.4523
3.75	1.28	0.1268	1.2827	0.3707
4.00	0.92	0.0907	1.3682	0.2652
4.25	0.94	0.0931	1.4537	0.2720
4.50	0.90	0.0896	1.5392	0.2618
4.75	0.81	0.0803	1.6247	0.2346
5.00	0.70	0.0698	1.7102	0.2040
5.25	0.60	0.0593	1.7957	0.1734
5.50	0.52	0.0512	1.8812	0.1496
5.75	0.45	0.0442	1.9668	0.1292
6.00	0.41	0.0407	2.0523	0.1190
6.25	0.36	0.0361	2.1378	0.1054
6.50	0.32	0.0314	2.2233	0.0918
6.75	0.29	0.0291	2.3088	0.0850
7.00	0.26	0.0256	2.3943	0.0748

7.25	0.22	0.0221	2.4798	0.0646
7.50	0.20	0.0198	2.5653	0.0578
7.75	0.18	0.0174	2.6508	0.0510
8.00	0.15	0.0151	2.7364	0.0442
8.25	0.14	0.0140	2.8219	0.0408
8.50	0.13	0.0128	2.9074	0.0374
8.75	0.11	0.0116	2.9929	0.0340
9.00	0.09	0.0093	3.0784	0.0272
9.25	0.09	0.0093	3.1639	0.0272
9.50	0.07	0.0070	3.2494	0.0204
9.75	0.07	0.0070	3.3349	0.0204
10.00	0.05	0.0047	3.4204	0.0136

6.8.6. Experimental conditions during tracer test 6

Mill ball Charge: 30% 2.4cm diameter and 70% 3.8cm diameter steel balls.

Tracer volume 250ml sodium chloride solution.

Table 6.8.6. Residence time distribution data from test 6

Time (min)	NaCl (g/l)	E (t)	θ	E (θ)
0.00	0.00	0.000	0.000	0.000
0.25	0.00	0.000	0.101	0.000
0.50	0.02	0.003	0.203	0.006
0.75	0.69	0.076	0.304	0.188
1.00	3.81	0.419	0.405	1.034
1.25	5.97	0.657	0.507	1.621
1.50	4.81	0.529	0.608	1.305
1.75	3.10	0.341	0.709	0.842
2.00	2.07	0.228	0.810	0.561
2.25	1.55	0.171	0.912	0.421
2.50	1.50	0.165	1.013	0.408
2.75	1.54	0.169	1.114	0.418
3.00	1.50	0.165	1.216	0.408
3.25	1.35	0.149	1.317	0.367
3.50	1.14	0.125	1.418	0.309

3.75	0.96	0.106	1.520	0.262
4.00	0.85	0.093	1.621	0.230
4.25	0.74	0.081	1.722	0.201
4.50	0.67	0.074	1.824	0.182
4.75	0.60	0.066	1.925	0.163
5.00	0.54	0.059	2.026	0.147
5.25	0.47	0.052	2.128	0.128
5.50	0.41	0.045	2.229	0.112
5.75	0.36	0.040	2.330	0.099
6.00	0.33	0.036	2.431	0.089
6.25	0.29	0.032	2.533	0.080
6.50	0.26	0.028	2.634	0.070
6.75	0.25	0.027	2.735	0.067
7.00	0.21	0.023	2.837	0.057
7.25	0.19	0.021	2.938	0.051
7.50	0.16	0.018	3.039	0.045

6.8.7 Experimental conditions during tracer test 7

Mill ball Charge: 20% 2.4cm diameter and 80% 3.8cm diameter steel balls.

Tracer volume 250ml sodium chloride solution.

Table 6.8.7. Residence time distribution data from test 7

Time (min)	NaCl (g/l)	E (t)	θ	E (θ)
0.00	0.00	0.000	0.000	0.000
0.25	0.00	0.000	0.075	0.000
0.50	0.02	0.002	0.151	0.007
0.75	0.06	0.005	0.226	0.018
1.00	0.93	0.084	0.302	0.279
1.25	3.02	0.274	0.377	0.908
1.50	4.48	0.406	0.452	1.346
1.75	4.38	0.397	0.528	1.318
2.00	3.55	0.322	0.603	1.067
2.25	2.68	0.243	0.679	0.805
2.50	2.11	0.192	0.754	0.636

2.75	1.87	0.169	0.829	0.562
3.00	1.80	0.163	0.905	0.540
3.25	1.76	0.160	0.980	0.530
3.50	1.68	0.152	1.056	0.505
3.75	1.54	0.140	1.131	0.463
4.00	1.40	0.127	1.206	0.420
4.25	1.26	0.114	1.282	0.378
4.50	1.12	0.101	1.357	0.336
4.75	1.01	0.092	1.433	0.304
5.00	0.94	0.085	1.508	0.283
5.25	0.86	0.078	1.583	0.258
5.50	0.76	0.069	1.659	0.230
5.75	0.74	0.067	1.734	0.223
6.00	0.66	0.060	1.809	0.198
6.25	0.61	0.055	1.885	0.184
6.50	0.55	0.050	1.960	0.166
6.75	0.51	0.046	2.036	0.152
7.00	0.47	0.043	2.111	0.141
7.25	0.43	0.039	2.186	0.131
7.50	0.39	0.035	2.262	0.117
7.75	0.35	0.032	2.337	0.106
8.00	0.33	0.030	2.413	0.099
8.25	0.31	0.028	2.488	0.092
8.50	0.28	0.026	2.563	0.085
8.75	0.25	0.022	2.639	0.074
9.00	0.23	0.021	2.714	0.071
9.25	0.22	0.020	2.790	0.067
9.50	0.20	0.018	2.865	0.060
9.75	0.19	0.017	2.940	0.057
10.00	0.18	0.016	3.016	0.053
10.25	0.16	0.015	3.091	0.049
10.50	0.15	0.014	3.167	0.046
10.75	0.14	0.013	3.242	0.042
11.00	0.13	0.012	3.317	0.039
11.25	0.12	0.011	3.393	0.035
11.50	0.11	0.010	3.468	0.032
11.75	0.09	0.009	3.544	0.028

12.00	0.08	0.007	3.619	0.025
12.25	0.09	0.009	3.694	0.028
12.50	0.07	0.006	3.770	0.021

APPENDIX I

6.9 RESULTS FOR THE DETERMINATION OF RTD CURVE FOR THE GRANULATION CIRCUIT

(For the experimental procedure refer to chapter 2 section 2.7.3).

6.9.1 Experimental conditions during tracer test 1

Rock feed rate: 129.3g/min

Degree of acidulation 50% (see appendix III for details of compositon).

Acid concentration: 70% H_2SO_4.

Tracer: 2 g Na_2SO_4 powder.

Mean residence time: 3.2 minutes.

Table 6.9.1. Residence time distribution data from test 1.

Time (min)	Na_2SO_4 (%)	E (t)	θ	E (θ)
0.0	0	0	0	0
0.5	0	0	0.1562	0
1.0	0.233605	0.1845	0.3124	0.5906
1.5	0.499691	0.3947	0.4686	1.2633
2.0	0.43442	0.3431	0.6248	1.0983
2.5	0.30442	0.2404	0.781	0.7696
3.0	0.155274	0.1226	0.9372	0.3926
3.5	0.201035	0.1588	1.0934	0.5083
4.0	0.035733	0.0282	1.2496	0.0903
4.5	0.089213	0.0705	1.4058	0.2255
5.0	0.088156	0.0696	1.562	0.2229
5.5	0.188633	0.149	1.7182	0.4769
6.0	0.025335	0.02	1.8744	0.0641
6.5	0.08758	0.0692	2.0306	0.2214
7.0	0.041306	0.0326	2.1868	0.1044
7.5	0.024559	0.0194	2.343	0.0621
8.0	0.012438	0.0098	2.4992	0.0314
8.5	0.055532	0.0439	2.6554	0.1404

9.0	0.042164	0.0333	2.8115	0.1066
9.5	0	0	2.9677	0
10.0	0	0	3.1239	0
10.5	0	0	3.2801	0
11.0	0.002312	0.0018	3.4363	0.0058
11.5	0.006332	0.005	3.5925	0.016
12.0	0	0	3.7487	0
12.5	0.00457	0.0036	3.9049	0.0116
13.0	0	0	4.0611	0
13.5	0	0	4.2173	0
14.0	0	0	4.3735	0
14.5	0	0	4.5297	0
15.0	0	0	4.6859	0
15.5	0	0	4.8421	0
16.0	0	0	4.9983	0
16.5	0	0	5.1545	0
17.0	0	0	5.3107	0
17.5	0	0	5.4669	0
18.0	0	0	5.6231	0
18.5	0	0	5.7793	0
19.0	0	0	5.9355	0
19.5	0	0	6.0917	0
20.0	0	0	6.2479	0
20.5	0	0	6.4041	0
21.0	0	0	6.5603	0
21.5	0	0	6.7165	0
22.0	0	0	6.8727	0
22.5	0	0	7.0289	0
23.0	0	0	7.1851	0
23.5	0	0	7.3413	0
24.0	0	0	7.4975	0

6.9.2 Experimental conditions during tracer test 2

Mean residence time increased to 6.7 minutes. Other conditions remained as in test 1.

Table 6.9.2. Residence time distribution data from test 2.

Time (min)	Na_2SO_4 (%)	E (t)	θ	E (θ)
0.0	0	0	0	0
0.5	0	0	0.0744	0
1.0	0	0	0.1489	0
1.5	0.000751	0.0013	0.2233	0.009
2.0	0.033339	0.0593	0.2978	0.3981
2.5	0.020842	0.0371	0.3722	0.2489
3.0	0.084872	0.1509	0.4466	1.0135
3.5	0.061701	0.1097	0.5211	0.7368
4.0	0.073544	0.1307	0.5955	0.8782
4.5	0.039546	0.0703	0.6699	0.4722
5.0	0.117967	0.2097	0.7444	1.4087
5.5	0.064437	0.1146	0.8188	0.7695
6.0	0.08075	0.1436	0.8933	0.9642
6.5	0.062512	0.1111	0.9677	0.7465
7.0	0.094616	0.1682	1.0421	1.1298
7.5	0.047469	0.0844	1.1166	0.5668
8.0	0.044267	0.0787	1.191	0.5286
8.5	0.052664	0.0936	1.2655	0.6289
9.0	0.049086	0.0873	1.3399	0.5861
9.5	0.037972	0.0675	1.4143	0.4534
10.0	0.01679	0.0298	1.4888	0.2005
10.5	0.013731	0.0244	1.5632	0.164
11.0	0.013554	0.0241	1.6376	0.1619
11.5	0.010102	0.018	1.7121	0.1206
12.0	0.026166	0.0465	1.7865	0.3124
12.5	0.019928	0.0354	1.861	0.238
13.0	0.007009	0.0125	1.9354	0.0837
13.5	0	0	2.0098	0
14.0	0.002008	0.0036	2.0843	0.024

14.5	0.01436	0.0255	2.1587	0.1715
15.0	0.018471	0.0328	2.2332	0.2206
15.5	0	0	2.3076	0
16.0	0.007382	0.0131	2.382	0.0882
16.5	0.000903	0.0016	2.4565	0.0108
17.0	0	0	2.5309	0
17.5	0.005458	0.0097	2.6053	0.0652
18.0	0	0	2.6798	0
18.5	0.000416	0.0007	2.7542	0.005
19.0	0	0	2.8287	0
19.5	0	0	2.9031	0
20.0	0	0	2.9775	0
20.5	0	0	3.052	0
21.0	0	0	3.1264	0
21.5	0	0	3.2009	0
22.0	0	0	3.2753	0
22.5	0	0	3.3497	0
23.0	0.0024	0.0043	3.4242	0.0287
23.5	0	0	3.4986	0

APPENDIX J

6.10 RESULTS FOR THE TESTING OF THE SHRINKING CORE MODEL

Table 6.10.1 Experimental data for the conversion of apatite to monocalcium phosphate using the Shrinking Core Model.

Total P_2O_5	P	$Ca_{10}(PO_4)_6F_2$	Total Wt (g)	Apatite (g)	Volume (cm^3)	
9.00	3.93	21.32	100.00	21.32	8.53X10^{-12}	
Available P_2O_5	**P**	**$Ca_{10}(PO_4)_6F_2$**	**Unreacted %**	**Weight (g)**	**Volume X10^{-12} (cm3)**	**Vunreacted/Vparti**
0	0.00	0.00	21.32	21.32	8.5268	1.000
0.05	0.02	0.12	21.20	21.20	8.4794	0.994
0.75	0.33	1.78	19.54	19.54	7.8162	0.917
1.5	0.65	3.55	17.76	17.76	7.1056	0.833
2.25	0.98	5.33	15.99	15.99	6.3951	0.750
3	1.31	7.11	14.21	14.21	5.6845	0.667
3.75	1.64	8.88	12.43	12.43	4.9739	0.583
4.5	1.96	10.66	10.66	10.66	4.2634	0.500
5	2.18	11.84	9.47	9.47	3.7897	0.444
5.5	2.40	13.03	8.29	8.29	3.3160	0.389
6	2.62	14.21	7.11	7.11	2.8423	0.333
6.25	2.73	14.80	6.51	6.51	2.6054	0.306
6.5	2.84	15.40	5.92	5.92	2.3685	0.278
6.75	2.95	15.99	5.33	5.33	2.1317	0.250
7	3.06	16.58	4.74	4.74	1.8948	0.222
7.25	3.17	17.17	4.14	4.14	1.6580	0.194
7.5	3.27	17.76	3.55	3.55	1.4211	0.167
7.75	3.38	18.36	2.96	2.96	1.1843	0.139
7.9	3.45	18.71	2.61	2.61	1.0422	0.122
8.1	3.54	19.19	2.13	2.13	0.8527	0.100
8.25	3.60	19.54	1.78	1.78	0.7106	0.083
8.5	3.71	20.13	1.18	1.18	0.4737	0.056
8.7	3.80	20.61	0.71	0.71	0.2842	0.033
9	3.93	21.32	0.00	0.00	0.0000	0.000

Table 6.10.2 Theoretical data for the conversion of apatite to monocalcium phosphate using the Shrinking Core Model.

					Fractional Conversion	Film Diffusion	Ash Diffusion	Reaction Controls
r_c	R	r_c/R	$(r_c/R)^3$	X_B	$1-X_B$	$X_B = t/T$	$t/T = 1-3(1-X_B)^{2/3} + 2(1-X_B)$	$t/T = 1-(1-X_B)^{1/3}$
0.0	37.5	0.000	0.000	1.000	0.000	1.000	1.000	1.000
5.0	37.5	0.133	0.002	0.998	0.002	0.998	0.951	0.867
10.0	37.5	0.267	0.019	0.981	0.019	0.981	0.825	0.733
15.0	37.5	0.400	0.064	0.936	0.064	0.936	0.648	0.600
20.0	37.5	0.533	0.152	0.848	0.152	0.848	0.450	0.467
25.0	37.5	0.667	0.296	0.704	0.296	0.704	0.259	0.333
30.0	37.5	0.800	0.512	0.488	0.512	0.488	0.104	0.200
35.0	37.5	0.933	0.813	0.187	0.813	0.187	0.013	0.067
37.5	37.5	1.000	1.000	0.000	1.000	0.000	0.000	0.000

APPENDIX K

Field Test Results of PAPR on food crops

ADEQUATE PHOSPHATE FERTILIZATION USING SIMPLY PROCESSED PHOSPHATE ROCK PRODUCTS

LUNGU O. AND MUNYINDA K.

School of Agricultural Sciences

JUSTIFICATON

- The single most important factor limiting crop yields worldwide especially among low-resource farmers is low soil fertility.
- In Zambia P is acutely deficient in soils, severely limiting crop yields. When P fertilizers are not applied, yields of cereal crops (Maize) are <1t/ha.
- High cost of fertilizers >3 to 4 times more expensive in developing compared to developed countries.
- Low-resource farmers cannot afford the high rates required to recapitalize the soil with P to maintain soil productivity.
- There is now rekindled interest in Zambia to develop local deposits of PR in order to substitute imported fertilizers.
- Local PRs are low grade and are not agronomically effective when directly applied to the soil.
- New approach in P fertilization aims at applying P from simply processed fertilizers.

OBJECTIVE

To evaluate the agronomic effectiveness of PAPR from Chilembwe PR produced from the Pilot Plant at the School of Mines, UNZA.

Treatments

On-Station

	P_2O_5	N	K	S
	----------------kg/ha------------------			
1.	0	200	70	26.4
2.	40	"	------------------	"
3.	80	"	------------------	"
4.	120	"	------------------	"
5.	160	"	------------------	"
6.	200	"	------------------	"

On-Farm

	P_2O_5	N	K	S
	------------------kg/ha----------------			
1.	0	120	70	26.4
2.	60	120	"	"
3.	120	200	"	"

Composition of Fertilizers

Table 1. Chemical composition (%) of phosphate sources used in the study

P source	Total P_2O_5	Available P_2O_5 [1]	Fe_2O_3	S	CaO	MgO
MAP	50.0	-	-	-	-	-
CGPR	16.0	1.3	6.4	-	29.8	-
50% PAPR	-	9.47	-	7.0	-	-

[1]. Water soluble plus neutral ammonium citrate soluble P as a percentage of the total sample
CGPR = Chilembwe Ground Phosphate Rock
MAP = mono-ammonium phosphate (also contains 11 % N and 0.75 % Zn)

Soils used in the study

Table 2. Soil classification and surface (0-15 cm) characteristics of the soil used in the study

Trial site	Region	Annual rainfall, mm	pH	Available P_2O_5, mg kg-1	Soil Classification, WRB/Soil Taxonomy
1.Mukonchi	II	800-1000	5.8	17.8	Haplic Lixisol/Typic andiustalfs
2.Chibwe/Kabwe	II	800-1000	4.7	24.0	Haplic Lixisols/Typic andiustalfs
3. GART, Chisamba	II	800-1000	4.4	5.0	Haplic Lixisols/Kandic Paleustalfs
4. UNZA FARM	II	800-1000	5.4	6.9	Haplic Lixisols/Typic Kandiustalfs
5. Magoye, CDT	II	800-1000	4.0	6.0	Haplic Lixisols/Kandic Paleustalfs
6.Magoye/Mwanachingwala	II	800-1000	4.3	3.0	Haplic Lixisols/Kandic Paleustalfs
7. Lusitu	I	<800	4.4	12.0	Chromic Luvisols/Rhodic Paleustalfs

WRB: FAO-ISRIC-ISSS. 1998 World Reference Base for Soil Resources. World Soil Resources Report No.84. FAO, Rome.

RESULTS AND DISCUSSIONS

Maize

- There was significant ($p<0.05$) response to P application regardless of P source at all locations
- This indicated that P was limiting crop yields
- Observed differences in the magnitudes of the responses reflected differences in initial P status inherent soil fertility

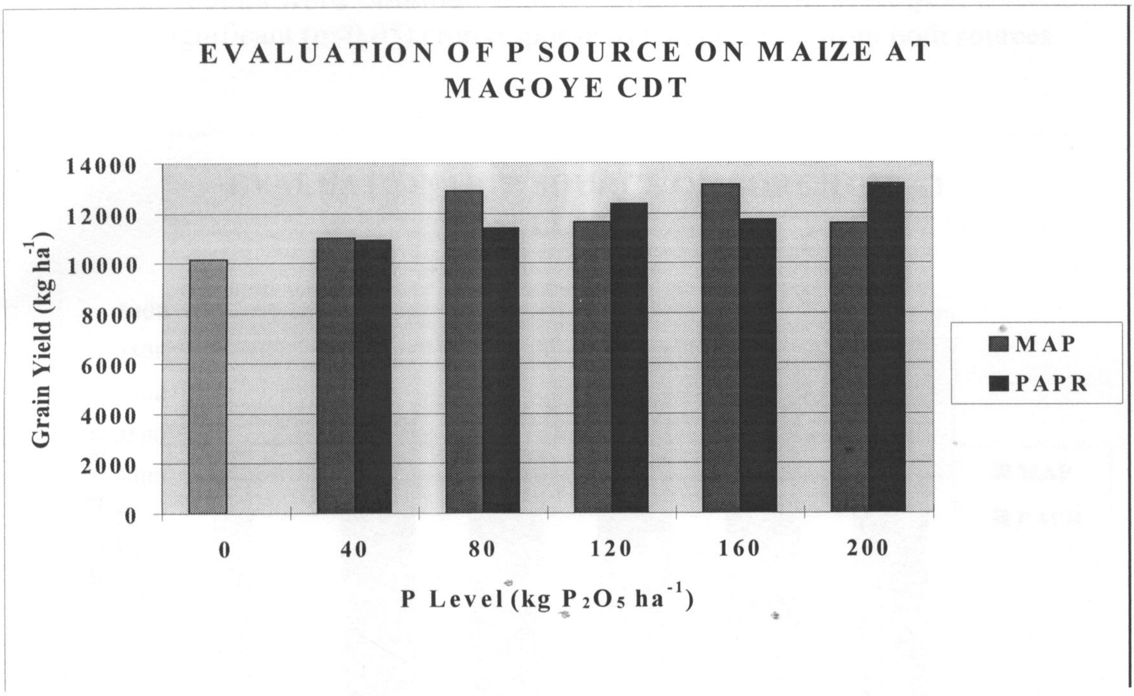

Figure 1.

When PAPR is compared to MAP in both on-station and on-farm trials, optimum Maize yields were generally obtained at lower rates of P with MAP than with PAPR

The rate of 80 kg P_2O_5/ha appeared to be optimum for MAP and there was a decline to yields with the application of MAP above this rate.

Similar rates of P application from PAPR resulted in larger cobs and higher grain yield than with MAP

- On sandy soils (Mukonchi, Chibwe and Mwanachingwala) the higher rates of P induced
- Zn, Mg, and Ca deficiencies
- This was not the case with PAPR

Sorghum

- Similar results were obtained with Sorghum at Lusitu in Region I.

There was a significant ($p<0.05$) crop response to P application from both sources.

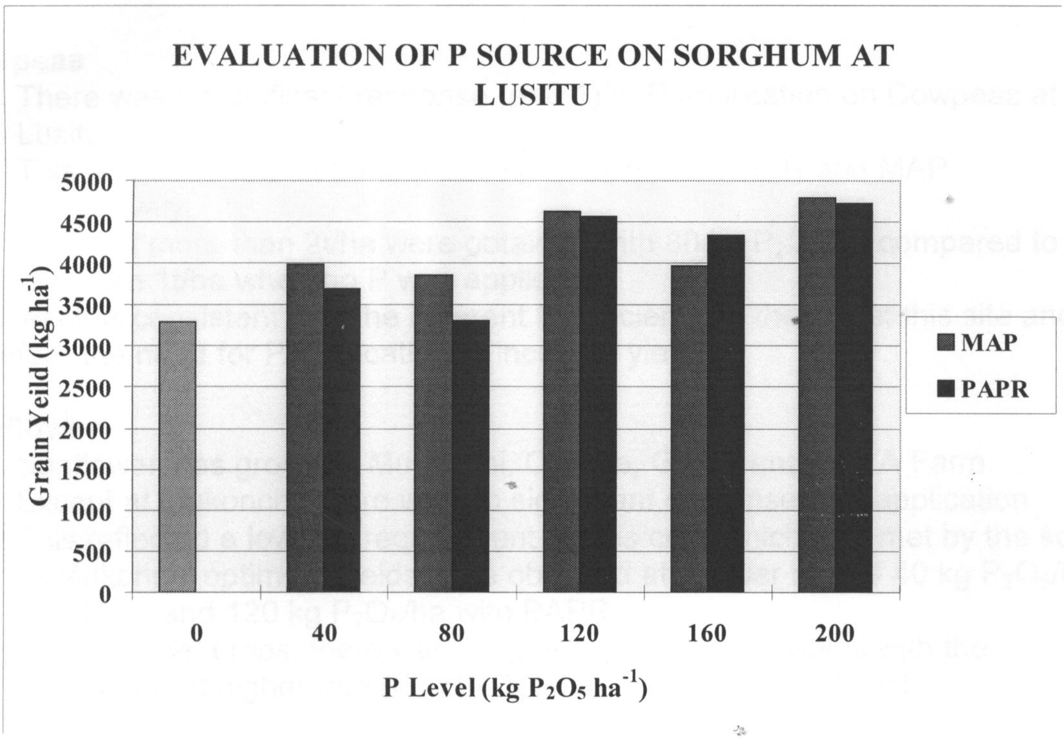

Figure 4.

- As for Maize at other sites, a significant response occurred with P application above 120 kg P_2O_5/ha. This indicates a higher P requirement for these sites than can be met by the recommended 60 P_2O_5/ha.

Soybeans

- There was a significant ($p<0.05$) response to P application only at GART

As with cereals a depression in yields was observed with the application of more than 80 kg P_2O_5/ha from MAP.

Groundnut

- At both sites (Magoye CDT and Mwanachingwala), there was no significant response to P application regardless of P source.
- The crop vigour that was observed was not translated into grain yield.
- There was a tendency for an increase in shelling % with P application especially at the higher rate of PAPR (>80 P_2O_5 kg/ha)
- This could be attributed to the supply of Ca from PAPR because the soils were very acid and no lime was applied to the soils. The soil thus requires to be limed.

Cowpeas

- There was a significant response ($p<0.1$) to P application on Cowpeas at Lusitu.
- This response was at 80 and 120 kg P_2O_5/ha for PAPR and MAP respectively.
- Yields of more than 2t/ha were obtained with 80 kg P_2O_5/ha compared to less than 1t/ha when no P was applied.

This result is consistent with the inherent P deficiency in the soil at this site and therefore the need for P application to increase yields.

Sunflower

- Sunflower was grown at Mukonchi, Chibwe, GART and UNZA Farm.
- Except at Mukonchi, there was no significant response to P application.
- This reflected a lower P requirement by this crop which was met by the soil.
- At Mukonchi optimum yields were obtained at a lower rate of 40 kg P_2O_5/ha with MAP and 120 kg P_2O_5/ha with PAPR.
- As with other crops, there was a significant decline in yields with the application of higher rate (>80 P_2O_5 kg/ha) of MAP than PAPR

The results of this experiment show that PAPR is as good as MAP in providing P to plants and improving yields of crops.

- At Mwanachingwala site where the soil was acutely P deficient and acid, PAPR was a significantly ($p<0.05$) better source of P than MAP for Maize.

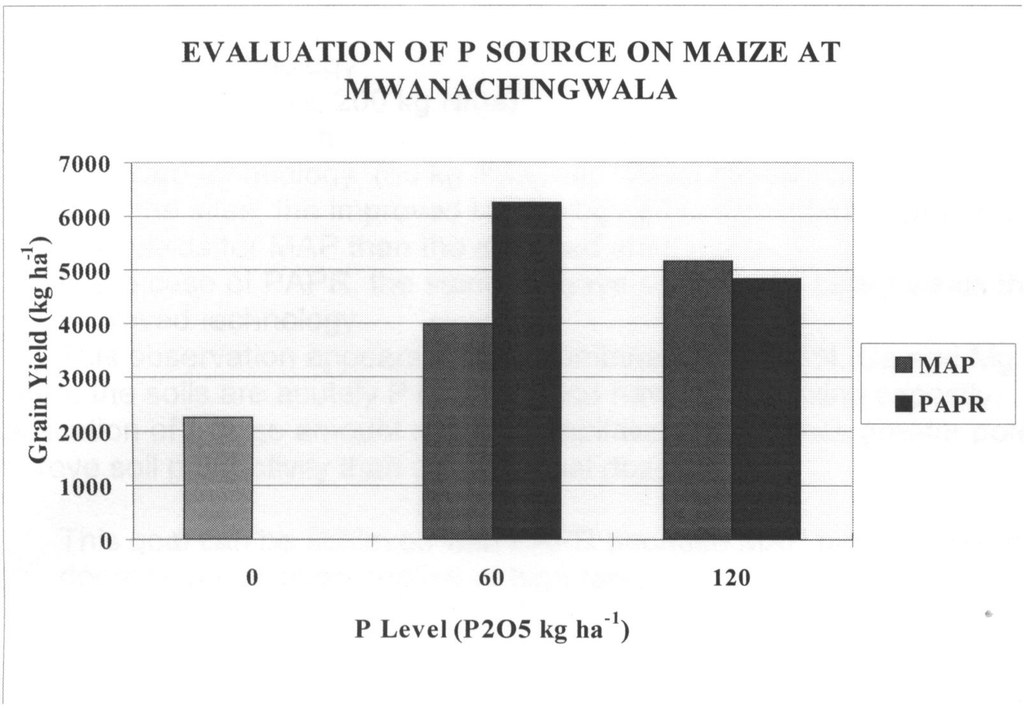
EVALUATION OF P SOURCE ON MAIZE AT MWANACHINGWALA
Grain Yield (kg ha-1)
7000
6000
5000
4000
3000
2000
1000
0
0
60
120
P Level (P2O5 kg ha-1)
MAP
PAPR


MAP 60
PAPR 60

Where soil P is low application of P of 80 kg P_2O_5/ha is more likely to increase crop yields than the currently recommended 60 kg P_2O_5/ha

- For on Farm sites,
- improved technology
  (120 kg P_2O_5/ha, 200 kg N/ha)
  was compared with
- Standard technology (60 kg P_2O_5/ha, 120 kg N/ha)
- In all the sites, the improved technology gave significantly ($p<0.05$) better crop yields for MAP than the standard technology.
- In the case of PAPR, the standard gave significantly better yields than the improved technology.
- This observation appears to be a combined effect of N, Ca and Mg.

Where the soils are acutely P deficient and have high P fixing capacity, application of a large amount of P to recapitalize the soil has greater potential to improve soil productivity than small annual dozes.

- This goal can be achieved with PAPR because MAP has a tendency to depress yields when applied at high rates.

REFERENCES

REFERENCES

Bank of Zambia (1987) Annual Report, Republic of Zambia, p19.

Bank of Zambia (1998) Annual Report, Republic of Zambia, p14

Bank of Zambia, (1978) Report and Statement of Accounts for the year ended December 31st , Republic of Zambia, p35.

Budget Speech (1998) Ministry of Finance and Economic Development. Republic of Zambia, January.

Bunyolo A. M (1991) Crop response to phosphate fertilization in Zambia. Utilization of phosphate deposits for the benefit of the Zambian farmer, proceedings of the first Zambian Seminar, ZFTDC pub. Siavonga, Zambia, 9 - 17 June, pp. 26 - 33.

Chein S. H and Hammond L. L (1989) Agronomic effectiveness of partially acidulated phosphate rock as influenced by soil phosphorus - fixing capacity. Plant and Soil 120: 159 - 164.

Chein S. H and Menon R. G (1989) Phosphate Rock (PR) compacted with Triple Superphosphate (TSP) or Single Superphosphate (SSP) versus Partially Acidulated Phosphate Rock (PAPR): A preliminary report on chemical, agronomic, and economic evaluations.

Chein S. H, Sompongse D, Henao J and Hellums D. T (1987) Greenhouse evaluation of phosphorus availability from compacted phosphate rocks with urea or with triple superphosphate. Fertilizer Research 14: 245 - 256.

Damaseke I. M, Sakala G. M and Muyunda K (1993) Agronomic Effectiveness of Partially Acidulated Phosphate rock in Southern Zambia. Proceedings of an international workshop: phosphate rock - derivatives and their use, Zambia Fertilizer Technology Development Committee, Aug. 29 – Sep. 2, Siavonga, Zambia, pp. 49 - 56.

Economic Report (1973) Ministry of Planning and Finance, p 181

Economic Report (1983) Office of the President, National commission for Development Planning, Lusaka

Economic Report (1997) Ministry of Finance and Economic development. Republic of Zambia, January, pp. 41 - 47.

Elsie M. Donaldson, (1982) Methods for the analysis of ores, rocks and related materials, Monograph 881 Second Edition, Minister of Supply and Services Canada.

Food and Agriculture Organization (FAO) (1999) Fertilizer, FAO Year Book, Vol.49.

Frederick T. M (1991) Production and Economics of Partially Acidulated Phosphate Rock - Implications for Zambia. Utilization of local phosphate deposits for the benefit of the Zambian farmer, proceeding of the first Zambian seminar, Siavonga, Zambia, 9 - 17 June, pp. 163 - 169.

Goma C. H, Phiri S, Mapiki A and Singh B. R (1991) Evaluation of fused magnesium phosphate in acid soils of the high rainfall zone of Zambia. Utilization of local phosphate deposits for the benefit of the Zambian farmer, proceedings of the first Zambian seminar, Siavonga, Zambia, 9 - 17 June, pp. 138 - 149.

Goma H. C, Mapiki A and Phiri S (1997) A review of evaluation of indigenous phosphate rock as a source of phosphorus. Phosphate resources and food security in Africa, conference proceedings, abstracts and program, Commonwealth Youth Center, Lusaka, Zambia, 3 - 5 Nov., p. 18.

Govere E. M (1993) Enhancing Phosphate Rock Agronomic Effectiveness by compaction technology. Proceedings of an international workshop: phosphate rock - derivatives and their use, Zambia Fertilizer Technology Development Committee, Siavonga, Zambia, Aug. 29 – Sep. 2, pp. 57 - 67.

Hagin J and Katz S (1985) Effectiveness of partially acidulated phosphate rock as a source of P to plants in calcareous soils. Fertilizer Research 8: 117 - 127.

Hammond L. L, Chein S. H, Roy A. H and Mokwunye A. U (1989) Solubility and agronomic effectiveness of partially acidulated phosphate rocks as influenced by their iron and aluminium oxide content. Fertilizer Research 19: 93 - 98.

Hardesty J. O (1964) Granulation. In Superphosphate: Its History, Chemistry and Manufacture, pp 251 – 271.

Hatfield J. D (1964) Normal Superphosphate: Chemistry: In Superphosphate: Its History, Chemistry and Manufacture, pp 116-130.

Hill, W. L, (1964) Raw Materials: In Superphosphate: Its History, Chemistry and Manufacture, pp 95-115.

Himmelblau D. M (1972) Fault detection and diagnosis in chemical and petrochemcal processes, Elsevier publishing company, pp 111 – 117.

Horwitz W (1965) Official methods of analysis of the association of official agricultural chemists, 10th Ed, pp13-14.

International Fertilizer Development Center (IFDC) (1984) Single-Step Partial Acidulation / Granulation of Phosphate Rock, Pilot-Plant Scale Studies, IFDC fertilizer Technology Division, June progress report.

International Fertilizer Development Center (IFDC) (1986) Sulphuric Acid-Based Partially Acidulated Phosphate Rock. It's Production, Cost and Use. Technical bulletin IFDC - T - 31, January.

International Fertilizer Development Center (IFDC) (1988) Agronomic Evaluation of Partially Acidulated Phosphate Rocks in the Tropics, IFDC's Experience, Paper Series IFDC-T- 7 October.

Japan International Cooperation Agency (JICA) (1985) A pre-feasibility study for the phosphate development project. The Republic of Zambia, Final Draft.

Kang B. T (1985) Cropping Systems and Soil Fertility Management in the humid and sub-humid tropicals with special reference to West Africa. In A.U. Mokwunye and P.L.G Vlek, Development in Plant and Soil Sciences. Management of Nitrogen and Phosphorus Fertilizers in sub - Saharan Africa, proceedings of a symposium, Lome, Togo, March 25 – 28, pp. 225- 252.

Levenspiel O (1972) Chemical reaction engineering, 2nd edition, p267-269, John Wiley and Sons, Inc.

Ibid, pp 253 – 265.

Lombe W. C (1985) Process Design Study for the Beneficiation of Chilembwe Phosphate Ore. Report prepared for ZIMCO Ltd, MINEX Department, School of Mines, University of Zambia.

Lombe W. C (1991) Phosphate beneficiation experiments in the School of Mines, University of Zambia. Fertilizer Research 30: 213 - 224.

Lukomona C (1989) Process Design Study for the Beneficiation of Mumbwa Sugar Loaf Phosphate Ore. B.Min.Sc. final year project report.

Lukomona C, Mwalula J. B, and Witika L. K (1997) The beneficiation of Mumbwa phosphate deposit by various techniques. Phosphate resources and food security in Africa, proceedings of an international conference, abstracts and program, Commonwealth Youth Center, Lusaka, Zambia, 3 - 5 Nov., p 9.

McClellan (1980) Chemistry of Carbonate apatites.

Menon R. G, Chein S. H and Abd el Nabi Gadalla (1991) Phosphate Rocks Compacted with Superphosphates vs. Partially Acidulated Phosphate Rock for beans and rice. Soil Science Society of America Journal 55, No. 5. Sep - Oct.

Menon R.G and Chein S. H (1990) Phosphorus availability to maize from partially acidulated phosphate rocks and phosphate rocks compacted with triple superphosphate. Plant and Soil 127: 123 - 128.

Monthly Digest of Statistics Feb/Mar (1991) Central Statistical Office, Lusaka, Republic of Zambia, p15.

Msiska A (1993) Fertilizer Marketing and Distribution Systems in Zambia - An overview. Proceedings of an international workshop: phosphate rock - derivatives and their use, Zambia Fertilizer Technology Development Committee, Siavonga, Zambia, Aug. 29 – Sep. 2, pp. 83 - 91.

Mulela D (1991) Igneous phosphate occurrences in Zambia. Utilization of local phosphate deposits for the benefit of the Zambian farmer, proceedings of the first Zambian seminar, ZFTDC pub. Siavonga, Zambia, pp. 15 - 27.

Nkonde G. K (1988) Analysis of joint distribution of number of cycles and residence time in a selective recycle system, Acta Polytechnica Scandinavica, Chemical Technology and Metallurgy Series No. 183.

Nkonde G. K (1989) Analysis of selective recycle systems, Analysis of joint distribution of number of cycles and residence time in a selective recycle system, Acta Polytechnica Scandinavica, Chemical Technology and Metallurgy Series No. 190.

Nkonde G. K and Simukanga S (1993) Determination of process variables in the production of partially acidulated phosphate rock. Proceedings of an international workshop: phosphate rock - derivatives and their use, Zambia Fertilizer Technology Development Committee, Siavonga, Zambia, Aug. 29 – Sep. 2.

Nkonde G. K and Simukanga S (1994) Production of Partially Acidulated Phosphate Rock (PAPR) : A local fertilizer product. The Zambian Engineer, March 32: 24 - 27.

Nkonde G. K, Simukanga S and Witika L. K (1991) Production of partially acidulated phosphate rock (PAPR) from Chilembwe Phosphate Ore. Utilization of local phosphate deposits for the benefit of the Zambian farmer, proceedings of the first Zambian seminar, Siavonga, Zambia, 9 - 17 June, pp. 63 - 73.

Nkonde G. K. and Simukanga S (1997) Compacting of Chilembwe phosphate rock of Zambia. Phosphate resources and food security in Africa, conference proceedings, abstracts and program, Commonwealth Youth Center, Lusaka, Zambia, 3 - 5 Nov., p. 12.

Phiri S, Goma H. C, Mapiki A and Singh B. R (1991) Agronomic Evaluation of Direct Application of Ground Phosphate Rock in the High Rainfall Zone of Zambia. Utilization of local phosphate deposits for the benefit of the Zambian farmer, proceedings of the first Zambian seminar, Siavonga, Zambia, 9 - 17 June, pp. 150 - 162.

Phiri S, Mapiki A, Goma H. C and Singh B. R (1993) Agronomic Evaluation of Partially Acidulated Phosphate Rock in Northern Zambia. Proceedings of an international workshop: phosphate rock - derivatives and their use, Zambia Fertilizer Technology Development Committee, Siavonga, Zambia, Aug. 29 – Sep. 2, pp. 41 - 48.

Phosphorus and Potassium (1987) Partial acidulation of phosphate rock, a fertilizer of growing importance. No. 150 PRODUCT PROFILE, July - August.

Roy H. A and McClellan H. G (1985) Processing Phosphate Ores into Fertilizers. In A.U. Mokwunye and P.L.G Vlek, Development in Plant and Soil Sciences. Management of Nitrogen and Phosphorus Fertilizers in sub - Saharan Africa, proceedings of a symposium, Lome, Togo, March 25 – 28, pp. 225- 252.

Simukanga (1986) Process Design Study for the Beneficiation of Kaluwe Phosphate Ore. M.Min.Sc. Thesis.

Simukanga S and Nkonde G. K (1993) A Preliminary Financial Evaluation for Production of PAPR at Chilembwe, Eastern Province. Proceedings of an international workshop: phosphate rock - derivatives and their use, Zambia Fertilizer Technology Development Committee, Aug 29 - Sep 2, Siavonga, Zambia, pp. 75 - 82.

Simukanga S, Lombe W. C and Nkonde G. K (1991) Chemical and Mineralogical Study of Chilembwe Phosphate Ore. Utilization of local phosphate deposits for the benefit of the Zambian farmer, proceedings of the first Zambian seminar, Siavonga, Zambia. 9 - 17 June, pp. 26 - 33.

Slack A. V and Rindt D. W (1964) Normal Superphosphate: Manufacturing Operations. In Superphosphate: Its History, Chemistry, and Manufacture, United States Department of Agriculture and Tennessee Valley Authority, pp. 165 - 183.

Sliwa A.S (1991) phosphate resources of Zambia and progress in their exploration. Fertilizer Research 30: 203 - 212.

Snell D. F (1970) Encyclopedia of Industrial Chemical Analysis, Vol. 9 p342, John Wiley and Sons, Inc.

Ssali H, P. M Ahn, and Mokwunye A (1985) Fertility of Soils in Tropical Africa: A historic perspective. In A.U. Mokwunye and P.L.G Vlek, Development in Plant and Soil Sciences. Management of Nitrogen and Phosphorus Fertilizers in sub - Saharan Africa, proceedings of a symposium, Lome, Togo, March 25 – 28, pp. 225- 252.

Stermole J. F and Stermole M. J (1996) Economic Evaluation and Investment Decission Methods, 9th Edition.

Tether J and Money N. J (1991) A review of agricultural minerals in Zambia. Fertilizer Research 30: 193 - 202.

Ukeles S. D, Ben-Yoseph E, and Finkelstein N. P (1994) Cadmium removal from phosphoric acid – Israeli experience. Hydrometallurgy '94', Institution of Mining and Metallurgy and the Society of Chemical Industry, Conf. Proceedings, Cambridge, England, 11 – 15 July, 1994, pp. 683 – 697.

Van Kauwenbergh S. J (1991) Overview of phosphate deposits in East and Southeast Africa. Fertlizer Research 30: 127 - 150.

World Population Prospects (1996) Zambia, Population Division, Department of Economic and Social Affairs of the United Nations Secretariat, pp. 836 - 837.

Young S. Roland (1971) Chemical analysis in extractive metallurgy, London, Griffin.

Zambezi P (1997) Phosphate resources of the Nkombwa Hill Carbonatite Complex of Isoka District, Northern Zambia: a new perspective. Phosphate resources and food security in Africa, proceedings of an international conference, abstracts and program, Commonwealth Youth Center, Lusaka, Zambia, 3 - 5 Nov., p.6.

Zambezi P and Chipola P (1991) Production of Partially Acidulated Phosphate Rock (PAPR) from Chilembwe Phosphate Ore at MINEX Department of ZIMCO. Utilization of local phosphate deposits for the benefit of the Zambian farmer, proceedings of the first Zambian seminar, Siavonga, Zambia, 9 - 17 June, pp. 57 - 62.